ISTANBUL TECHNICAL UNIVERSITY★ INSTITUTE OF SCIENCE AND TECHNOLOGY

DESIGN OF COMPOSITE SANDWICH SHIPBORNE PLATES

M.Sc. Thesis by

Barış A. GÜMÜŞLÜOĞLU, B.Sc.

Department: **Mechanical Egineering**
Programme: **Solid Mechanics**

DECEMBER 2006

ISTANBUL TECHNICAL UNIVERSITY★ INSTITUTE OF SCIENCE AND TECHNOLOGY

DESIGN OF COMPOSITE SANDWICH SHIPBORNE PLATES

M.Sc. THESIS by
Barış A. GÜMÜŞLÜOĞLU, B.Sc.

503031502

Date of Submition:	**20 December 2006**
Date of Defence Examination:	**30 January 2007**
Supervisor (Chairman):	**Assoc. Prof. Dr. Ata MUĞAN**
Members of the Examining Committee:	**Prof. Dr. Alaeddin ARPACI**
	Prof. Dr. Zahit MECİTOĞLU

DECEMBER 2006

İSTANBUL TEKNİK ÜNİVERSİTESİ ★ FEN BİLİMLERİ ENSTİTÜSÜ

KOMPOZİT SANDVİÇ GEMİ PLAKLARININ TASARIMI

YÜKSEK LİSANS TEZİ

Barış A. GÜMÜŞLÜOĞLU, B.Sc.

503031502

Tezin Enstitüye Verildiği Tarih:	**20 Aralık 2006**
Tezin Savunulduğu Tarih:	**30 Ocak 2007**
Tez Danışmanı:	**Doç. Dr. Ata MUĞAN**
Diğer Jüri Üyeleri:	**Prof. Dr. Alaeddin ARPACI**
	Prof. Dr. Zahit MECİTOĞLU

ARALIK 2006

Acknowledgements

I wish to take the opportunity to thank to my supervisor Assoc. Prof. Dr. Ata MUĞAN for his continuous support and encouragement throughout my entire study since the beginning. I would also like to thank to Prof. Dr. Zahit MECİTOĞLU and Prof. Dr. Muhittin ORAL from whom I have had the chance to learn a lot. I have always felt grateful to have the occasion to meet and to work with such influencing scientists and personalities.

I would like to express my very special gratitude to my lifetime mentor (*Uncle*) Dr. I. N. Ekber ONUK, who has dramatically influenced and directed the heading of my entire life. He is the one who has done everything possible to make all my ambitions become reality without revealing any sight of weariness.

I am grateful to my parents who have done every effort to support me all through my life.

I am also exceptionally grateful to have the chance to marry my wife, who has sacrificed her times, without any complaint, to support and encourage me in any situation, how hard it was, throughout my everlasting working times. And I have my best wishes for my little daughter of two and a half years old. She has cheerfully forfeited her playing times to let her father work.

And special thanks to the distinguished people of Yonca-Onuk JV/ Istanbul, especially; Navy Captain (r) Yıldıray ÖZEL, without them my professional career would not be possible.

DECEMBER 2006 Barış A. GÜMÜŞLÜOĞLU

TABLE OF CONTENTS

LIST OF TABLES **v**
LIST OF FIGURES **vi**
LIST OF SYMBOLS **ix**
SUMMARY **xi**
ÖZET **xii**

1 INTRODUCTION **1**
1.1 Composite Materials 1
1.2 Composite Sandwich Structures 1
1.3 Background and Literature Survey 5
1.4 Outline of the Study 7

2 CONSTITUTIVE RELATIONS of ORTHOTROPIC MATERIALS **9**
2.1 Hooke's Law 9
2.2 Material Type Independent Symmetry Conditions (MTISC) 10
2.2.1 Condition 01 $E_{mnpr} = E_{nmpr}$: 10
2.2.2 Condition 02 $E_{mnpr} = E_{mnrp}$: 12
2.2.3 Condition 03 $E_{mnpr} = E_{prmn}$: 12
2.3 Simplified Constitutive Relations Equation Following the Application of MTISC 14
2.4 Material Type Dependent Symmetry Conditions (MTDSC) 15
2.4.1 Monoclinic Materials 15
2.4.2 Orthotropic Materials 17
2.4.3 Tetragonal Materials 19
2.4.4 Cubic Materials 21
2.4.5 Isotropic Materials 23

3 FIBER REINFORCED COMPOSITE MATERIALS **26**
3.1 Stress-Strain Characteristics of Fiber Reinforced Composite Materials 26
3.1.1 Elasticity Constants of Fiber Reinforced Composite Materials 27
3.1.2 Relationship among Elasticity Constants 29
3.1.3 Stiffness and Compliance Matrices 30
3.2 Plane Stress Assumption 32

3.2.1 Stress-Strain Relations for Plane Stress 34
3.2.2 Strain-Stress Relations for Plane Stress in a Global Coordinate System 37
3.2.3 Transformed Reduced Compliance Matrix 44
3.2.4 Transformed Reduced Stiffness Matrix 46
3.2.5 Reduced Stiffness and Compliance Matrices in Terms of Engineering Constants 47

4 CLASSICAL LAMINATION THEORY 51
4.1 Coordinate System and Layer Nomenclature 51
4.1.1 Coordinate System 51
4.1.2 Laminate Nomenclature 51
4.2 Kirchoff Hypothesis 53
4.2.1 Assumptions of Kirchoff Hypothesis 53
4.2.2 Bending of a Plate 55
4.3 Laminate Strains 57
4.4 Laminate Stresses 58
4.5 Force and Moment Resultants 59
4.5.1 Force Resultants 60
4.5.2 Moment Resultants 62
4.6 Laminate Stiffness Matrix 63
4.6.1 Force Expressions 64
4.6.2 Moment Expressions 67
4.6.3 Laminate Stiffness Matrix 69

5 FIBER REINFORCED LAMINATED PLATES 71
5.1.1 Governing Rectangular Plate Equations 71
5.1.2 Forces along the x-Direction 73
5.1.3 Forces along the y-Direction 74
5.1.4 Forces Along the z-Direction 75
5.1.5 Moments About the x-Axis 76
5.1.6 Moments About the y-Axis 77
5.1.7 Moments about the z-Axis 78
5.1.8 Generic Rectangular Plate Equations 78
5.2 Boundary Conditions 79
5.3 Governing Equations in Terms of Displacements 80
5.4 Boundary Conditions in Terms of Displacements 82

6 PLATE PROBLEM SOLUTION 85
6.1 Simplified Governing Differential Equations 85
6.2 Simplified Boundary Conditions 86
6.3 Solution of the Differential Equations Given the Boundary Conditions 86

7 ANALYTICAL SOLUTION TOOL 88
7.1 Analytical Tool Flow Chart 88
7.2 Flow Charts' Step Details 89

8 CONCLUSION AND DISCUSSIONS 91
8.1 Trapezoidal Plate Configuration 91
8.2 Curved Plate Configuration 91

9 RECOMMENDATIONS FOR FUTURE STUDY 92

REFERENCES 93
APPENDIXES 99
A PLATE SOLUTIONS 99
B STRESS DISTRIBUTION ABOUT x_o 123
C LENGTH OF AN INFINITESIMAL LINE ELEMENT 125
D DEFORMATION OF A PARTICLE 128
E MTDSC BASICS; COORDINATE TRANSFORMATIONS 130
F STRAIN TENSOR TRANSFORMATIONS 133
G STRESS TENSOR TRANSFORMATIONS 134
H MAXWELL-BETTI RECIPROCAL THEOREM 144
I GRADIENT (SLOPE) OF A CURVE AT A POINT 146
J STRAIN TENSOR 147
K NOTES ON DISPLACEMENT COMPONENTS 151
L SIGN CONVENTIONS 153
M EXPERIMENT 154
RESUME 166

LIST OF TABLES

Page No.

Table A.1:	Mechanical Properties of Fiber Reinforcement	100
Table A.2:	Mechanical Properties of Core Material	100
Table A.3:	Analytical Tool vs. Experiment Results	101
Table A.4:	Element Properties	102
Table A.5:	Mesh Properties	102
Table A.6:	Constraints on Edges along Direction x	102
Table A.7:	Constraints on Edges along Direction y	102
Table A.8:	Loading Conditions	103
Table A.9:	Type of Analysis	103
Table A.10:	Analytical Tool vs. FEA Res. For Trapezoidal Plates for L.01	103
Table A.11:	Analytical Tool vs. FEA Res. for Trapezoidal Plates for L.02	104
Table A.12:	Analytical Tool vs. FEA Res. for Trapezoidal Plates for L.03	104
Table A.13:	Analytical Tool vs. FEA Res. for Trapezoidal Plates for L.04	104
Table A.14:	Analytical Tool vs. FEA Res. for Trapezoidal Plates for L.05	104
Table A.15:	Analytical Tool vs. FEA Res. for Trapezoidal Plates for L.06	104
Table A.16:	Analytical Tool vs. FEA Res. for Trapezoidal Plates for L.07	105
Table A.17:	Analytical Tool vs. FEA Res. for Trapezoidal Plates for L.08	105
Table A.18:	Analytical Tool vs. FEA Res. for Trapezoidal Plates for L.09	105
Table A.19:	Analytical Tool vs. FEA for Curved Plates for L.01	111
Table A.20:	Analytical Tool vs. FEA for Curved Plates for L.02	111
Table A.21:	Analytical Tool vs. FEA for Curved Plates for L.03	112
Table A.22:	Analytical Tool vs. FEA for Curved Plates for L.04	112
Table A.23:	Analytical Tool vs. FEA for Curved Plates for L.05	112
Table A.24:	Analytical Tool vs. FEA for Curved Plates for L.06	112
Table A.25:	Analytical Tool vs. FEA for Curved Plates for L.07	112
Table A.26:	Analytical Tool vs. FEA for Curved Plates for L.08	113
Table A.27:	Analytical Tool vs. FEA for Curved Plates for L.09	113
Table M.1:	Mechanical Properties of Fiber Reinforcement	157
Table M.2:	Mechanical Properties of Fiber Reinforcement	157
Table M.3:	Measurements Summary Table.	161

LIST OF FIGURES

		Page No.
Figure 1.1:	Typical Sandwich Structure	2
Figure 1.2:	ONUK MRTP33 Fast Attack Craft	4
Figure 1.3:	ONUK MRTP29 Fast Patrol Craft	4
Figure 1.4:	Visby Class Corvette	5
Figure 1.5:	US Submarine SSN711	5
Figure 2.1:	Representation of Infinitesimal Cubic Element	11
Figure 3.1:	Infinitesimal Fiber Reinforced Cubic Element	26
Figure 3.2:	Small Volume Of Fiber Reinforced Composite Material	29
Figure 3.3:	Interaction Between Two Layers	33
Figure 3.4:	Plate Stiffened With A Stiffener	33
Figure 3.5:	Local Gradual Layer Termination Detail	34
Figure 3.6:	Plane Stress Case Coordinate Transformation	37
Figure 3.7:	Tensor Shear Strain	41
Figure 3.8:	Engineering Shear Strain	41
Figure 4.1:	Plate Coordinate System	51
Figure 4.2:	Layer Nomenclature	51
Figure 4.3:	Fiber Orientation	52
Figure 4.4:	Laminate Notation 01	52
Figure 4.5:	Laminate Notation 02	52
Figure 4.6:	Laminate Notation 03	52
Figure 4.7:	Laminate Notation	53
Figure 4.8:	Kirchoff Hypothesis 01, Plate Loading Conditions	53
Figure 4.9:	Kirchoff Hypothesis 02	53
Figure 4.10:	Kirchoff Hypothesis 03	54
Figure 4.11:	Bending of a Plate.	55
Figure 4.12:	Line Segment Assumption	56
Figure 4.13:	Distribution Of σ_x within a Cross Section	59
Figure 4.14:	Stress Distribution within Layer 1	60
Figure 5.1:	Force and Moment Resultants On The Boundaries Of A Plate	71
Figure 5.2:	Differential Element within a Laminated Plate	73
Figure 5.3:	Forces Along the x-Direction On The Differential Element	73
Figure 5.4:	Forces Along the y-Direction on the Differential Element	74
Figure 5.5:	Forces Along the z-Direction on the Differential Element	75
Figure 5.6:	Moments about the x-Axis on the Differential Element	76
Figure 5.7:	Moments about the y-Axis on the Differential Element	77
Figure 5.8:	Moments about the z-Axis on the Differential Element	78
Figure 7.1:	Analytical Tool Flow Chart	88
Figure A.1:	Reference Plate Cross Section Details	99
Figure A.2:	Deviation, Analytical vs. Experiment Results	101
Figure A.3:	Trapezoidal Plate Configuration	103

Figure A.4: Analytical Tool vs. FEA for Trapezoidal Plates for $\sigma_{1\max}$ of L.01 105
Figure A.5: Analytical Tool vs. FEA for Trapezoidal Plates for $\sigma_{1\max}$ of L.02 106
Figure A.6: Analytical Tool vs. FEA for Trapezoidal Plates for $\sigma_{1\max}$ of L.03 106
Figure A.7: Analytical Tool vs. FEA for Trapezoidal Plates for $\sigma_{1\max}$ of L.04 107
Figure A.8: Analytical Tool vs. FEA for Trapezoidal Plates for $\sigma_{1\max}$ of L.05 107
Figure A.9: Analytical Tool vs. FEA for Trapezoidal Plates for $\sigma_{2\max}$ of L.01 108
Figure A.10: Analytical Tool vs. FEA for Trapezoidal Plates for $\sigma_{2\max}$ of L.02 108
Figure A.11: Analytical Tool vs. FEA for Trapezoidal Plates for $\sigma_{2\max}$ of L.03 109
Figure A.12: Analytical Tool vs. FEA for Trapezoidal Plates for $\sigma_{2\max}$ of L.04 109
Figure A.13: Analytical Tool vs. FEA for Trapezoidal Plates for $\sigma_{2\max}$ of L.05 110
Figure A.14: Analytical Tool vs. FEA for Trapezoidal Plates, $w_{o\max}$ 110
Figure A.15: Curved Plate Configuration. 111
Figure A.16: Analytical Tool vs. FEA for Curved Plates for $\sigma_{1\max}$ of L.01 113
Figure A.17: Analytical Tool vs. FEA for Curved Plates for $\sigma_{1\max}$ of L.02 114
Figure A.18: Analytical Tool vs. FEA for Curved Plates for $\sigma_{1\max}$ of L.03 114
Figure A.19: Analytical Tool vs. FEA for Curved Plates for $\sigma_{1\max}$ Of L.04 115
Figure A.20: Analytical Tool vs. FEA for Curved Plates for $\sigma_{1\max}$ of L.05 115
Figure A.21: Analytical Tool vs. FEA for Curved Plates for $\sigma_{1\max}$ of L.06 116
Figure A.22: Analytical Tool vs. FEA for Curved Plates for $\sigma_{1\max}$ of L.07 116
Figure A.23: Analytical Tool vs. FEA for Curved Plates for $\sigma_{1\max}$ of L.08 117
Figure A.24: Analytical Tool vs. FEA for Curved Plates for $\sigma_{1\max}$ of L.09 117
Figure A.25: Analytical Tool vs. FEA for Curved Plates for $\sigma_{2\max}$ of L.01 118
Figure A.26: Analytical Tool vs. FEA for Curved Plates for $\sigma_{2\max}$ of L.02 118
Figure A.27: Analytical Tool vs. FEA for Curved Plates for $\sigma_{2\max}$ of L.03 119
Figure A.28: Analytical Tool vs. FEA for Curved Plates for $\sigma_{2\max}$ of L.04 119
Figure A.29: Analytical Tool vs. FEA for Curved Plates for $\sigma_{2\max}$ of L.05 120
Figure A.30: Analytical Tool vs. FEA for Curved Plates for $\sigma_{2\max}$ of L.06 120
Figure A.31: Analytical Tool vs. FEA for Curved Plates for $\sigma_{2\max}$ of L.07 121
Figure A.32: Analytical Tool vs. FEA for Curved Plates for $\sigma_{2\max}$ of L.08 121
Figure A.33: Analytical Tool vs. FEA for Curved Plates for $\sigma_{2\max}$ of L09 122
Figure A.34: Analytical Tool vs. FEA for Curved Plates, $w_{o\max}$ 122
Figure C.1: Length of an Infinitesimal Line Element 125
Figure D.1: Deformation of a Particle. 128
Figure E.1: 2D Coordinate System Transformation 130
Figure G.1: Stress Tensor Transformations 01 134
Figure G.2: Stress Tensor Transformations 02 136
Figure G.3: Stress Tensor Transformations 03 136
Figure G.4: Stress Tensor Transformations 04 140
Figure G.5: Stress Tensor Transformations 05 141
Figure H.1: Maxwell-Betti Reciprocal Theorem 01 144
Figure H.2: Maxwell-Betti Reciprocal Theorem 02. 145

Figure I.1: Gradient (slope) of a Curve. 146
Figure J.1: Strain Tensor. 148
Figure K.1: Displacement Components, $\underline{u}$. 151
Figure K.2: Displacement Components, $\underline{v}$. 151
Figure K.3: Displacement Components; $\underline{u}$ and $\underline{v}$. 152
Figure L.1: Typical Plate Cross Section 153
Figure L.2: Moments Acting on a Plate Reference Surface 153
Figure M.1: Experiment Set Lay-Out 155
Figure M.2: Plate Cross Section Details 156
Figure M.3: 3-D Model of the Supporting Structure 158
Figure M.4: FEA Results: Maximum Deformation along the Vertical Axis 158
Figure M.5: Shop Drawing Of The Supporting Structure 159
Figure M.6: FEA Results: Maximum Deflection along Vertical Axis 159
Figure M.7: Support Structure: Sandwich Plate and Side Panels 160
Figure M.8: Measurements and Calculations 160
Figure M.9: Measurements Summary Graph. 162
Figure M.10: Strain Gauge Installation. 163
Figure M.11: The Supporting Structure and the Sandwich Panel. 163
Figure M.12: The Sand Block at 450mm Height. 164
Figure M.13: The Strain Indicator. 164
Figure M.14: The Deflection Gauge. 165

LIST OF SYMBOLS

a_{ij}	:	Base vectors for curvilinear coordinate system
a_{kl}	:	Direction cosines
A_{ij}, B_{ij}, C_{ij}	:	Extension, coupling and bending stiffness matrices
B	:	Body force
C_{ij}	:	Stiffness matrix
ds	:	Length of a infinitesimal line element
E^3	:	Three dimensional Euclidian Space
E_{mnpr}	:	Elasticity tensor
E_1, E_2, E_3	:	Young's modulus
F_x, F_y, F_{xy}	:	Force
g_i	:	Base vector for curvilinear coordinate system
g_{ij}	:	Fundamental metric tensor
G_{12}, G_{13}, G_{23}	:	Shear modulus
h	:	Ply thickness
H	:	Laminate thickness
I_i	:	Orthogonal base vectors
N_x, N_y, N_{xy}	:	Force resultants
M_x, M_y, M_{xy}	:	Moment resultants
Q_x, Q_y	:	Shear force resultants
q	:	Distributed load
q_o	:	Uniform distributed load
Q_{ij}	:	Reduced stiffness matrix
$\overline{Q}_{ij}$	:	Transformed reduced stiffness matrix
S_{ij}	:	Compliance matrix
$\overline{S}_{ij}$	:	Transformed reduced compliance matrix
T_ε	:	Plane stress transformation matrix for strain
T_σ	:	Plane stress transformation matrix for stress
$u^o(x,y)$	:	Reference surface translation along x axis
$u(x,y,z)$	:	Translation along x axis
U^*	:	Strain energy density
$v^o(x,y)$	:	Reference surface translation along y axis
$v(x,y,z)$	:	Translation along y axis

V	:	Volume
$w^o(x,y)$	:	Reference surface deflection
$w(x,y,z)$	:	Deflection
W	:	Work
δ_{ij}	:	Kronecker delta function
$\varepsilon_1, \varepsilon_2, \varepsilon_3$	:	Engineering extensional strains in material coordinates
$\varepsilon_x, \varepsilon_y, \varepsilon_z$	:	Engineering extensional strains in global coordinates
$\gamma_{12}, \gamma_{13}, \gamma_{23}$	:	Engineering shear strains in material coordinates
$\gamma_{xy}, \gamma_{xz}, \gamma_{yz}$	:	Engineering shear strains in global coordinates
γ_{ij}	:	Strain tensor
$\kappa^o{}_x(x,y)$	:	Reference surface curvature along x axis
$\kappa^o{}_y(x,y)$	:	Reference surface curvature along y axis
$\kappa^o{}_{xy}(x,y)$	:	Reference surface curvature along xy axis
λ, μ	:	Lamé constants
$\nu_{12}, \nu_{13}, \nu_{23}$	:	Poisson ratios in material coordinates
$\nu_{xy}, \nu_{xz}, \nu_{yz}$	:	Poisson ratios in global coordinates
θ	:	Fiber orientation wrt x axis
$\sigma_1, \sigma_2, \sigma_3$	:	Engineering extensional stresses in material coordinates
$\sigma_x, \sigma_y, \sigma_z$	:	Engineering extensional stresses in global coordinates
σ_{ij}	:	Stress tensor
$\tau_{12}, \tau_{13}, \tau_{23}$	:	Engineering shear stresses in material coordinates
$\tau_{xy}, \tau_{xz}, \tau_{yz}$	:	Engineering shear stresses in global coordinates
ψ	:	Stored energy

DESIGN OF COMPOSITE SANDWICH SHIPBORNE PLATES

Abstract

From the local strength analysis perspective in ship structures, ship panels consist of plates supported by beams, webs, bulkheads and other supporting structures. Therefore, structural analysis of plates constitutes a significant importance in ship panel analysis.

In ship structural analysis, plates are usually assumed to be simply supported and loads are usually defined as out of plane pressures distributed evenly on the surface in question. On the other hand, because of the generally complex geometry of the hull shape of a ship, plates within panels are rarely perfect rectangles. However, in most cases, these plates are trapezoids. Moreover, in many cases, plates are also curved where the convexity is towards the force direction.

Theoretically, structural analysis of non-rectangular and/ or curved composite sandwich plates cannot be carried out with closed form analytical methods in most of the circumstances. Nevertheless, numerical approximation methods can always be employed. FEA is the most commonly used method for the structural analysis of such problems. However, depending on the actual requirement, commercially available FEA tools can sometimes be expensive and utilizing them may be time consuming for the purpose of local strength analysis of shipborne panels.

The purpose of this study is to demonstrate that Classical Laminated Plate Theory (CLPT) based closed form methods can also be considered as a viable alternative for the analysis of sandwich plates having geometries deviating, to a certain extent, from a perfect rectangular or a flat shape. Obviously, the solution is expected to include errors; thus, it can only be an approximation. Within the context of this study the limits of this deviation, above which closed form methods start producing irrelevant results for simply supported plates of composite sandwich construction operating under evenly distributed out of plane pressures, will be demonstrated.

KOMPOZİT SANDVİÇ GEMİ PLAKLARININ TASARIMI

Özet

Gemi yapılarının bölgesel yapısal analizi çerçevesinden bakıldığında, gemi panelleri çeşitli yapısal takfiyeler ve bu yapısal takfiyeler tarafından desteklenen plaklardan meydana gelir. Dolayısıyla plakların analizi gemi yapı tasarımlarında önemli yer tutar.

Gemi yapısal analizlerinde, plaklar genellikle yüzeye dik doğrultuda ve düzgün dağılmış basınç altında çalışan serbest mesnetli elemanlar olarak değerlendirilirler. Diğer yandan gemi formlarının çoğunlukla eğrisel geometrik yapıları nedeniyle plaklar nadir durumlarda düzgün bir dikdörtgen geometriye sahiptirler. Şekilleri ekseriyetle yamuğa yakındır. Bunun ötesinde plaklar, çoğu durumlarda, konveks yük tarafında olacak şekilde, belli bir bükümede sahiptirler.

Teorik olarak düzgün bir dikdörtgen yapıya sahip olmayan ve/veya belli bir bükümü olan kompozit sandviç plakların analizi kapalı analitik yöntemlerle çok sınırlı durumlar haricinde yapılamaz. Bu noktada nümerik yaklaşım yöntemleri tercih edilir. Sonlu elemanlar analiz yöntemi bu tip problemlerin çözümünde en sık başvurulan yöntemdir. Ancak ihtiyaçlar göz önüne alındığında ticari sonlu elemanlar analiz yazılımları hem pahalı hemde kullanım açısından gemi panel çözümleri için zaman alıcı olabilirler.

Bu çalışmanın amacı, Klasik Çok Katmanlı Plak Teorisi türevli kapalı çözüm metodlarının da belirli ölçüde dikdörtgen geometriden sapan veya belirli ölçüde bükümlü sandviç plakların analizinde kullanım alanı bulabileceğini göstermektir. Ancak bu yöntemle üretilen sonuçların hata içereceği unutulmamalıdır. Bu çalışma çerçevesinde geometrik sapma ile ilgili, düzgün dağılmış ve yüzeye dik etkiyen basınç altında çalışan serbest mesnetli kompozit sandviç plaklar için, yöntemin büyük hatalar üretmeye başladığı limit değerleri belirlenmiştir.

1 INTRODUCTION

1.1 Composite Materials

A composite material is a macroscopic combination of two or more physically and chemically distinctive materials. Although the constituents act together, they retain their physical and chemical features within the combination.

Composite materials consist of two main phases which are the matrix and the reinforcement. Matrix is the homogenous separating media in between the reinforcement whereas the reinforcement is generally heterogeneous. Matrix keeps the reinforcement together while providing the load transfer in between the reinforcement. On the other hand, the reinforcement provides the combination with mechanical strength.

With its broad definition composites cover an immense variety of materials, including reinforced concrete, asphalt, metal-metal composites and fiber reinforced thermoset plastics. However, within the scope of this thesis, only advanced fiber reinforced thermoset plastic composites is of concern.

High specific stiffness, high specific strength, availability of constructing tailor made structures (by utilizing various resins and reinforcements and by utilizing the flexibility of orienting fibers etc.) depending on the demands, creep resistance, corrosion resistance, dimensional stability, radar wave transparency, non-magnetic characteristics and low maintenance cost are among the major advantages of advanced fiber reinforced thermoset plastic composites.

For further details references can be consulted.

1.2 Composite Sandwich Structures

Because of their advantages sandwich structures is widely used and the use continues to spread with impetus in variety of industries such as aerospace, aeronautics, civil construction, transport and marine. High strength to weight ratio, high stiffness to weight ratio, higher buckling and wrinkling resistance, higher natural frequencies compared to monocoque thin-walled constructions, excellent thermal insulation characteristics and low maintenance costs are among the major advantages of utilizing sandwich structures in industrial applications where high performance is a leading requirement.

Sandwich panels are considered to be layered mediums consisting of three principal elements. The element between top and bottom elements is called the core and the top and the bottom elements are called the faces. The core material is a thick, light weight but relatively low performing material whereas faces usually consist of thin and high performing materials. The core resists shear, keeps the faces at a certain distance apart and stabilizes the faces against buckling and wrinkling. On the other hand, the faces carry the load similar to an I-beam. [1, 2]

The aim of Sandwich construction is to use the materials with maximum efficiency while the particular attention is paid to reduce the structural weight as much as possible. The two faces are placed at a distance from each other to increase the moment of inertia and thereby the flexural rigidity about the neutral axis of the structure [3].

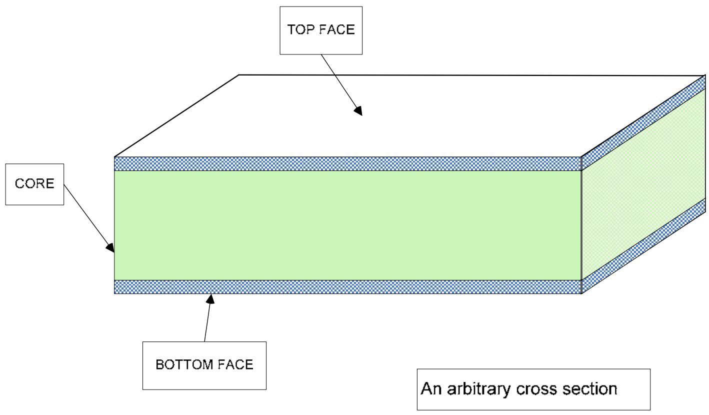

Figure 1.1: Typical Sandwich Structure

There are a vast variety of materials which can be used for the construction of sandwich structures depending on the type of application and the requirements. Metallic or non-metallic materials can be of choice both for the faces and the core. Commonly preferred metallic materials used for the construction of the faces are steel alloys, stainless steel and aluminum. However, preferential non-metallic materials of choice are plywood, asbestos/ cement, veneer, reinforced thermoplastics and fiber composites. On the other hand, generally used materials as cores are metallic or non-metallic corrugated boards, metallic or non-metallic honeycombs, wood and cellular foams. Further information can be found in references [1, 2, 3, 4, 5, 6, 7, 8].

Although there are some earlier examples as reported by Allen [9], the history of sandwich construction in industrial applications is rather recent. The first industrial scale application is considered to be Mosquito Airplane built during the Second World War [10]. However within a considerably very short period of time, with the support by immense academic research especially in the fields of mechanics and material science, application of sandwich structures has gained remarkable importance in variety of areas. Traditionally, aerospace and aeronautical industries have always been the locomotive force behind the spread. Nevertheless, today, there are very successful applications both in the aerospace, marine and transport industries. And most incorporate the novel fiber reinforced advanced composites due to their advantages as sandwich construction materials.

As mentioned, there are numerous successful applications of sandwich structures in the areas of marine industry. Some of these application areas are as follows [7]:

- Small crafts
- Fishing boats
- Passenger and cargo vessels
- Naval vessels
- High performance craft
- Underwater vehicles
- Submarine casings and appendages
- Radomes
- Sonar domes

Figure 1.2: ONUK MRTP33 Fast Attack Craft
Of Yonca-Onuk J.V./ Istanbul Incorporates Advanced Sandwich Construction

Figure 1.3: ONUK MRTP29 Fast Patrol Craft
Of Yonca-Onuk J.V./ Istanbul Incorporates Advanced Sandwich Construction (Craft Operational Under The Command Of Turkish Coast Guard)

Figure 1.4: Visby Class Corvette
of Karlskronavarvet Ab/ Sweden Incorporates Advanced Sandwich Construction

Figure 1.5: US Submarine SSN711
Incorporates Advanced Sandwich Construction.

1.3 Background and Literature Survey

Sandwich construction and the structural analysis of sandwich construction have been a highly active research topic for the last half century.

First papers on the topic started appearing during mid 1940s. These papers were mostly on the principals, advantages and disadvantages of sandwich construction. Garrard [11, 12], Hoff and Mautner [13] were among the authors.

In the end of 1940s, papers dealing with fundamental theoretical approaches, governing differential equations and boundary conditions for bending and buckling, were published. These approaches were based on the membrane theories for small deflection. In this case, the structure was assumed to be membrane and the faces were assumed to be separated by the core which only transmitted the shear stresses through the thickness. However, the assumption was that the faces and the core were of isotropic materials. Reissner [14], Libove and Batdoff [18] and Eringen [16] were among the researchers.

1960s and 1970s witnessed the appearance of the classical text books by Allen [9] and Plantema [10]. These books have been among the most significant resources in the field for many years. In their books the writers dealt with bending, buckling and local instability problems based on the knowledge available at the time.

Most recently, during 1990s, Bitzer [17], Vinson [8] and Zenkert [1, 2] published books on the topic. They supplemented the earlier studies of the contributing researchers and Allen[9] and Plantema [10]. On the other hand, researchers, Corden [18], Marshall [19], Frostig [20], Librescu and Hause [21] contributed to the subject with book sections and articles.

Basically, there are two distinct fundamental approaches used for the modeling of sandwich structures. These are equivalent single layer theories (ESL) and 3-D or Layerwise Theories. The Classical Laminated Plate Theory (CLPT) and First Order Shear Deformation Theory are among the most common ESL theories. ESL theories are based on the plane stress assumption. Thus, by ignoring the transverse shear stresses through the thickness of the structure, ESL theories reduce 3-D problems to 2-D problems. However, although this approach provides with fairly adequate results for thin plates and beams, it generates in accuracies for thick plates or beams and for local structural problems. In contrast to ESL theories, the Layerwise Theories are developed by assuming that the displacement field exhibits C^o-continuity through the laminate thickness with full constitutive relations. Thus, the displacement components are continuous through the laminate thickness but the derivatives of the displacements are discontinuous. [22] Both ESL theories and 3-D or Layerwise Theories are widely used. The choice among them depends on the problem. Though, because solutions involving ESL Theories deal with reduced number of parameters compared to the counterparts they require less computational effort.

Recently, successful ESL approaches were demonstrated by Barut et al [23, 24] based on the work by Cook and Tessler [25]. In their work they introduced the utilization of weighted average displacement functions through the thickness for the analysis of plane sandwich plates. On the other hand, Meunier and Shenoi [26, 27] successfully applied Reddy's [28] refined higher order shear deformation theory based on ESL Theories to solve for the vibration problems of sandwich plates.

Nevertheless, Frostig [20] and Swanson [29] published articles on problems addressing particularly localized structural problems for beams and plates by utilizing Layerwise Theories.

The advantages of advanced anisotropic composite materials over isotropic conventional materials led to an extensive research on mechanical behavior of sandwich construction involving advanced composite materials. Researchers like Pearce and Webber [30, 31], Roa and Meyer-Piening [32] worked on the effects of anisotropy on mechanical behavior of sandwich structures.

However, there is also an extensive research on the design and analysis of sandwich structure by utilizing numerical methods. Dedicated element formulations based on the structural theories mentioned above were developed by researchers. Carrera [33] and Ferreira et al. [34, 35] are among these researchers.

1.4 Outline of the Study

The thesis starts with the fundamentals of the elasticity theory with the objective to define the constitutive relations of fiber reinforced composites. It briefly gives answers to the following questions: What is an orthotropic material? And why fiber reinforced composite materials are assumed to be orthotropic? Obtaining the constitutive relations, the focus is then turned to the mechanical behavior of fiber reinforced composite materials. Based on the findings in this step and based on the Kirchoff Hypothesis, the Classical Lamination Theory is developed. Afterward governing rectangular plate equations are obtained for fiber reinforced laminated plates. Then, the problem of fiber reinforced, simply supported, rectangular laminated composite plates operating under evenly distributed pressure is solved.

All the findings detailed in the theoretical background section of this thesis are utilized to develop a computer code for the solution of the problem of fiber reinforced, simply supported, rectangular laminated composite plates operating under evenly distributed pressure given the material, plate and loading details.

Within the scope of this study the experiment detailed in Appendix M is carried out. The computer code results are compared with the findings of the experiment for code result verification purposes.

However, solutions for various trapezoidal and curved plates are obtained by utilizing Ansys 9.0 of Ansys Inc. FEA tool and these solutions are compared with the corresponding results obtained by utilizing the computer code. At the end, conclusions on the limits of the analytical approach with respect to geometrical deviations are drawn.

On the other hand, supplementary notes are provided at the end of the text in the Appendixes to support the theory. The aim is to give insight into the basics.

2 CONSTITUTIVE RELATIONS of ORTHOTROPIC MATERIALS

2.1 Hooke's Law

Constitutive relations defined by Hooke's law in the general form which represents the behavior of a material showing anisotropy in all directions can be written in explicit form as follows:

Details of the derivations in this section can be found in the references [8, 36, 37, 38]:

$$\begin{pmatrix} \sigma_{11} \\ \sigma_{12} \\ \sigma_{13} \\ \sigma_{21} \\ \sigma_{22} \\ \sigma_{23} \\ \sigma_{31} \\ \sigma_{32} \\ \sigma_{33} \end{pmatrix} = \begin{pmatrix} E_{1111} & E_{1112} & E_{1113} & E_{1121} & E_{1122} & E_{1123} & E_{1131} & E_{1132} & E_{1133} \\ E_{1211} & E_{1212} & E_{1213} & E_{1221} & E_{1222} & E_{1223} & E_{1231} & E_{1232} & E_{1233} \\ E_{1311} & E_{1312} & E_{1313} & E_{1321} & E_{1322} & E_{1323} & E_{1331} & E_{1332} & E_{1333} \\ E_{2111} & E_{2112} & E_{2113} & E_{2121} & E_{2122} & E_{2123} & E_{2131} & E_{2132} & E_{2133} \\ E_{2211} & E_{2212} & E_{2213} & E_{2221} & E_{2222} & E_{2223} & E_{2231} & E_{2232} & E_{2233} \\ E_{2311} & E_{2312} & E_{2313} & E_{2321} & E_{2322} & E_{2323} & E_{2331} & E_{2332} & E_{2333} \\ E_{3111} & E_{3112} & E_{3113} & E_{3121} & E_{3122} & E_{3123} & E_{3131} & E_{3132} & E_{3133} \\ E_{3211} & E_{3212} & E_{3213} & E_{3221} & E_{3222} & E_{3223} & E_{3231} & E_{3232} & E_{3233} \\ E_{3311} & E_{3312} & E_{3313} & E_{3321} & E_{3322} & E_{3323} & E_{3331} & E_{3332} & E_{3333} \end{pmatrix} \cdot \begin{pmatrix} \gamma_{11} \\ \gamma_{12} \\ \gamma_{13} \\ \gamma_{21} \\ \gamma_{22} \\ \gamma_{23} \\ \gamma_{31} \\ \gamma_{32} \\ \gamma_{33} \end{pmatrix}$$

or in closed form; **(2.1)**

$$\sigma_{mn} = \mathrm{E}_{mnpr}\gamma_{pr} \tag{2.2}$$

where; σ_{mn} is the stress tensor, E_{mnpr} is the elasticity tensor and γ_{pr} is the strain tensor.

However, utilizing symmetry conditions of stress and strain tensor components and the first law of thermodynamics, this equation can be simplified such that it shows only the independent components and elasticity constants.

2.2 Material Type Independent Symmetry Conditions (MTISC)

The below symmetry conditions are independent of the material type chosen. These conditions originate from the physical definitions of stress and strain tensors and the requirements of the first law of thermodynamics. [36, 37]

2.2.1 Condition 01 $E_{mnpr} = E_{nmpr}$:

Elasticity tensor has symmetry under the following transformation:

$$E_{mnpr} = E_{nmpr} \tag{2.3}$$

Proof 2-1: $E_{mnpr} = E_{nmpr}$

If we can show that the stress tensor is symmetric, $\sigma_{mn} = \sigma_{nm}$, then we can conclude that the elasticity tensor is also symmetric under the above transformation for instance;

$$\begin{aligned} \sigma_{12} &= E_{1211}\gamma_{11} + E_{1212}\gamma_{12} + E_{1213}\gamma_{13} + E_{1221}\gamma_{21} + E_{1222}\gamma_{22} \\ &+ E_{1223}\gamma_{23} + E_{1231}\gamma_{31} + E_{1232}\gamma_{32} + E_{1233}\gamma_{33} \end{aligned} \tag{2.4}$$

and

$$\begin{aligned} \sigma_{21} &= E_{2111}\gamma_{11} + E_{2112}\gamma_{12} + E_{2113}\gamma_{13} + E_{2121}\gamma_{21} + E_{2122}\gamma_{22} \\ &+ E_{2123}\gamma_{23} + E_{2131}\gamma_{31} + E_{2132}\gamma_{32} + E_{2133}\gamma_{33} \end{aligned} \tag{2.5}$$

The symmetry of stress tensor can be demonstrated as follows [37, 38, 39]:

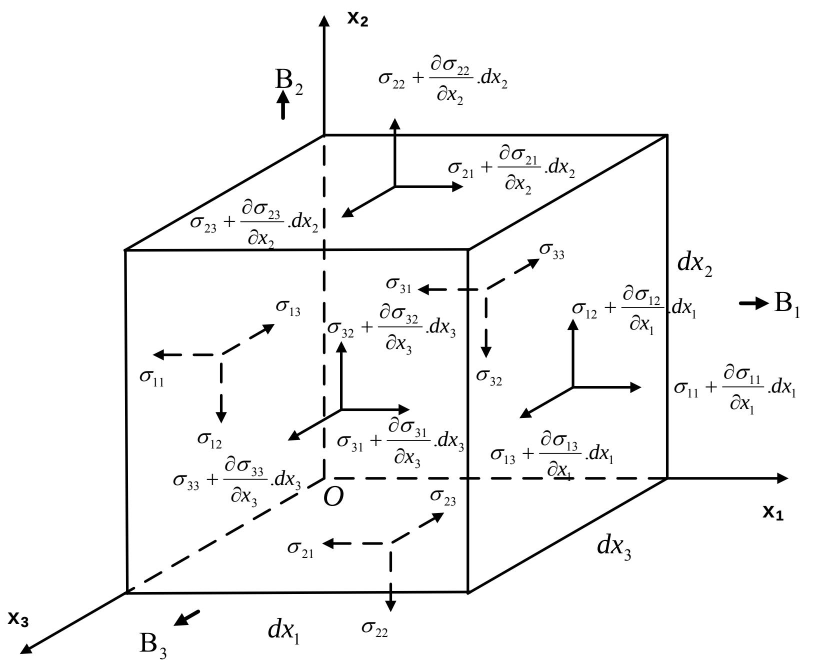

Figure 2.1: Representation of Infinitesimal Cubic Element

Force equilibrium along each principal axis for the cubic element results in;

$$\frac{\partial \sigma_{11}}{\partial x_1} + \frac{\partial \sigma_{21}}{\partial x_2} + \frac{\partial \sigma_{31}}{\partial x_3} + \mathrm{B}_1 = 0 \tag{2.7}$$

$$\frac{\partial \sigma_{12}}{\partial x_1} + \frac{\partial \sigma_{22}}{\partial x_2} + \frac{\partial \sigma_{32}}{\partial x_3} + \mathrm{B}_2 = 0 \tag{2.6}$$

$$\frac{\partial \sigma_{13}}{\partial x_1} + \frac{\partial \sigma_{23}}{\partial x_2} + \frac{\partial \sigma_{33}}{\partial x_3} + \mathrm{B}_3 = 0 \tag{2.8}$$

And moment equilibrium about Ox_3 results in;

$$\begin{aligned}
&-\frac{1}{2}\frac{\partial \sigma_{11}}{\partial x_1}dx_2 + \sigma_{12} + \frac{\partial \sigma_{12}}{\partial x_1}dx_1 - \sigma_{21} - \frac{\partial \sigma_{21}}{\partial x_2}dx_2 \\
&+\frac{1}{2}\frac{\partial \sigma_{22}}{\partial x_2}dx_1 - \frac{1}{2}\frac{\partial \sigma_{31}}{\partial x_3}dx_2 + \frac{1}{2}\frac{\partial \sigma_{32}}{\partial x_3}dx_1 \\
&-\frac{1}{2}\mathrm{B}_1 dx_2 + \frac{1}{2}\mathrm{B}_2 dx_1 = 0
\end{aligned} \tag{2.9}$$

For $dx_1 \to 0$, $dx_2 \to 0$

$$\sigma_{12} = \sigma_{21} \tag{2.10}$$

We can carry out similar moment equilibrium calculations about Ox_1 and Ox_2 to obtain;

$\sigma_{13} = \sigma_{31}$ and $\sigma_{32} = \sigma_{23}$ which shows that the stress tensor is symmetrical.

2.2.2 Condition 02 $E_{mnpr} = E_{mnrp}$:

Elasticity tensor has symmetry under the following transformation:

$$E_{mnpr} = E_{mnrp} \tag{2.11}$$

Proof 2-2: $E_{mnpr} = E_{mnrp}$

Recalling from (2.2); if we can show that the strain tensor is symmetric, $\gamma_{pr} = \gamma_{rp}$, then we can conclude that the material property tensor is also symmetric under the above transformation.

As shown in Appendix C, symmetry of the strain tensor requires that the elasticity tensor is symmetric under the transformation $E_{mnpr} = E_{mnrp}$.

2.2.3 Condition 03 $E_{mnpr} = E_{prmn}$:

Elasticity tensor has symmetry under the following transformation:

$$E_{mnpr} = E_{prnm} \tag{2.12}$$

Proof 2-3: $E_{mnpr} = E_{prnm}$

Using the energy approach we will prove that $E_{mnpr} = E_{prnm}$. [37]

Let U^* be the strain energy density. Then, the work done by the stress components resulting a change $d\gamma_{mn}$ is;

$$\begin{aligned} dU^* &= \sigma_{mn} d\gamma_{mn} \\ &= \sigma_{11} d\gamma_{11} + \sigma_{12} d\gamma_{12} + \sigma_{13} d\gamma_{13} \\ &+\sigma_{21} d\gamma_{21} + \sigma_{22} d\gamma_{22} + \sigma_{23} d\gamma_{23} \\ &+\sigma_{31} d\gamma_{31} + \sigma_{32} d\gamma_{32} + \sigma_{33} d\gamma_{33} \end{aligned} \tag{2.13}$$

equivalently,

$$dU^* = \sigma_{mn} d\gamma_{mn}$$
$$= \sigma_{11} d\gamma_{11} + \sigma_{22} d\gamma_{22} + \sigma_{33} d\gamma_{33}$$
$$+2(\sigma_{12} d\gamma_{12} + \sigma_{13} d\gamma_{13} + \sigma_{23} d\gamma_{23})$$

According to the first law of thermodynamics, if this deformation process is adiabatic then the work done by the stress components should be equal to the stored energy. Normally,

$$d\Psi = dU^* = \sigma_{mn} d\gamma_{mn} \quad \textbf{(2.14)}$$

We know that

$$\sigma_{mn} = E_{mnpr} \gamma_{pr} \quad \textbf{(2.15)}$$

thus,

$$d\Psi = E_{mnpr} \gamma_{pr} d\gamma_{mn} \quad \textbf{(2.16)}$$

Since Ψ is a function of γ_{mn} we can write the total differential as follows:

$$d\Psi = \frac{\partial \Psi}{\partial \gamma_{mn}} d\gamma_{mn} \quad \textbf{(2.17)}$$

hence,

$$\frac{\partial \Psi}{\partial \gamma_{mn}} d\gamma_{mn} = E_{mnpr} \gamma_{pr} d\gamma_{mn} \quad \textbf{(2.18)}$$

$$\Rightarrow \frac{\partial \Psi}{\partial \gamma_{mn}} = E_{mnpr} \gamma_{pr} \quad \textbf{(2.19)}$$

$$\frac{\partial}{\partial \gamma_{pr}} \left(\frac{\partial \Psi}{\partial \gamma_{mn}} \right) = \frac{\partial}{\partial \gamma_{pr}} (E_{mnpr} \gamma_{pr}) \quad \textbf{(2.20)}$$

$$\Rightarrow \frac{\partial}{\partial \gamma_{pr}} \left(\frac{\partial \Psi}{\partial \gamma_{mn}} \right) = E_{mnpr} \quad \textbf{(2.21)}$$

on the other hand,

$$\frac{\partial}{\partial \gamma_{mn}} \left(\frac{\partial \Psi}{\partial \gamma_{pr}} \right) = E_{prmn} \quad \textbf{(2.22)}$$

However, since the above two differential equations are equal:

$$E_{mnpr} = E_{prmn}$$

2.3 Simplified Constitutive Relations Equation Following the Application of MTISC

Constitutive relations equation simplified under the material type independent symmetry conditions $E_{mnpr} = E_{nmpr}$ (condition 01) and $E_{mnpr} = E_{mnrp}$ (condition 02) is as follows: [36]

$$\begin{pmatrix} \sigma_{11} \\ \sigma_{12} \\ \sigma_{13} \\ \sigma_{22} \\ \sigma_{23} \\ \sigma_{33} \end{pmatrix} = \begin{pmatrix} E_{1111} & E_{1112} & E_{1113} & E_{1122} & E_{1123} & E_{1133} \\ E_{1211} & E_{1212} & E_{1213} & E_{1222} & E_{1223} & E_{1233} \\ E_{1311} & E_{1312} & E_{1313} & E_{1322} & E_{1323} & E_{1333} \\ E_{2211} & E_{2212} & E_{2213} & E_{2222} & E_{2223} & E_{2233} \\ E_{2311} & E_{2312} & E_{2313} & E_{2322} & E_{2323} & E_{2333} \\ E_{3311} & E_{3312} & E_{3313} & E_{3322} & E_{3323} & E_{3333} \end{pmatrix} \cdot \begin{pmatrix} \gamma_{11} \\ \gamma_{12} \\ \gamma_{13} \\ \gamma_{22} \\ \gamma_{23} \\ \gamma_{33} \end{pmatrix} \quad \textbf{(2.23)}$$

As can be seen above there are 36 elasticity constants however only 21 of these constants are independent for anisotropic materials. By using the anisotropic material definition, it is assumed that all available materials under the small deformation assumption can be modeled by the Hooke's law.

Moreover, we should apply the condition $E_{mnpr} = E_{nmpr}$ (condition 03) to obtain the representation of the constitutive relations equation with 21 independent constants.

Thus, we finally obtain the below equation: [37]

$$\begin{pmatrix} \sigma_{11} \\ \sigma_{12} \\ \sigma_{13} \\ \sigma_{22} \\ \sigma_{23} \\ \sigma_{33} \end{pmatrix} = \begin{pmatrix} C_{11} & C_{12} & C_{13} & C_{14} & C_{15} & C_{16} \\ C_{12} & C_{22} & C_{23} & C_{24} & C_{25} & C_{26} \\ C_{13} & C_{23} & C_{33} & C_{34} & C_{35} & C_{36} \\ C_{14} & C_{24} & C_{34} & C_{44} & C_{45} & C_{46} \\ C_{15} & C_{25} & C_{35} & C_{45} & C_{55} & C_{56} \\ C_{16} & C_{26} & C_{36} & C_{46} & C_{56} & C_{66} \end{pmatrix} \cdot \begin{pmatrix} \gamma_{11} \\ \gamma_{12} \\ \gamma_{13} \\ \gamma_{22} \\ \gamma_{23} \\ \gamma_{33} \end{pmatrix} \quad \textbf{(2.24)}$$

2.4 Material Type Dependent Symmetry Conditions (MTDSC)

For the details of the derivations in this section references [36, 37, 38, 39] are referred.

2.4.1 Monoclinic Materials

Let's consider a coordinate transformation $\underline{x} \to \underline{x}$, $\underline{y} \to \underline{y}$, $\underline{z} \to -\underline{z}$. This transformation represents a reflection with respect to xy plane. If the material properties are invariant under this transformation than the material is assumed to be monoclinic. A monoclinic material shows symmetry with respect to one plane only.

If the material properties are invariant under this transformation, then;

$$\sigma_{mn}{}' = \sigma_{nm} \text{ (i.e. } \sigma_{11}{}' = \sigma_{11}, \ \sigma_{23}{}' = \sigma_{32}) \tag{2.25}$$

Direction cosine array of this transformation is;

$$\begin{array}{cccc} & \underline{x}_1 & \underline{x}_2 & \underline{x}_3 \\ \underline{y}_1 & 1 & 0 & 0 \\ \underline{y}_2 & 0 & 1 & 0 \\ \underline{y}_3 & 0 & 0 & -1 \end{array}$$

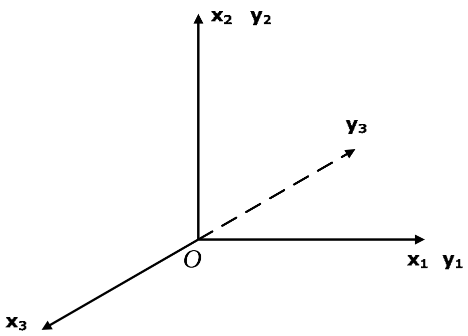

From (G.60);

$$\sigma_{11}{}' = a_{1\alpha} a_{1\beta} \sigma_{\alpha\beta} \tag{2.26}$$

$$\begin{aligned} \Rightarrow \sigma_{11}{}' &= a_{11}a_{11}\sigma_{11} + a_{12}a_{11}\sigma_{21} + a_{13}a_{11}\sigma_{31} \\ &+ a_{11}a_{12}\sigma_{12} + a_{12}a_{12}\sigma_{22} + a_{13}a_{12}\sigma_{32} \\ &+ a_{11}a_{13}\sigma_{13} + a_{12}a_{13}\sigma_{23} + a_{13}a_{13}\sigma_{33} = \sigma_{11} \end{aligned} \tag{2.27}$$

Similarly,

$$\sigma_{22}{}' = \sigma_{22}, \ \sigma_{33}{}' = \sigma_{33} \tag{2.28}$$

and

$$\sigma_{12}{}' = a_{1\alpha} a_{2\beta} \sigma_{\alpha\beta} = \sigma_{12} \tag{2.29}$$

$$\sigma_{13}{}' = a_{1\alpha} a_{3\beta} \sigma_{\alpha\beta} = -\sigma_{13} \tag{2.30}$$

$$\sigma_{23}{}' = a_{2\alpha} a_{3\beta} \sigma_{\alpha\beta} = -\sigma_{23} \tag{2.31}$$

In sum;

$$\sigma_{11}{}' = \sigma_{11} \tag{2.32}$$

$$\sigma_{22}{}' = \sigma_{22} \tag{2.33}$$

$$\sigma_{33}{}' = \sigma_{33} \tag{2.34}$$

$$\sigma_{12}{}' = \sigma_{12} \tag{2.35}$$

$$\sigma_{13}{}' = -\sigma_{13} \tag{2.36}$$

$$\sigma_{23}{}' = -\sigma_{23} \tag{2.37}$$

On the other hand, (F.6) yields;

$$\gamma_{kp}{}' = a_{km} a_{pl} \gamma_{ml} \tag{2.38}$$

$$\Rightarrow \gamma_{11}{}' = a_{1m} a_{1l} \gamma_{ml} = \gamma_{11} \tag{2.39}$$

Similarly,

$$\gamma_{22}{}' = \gamma_{22}\,,\ \gamma_{33}{}' = \gamma_{33} \tag{2.40}$$

and

$$\gamma_{12}{}' = a_{1m} a_{2l} \gamma_{ml} = \gamma_{12} \tag{2.41}$$

$$\gamma_{13}{}' = a_{1m} a_{3l} \gamma_{ml} = -\gamma_{13} \tag{2.42}$$

$$\gamma_{23}{}' = a_{2m} a_{3l} \gamma_{ml} = -\gamma_{23} \tag{2.43}$$

From (D.7);

$$\sigma_{11} = C_{11}\gamma_{11} + C_{12}\gamma_{22} + C_{13}\gamma_{33} + C_{14}\gamma_{12} + C_{15}\gamma_{13} + C_{16}\gamma_{23} \tag{2.44}$$

(2.45)

$$\sigma_{11}' = C_{11}\gamma_{11}' + C_{12}\gamma_{22}' + C_{13}\gamma_{33}' + C_{14}\gamma_{12}' + C_{15}\gamma_{13}' + C_{16}\gamma_{23}'$$

$$\sigma_{11}' = C_{11}\gamma_{11} + C_{12}\gamma_{22} + C_{13}\gamma_{33} + C_{14}\gamma_{12} - C_{15}\gamma_{13} - C_{16}\gamma_{23} \quad \textbf{(2.46)}$$

For $\sigma_{11} = \sigma_{11}'$ to be valid, $C_{15} = C_{16} = 0$ should hold. Similarly,

For $\sigma_{22} = \sigma_{22}'$ to be valid, $C_{25} = C_{26} = 0$ should hold.

For $\sigma_{33} = \sigma_{33}'$ to be valid, $C_{35} = C_{36} = 0$ should hold.

For $\sigma_{12} = \sigma_{12}'$ to be valid, $C_{45} = C_{46} = 0$ should hold.

For $\sigma_{13} = -\sigma_{13}'$ to be valid, $C_{15} = C_{25} = C_{35} = C_{45} = 0$ should hold.

For $\sigma_{23} = -\sigma_{23}'$ to be valid, $C_{16} = C_{26} = C_{36} = C_{46} = 0$ should hold.

Using the above findings, we can obtain the elasticity matrix for a monoclinic material as follows:

$$C_{ij} = \begin{pmatrix} C_{11} & C_{12} & C_{13} & C_{14} & 0 & 0 \\ C_{12} & C_{22} & C_{23} & C_{24} & 0 & 0 \\ C_{13} & C_{23} & C_{33} & C_{34} & 0 & 0 \\ C_{14} & C_{24} & C_{34} & C_{44} & 0 & 0 \\ 0 & 0 & 0 & 0 & C_{55} & C_{56} \\ 0 & 0 & 0 & 0 & C_{56} & C_{66} \end{pmatrix} \quad \textbf{(2.47)}$$

Nevertheless, as can be observed above, monoclinic materials have 13 independent elasticity constants.

On the other hand it should also be remarked that symmetry with respect to x_1x_2 plane requires the effect of shear stresses σ_{13}, σ_{23} and $-\sigma_{13}$, $-\sigma_{23}$ to be the same.

2.4.2 Orthotropic Materials

Orthotropic materials have two orthogonal plane material property symmetries. Having calculated symmetry with respect to x_1x_2 plane for monoclinic materials above, now we can calculate an additional symmetry with respect to for instance x_1x_3 plane which is an orthogonal plane to x_1x_2. This corresponds to a coordinate transformation $\underline{x} \to \underline{x}$, $\underline{y} \to -\underline{y}$, $\underline{z} \to \underline{z}$ in addition to $\underline{x} \to \underline{x}$, $\underline{y} \to \underline{y}$, $\underline{z} \to -\underline{z}$ which was the case for monoclinic materials.

The direction cosine array of this transformation is as follows:

	$\underline{x}_1$	$\underline{x}_2$	$\underline{x}_3$
$\underline{y}_1$	1	0	0
$\underline{y}_2$	0	-1	0
$\underline{y}_3$	0	0	1

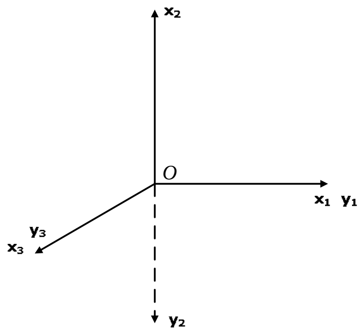

Using the stress and strain transformation laws, we can carry out similar calculations as we did for monoclinic materials to obtain:

$$\sigma_{11}' = \sigma_{11} \qquad \gamma_{11}' = \gamma_{11} \tag{2.48}$$

$$\sigma_{22}' = \sigma_{22} \qquad \gamma_{22}' = \gamma_{22} \tag{2.49}$$

$$\sigma_{33}' = \sigma_{33} \qquad \gamma_{33}' = \gamma_{33} \tag{2.50}$$

$$\sigma_{12}' = -\sigma_{12} \qquad \gamma_{12}' = -\gamma_{12} \tag{2.51}$$

$$\sigma_{13}' = \sigma_{13} \qquad \gamma_{13}' = \gamma_{13} \tag{2.52}$$

$$\sigma_{23}' = -\sigma_{23} \qquad \gamma_{23}' = -\gamma_{23} \tag{2.53}$$

Based on our findings for monoclinic materials and using the above equations, we can obtain the following additional elasticity matrix properties for orthotropic materials:

For $\sigma_{11} = \sigma_{11}'$ to be valid, $C_{14} = 0$ should hold.

For $\sigma_{22} = \sigma_{22}'$ to be valid, $C_{24} = 0$ should hold.

For $\sigma_{33} = \sigma_{33}'$ to be valid, $C_{34} = 0$ should hold.

For $\sigma_{12} = -\sigma_{12}'$ to be valid, $C_{14} = C_{24} = C_{34} = 0$ should hold.

For $\sigma_{13} = \sigma_{13}'$ to be valid, $C_{56} = 0$ should hold.

For $\sigma_{23} = -\sigma_{23}'$ to be valid, $C_{66} \neq 0$ should hold.

Thus, the elasticity matrix for orthotropic materials can be obtained as follows;

$$C_{ij} = \begin{pmatrix} C_{11} & C_{12} & C_{13} & 0 & 0 & 0 \\ C_{12} & C_{22} & C_{23} & 0 & 0 & 0 \\ C_{13} & C_{23} & C_{33} & 0 & 0 & 0 \\ 0 & 0 & 0 & C_{44} & 0 & 0 \\ 0 & 0 & 0 & 0 & C_{55} & 0 \\ 0 & 0 & 0 & 0 & 0 & C_{66} \end{pmatrix} \tag{2.54}$$

However as can be observed above, orthotropic materials have 9 independent elasticity constants.

2.4.3 Tetragonal Materials

In addition to orthotropic material symmetries let us consider an invariant transformation $\underline{x} \to \underline{x}$, $\underline{y} \to -\underline{z}$, $\underline{z} \to \underline{y}$ which requires the material behavior be the same along $\underline{x}_2$ and $\underline{x}_3$ but different along $\underline{x}_1$. This is in fact a -90deg rotation of $x_1 x_2 x_3$ coordinate system about x_1.

The direction cosine array of this transformation is as follows:

	$\underline{x}_1$	$\underline{x}_2$	$\underline{x}_3$
$\underline{y}_1$	1	0	0
$\underline{y}_2$	0	0	-1
$\underline{y}_3$	0	1	0

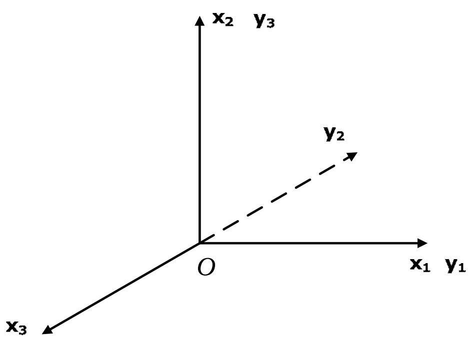

Using the stress and strain transformation laws, as before, we can carry out similar calculations as we did for orthotropic materials to obtain the below expressions:

$$\sigma_{11}{}' = \sigma_{11} \qquad \gamma_{11}{}' = \gamma_{11} \tag{2.55}$$

$$\sigma_{22}{}' = \sigma_{33} \qquad \gamma_{22}{}' = \gamma_{33} \tag{2.56}$$

$$\sigma_{33}{}' = \sigma_{22} \qquad \gamma_{33}{}' = \gamma_{22} \tag{2.57}$$

$$\sigma_{12}{}' = -\sigma_{13} \qquad \gamma_{12}{}' = -\gamma_{13} \tag{2.58}$$

$$\sigma_{13}{}' = \sigma_{12} \qquad \gamma_{13}{}' = \gamma_{12} \tag{2.59}$$

$$\sigma_{23}{}' = -\sigma_{23} \qquad \gamma_{23}{}' = -\gamma_{23} \tag{2.60}$$

Based on our findings for orthotropic materials and using the above expressions, we can obtain the following additional elasticity matrix properties for tetragonal materials:

For $\sigma_{11} = \sigma_{11}{}'$ to be valid, $C_{11} = C_{11}$, $C_{12} = C_{13}$ should hold.

For $\sigma_{22}{}' = \sigma_{33}$ and $\sigma_{33}{}' = \sigma_{22}$ to be valid, $C_{33} = C_{22}$ should hold.

For $\sigma_{12}{}' = -\sigma_{13}$ to be valid, $C_{44} = C_{55}$ should hold.

For $\sigma_{13}{}' = -\sigma_{12}$ to be valid, $C_{44} = C_{55}$ should hold.

For $\sigma_{23}{}' = -\sigma_{23}$ to be valid, $C_{66} = C_{66}$ should hold.

Thus, we can obtain the elasticity matrix for tetragonal materials as follows:

$$C_{ij} = \begin{pmatrix} C_{11} & C_{12} & C_{12} & 0 & 0 & 0 \\ C_{12} & C_{22} & C_{23} & 0 & 0 & 0 \\ C_{12} & C_{23} & C_{22} & 0 & 0 & 0 \\ 0 & 0 & 0 & C_{44} & 0 & 0 \\ 0 & 0 & 0 & 0 & C_{44} & 0 \\ 0 & 0 & 0 & 0 & 0 & C_{66} \end{pmatrix} \qquad \textbf{(2.61)}$$

As can be noticed, tetragonal materials have 6 independent elasticity constants.

2.4.4 Cubic Materials

In addition to tetragonal material symmetries now let us consider an invariant transformation $\underline{x} \to -\underline{y}$, $\underline{y} \to \underline{x}$, $\underline{z} \to \underline{z}$ which requires material behavior be the same along $\underline{x}_1$, $\underline{x}_2$ and $\underline{x}_3$ in addition to tetragonal material behavior characteristics.

The direction cosine array of this transformation is as follows:

$$\begin{array}{cccc} & \underline{x}_1 & \underline{x}_2 & \underline{x}_3 \\ \underline{y}_1 & 1 & 0 & 0 \\ \underline{y}_2 & 0 & 0 & -1 \\ \underline{y}_3 & 0 & 1 & 0 \end{array}$$

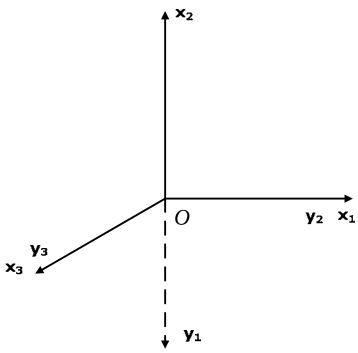

Using the stress and strain transformation laws, as before, we can carry out similar calculations as we did for tetragonal materials to obtain the below expressions:

$$\sigma_{11}' = \sigma_{22} \qquad \gamma_{11}' = \gamma_{22} \qquad \textbf{(2.62)}$$

$$\sigma_{22}' = \sigma_{11} \qquad \gamma_{22}' = \gamma_{11} \qquad \textbf{(2.63)}$$

$$\sigma_{33}' = \sigma_{33} \qquad \gamma_{33}' = \gamma_{33} \qquad \textbf{(2.64)}$$

$$\sigma_{12}' = -\sigma_{12} \qquad \gamma_{12}' = -\gamma_{12} \tag{2.65}$$

$$\sigma_{13}' = -\sigma_{23} \qquad \gamma_{13}' = -\gamma_{23} \tag{2.66}$$

$$\sigma_{23}' = \sigma_{13} \qquad \gamma_{23}' = \gamma_{13} \tag{2.67}$$

Similarly, based on our findings for tetragonal materials and using the above expressions, we can obtain the following additional elasticity matrix properties for cubic materials:

For $\sigma_{11}' = \sigma_{22}$ and $\sigma_{22}' = \sigma_{11}$ to be valid, $C_{11} = C_{22}$, $C_{12} = C_{23}$ should hold.

For $\sigma_{33}' = \sigma_{33}$ to be valid, $C_{12} = C_{23}$ should hold.

For $\sigma_{12}' = -\sigma_{12}$ to be valid, $C_{44} = C_{44}$ should hold.

For $\sigma_{13}' = -\sigma_{23}$ to be valid, $C_{44} = C_{66}$ should hold.

For $\sigma_{23}' = \sigma_{13}$ to be valid, $C_{66} = C_{44}$ should hold.

Thus, the elasticity matrix for orthotropic materials can be obtained as follows;

$$c_{ij} = \begin{pmatrix} c_{11} & c_{12} & c_{12} & 0 & 0 & 0 \\ c_{12} & c_{11} & c_{12} & 0 & 0 & 0 \\ c_{12} & c_{12} & c_{11} & 0 & 0 & 0 \\ 0 & 0 & 0 & c_{44} & 0 & 0 \\ 0 & 0 & 0 & 0 & c_{44} & 0 \\ 0 & 0 & 0 & 0 & 0 & c_{44} \end{pmatrix} \tag{2.68}$$

As can be seen above cubic materials have 3 independent elasticity constants.

2.4.5 Isotropic Materials

An isotropic material requires symmetry with respect to any plane. In addition to cubic material symmetries let us consider a further invariant transformation $x \to x$, $\underline{y} \to \frac{\sqrt{2}}{2}.\underline{y} + \frac{\sqrt{2}}{2}.\underline{z}$, $\underline{z} \to -\frac{\sqrt{2}}{2}.\underline{y} + \frac{\sqrt{2}}{2}.\underline{z}$. This transformation represents a 45deg. rotation about x_1.

The direction cosine array of this transformation is as follows:

$$\begin{array}{cccc} & \underline{x}_1 & \underline{x}_2 & \underline{x}_3 \\ \underline{y}_1 & 1 & 0 & 0 \\ \underline{y}_2 & 0 & \frac{\sqrt{2}}{2} & \frac{\sqrt{2}}{2} \\ \underline{y}_3 & 0 & \frac{\sqrt{2}}{2} & -\frac{\sqrt{2}}{2} \end{array}$$

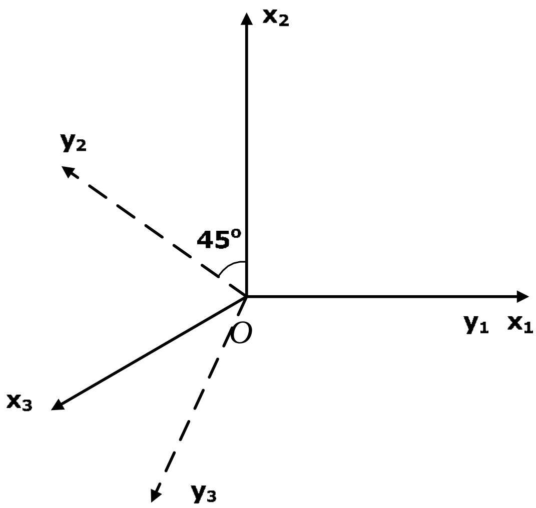

Using the stress and strain transformation laws, we can obtain the below expressions:

$$\sigma_{11}' = \sigma_{11} \qquad \gamma_{11}' = \gamma_{22} \qquad \textbf{(2.69)}$$

$$\sigma_{22}' = \frac{1}{2}\sigma_{22} + \frac{1}{2}\sigma_{33} + \sigma_{23} \qquad \gamma_{22}' = \frac{1}{2}\gamma_{22} + \frac{1}{2}\gamma_{33} + \gamma_{23} \qquad \textbf{(2.70)}$$

$$\sigma_{33}' = \frac{1}{2}\sigma_{22} + \frac{1}{2}\sigma_{33} - \sigma_{23} \qquad \gamma_{33}' = \frac{1}{2}\gamma_{22} + \frac{1}{2}\gamma_{33} - \gamma_{23} \qquad \textbf{(2.71)}$$

$$\sigma_{12}' = \frac{\sqrt{2}}{2}\sigma_{12} + \frac{\sqrt{2}}{2}\sigma_{13} \qquad \gamma_{12}' = \frac{\sqrt{2}}{2}\gamma_{12} + \frac{\sqrt{2}}{2}\gamma_{13} \qquad \textbf{(2.72)}$$

$$\sigma_{13}' = -\frac{\sqrt{2}}{2}\sigma_{12} + \frac{\sqrt{2}}{2}\sigma_{13} \qquad \gamma_{13}' = -\frac{\sqrt{2}}{2}\gamma_{12} + \frac{\sqrt{2}}{2}\gamma_{13} \qquad \textbf{(2.73)}$$

$$\sigma_{23}{}' = -\frac{1}{2}\sigma_{22} + \frac{1}{2}\sigma_{33} \qquad \gamma_{23}{}' = -\frac{1}{2}\gamma_{22} + \frac{1}{2}\gamma_{33} \tag{2.74}$$

Based on the findings for cubic materials and using the above expressions, we can obtain the following additional elasticity matrix properties for isotropic materials:

For $\sigma_{11}{}' = \sigma_{11}$ to be valid, $C_{11} = C_{11}$ should hold.

For $\sigma_{22}{}' = \frac{1}{2}.\sigma_{22} + \frac{1}{2}.\sigma_{33} + \sigma_{23}$ to be valid,

$$\begin{aligned}&\frac{1}{2}C_{12}(\gamma_{11} + \gamma_{33} + \gamma_{11} + \gamma_{22}) + \frac{1}{2}C_{11}(\gamma_{22} + \gamma_{33}) + C_{44}\gamma_{23} \\ &= \frac{1}{2}C_{12}(2\gamma_{11} + \gamma_{22} + \gamma_{33}) + \frac{1}{2}C_{11}(\gamma_{22} + \gamma_{33}) + C_{44}\gamma_{23}\end{aligned} \tag{2.75}$$

Equivalently,

$$\begin{aligned}&\gamma_{11}C_{12} + \gamma_{22}(\frac{1}{2}C_{11} + \frac{1}{2}C_{12}) + \gamma_{33}(\frac{1}{2}C_{11} + \frac{1}{2}C_{12}) + \gamma_{23}(C_{11} - C_{12}) \\ &= \gamma_{11}C_{12} + \gamma_{22}(\frac{1}{2}.C_{11} + \frac{1}{2}C_{12}) + \gamma_{33}(\frac{1}{2}C_{12} + \frac{1}{2}C_{11}) + \gamma_{23}C_{44}\end{aligned} \tag{2.76}$$

should hold. Thus,

$$C_{44} = C_{11} - C_{12}$$

Therefore, we conclude that C_{44} is not independent for isotropic materials.

If we use the engineering definition of strain, $\gamma_{ij} = 2.\varepsilon_{ij} \ (i \neq j)$, then;

$$2C_{44} = C_{11} - C_{12} \tag{2.77}$$

Let $C_{44} = \mu$ and $C_{11} = 2.\mu + \lambda$ where μ and λ are Lamé constants. Hence,

$$C_{11} = 2\mu + \lambda \tag{2.78}$$

Thus, the elasticity matrix for isotropic materials can be obtained as follows;

$$C_{ij} = \begin{pmatrix} \lambda + 2\mu & \lambda & \lambda & 0 & 0 & 0 \\ \lambda & \lambda + 2\mu & \lambda & 0 & 0 & 0 \\ \lambda & \lambda & \lambda + 2\mu & 0 & 0 & 0 \\ 0 & 0 & 0 & \mu & 0 & 0 \\ 0 & 0 & 0 & 0 & \mu & 0 \\ 0 & 0 & 0 & 0 & 0 & \mu \end{pmatrix} \qquad \mathbf{(2.79)}$$

As can be seen, cubic materials have 2 independent elasticity constants.

3 FIBER REINFORCED COMPOSITE MATERIALS

3.1 Stress-Strain Characteristics of Fiber Reinforced Composite Materials

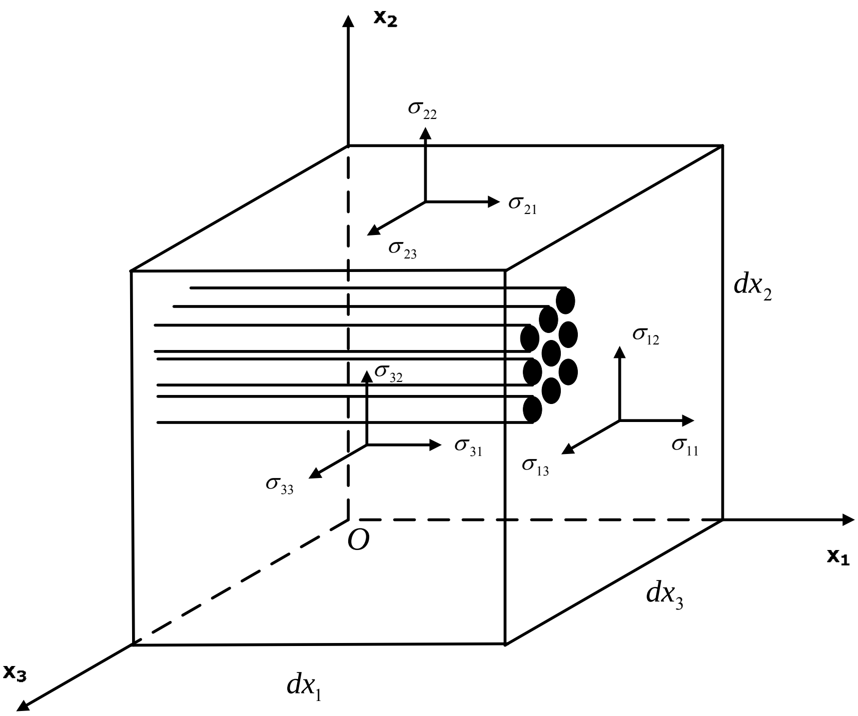

Figure 3.1: Infinitesimal Fiber Reinforced Cubic Element

In the Figure 3.1, we see the representation of an infinitesimal fiber reinforced composite cubic element. [40] We assume that the fibers are aligned with direction 01 ($\underline{x}_1$). Direction 01 is called the fiber direction. Direction 02 (x_2) and direction 03 (x_3) are called the matrix directions.

For the rest of our discussion, to facilitate the ease of our calculations, we will assume that the material properties of different phases of a fiber reinforced material (fiber and the matrix) are combined into one single material and thus we will be arguing about the material properties of this material. [5, 19]

As we have demonstrated earlier, materials having two orthogonal symmetries are called orthotropic materials. [36] Fiber reinforced composite materials show different properties along three mutually perpendicular directions (01, 02, 03). Hence they have two perpendicular planes of symmetry. Therefore, composite materials are assumed to be orthotropic.

3.1.1 Elasticity Constants of Fiber Reinforced Composite Materials

If we omit the Poisson effects for a while, we can write the stress-strain relations of fiber reinforced composite materials, using the engineering definitions of elasticity constants, as follows: [8, 40, 41]

$$\varepsilon_1 = \frac{\sigma_1}{E_1} \qquad \gamma_{12} = \frac{\tau_{12}}{G_{12}} \tag{3.1}$$

$$\varepsilon_2 = \frac{\sigma_2}{E_2} \qquad \gamma_{13} = \frac{\tau_{13}}{G_{13}} \tag{3.2}$$

$$\varepsilon_3 = \frac{\sigma_3}{E_3} \qquad \gamma_{23} = \frac{\tau_{23}}{G_{23}} \tag{3.3}$$

On the other hand, Poisson constants are as follows:

$$\nu_{12} = -\frac{\varepsilon_2}{\varepsilon_1} \qquad \nu_{21} = -\frac{\varepsilon_1}{\varepsilon_2} \tag{3.4}$$

$$\nu_{13} = -\frac{\varepsilon_3}{\varepsilon_1} \qquad \nu_{31} = -\frac{\varepsilon_1}{\varepsilon_3} \tag{3.5}$$

$$\nu_{23} = -\frac{\varepsilon_3}{\varepsilon_2} \qquad \nu_{32} = -\frac{\varepsilon_2}{\varepsilon_3} \tag{3.6}$$

Thus, the stress-strain relations with Poisson effects can be obtained as follows:

$$\varepsilon_1 = \frac{\sigma_1}{E_1} - \nu_{21}\frac{\sigma_2}{E_2} - \nu_{31}\frac{\sigma_3}{E_3} \tag{3.7}$$

$$\varepsilon_2 = \frac{\sigma_2}{E_2} - \nu_{12}\frac{\sigma_1}{E_1} - \nu_{32}\frac{\sigma_3}{E_3} \tag{3.8}$$

$$\varepsilon_3 = \frac{\sigma_3}{E_3} - \nu_{13}\frac{\sigma_1}{E_1} - \nu_{23}\frac{\sigma_2}{E_2} \tag{3.9}$$

$$\gamma_{12} = \frac{\tau_{12}}{G_{12}} \tag{3.10}$$

$$\gamma_{13} = \frac{\tau_{13}}{G_{13}} \tag{3.11}$$

$$\gamma_{23} = \frac{\tau_{23}}{G_{23}} \tag{3.12}$$

Hence,

$$\begin{pmatrix} \varepsilon_1 \\ \varepsilon_2 \\ \varepsilon_3 \\ \gamma_{12} \\ \gamma_{13} \\ \gamma_{23} \end{pmatrix} = \begin{pmatrix} \frac{1}{E_1} & -\frac{\nu_{21}}{E_2} & -\frac{\nu_{31}}{E_3} & 0 & 0 & 0 \\ -\frac{\nu_{12}}{E_1} & \frac{1}{E_2} & -\frac{\nu_{32}}{E_3} & 0 & 0 & 0 \\ -\frac{\nu_{13}}{E_3} & -\frac{\nu_{23}}{E_2} & \frac{1}{E_3} & 0 & 0 & 0 \\ 0 & 0 & 0 & \frac{1}{G_{12}} & 0 & 0 \\ 0 & 0 & 0 & 0 & \frac{1}{G_{13}} & 0 \\ 0 & 0 & 0 & 0 & 0 & \frac{1}{G23} \end{pmatrix} \cdot \begin{pmatrix} \sigma_1 \\ \sigma_2 \\ \sigma_3 \\ \tau_{12} \\ \tau_{13} \\ \tau_{23} \end{pmatrix} \tag{3.13}$$

Or in the short form; [8]

$$\varepsilon_{ij} = S_{ij}\sigma_{ij} \tag{3.14}$$

where, S_{ij} is the compliance matrix and the elasticity constants are called the compliance matrix coefficients.

As can be seen at the first glance from the above equation, there exist 12 elasticity constants. However, as we showed earlier, orthotropic materials have only 9 independent elasticity constants. We will soon prove that only 9 of these 12 constants are independent by utilizing Maxwell-Betti Reciprocal Theorem. [40]

The inverse of the compliance matrix is called the stiffness matrix as defined earlier as follows:

$$\sigma_{ij} = C_{ij}\varepsilon_{ij} \tag{3.15}$$

3.1.2 Relationship among Elasticity Constants

Consider a small volume of fiber reinforced composite material under the following loading condition.

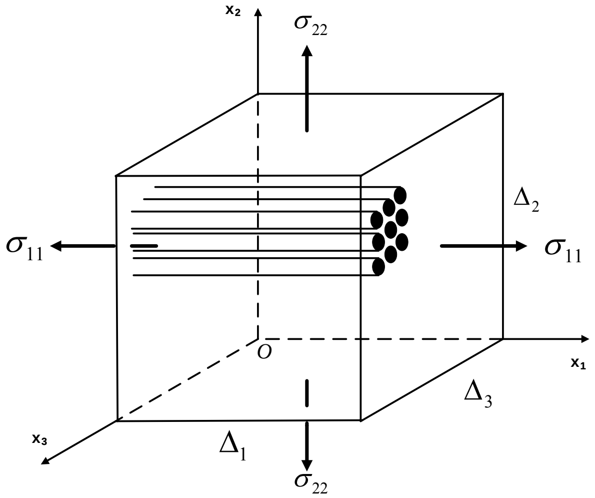

Figure 3.2: Small Volume Of Fiber Reinforced Composite Material

In order to obtain a relationship among elasticity constants, we will apply the Maxwell-Betti Reciprocal Theorem as detailed in [40]. Consider that σ_{22} is initially applied. Following the application of σ_{22}, σ_{11} is applied. The latter causes contraction along direction 2 due to Poisson effects. Thus,

$$\varepsilon_2 = -\varepsilon_1 \nu_{12} \tag{3.16}$$

$$W_{2/1} = F_2 \delta\Delta_2 \tag{3.17}$$

$$F_2 = \sigma_2 \Delta_1 \Delta_3 \tag{3.18}$$

$$\delta\Delta_2 = \Delta_2 \varepsilon_2 \tag{3.19}$$

$$\begin{aligned} \Rightarrow \delta\Delta_2 &= -\Delta_2 \varepsilon_1 \nu_{12} \\ &= -\Delta_2 \frac{\sigma_1}{E_1} \nu_{12} \end{aligned} \tag{3.20}$$

Thus,

$$\begin{aligned} W_{2/1} &= -\sigma_2 \Delta_1 \Delta_2 \Delta_3 \frac{\sigma_1}{E_1} \nu_{12} \\ &= -\frac{\sigma_1 \sigma_2}{E_1} \nu_{12} \Delta V \end{aligned} \tag{3.21}$$

Similarly,

$$W_{1/2} = -\frac{\sigma_1\sigma_2}{E_2}\nu_{21}\Delta V \quad \textbf{(3.22)}$$

From (H.3);

$$W_{2/1} = W_{1/2} \quad \textbf{(3.23)}$$

$$\Rightarrow -\frac{\sigma_1\sigma_2}{E_1}\nu_{12}\Delta V = -\frac{\sigma_1\sigma_2}{E_2}\nu_{21}\Delta V \quad \textbf{(3.24)}$$

$$\Rightarrow \frac{\nu_{12}}{E_1} = \frac{\nu_{21}}{E_2} \quad \textbf{(3.25)}$$

Similarly,

$$\frac{\nu_{13}}{E_1} = \frac{\nu_{31}}{E_3} \quad \textbf{(3.26)}$$

and

$$\frac{\nu_{23}}{E_2} = \frac{\nu_{32}}{E_3} \quad \textbf{(3.27)}$$

Thus, we can confirm that,

$$S_{12} = S_{21} \quad \textbf{(3.28)}$$

$$S_{13} = S_{31} \quad \textbf{(3.29)}$$

$$S_{23} = S_{32} \quad \textbf{(3.30)}$$

3.1.3 Stiffness and Compliance Matrices

We can obtain the stiffness and compliance matrices of fiber reinforced composite materials as follows [22, 40, 41, 42]:

Compliance matrix:

$$S = \begin{pmatrix} S_{11} & S_{12} & S_{13} & 0 & 0 & 0 \\ S_{12} & S_{22} & S_{23} & 0 & 0 & 0 \\ S_{13} & S_{23} & S_{33} & 0 & 0 & 0 \\ 0 & 0 & 0 & S_{44} & 0 & 0 \\ 0 & 0 & 0 & 0 & S_{55} & 0 \\ 0 & 0 & 0 & 0 & 0 & S_{66} \end{pmatrix} \quad \textbf{(3.31)}$$

where,

$$S_{11} = \frac{1}{E_1} \qquad S_{12} = S_{21} = -\frac{\nu_{21}}{E_2} = -\frac{\nu_{12}}{E_1} \qquad S_{13} = S_{31} = -\frac{\nu_{31}}{E_3} = -\frac{\nu_{13}}{E_1}$$

$$S_{22} = \frac{1}{E_2} \qquad S_{23} = S_{32} = -\frac{\nu_{32}}{E_3} = -\frac{\nu_{23}}{E_2} \quad \textbf{(3.32)}$$

$$S_{33} = \frac{1}{E_1}$$

$$S_{44} = \frac{1}{G_{12}} \qquad S_{55} = \frac{1}{G_{13}} \qquad S_{66} = \frac{1}{G_{23}}$$

Stiffness matrix:

$$C = \begin{pmatrix} C_{11} & C_{12} & C_{13} & 0 & 0 & 0 \\ C_{12} & C_{22} & C_{23} & 0 & 0 & 0 \\ C_{13} & C_{23} & C_{33} & 0 & 0 & 0 \\ 0 & 0 & 0 & C_{44} & 0 & 0 \\ 0 & 0 & 0 & 0 & C_{55} & 0 \\ 0 & 0 & 0 & 0 & 0 & C_{66} \end{pmatrix} \quad \textbf{(3.33)}$$

$$C_{11} = \frac{S_{22}S_{33} - S_{23}S_{23}}{S} \quad \textbf{(3.34)}$$

$$C_{12} = C_{21} = \frac{S_{23}S_{13} - S_{12}S_{33}}{S} \quad \textbf{(3.35)}$$

$$C_{13} = C_{31} = \frac{S_{12}S_{23} - S_{13}S_{22}}{S} \quad \textbf{(3.36)}$$

$$C_{22} = \frac{S_{11}S_{33} - S_{13}S_{13}}{S}$$

$$C_{23} = C_{32} = \frac{S_{12}S_{13} - S_{11}S_{23}}{S} \quad \textbf{(3.37)}$$

$$C_{33} = \frac{S_{11}S_{22} - S_{12}S_{12}}{S} \quad \textbf{(3.39)}$$

$$C_{44} = \frac{1}{S_{44}} \quad \textbf{(3.40)}$$

$$C_{55} = \frac{1}{S_{55}} \quad \textbf{(3.41)}$$

$$C_{66} = \frac{1}{S_{66}} \quad \textbf{(3.42)}$$

$$S = S_{11}S_{22}S_{33} + 2S_{12}S_{13}S_{23} - S_{11}S_{23}{}^{2} - S_{22}S_{13}{}^{2} - S_{12}{}^{2}S_{33} \quad \textbf{(3.43)}$$

3.2 Plane Stress Assumption

Basically, there are two fundamental assumptions in the analysis of composite materials which simplify the problems to a manageable level. [40]

1. Equivalent material assumption:

   Matrix and fiber come together to form an equivalent material. Therefore, the problem of dealing with each of the ingredients separately and dealing with the interaction among them is eliminated.

2. Plane stress assumption:

   Fiber reinforced composite materials are generally utilized in structures where at least one dimension is considerably small compared to the other dimensions of the structure. Therefore, stress components out of plane are negligible compared to stress components in plane, i.e., $\sigma_1 \neq 0$, $\sigma_2 \neq 0$, $\tau_{12} \neq 0$ whereas $\sigma_3 = \tau_{13} = \tau_{23}$ =0.

Inaccuracies of plane stress assumptions can be summarized as follows [5, 22, 40]:

1. Even if the thickness is small, theoretically, $\sigma_3 \neq 0$, $\tau_{13} \neq 0, \tau_{23} \neq 0$. Therefore, there is always an inaccuracy. However, this inaccuracy is important in some particular problems:

   - Near the structure edge where delamination generally starts. By nature, the analysis of delamination phenomenon is three dimensional. σ_3, τ_{13} and τ_{23} play the major roles during delamination.

   - At particular locations where there are defects between layers being prone to delamination.

   - Problems involving the interactions between two layers.

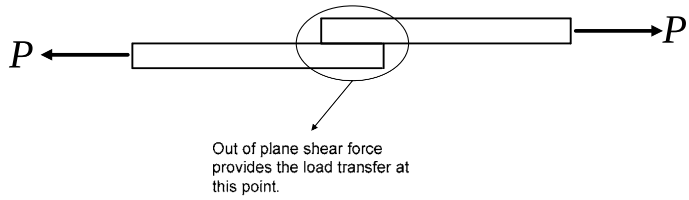

Figure 3.3: Interaction Between Two Layers

   - In problems where for instance a plate is supported by a stiffener.

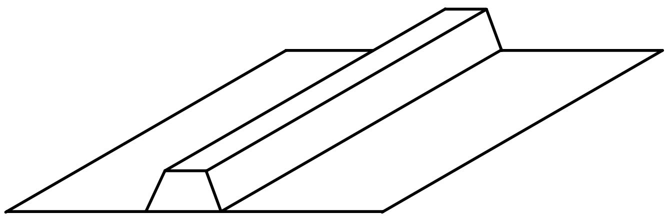

Figure 3.4: Plate Stiffened With A Stiffener

   Plane stress assumption may not introduce much inaccuracy away form the stiffener. However, around the stiffener region, because load is transferred from the plate to the stiffener by out of plane stresses, the assumption is prone to generate inaccuracies.

   - Problems involving local gradual layer terminations.

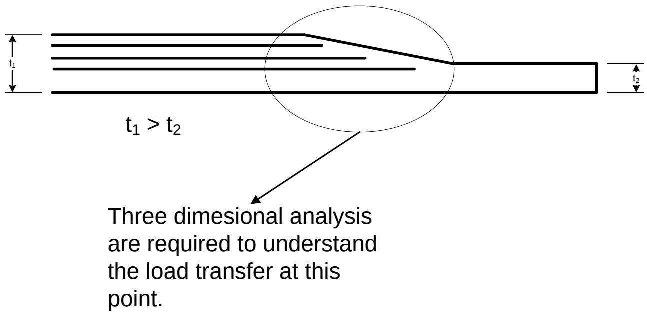

Figure 3.5: Local Gradual Layer Termination Detail

There are also two major points to be considered when using the plane stress assumption:

- Assure that out of plane stresses are really small compared to in plane stresses.
- Due to Poisson effects, ε_3 is not zero although $\sigma_3 \cong 0$.

3.2.1 Stress-Strain Relations for Plane Stress

Details of the derivations in this section can be found in the references [5, 22, 36, 37, 40, 43].

We have showed earlier that for plane stress case,

$$\sigma_3 = \tau_{13} = \tau_{23} = 0 \tag{3.44}$$

Thus,

$$\begin{pmatrix} \varepsilon_{11} \\ \varepsilon_{22} \\ \varepsilon_{33} \\ \gamma_{23} \\ \gamma_{13} \\ \gamma_{12} \end{pmatrix} = \begin{pmatrix} S_{11} & S_{12} & S_{13} & 0 & 0 & 0 \\ S_{12} & S_{22} & S_{23} & 0 & 0 & 0 \\ S_{13} & S_{23} & S_{33} & 0 & 0 & 0 \\ 0 & 0 & 0 & S_{44} & 0 & 0 \\ 0 & 0 & 0 & 0 & S_{55} & 0 \\ 0 & 0 & 0 & 0 & 0 & S_{66} \end{pmatrix} \cdot \begin{pmatrix} \sigma_1 \\ \sigma_2 \\ 0 \\ 0 \\ 0 \\ \tau_{12} \end{pmatrix} \tag{3.45}$$

We should note that $\gamma_{23} = \gamma_{13} = 0$.

However,

$$\varepsilon_3 = S_{13}\sigma_1 + S_{23}\sigma_2 \tag{3.46}$$

Despite $\varepsilon_3 \neq 0$, in plane stress case, we can obtain the reduced compliance matrix as follows:

$$\begin{pmatrix} \varepsilon_1 \\ \varepsilon_2 \\ \gamma_{12} \end{pmatrix} = \begin{pmatrix} S_{11} & S_{12} & 0 \\ S_{12} & S_{22} & 0 \\ 0 & 0 & S_{66} \end{pmatrix} \cdot \begin{pmatrix} \sigma_1 \\ \sigma_2 \\ \tau_{12} \end{pmatrix} \quad \textbf{(3.47)}$$

Material constants are as per (3.32).

Nevertheless, the inverse form of the stress-strain relation is given by;

$$\sigma = C\varepsilon \quad \textbf{(3.48)}$$

$$\begin{pmatrix} \sigma_1 \\ \sigma_2 \\ 0 \\ 0 \\ 0 \\ \tau_{12} \end{pmatrix} = \begin{pmatrix} C_{11} & C_{12} & C_{13} & 0 & 0 & 0 \\ C_{12} & C_{22} & C_{23} & 0 & 0 & 0 \\ C_{13} & C_{23} & C_{33} & 0 & 0 & 0 \\ 0 & 0 & 0 & C_{44} & 0 & 0 \\ 0 & 0 & 0 & 0 & C_{55} & 0 \\ 0 & 0 & 0 & 0 & 0 & C_{66} \end{pmatrix} \begin{pmatrix} \varepsilon_{11} \\ \varepsilon_{22} \\ \varepsilon_{33} \\ 0 \\ 0 \\ \gamma_{12} \end{pmatrix} \quad \textbf{(3.49)}$$

Since $\sigma_3 = 0$,

$$\sigma_3 = 0 = C_{13}\varepsilon_1 + C_{23}\varepsilon_2 + C_{33}\varepsilon_3 \quad \textbf{(3.50)}$$

Hence,

$$\varepsilon_3 = -\frac{C_{13}}{C_{33}}\varepsilon_1 - \frac{C_{23}}{C_{33}}\varepsilon_2 \quad \textbf{(3.51)}$$

On the other hand,

$$\sigma_1 = C_{11}\varepsilon_1 + C_{12}\varepsilon_2 + C_{13}\varepsilon_3 \quad \textbf{(3.52)}$$

$$\sigma_2 = C_{12}\varepsilon_1 + C_{22}\varepsilon_2 + C_{23}\varepsilon_3 \quad \textbf{(3.53)}$$

$$\Rightarrow \sigma_1 = \varepsilon_1(C_{11} - \frac{C_{13}^{\ 2}}{C_{33}}) + \varepsilon_2(C_{12} - \frac{C_{13}C_{23}}{C_{33}}) \quad \textbf{(3.54)}$$

Similarly,

$$\sigma_2 = \varepsilon_1 (C_{12} - \frac{C_{13}C_{23}}{C_{33}}) + \varepsilon_2 (C_{22} - \frac{{C_{23}}^2}{C_{33}}) \tag{3.55}$$

Let us define the below constants:

$$Q_{11} = C_{11} - \frac{{C_{13}}^2}{C_{33}} \tag{3.56}$$

$$Q_{12} = C_{12} - \frac{C_{13}C_{23}}{C_{33}} \tag{3.57}$$

$$Q_{22} = C_{22} - \frac{{C_{23}}^2}{C_{33}} \tag{3.58}$$

$$Q_{66} = C_{66} \tag{3.59}$$

Thus we can obtain the reduced stiffness matrix as follows:

$$\begin{pmatrix} \sigma_1 \\ \sigma_2 \\ \tau_{12} \end{pmatrix} = \begin{pmatrix} Q_{11} & Q_{12} & 0 \\ Q_{12} & Q_{22} & 0 \\ 0 & 0 & Q_{66} \end{pmatrix} . \begin{pmatrix} \varepsilon_1 \\ \varepsilon_2 \\ \gamma_{12} \end{pmatrix} \tag{3.60}$$

Or, since $C_{red} = S_{red}^{-1}$,

$$\left. \begin{aligned} Q_{11} &= \frac{S_{22}}{S_{11}S_{22} - {S_{12}}^2} \\ Q_{12} &= -\frac{S_{12}}{S_{11}S_{22} - {S_{12}}^2} \\ Q_{22} &= \frac{S_{11}}{S_{11}S_{22} - {S_{12}}^2} \\ Q_{66} &= \frac{1}{S_{66}} \end{aligned} \right| \tag{3.61}$$

3.2.2 Strain-Stress Relations for Plane Stress in a Global Coordinate System

Consider the below transformation in rectangular cartesian coordinate system:

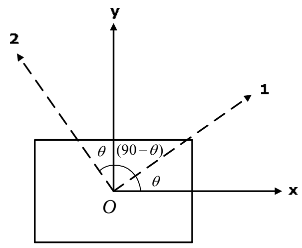

Figure 3.6: Plane Stress Case Coordinate Transformation

Coordinate system xy is referred to global coordinate system. On the other hand, coordinate system 12 is referred to material coordinate system. In this case, both global and material coordinate systems are chosen as rectangular Cartesian coordinate systems. However, they could have been chosen to be any orthogonal coordinate systems.

This transformation corresponds to:

	x	y	z
1	$\cos(\theta)$	$\cos(90-\theta)$	$\cos(90)$
2	$\cos(90+\theta)$	$\cos(\theta)$	$\cos(90)$
3	$\cos(90)$	$\cos(90)$	$\cos(0)$

Or,

	x	y	z
1	$\cos(\theta)$	$\sin(\theta)$	0
2	$-\sin(\theta)$	$\cos(\theta)$	0
3	0	0	1

It is wise to note here that, due to the existence of Sine function, angle θ will always be defined within the range $-90^o \leq \theta \leq 90^o$ this point forward.

Let us define;

$$m = \cos(\theta) \tag{3.62}$$

$$n = \sin(\theta) \tag{3.63}$$

By utilizing (G.60), we can obtain the transformed stresses as follows:

$$\sigma_1 = m^2\sigma_x + n^2\sigma_y + 2mn\tau_{xy} \tag{3.64}$$

Equivalently,

$$\sigma_1 = \cos^2(\theta)\sigma_x + \sin^2(\theta)\sigma_y + 2\cos(\theta)\sin(\theta)\tau_{xy} \tag{3.65}$$

Similarly,

$$\sigma_2 = n^2\sigma_x + m^2\sigma_y - 2mn\tau_{xy} \tag{3.66}$$

Equivalently,

$$\sigma_2 = \sin^2(\theta)\sigma_x + \cos^2(\theta)\sigma_y - 2\cos(\theta)\sin(\theta)\tau_{xy} \tag{3.67}$$

$$\sigma_3 = \sigma_z$$

$$\tau_{12} = -mn\sigma_x + mn\sigma_y + (m^2 - n^2)\tau_{xy} \tag{3.68}$$

that becomes,

$$\tau_{12} = \cos(\theta)\sin(\theta)(\sigma_y - \sigma_x) + \left[\cos^2(\theta) - \sin^2(\theta)\right]\tau_{xy} \tag{3.69}$$

$$\tau_{13} = m\tau_{xz} + n\tau_{yz} \tag{3.70}$$

which is equivalent to,

$$\tau_{13} = \cos(\theta)\tau_{xz} + \sin(\theta)\tau_{yz} \tag{3.71}$$

and

$$\tau_{23} = -n\tau_{xz} + m\tau_{yz} \tag{3.72}$$

that reduces to,

$$\tau_{23} = -\sin(\theta)\tau_{xz} + \cos(\theta)\tau_{yz} \tag{3.73}$$

As we have stated before for plane stress case;

$$\sigma_3 = \tau_{13} = \tau_{23} = 0 \tag{3.74}$$

Thus, from (3.68), (3.42) and (3.73);

$$\sigma_z = 0 \tag{3.75}$$

$$\cos(\theta)\tau_{xz} = -\sin(\theta)\tau_{yz} \tag{3.76}$$

$$\sin(\theta)\tau_{xz} = \cos(\theta)\tau_{yz} \tag{3.77}$$

From (3.80),

$$\tau_{xz} = -\frac{\sin(\theta)}{\cos(\theta)}\tau_{yz} \tag{3.78}$$

Thus, from (3.77) and (3.78)

$$\sin(\theta)\left[-\frac{\sin(\theta)}{\cos(\theta)}\tau_{yz}\right] = \cos(\theta)\tau_{yz} \tag{3.79}$$

This requires that

$-\sin^2(\theta) = \cos^2(\theta)$ should hold. However, since this is not a valid condition, we can conclude that $\tau_{xz} = \tau_{yz} = 0$.

Hence, the stress transformation equations for plane stress case can be summarized as follows:

$$\sigma_1 = \cos^2(\theta)\sigma_x + \sin^2(\theta)\sigma_y + 2\cos(\theta)\sin(\theta)\tau_{xy} \tag{3.80}$$

$$\sigma_2 = \sin^2(\theta)\sigma_x + \cos^2(\theta)\sigma_y - 2\cos(\theta)\sin(\theta).\tau_{xy} \tag{3.81}$$

$$\tau_{12} = \cos(\theta).\sin(\theta)(\sigma_y - \sigma_x) + \left[\cos^2(\theta) - \sin^2(\theta)\right]\tau_{xy} \tag{3.82}$$

However, with some mathematical manipulations these equations can be obtained in a more familiar form;

$$\sigma_1 = (\frac{\sigma_x + \sigma_y}{2}) + (\frac{\sigma_x - \sigma_y}{2})\cos(2\theta) + \sin(2\theta)\tau_{xy} \tag{3.83}$$

$$\sigma_1 = (\frac{\sigma_x + \sigma_y}{2}) - (\frac{\sigma_x - \sigma_y}{2})\cos(2\theta) - \sin(2\theta)\tau_{xy} \quad \textbf{(3.84)}$$

$$\tau_{12} = -(\frac{\sigma_x - \sigma_y}{2})\sin(2\theta) + \tau_{xy}\cos(2\theta) \quad \textbf{(3.85)}$$

(3.81), (3.80) and (3.82) can also be written in matrix form as follows:

$$\begin{pmatrix} \sigma_1 \\ \sigma_2 \\ \tau_{12} \end{pmatrix} = \begin{pmatrix} m^2 & n^2 & 2mn \\ n^2 & m^2 & -2mn \\ -mn & mn & m^2 - n^2 \end{pmatrix} \cdot \begin{pmatrix} \sigma_x \\ \sigma_y \\ \tau_{xy} \end{pmatrix} \quad \textbf{(3.86)}$$

Where,

$$T_\sigma = \begin{pmatrix} m^2 & n^2 & 2mn \\ n^2 & m^2 & -2mn \\ -mn & mn & m^2 - n^2 \end{pmatrix} \quad \textbf{(3.87)}$$

T_σ is the stress transformation matrix for the plane stress case.

The inverse of this matrix is;

$$T_\sigma^{-1} = \begin{pmatrix} m^2 & n^2 & -2mn \\ n^2 & m^2 & 2mn \\ mn & -mn & m^2 - n^2 \end{pmatrix} \quad \textbf{(3.88)}$$

Thus,

$$\begin{pmatrix} \sigma_x \\ \sigma_y \\ \tau_{xy} \end{pmatrix} = \begin{pmatrix} m^2 & n^2 & -2mn \\ n^2 & m^2 & 2mn \\ mn & -mn & m^2 - n^2 \end{pmatrix} \cdot \begin{pmatrix} \sigma_1 \\ \sigma_2 \\ \tau_{12} \end{pmatrix} \quad \textbf{(3.89)}$$

Utilizing the above transformation, any in plane stress state can be transformed into global stress state. We will use this feature later in our calculations to provide with a consistent calculation basis.

Recall from (G.60) that,

$$\sigma_{\gamma\delta}' = a_{\gamma\alpha} a_{\delta\beta} \sigma_{\alpha\beta} \quad \textbf{(3.90)}$$

And recall from (F.6) that,

$$\overline{\gamma}_{kp} = \gamma_{ml} a_{\bar{k}m} a_{\bar{p}l} \quad \textbf{(3.91)}$$

Notice the similarity between the two equations given above. This similarity clearly leads to the below conclusions:

$$\varepsilon_1 = \cos^2(\theta)\varepsilon_x + \sin^2(\theta)\varepsilon_y + 2\cos(\theta)\sin(\theta)\varepsilon_{xy} \quad \textbf{(3.92)}$$

$$\varepsilon_2 = \sin^2(\theta)\varepsilon_x + \cos^2(\theta)\varepsilon_y - 2\cos(\theta)\sin(\theta)\varepsilon_{xy} \quad \textbf{(3.93)}$$

$$\varepsilon_3 = \varepsilon_z \quad \textbf{(3.94)}$$

$$\varepsilon_{12} = -\cos(\theta)\sin(\theta)\varepsilon_x + \cos(\theta)\sin(\theta)\varepsilon_y + \left[\cos^2(\theta) - \sin^2(\theta)\right]\varepsilon_{xy} \quad \textbf{(3.95)}$$

$$\varepsilon_{13} = \cos(\theta)\varepsilon_{xz} + \sin(\theta)\varepsilon_{yz} \quad \textbf{(3.96)}$$

$$\varepsilon_{23} = -\sin(\theta)\varepsilon_{xz} + \cos(\theta)\varepsilon_{yz} \quad \textbf{(3.97)}$$

Notice ε is used instead of γ above for shear strains. Although both ε and γ define strain at a point, they are different in magnitude. The relationship among them is as follows:

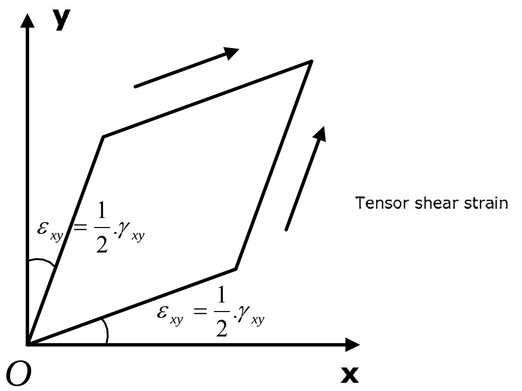

Figure 3.7: Tensor Shear Strain

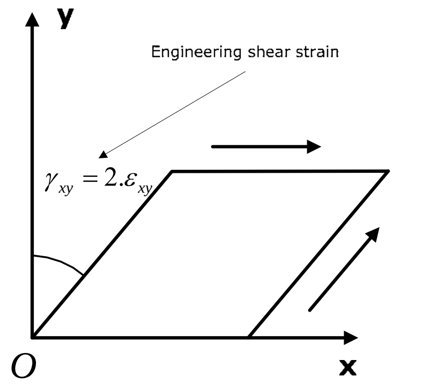

Figure 3.8: Engineering Shear Strain

In shear strain tensor definition, it is assumed that horizontal edges of the element also rotate as the vertical edges. Whereas in engineering shear strain definition it is assumed that shear deformation is coupled with rigid body rotation. Therefore, horizontal edges remain horizontal after the deformation.

The above given two assumptions provide identical results. However, one should notice from the figures that,

$$\varepsilon_{12} = \frac{1}{2}\gamma_{12} \tag{3.98}$$

$$\varepsilon_{13} = \frac{1}{2}\gamma_{13} \tag{3.99}$$

$$\varepsilon_{23} = \frac{1}{2}\gamma_{23} \tag{3.100}$$

Now, one can use the engineering strain in transformation equations:

$$\varepsilon_1 = \cos^2(\theta)\varepsilon_x + \sin^2(\theta)\varepsilon_y + 2\cos(\theta)\sin(\theta)\frac{1}{2}\gamma_{xy} \tag{3.101}$$

$$\varepsilon_2 = \sin^2(\theta)\varepsilon_x + \cos^2(\theta)\varepsilon_y - 2\cos(\theta)\sin(\theta)\frac{1}{2}\gamma_{xy} \tag{3.102}$$

$$\varepsilon_3 = \varepsilon_z \tag{3.103}$$

$$\frac{1}{2}\gamma_{12} = -\cos(\theta)\sin(\theta)\varepsilon_x + \cos(\theta)\sin(\theta)\varepsilon_y + \left[\cos^2(\theta) - \sin^2(\theta)\right]\frac{1}{2}\gamma_{12} \tag{3.104}$$

$$\frac{1}{2}\gamma_{13} = \cos(\theta)\frac{1}{2}\gamma_{13} + \sin(\theta)\frac{1}{2}\gamma_{23} \tag{3.105}$$

$$\frac{1}{2}\gamma_{23} = -\sin(\theta)\frac{1}{2}\gamma_{13} + \cos(\theta)\frac{1}{2}\gamma_{23} \tag{3.106}$$

For the plane stress case, recalling from our earlier findings, $\tau_{13} = \tau_{23} = 0$ and $\gamma_{13} = \gamma_{23} = 0$.

Thus,

$$\frac{1}{2}\cos(\theta)\gamma_{xz} + \frac{1}{2}\sin(\theta)\gamma_{yz} = 0 \tag{3.107}$$

and

$$-\frac{1}{2}\sin(\theta)\gamma_{xz} + \frac{1}{2}\cos(\theta)\gamma_{yz} = 0 \tag{3.108}$$

that yields,

$$\gamma_{yz} = \frac{\sin(\theta)}{\cos(\theta)}\cdot_{xz} \quad \textbf{(3.109)}$$

By substituting into the previous equation, we get

$$\frac{1}{2}\cos(\theta)\gamma_{xz} + \frac{1}{2}\sin(\theta)\frac{\sin(\theta)}{\cos(\theta)}\gamma_{xz} = 0 \quad \textbf{(3.110)}$$

which requires that, $\cos^2(\theta) + \sin^2(\theta) = 0$ should hold. However, this is not a valid condition. Thus, one can conclude that,

$$\gamma_{xz} = \gamma_{yz} = 0 \quad \textbf{(3.111)}$$

On the other hand, (3.45) yields

$$\begin{aligned}\varepsilon_3 &= S_{13}\sigma_1 + S_{23}\sigma_2 \\ &= S_{13}\left[\cos^2(\theta)\sigma_x + \sin^2(\theta)\sigma_y + 2\cos(\theta)\sin(\theta)\tau_{xy}\right] \\ &+ S_{23}\left[\sin^2(\theta)\sigma_x + \cos^2(\theta)\sigma_y - 2\cos(\theta)\sin(\theta)\tau_{xy}\right]\end{aligned} \quad \textbf{(3.112)}$$

Hence,

$$\begin{aligned}\varepsilon_3 &= \left[(S_{13}\cos^2(\theta) + S_{23}\sin^2(\theta)\right]\sigma_x + \left[S_{13}\sin^2(\theta) + S_2\cos^2(\theta)\right]\sigma_y \\ &+ 2(S_{13} - S_{23})\cos(\theta)\sin(\theta)\tau_{xy}\end{aligned} \quad \textbf{(3.113)}$$

Notice that ε_3 is dependent on shear stress τ_{xy}. We know that for orthotropic materials $S_{13} \neq S_{23}$ this implies that in-plane shear stress τ_{xy} causes out-of-plane extension/ contraction for orthotropic materials. This phenomenon is not a case for isotropic materials since for isotropic materials $S_{13} = S_{23}$ and thus $S_{13} - S_{23} = 0$.

For plane stress case, we can summarize the strain transformation equations as follows:

$$\varepsilon_1 = \cos^2(\theta)\varepsilon_x + \sin^2(\theta)\varepsilon_y + 2\cos(\theta)\sin(\theta)\frac{1}{2}\gamma_{xy} \quad \textbf{(3.114)}$$

$$\varepsilon_2 = \sin^2(\theta)\varepsilon_x + \cos^2(\theta)\varepsilon_y - 2\cos(\theta)\sin(\theta)\frac{1}{2}\gamma_{xy} \quad \textbf{(3.115)}$$

$$\gamma_{12} = -2\cos(\theta)\sin(\theta)\varepsilon_x + 2\cos(\theta)\sin(\theta)\varepsilon_y + \left[\cos^2(\theta) - \sin^2(\theta)\right]\gamma_{12} \quad \textbf{(3.116)}$$

The above equations can be written in matrix form as follows:

$$\begin{pmatrix} \varepsilon_1 \\ \varepsilon_2 \\ \gamma_{12} \end{pmatrix} = \begin{bmatrix} \cos^2(\theta) & \sin^2(\theta) & \cos(\theta)\sin(\theta) \\ \sin^2(\theta) & \cos^2(\theta) & -\sin(\theta)\cos(\theta) \\ -2\cos(\theta)\sin(\theta) & 2\cos(\theta)\sin(\theta) & \left[\cos^2(\theta) - \sin^2(\theta)\right] \end{bmatrix} \cdot \begin{pmatrix} \varepsilon_x \\ \varepsilon_y \\ \gamma_{xy} \end{pmatrix} \quad \textbf{(3.117)}$$

that becomes,

$$\begin{pmatrix} \varepsilon_1 \\ \varepsilon_2 \\ \gamma_{12} \end{pmatrix} = \begin{bmatrix} m^2 & n^2 & mn \\ n^2 & m^2 & -mn \\ -2mn & 2mn & \left(m^2 - n^2\right) \end{bmatrix} \cdot \begin{pmatrix} \varepsilon_x \\ \varepsilon_y \\ \gamma_{xy} \end{pmatrix} \quad \textbf{(3.118)}$$

where,

$$T_\varepsilon = \begin{bmatrix} m^2 & n^2 & mn \\ n^2 & m^2 & -mn \\ -2mn & 2mn & \left(m^2 - n^2\right) \end{bmatrix} \quad \textbf{(3.119)}$$

T_ε is the strain transformation matrix for the plane stress case. The inverse of this matrix is as follows:

$$T_\varepsilon^{-1} = \begin{bmatrix} m^2 & n^2 & -mn \\ n^2 & m^2 & mn \\ 2mn & -2mn & \left(m^2 - n^2\right) \end{bmatrix} \quad \textbf{(3.120)}$$

Hence,

$$\begin{pmatrix} \varepsilon_x \\ \varepsilon_y \\ \gamma_{xy} \end{pmatrix} = \begin{bmatrix} m^2 & n^2 & -mn \\ n^2 & m^2 & mn \\ 2mn & -2mn & \left(m^2 - n^2\right) \end{bmatrix} \cdot \begin{pmatrix} \varepsilon_1 \\ \varepsilon_2 \\ \gamma_{12} \end{pmatrix} \quad \textbf{(3.121)}$$

3.2.3 Transformed Reduced Compliance Matrix

From (3.47), we know that

$$\begin{pmatrix} \varepsilon_1 \\ \varepsilon_2 \\ \gamma_{12} \end{pmatrix} = \begin{pmatrix} S_{11} & S_{12} & 0 \\ S_{12} & S_{22} & 0 \\ 0 & 0 & S_{66} \end{pmatrix} \cdot \begin{pmatrix} \sigma_1 \\ \sigma_2 \\ \tau_{12} \end{pmatrix} \quad \textbf{(3.122)}$$

However, by utilizing (3.86) and (3.118), we can obtain the below expression:

$$T_{\varepsilon}\begin{pmatrix}\varepsilon_x\\ \varepsilon_y\\ \gamma_{xy}\end{pmatrix}=\begin{pmatrix}S_{11} & S_{12} & 0\\ S_{12} & S_{22} & 0\\ 0 & 0 & S_{66}\end{pmatrix}T_{\sigma}\begin{pmatrix}\sigma_x\\ \sigma_y\\ \tau_{xy}\end{pmatrix} \tag{3.123}$$

Thus,

$$T_{\varepsilon}^{-1}\cdot T_{\varepsilon}\begin{pmatrix}\varepsilon_x\\ \varepsilon_y\\ \gamma_{xy}\end{pmatrix}=T_{\varepsilon}^{-1}\begin{pmatrix}S_{11} & S_{12} & 0\\ S_{12} & S_{22} & 0\\ 0 & 0 & S_{66}\end{pmatrix}T_{\sigma}\begin{pmatrix}\sigma_x\\ \sigma_y\\ \tau_{xy}\end{pmatrix} \tag{3.124}$$

Hence,

$$\begin{pmatrix}\varepsilon_x\\ \varepsilon_y\\ \gamma_{xy}\end{pmatrix}=\overline{S}\begin{pmatrix}\sigma_x\\ \sigma_y\\ \tau_{xy}\end{pmatrix} \tag{3.125}$$

where,

$$\overline{S}=\begin{pmatrix}\overline{S}_{11} & \overline{S}_{12} & \overline{S}_{16}\\ \overline{S}_{12} & \overline{S}_{22} & \overline{S}_{26}\\ \overline{S}_{16} & \overline{S}_{26} & \overline{S}_{66}\end{pmatrix}=T_{\varepsilon}^{-1}\begin{pmatrix}S_{11} & S_{12} & 0\\ S_{12} & S_{22} & 0\\ 0 & 0 & S_{66}\end{pmatrix}T_{\sigma} \tag{3.126}$$

The components of reduced compliance matrix are as follows [22, 40]

$$\begin{aligned}
\overline{S}_{11} &= m^4S_{11}+m^2n^2(2S_{12}+S_{66})+n^4S_{22}\\
\overline{S}_{12} &= m^2n^2(S_{11}+S_{22}-S_{66})+(m^4+n^4)S_{12}\\
\overline{S}_{16} &= m^3n(2S_{11}-2S_{12}-S_{66})+n^3m(S_{12}-2S_{22}+S_{66})\\
\overline{S}_{22} &= n^4S_{11}+m^2n^2(2S_{12}+S_{66})+m^4S_{22}\\
\overline{S}_{26} &= n^3m(2S_{11}-2S_{12}-S_{66})+m^3n(2S_{12}-2S_{22}+S_{66})\\
\overline{S}_{66} &= 2m^2n^2(2S_{11}-4S_{12}+2S_{22}-S_{66})+(m^4+n^4)S_{66}
\end{aligned} \tag{3.127}$$

(3.125) implies that through the existence of $\overline{S}_{16}$ and $\overline{S}_{26}$, shear stresses cause extensional strains and normal stresses cause shear strains. This is a major difference of orthogonal materials compared to metals. This phenomenon in composites is called shear-extension coupling.

Also note that for $\theta = 0$, this happens when the material coordinate system coincides with the global coordinate system;

$$\left.\begin{array}{lll} \overline{S}_{11} = S_{11} & \overline{S}_{22} = S_{22} & \overline{S}_{66} = S_{66} \\ \overline{S}_{12} = S_{12} & \overline{S}_{26} = 0 & \\ \overline{S}_{16} = 0 & & \end{array}\right| \tag{3.128}$$

That means for $\theta = 0$, the compliance matrix and transformed compliance matrix coincide.

3.2.4 Transformed Reduced Stiffness Matrix

From (3.60) we know that

$$\begin{pmatrix} \sigma_1 \\ \sigma_2 \\ \tau_{12} \end{pmatrix} = \begin{pmatrix} Q_{11} & Q_{12} & 0 \\ Q_{12} & Q_{22} & 0 \\ 0 & 0 & Q_{66} \end{pmatrix} \cdot \begin{pmatrix} \varepsilon_1 \\ \varepsilon_2 \\ \gamma_{12} \end{pmatrix} \tag{3.129}$$

However, by utilizing (3.86) and (3.118), we can obtain the below expression:

$$T_\sigma \begin{pmatrix} \sigma_x \\ \sigma_y \\ \tau_{xy} \end{pmatrix} = \begin{pmatrix} Q_{11} & Q_{12} & 0 \\ Q_{12} & Q_{22} & 0 \\ 0 & 0 & Q_{66} \end{pmatrix} T_\varepsilon \begin{pmatrix} \varepsilon_x \\ \varepsilon_y \\ \gamma_{xy} \end{pmatrix} \tag{3.130}$$

Thus,

$$T_\sigma^{-1} \cdot T_\sigma \begin{pmatrix} \sigma_x \\ \sigma_y \\ \tau_{xy} \end{pmatrix} = T_\sigma^{-1} \begin{pmatrix} Q_{11} & Q_{12} & 0 \\ Q_{12} & Q_{22} & 0 \\ 0 & 0 & Q_{66} \end{pmatrix} T_\varepsilon \begin{pmatrix} \varepsilon_x \\ \varepsilon_y \\ \gamma_{xy} \end{pmatrix} \tag{3.131}$$

Hence,

$$\begin{pmatrix} \sigma_x \\ \sigma_y \\ \tau_{xy} \end{pmatrix} = \overline{Q} \begin{pmatrix} \varepsilon_x \\ \varepsilon_y \\ \gamma_{xy} \end{pmatrix} \tag{3.132}$$

where,

$$\overline{Q} = \begin{pmatrix} \overline{Q}_{11} & \overline{Q}_{12} & \overline{Q}_{16} \\ \overline{Q}_{12} & \overline{Q}_{22} & \overline{Q}_{26} \\ \overline{Q}_{16} & \overline{Q}_{26} & \overline{Q}_{66} \end{pmatrix} = T_\sigma \begin{pmatrix} Q_{11} & Q_{12} & Q_{16} \\ Q_{12} & Q_{22} & Q_{26} \\ Q_{16} & Q_{26} & Q_{66} \end{pmatrix} T_\varepsilon \quad \textbf{(3.133)}$$

After some mathematical manipulations, the components of reduced stiffness matrix can be obtained as follows [22, 40]:

$$\left.\begin{aligned}
\overline{Q}_{11} &= m^4 Q_{11} + 2m^2 n^2 (Q_{12} + 2Q_{66}) + n^4 Q_{22} \\
\overline{Q}_{12} &= m^2 n^2 (Q_{11} + Q_{22} - 4Q_{66}) + (m^4 + n^4) Q_{12} \\
\overline{Q}_{16} &= m^3 n (Q_{11} - Q_{12} - 2Q_{66}) + n^3 m (Q_{12} - Q_{22} + 2Q_{66}) \\
\overline{Q}_{22} &= n^4 Q_{11} + 2m^2 n^2 (Q_{12} + 2Q_{66}) + m^4 Q_{22} \\
\overline{Q}_{26} &= n^3 m (Q_{11} - Q_{12} - 2Q_{66}) + m^3 n (Q_{12} - Q_{22} + 2Q_{66}) \\
\overline{Q}_{66} &= m^2 n^2 (Q_{11} - 2Q_{12} + Q_{22} - 2Q_{66}) + (m^4 + n^4) Q_{66}
\end{aligned}\right| \quad \textbf{(3.134)}$$

3.2.5 Reduced Stiffness and Compliance Matrices in Terms of Engineering Constants

From (3.32), we know that

$$S_{11} = \frac{1}{E_1} \quad \textbf{(3.135)}$$

$$S_{12} = -\frac{\nu_{12}}{E_1} \quad \textbf{(3.136)}$$

$$S_{22} = \frac{1}{E_2} \quad \textbf{(3.137)}$$

$$S_{66} = \frac{1}{G_{12}} \quad \textbf{(3.138)}$$

$$\overline{S} = \begin{pmatrix} \frac{1}{E_1} & -\frac{\nu_{12}}{E_1} & 0 \\ -\frac{\nu_{12}}{E_1} & \frac{1}{E_2} & 0 \\ 0 & 0 & \frac{1}{G_{12}} \end{pmatrix} \quad \textbf{(3.139)}$$

On the other hand, utilizing the equations (3.34) to (3.43), we can obtain the stiffness matrix coefficients in terms of engineering constants [40, 42]

$$C_{11} = \frac{-E_2 E_1^{2} + \nu_{23}^{2} E_3 E_1^{2}}{C} \quad \textbf{(3.140)}$$

$$C_{12} = -\frac{(\nu_{12} E_2 + \nu_{23} \nu_{13} E_3) E_1 E_2}{C} \quad \textbf{(3.141)}$$

$$C_{13} = \frac{-(\nu_{12} \nu_{23} + \nu_{13}) E_1 E_2 E_3}{C} \quad \textbf{(3.142)}$$

$$C_{22} = \frac{-E_1 E_2^{2} + \nu_{13}^{2} E_3}{C} \quad \textbf{(3.143)}$$

$$C_{23} = -\frac{(\nu_{23} E_1 + \nu_{13} \nu_{12} E_2) E_2 E_3}{C} \quad \textbf{(3.144)}$$

$$C_{33} = \frac{(-E_1 + \nu_{12}^{2} E_2) E_2 E_3}{C} \quad \textbf{(3.145)}$$

$$C_{44} = G_{23} \quad \textbf{(3.146)}$$

$$C_{55} = G_{13} \quad \textbf{(3.147)}$$

$$C_{66} = G_{12} \quad \textbf{(3.148)}$$

and

$$C = -E_1 E_2 + E_1 \nu_{23}^{2} E_3 + \nu_{12}^{2} E_2^{2} + 2\nu_{12} E_2 \nu_{23} \nu_{13} E_3 + \nu_{13}^{2} E_2 E_3 \quad \textbf{(3.149)}$$

However, by incorporating (3.32) and (3.60), we can obtain the reduced stiffness matrix coefficients in terms of engineering material constants as follows:

$$\left.\begin{aligned} Q_{11} &= \frac{E_1}{1-\nu_{12}\nu_{21}} \\ Q_{12} &= \frac{\nu_{21} E_1}{1-\nu_{21}\nu_{12}} \\ Q_{22} &= \frac{E_2}{1-\nu_{12}\nu_{21}} \\ Q_{66} &= G_{12} \end{aligned}\right| \quad \textbf{(3.150)}$$

Now, we can derive the transformed reduced compliance and stiffness matrices.

By utilizing (3.32) and (3.127), we can obtain the reduced compliance matrix coefficients in terms of engineering constants as follows [40]:

$$\overline{S}_{11} = \frac{m^4E_2G_{12} - 2n^2m^2\nu_{12}E_2G_{12} + n^4E_1G_{12} + n^2m^2E_1E_2}{E_1E_2G_{12}} \quad \textbf{(3.151)}$$

$$\overline{S}_{12} = -\frac{(-n^2m^2E_2G_{12} - n^2m^2E_1G_{12} + n^2m^2E_1E_2 + m^4\nu_{12}E_2G_{12} + n^4\nu_{12}E_2G_{12})}{E_1E_2G_{12}} \quad \textbf{(3.152)}$$

$$\overline{S}_{16} = \frac{mn(2m^2E_2G_{12} + 2m^2E_2\nu_{12}G_{12} - m^2E_2E_1 - n^2\nu_{12}E_2G_{12} - 2n^2E_1G_{12} + n^2E}{E_1E_2G_{12}} \quad \textbf{(3.153)}$$

$$\overline{S}_{22} = \frac{n^4E_2G_{12} - 2m^2n^2\nu_{12}E_2G_{12} + n^2m^2E_1.E_2 + m^4E_1G_{12}}{E_1E_2G_{12}} \quad \textbf{(3.154)}$$

$$\overline{S}_{26} = \frac{n^3m(2 + 2\nu_{12} - \frac{E_1}{G_{12}}) - m^3n(2\nu_{12} + 2\frac{E_1}{E_2} - \frac{E_1}{G_{12}})}{E_1} \quad \textbf{(3.155)}$$

$$\overline{S}_{66} = \frac{4n^2m^2E_2G_{12} + 8n^2m^2\nu_{12}E_2G_{12} + 4n^2m^2E_1G_{12} - 2n^2m^2E_1E_2 + m^4E_1E_2 + n^4E_1E_2}{E_1E_2G_{12}} \quad \textbf{(3.156)}$$

On the other hand, incorporating (3.134) and (3.150), we can obtain the below reduced stiffness matrix coefficients.

$$\overline{Q}_{11} = -\frac{(-4E_2m^2n^2G_{12}\nu_{12}{}^2 + 2E_2m^2n^2E_1\nu_{12} + E_1E_2n^4 + 4n^2m^2E_1G_{12} + m^4E_1{}^2)}{-E_1 + \nu_{12}{}^2E_2} \quad \textbf{(3.157)}$$

$$\overline{Q}_{12} = -\frac{(4E_2m^2n^2G_{12}\nu_{12}{}^2 + E_2\nu_{12}E_1m^4 + E_2\nu_{12}E_1n^4 + n^2m^2E_1E_2 - 4n^2m^2E_1G_{12} + m^2n^2E_1{}^2)}{-E_1 + \nu_{12}{}^2E_2} \quad \textbf{(3.158)}$$

$$\overline{Q}_{16} = \frac{-mn(-2E_2\nu_{12}{}^2n^2G_{12} + E_2\nu_{12}{}^2m^2G_{12} - E_2\nu_{12}m^2E_1}{-E_1 + \nu_{12}{}^2E_2} + \frac{E_2\nu_{12}n^2E_1 - n^2E_1E_2 + 2n^2E_1G_{12} - m^2G_{12}E_1 + m^2E_1}{-E_1 + \nu_{12}{}^2E_2} \quad \textbf{(3.159)}$$

$$\overline{Q}_{22} = -\frac{(-4E_2m^2n^2G_{12}\nu_{12}{}^2 + 2E_2m^2n^2E_1\nu_{12} + E_1E_2m^4 + 4n^2m^2E_1G_{12} + n^4E_1}{-E_1 + \nu_{12}{}^2E_2} \quad \textbf{(3.160)}$$

$$\overline{Q}_{26}=\frac{(2E_2\nu_{12}{}^2m^2G_{12}-2E_2\nu_{12}{}^2n^2G_{12}+E_2\nu_{12}nE_1{}^2-E_2\nu_{12}m^2E_1)mn}{-E_1+\nu_{12}{}^2E_2}$$

$$+\frac{(m^2E_1E_2-n^2E_1{}^2-2m^2G_{12}E_1+2n^2E_1G_{12})nm}{-E_1+\nu_{12}{}^2E_2} \tag{3.161}$$

$$\overline{Q}_{66}=-\frac{-E_2\nu_{12}{}^2n^2G_{12}-E_2\nu_{12}{}^2m^2G_{12}+2E_2m^2n^2G_{12}\nu_{12}{}^2-2E_2m^2n^2E_1\nu_{12}}{-E_1+\nu_{12}{}^2E_2}$$

$$-\frac{n^2m^2E_1E_2-2n^2m^2E_1G_{12}+m^2G_{12}E_1+n^2E_1G_{12}+m^2n^2E_1{}^2}{-E_1+\nu_{12}{}^2E_2} \tag{3.162}$$

Obviously, when the material coordinate system coincides with the global coordinate system, i.e. $\theta=0$;

$$\overline{S}=S=\begin{pmatrix}\frac{1}{E_1} & -\frac{\nu_{12}}{E_1} & 0\\ -\frac{\nu_{12}}{E_1} & \frac{1}{E_2} & 0\\ 0 & 0 & \frac{1}{G_{12}}\end{pmatrix} \tag{3.163}$$

$$\overline{Q}=Q=\begin{pmatrix}\frac{E_1}{1-\nu_{12}\nu_{21}} & \frac{E_1\nu_{21}}{1-\nu_{12}\nu_{21}} & 0\\ \frac{E_1\nu_{21}}{1-\nu_{12}\nu_{21}} & \frac{E_2}{1-\nu_{12}\nu_{21}} & 0\\ 0 & 0 & G_{12}\end{pmatrix} \tag{3.164}$$

4 CLASSICAL LAMINATION THEORY

4.1 Coordinate System and Layer Nomenclature

4.1.1 Coordinate System

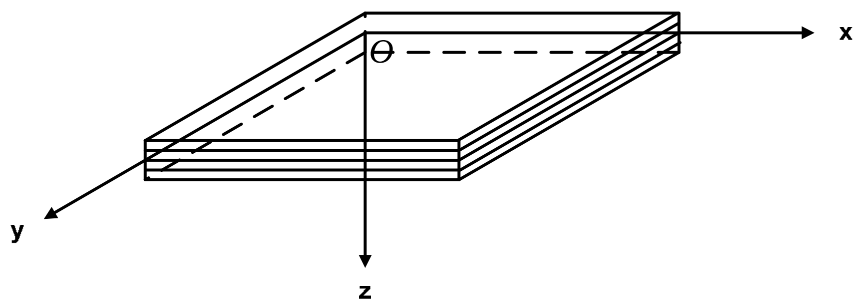

Figure 4.1: Plate Coordinate System

As can be noticed from Figure 4.1, the *xy* plane coincides with the geometrical midplane of the plate. [22, 44]

4.1.2 Laminate Nomenclature

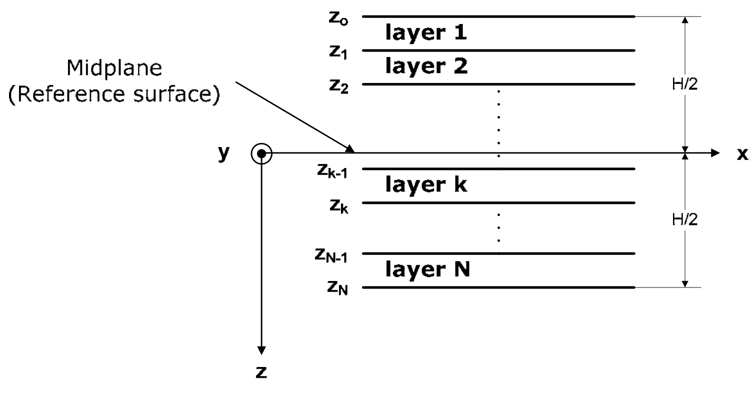

Figure 4.2: Layer Nomenclature

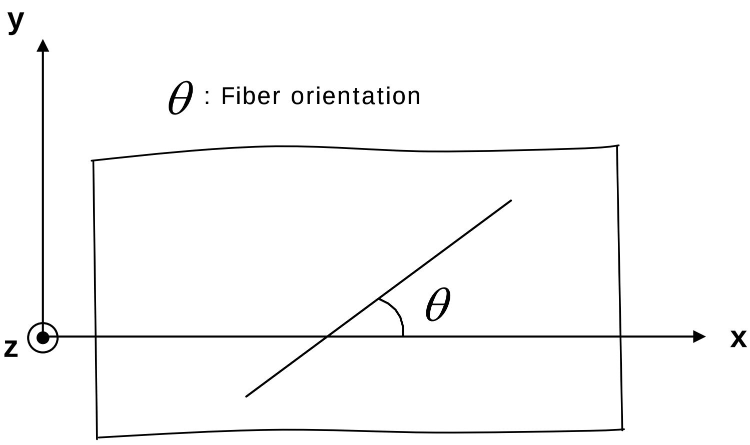

Figure 4.3: Fiber Orientation

In order to identify the total number and fiber orientation of various layers, we will use the below notations [40]:

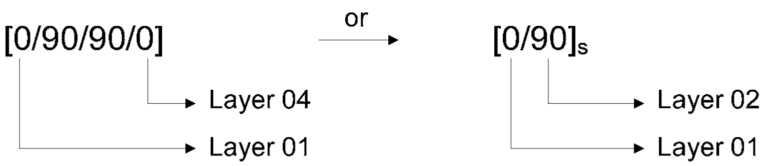

Figure 4.4: Laminate Notation 01

Numbers between brackets represents fiber angles (orientations) with respect to $+x$ as defined in Figure 4.3. On the other hand, the subscript "s" on the right hand side represents symmetry with respect to the midplane of the plate.

However, the below notation is generally preferred in the literature:

$$[0/90/90/0] \xrightarrow{\text{or}} [0/90/90/0]_s$$

Figure 4.5: Laminate Notation 02

When there is no subscript, the meaning is that there is symmetry with respect to the midplane of the plate. Nevertheless, if the total number of layers is only four, then the below notation should be used:

$$[0/90/90/0]_T$$

Figure 4.6: Laminate Notation 03

The subscript "T" means that the total number of layers is four in this case.

On the other hand,

$$[+45/-45/0/+45/-45/0/0/-45/+45/0/-45/+45]_T$$

$$\xrightarrow{\text{or}} [+45/-45/0/+45/-45/0]_s$$

$$\xrightarrow{\text{or}} [\pm 45/0/\pm 45/0]_s$$

$$\xrightarrow{\text{or}} [(\pm 45/0)_s]_s$$

Figure 4.7: Laminate Notation

4.2 Kirchoff Hypothesis

4.2.1 Assumptions of Kirchoff Hypothesis

The coordinate system and loading conditions are defined as follows:

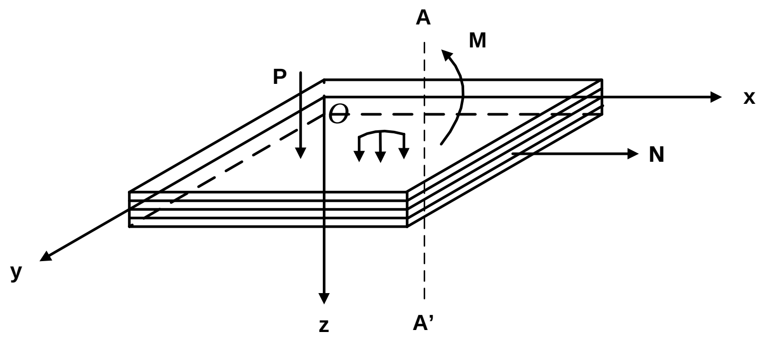

Figure 4.8: Kirchoff Hypothesis 01, Plate Loading Conditions

Cross section of a laminate on *xz* plane is as follows:

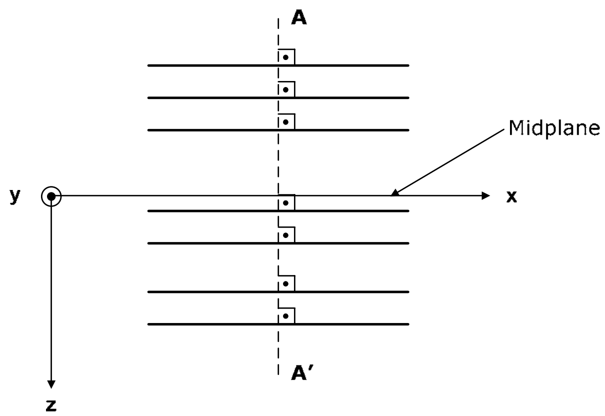

Figure 4.9: Kirchoff Hypothesis 02

Cross section of a laminate on yz plane is as follows:

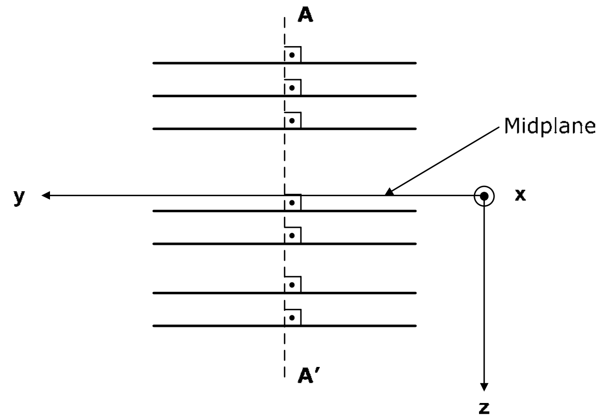

Figure 4.10: Kirchoff Hypothesis 03

1. All layers are perfectly bonded.
2. There is no slippage between layers.
3. Straight lines (AA') remain straight after deformation. These lines only rotate and translate during deformation.
4. Straight lines do not change their lengths.
5. A point on the neutral surface does not change its position during deformation.

Notice that assumption 4 ignores ε_z. The magnitude of ε_z is important for increased laminate thicknesses. However, when thicknesses are small (i.e. shell elements) ε_z can be easily ignored.

On the other hand, for the Kirchoff hypothesis assumptions to be valid; deformations will be small and, in addition to this, through thickness dimension of the plate will also be small compared with the other plate dimensions. This is also known as the shell assumption.

4.2.2 Bending of a Plate

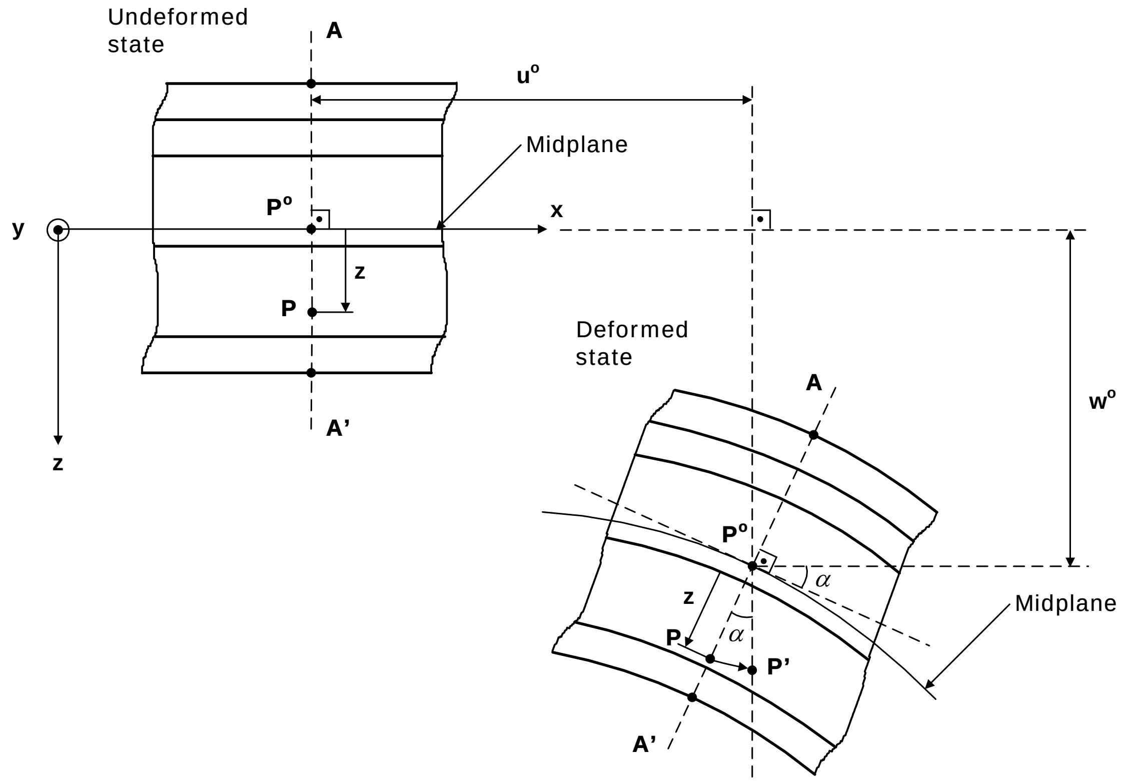

Figure 4.11: Bending of a Plate.

Figure notes:

1. P^o is an arbitrary point on the reference surface. The superscript is used to indicate any relation to the reference surface.
2. P is an arbitrary point on AA' having the distance z from P^o.
3. u^o is the horizontal displacement of P^o along x axis.
4. w^o is the vertical displacement of P^o along y axis.
5. As stated earlier, according to the Kirchoff hypothesis, $|AA'|$ does not change during deformation; thus, $|P^oP|$ does not change as well.

We assume that under the loading conditions defined in Figure 4.8, a plate deforms as in Figure 4.11 fulfilling the Kirchoff Hypothesis assumptions. Thus,

$$\alpha = \frac{\partial w^o(x,y)}{\partial x}$$ (refer to Appendix H for the underlying logic)

Thus the distance $|PP'|$ can be obtained as $z\dfrac{\partial w^{o}(x,y)}{\partial x}$

Since it is assumed that $\dfrac{\partial w^{o}(x,y)}{\partial x} \approx 0$ (small deformation assumption), PP' is assumed to be a line segment.

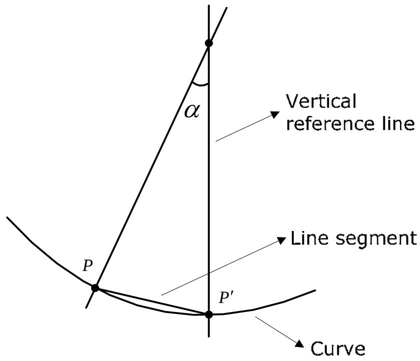

Length of the arc approaches to the length of the line segment PP'.

Figure 4.12: Line Segment Assumption

Therefore, the total displacement of P along x can be obtained as follows:

$$u(x,y,z) = u^{o}(x,y) - z\frac{\partial w^{o}(x,y)}{\partial x} \tag{4.1}$$

The term $u^{o}(x,y)$ is the extensional effect and the term $z\dfrac{\partial w^{o}(x,y)}{\partial x}$ is the rotational effect.

Similarly, the total displacement of P along y and along z are as follows respectively:

$$v(x,y,z) = v^{o}(x,y) - z\frac{\partial w^{o}(x,y)}{\partial y} \tag{4.2}$$

$$w(x,y,z) = w^{o}(x,y) \tag{4.3}$$

There is, however, a contradiction in (4.3). The right hand side of the equation is independent of z whereas the left hand side of the equation is depending on z. The reason for this phenomenon is that the position of P is depended on x, y, z whereas the vertical deformation function is only depending on x and y. This implies that the vertical displacement of P is the same as the vertical displacement of P^{o}. This assumption is the reason why through thickness strains are ignored. Thus, we can intuitively think that Kirchoff Hypothesis is valid for the small deformation of thin plates.

4.3 Laminate Strains

We can obtain the laminate strains by substituting (4.1) to (4.3) into (J.17) and (J.18). Thus,

$$\varepsilon_x = \frac{\partial u^o(x,y)}{\partial x} - z\frac{\partial^2 w^o}{\partial x^2} \tag{4.4}$$

$$\varepsilon_y = \frac{\partial v^o(x,y)}{\partial y} - z\frac{\partial^2 w^o}{\partial y^2} \tag{4.5}$$

$$\varepsilon_z = \frac{\partial w^o(x,y)}{\partial z} = 0 \tag{4.6}$$

$$\gamma_{xy} = \frac{\partial u^o}{\partial y} + \frac{\partial v^o}{\partial x} - 2z\frac{\partial^2 w^o}{\partial x \partial y} \tag{4.7}$$

$$\gamma_{xz} = -\frac{\partial w^o}{\partial x} + \frac{\partial w^o}{\partial x} = 0 \tag{4.8}$$

$$\gamma_{yz} = -\frac{\partial w^o}{\partial y} + \frac{\partial w^o}{\partial y} = 0 \tag{4.9}$$

Shortly, we can obtain the non-zero strain components as follows:

$$\left.\begin{aligned} \varepsilon_x &= \varepsilon_x{}^o(x,y) + z.\kappa_x{}^o(x,y) \\ \varepsilon_y &= \varepsilon_y{}^o(x,y) + z.\kappa_y{}^o(x,y) \\ \gamma_{xy} &= \gamma_{xy}{}^o + z.\kappa_{xy}{}^o \end{aligned}\right| \tag{4.10}$$

where,

$$\varepsilon_x{}^o(x,y) = \frac{\partial u^o(x,y)}{\partial x} \qquad \kappa_x{}^o(x,y) = -\frac{\partial^2 w^o}{\partial x^2}$$

$$\varepsilon_y{}^o(x,y) = \frac{\partial v^o(x,y)}{\partial y} \qquad \kappa_y{}^o(x,y) = -\frac{\partial^2 w^o}{\partial y^2} \tag{4.11}$$

$$\gamma_{xy}{}^o(x,y) = \frac{\partial u^o(x,y)}{\partial y} + \frac{\partial v(x,y)}{\partial x} \qquad \kappa_{xy}{}^o(x,y) = -2.\frac{\partial^2 w^o}{\partial x \partial y}$$

4.4 Laminate Stresses

One other important assumption of Classical Lamination Theory is that each point within the volume of a laminate is in a state of plane stress. [22]

From 3.2.4, we know that

$$\begin{bmatrix} \sigma_x \\ \sigma_y \\ \tau_{xy} \end{bmatrix} = \begin{bmatrix} \overline{Q}_{11} & \overline{Q}_{12} & \overline{Q}_{16} \\ \overline{Q}_{21} & \overline{Q}_{22} & \overline{Q}_{26} \\ \overline{Q}_{16} & \overline{Q}_{26} & \overline{Q}_{66} \end{bmatrix} . \begin{bmatrix} \varepsilon_x \\ \varepsilon_y \\ \gamma_{xy} \end{bmatrix} \tag{4.12}$$

By substituting (4.10) into (4.12), we can obtain the following expression:

$$\begin{bmatrix} \sigma_x \\ \sigma_y \\ \tau_{xy} \end{bmatrix} = \begin{bmatrix} \overline{Q}_{11} & \overline{Q}_{12} & \overline{Q}_{16} \\ \overline{Q}_{21} & \overline{Q}_{22} & \overline{Q}_{26} \\ \overline{Q}_{16} & \overline{Q}_{26} & \overline{Q}_{66} \end{bmatrix} . \begin{bmatrix} \varepsilon_x{}^o + z\kappa_x{}^o \\ \varepsilon_y{}^o + z\kappa_y{}^o \\ \gamma_{xy}{}^o + z\kappa_{xy}{}^o \end{bmatrix} \tag{4.13}$$

Notice that strains vary with z through the thickness of a laminate; therefore, stresses also vary with z. However, stresses also vary with z, because mechanical properties also vary with z. Each layer may have different mechanical properties and may have different fiber orientation.

Similarly, instead of strain values, given the stress values in global coordinate system we can obtain the corresponding strain values in principal material coordinate system by utilizing the below expressions:

$$\begin{bmatrix} \sigma_1 \\ \sigma_2 \\ \tau_{12} \end{bmatrix} = [T]_\sigma \begin{bmatrix} \sigma_x \\ \sigma_y \\ \tau_{xy} \end{bmatrix} \tag{4.14}$$

and

$$\begin{bmatrix} \varepsilon_1 \\ \varepsilon_2 \\ \gamma_{12} \end{bmatrix} = [T]_\varepsilon \begin{bmatrix} \varepsilon_x \\ \varepsilon_y \\ \gamma_{xy} \end{bmatrix} \tag{4.15}$$

4.5 Force and Moment Resultants

For a given midplane deformation state of a plate to occur, in-plane loads and/ or out-of-plane moments are required. These loads and moments are applied along the edges of the plate or along the edges of a region defined within a plate. These loads and moments can be obtained by through laminate thickness integrals of corresponding stresses at a given point on the plate [40]; that is,

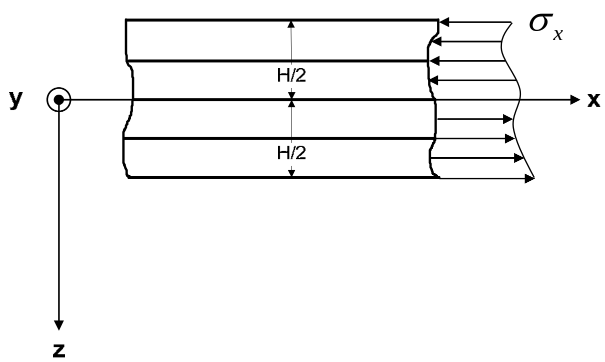

Figure 4.13: Distribution Of σ_x within a Cross Section

$$N_x = \int_{-H/2}^{H/2} \sigma_x dz \tag{4.16}$$

and

$$M_x = \int_{-H/2}^{H/2} \sigma_x z dz \tag{4.17}$$

4.5.1 Force Resultants

The layered fashion of a laminated plate enforces stepwise distribution of stresses through the thickness of the plate. This phenomenon has been discussed earlier.

Thus,

$$N_x = \int_{z_o}^{z_1} \sigma_{x_1} dz + \int_{z_1}^{z_2} \sigma_{x_2} dz + \int_{z_2}^{z_3} \sigma_{x_3} + \ldots \tag{4.18}$$

where σ_{x_1} corresponds to stress distribution within *layer* 1 and σ_{x_2} corresponds to stress distribution within *layer* 2 and so on.

If we assume that stress values within each layer are constant, then

$$N_x = \sigma_{x_1} \int_{z_o}^{z_1} dz + \sigma_{x_2} \int_{z_1}^{z_2} dz + \sigma_{x_3} \int_{z_2}^{z_3} dz + \ldots \tag{4.19}$$

Thus,

$$N_x = \sigma_{x_1}(z_1 - z_o) + \sigma_{x_2}(z_2 - z_1) + \sigma_{x_3}(z_3 - z_2) + \ldots \tag{4.20}$$

However, if σ_x values are not constant within each layer, then step-by-step approach is necessary; that is,

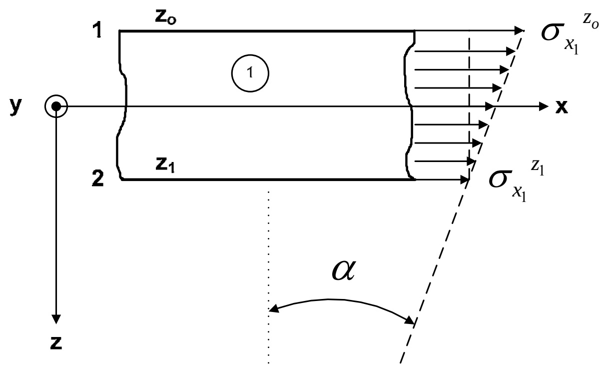

Figure 4.14: Stress Distribution within Layer 1

Obviously from Figure 4.14,

$$\tan(\alpha) = \frac{\sigma_{x_1}^{z_o} - \sigma_{x_1}^{z_1}}{z_o - z_1} \tag{4.21}$$

and

$$\sigma_{x_1}(z) = z\tan(\alpha) \tag{4.22}$$

Thus,

$$N_{x_1} = \int_{z_1}^{z_o} z\tan(\alpha)dz = \frac{1}{2}z^2\tan(\alpha)\Big|_{z_1}^{z_o} \tag{4.23}$$

$$\Rightarrow N_{x_1} = \frac{1}{2}(z_0^{\;2} - z_1^{\;2})\tan(\alpha) = \frac{1}{2}(z_o^{\;2} - z_1^{\;2})\frac{\sigma_{x_1}^{\;z_o} - \sigma_{x_1}^{\;z_1}}{z_o - z_1} \tag{4.24}$$

However, notice above that when $\sigma_{x_1}^{\;z_o} = \sigma_{x_1}^{\;z_1}$ (this happens when $\kappa_x^{\;o} = 0$ and $\varepsilon_x^{\;o} \neq 0$), N_{x_1} leads to zero although it is not.

In such a case, with the addition of a correction term, N_{x_1} can be obtained as follows:

$$N_{x_1} = \sigma_{x_1}^{\;z_1}(z_o - z_1) + \frac{1}{2}(z_o^{\;2} - z_1^{\;2})\frac{\sigma_{x_1}^{\;z_o} - \sigma_{x_1}^{\;z_1}}{z_o - z_1} \tag{4.25}$$

But in this case when $\kappa_x^{\;o} \neq 0$, the above equation leads to errors. Therefore, for the calculation of N_{x_1}, it is more convenient to use the below equation which is also a better approach when doing computational calculations.

$$N_{x_1} = \frac{\sigma_{x_1}^{\;z_o} - \sigma_{x_1}^{\;z_1}}{2}(z_o - z_1) \tag{4.26}$$

This is some sort of calculating a cross sectional area.

Notice that the unit of the above equation is N/mm. Therefore, in order to obtain the force along direction x, we need to multiply the resultant with the width along y. Thus,

$$F_x = N_x L_y \tag{4.27}$$

Similarly,

$$N_y = \int_{-H/2}^{H/2} \sigma_y dz \text{ and } F_y = N_y L_x \tag{4.28}$$

and

$$N_{xy} = \int_{-H/2}^{H/2} \tau_{xy} dz \text{ and } F_{xy} = N_{xy} L_x \tag{4.29}$$

4.5.2 Moment Resultants

$$M_x = \int_{-H/2}^{H/2} \sigma_x . z . dz \tag{4.30}$$

that becomes,

$$M_x = \int_{z_o}^{z_1} \sigma_{x_1} zdz + \int_{z_1}^{z_2} \sigma_{x_2} zdz + \int_{z_2}^{z_3} \sigma_{x_3} zdz + ... \tag{4.31}$$

If σ_x is constant within each layer, then, recalling from section 4.5.1, we get

$$\sigma_x(z) = z\tan(\alpha) = z \frac{\sigma_{x_1}^{z_o} - \sigma_{x_1}^{z_1}}{z_o - z_1} \tag{4.32}$$

Thus,

$$M_{x_1} = \int_{z_1}^{z_o} z \frac{\sigma_{x_1}^{z_o} - \sigma_{x_1}^{z_1}}{z_o - z_1} zdz \tag{4.33}$$

$$\Rightarrow M_{x_1} = \frac{1}{3}(z_o^3 - z_1^3) \frac{\sigma_{x_1}^{z_o} - \sigma_{x_1}^{z_1}}{z_o - z_1} \tag{4.34}$$

Notice in the above equation that when $\sigma_{x_1}^{z_o} = \sigma_{x_1}^{z_1}$, which requires that $\kappa_x^o = M_{x_1} = M_x = 0$. This is clear if the laminate is symmetric. If it is not symmetric, depending on the fiber orientations, M_x may be non zero although $\kappa_x^o = 0$. In this case, for convenience, a correction term is required in the above equation. Thus, the above equation turns out to be;

$$M_{x_1} = \frac{1}{2}(z_o^2 - z_1^2)\sigma_{x_1}^{z_1} + \frac{1}{3}(z_o^3 - z_1^3) \frac{\sigma_{x_1}^{z_o} - \sigma_{x_1}^{z_1}}{z_o - z_1} \tag{4.35}$$

For computational purposes, when M_{x_1} is calculated

- Check weather $\sigma_{x_1}^{z_o} = \sigma_{x_1}^{z_1}$ or not

- Utilize either (4.34) or (4.35) depending on the result.

Notice that the unit of moment resultant M_{x_1} is Nmm/mm. In order to obtain the moment value along x, we need to multiply the resultant with the width along y. Thus,

$$Mom_x = M_x L_y \tag{4.36}$$

Similarly,

$$M_y = \int_{-H/2}^{H/2} \sigma_y z dz, \; Mom_y = M_y L_x \tag{4.37}$$

$$M_{xy} = \int_{-H/2}^{H/2} \tau_{xy} z dz, \; Mom_{xy} = M_{xy} L_x \tag{4.38}$$

4.6 Laminate Stiffness Matrix

By developing the laminate stiffness matrix, we will link the force and moment resultants to laminate strains and curvatures given the force and moment resultants.

Force and moment resultants are considered to act on the reference surface.

Details of the derivations in this section can be found in the references [22, 40]

From 4.5 know that,

$$N_x = \int_{-H/2}^{H/2} \sigma_x dz \tag{4.39}$$

$$N_y = \int_{-H/2}^{H/2} \sigma_y dz \tag{4.40}$$

$$N_{xy} = \int_{-H/2}^{H/2} \tau_{xy} dz \tag{4.41}$$

$$M_x = \int_{-H/2}^{H/2} \sigma_x z dz \tag{4.42}$$

$$M_y = \int_{-H/2}^{H/2} \sigma_y z dz \tag{4.43}$$

$$M_{xy} = \int_{-H/2}^{H/2} \tau_{xy} z dz \tag{4.44}$$

M_x and M_y are denoted as bending moments and M_{xy} is denoted as twisting moment.

From (4.13), we know that

$$\begin{aligned} \sigma_x &= \overline{Q}_{11}(\varepsilon_x{}^o + z\kappa_x{}^o) + \overline{Q}_{12}(\varepsilon_y{}^o + z\kappa_y{}^o) + \overline{Q}_{16}(\gamma_{xy}{}^o + z\kappa_{xy}{}^o) \\ &= \overline{Q}_{11}\varepsilon_x{}^o + \overline{Q}_{11}z\kappa_x{}^o + \overline{Q}_{12}\varepsilon_y{}^o + \overline{Q}_{12}z\kappa_y + \overline{Q}_{16}\gamma_{xy}{}^o + \overline{Q}_{16}z\kappa_{xy}{}^o \end{aligned} \tag{4.45}$$

4.6.1 Force Expressions

If we substitute (4.45) into (4.40), we obtain

$$N_x = \int_{-H/2}^{H/2} \left[\overline{Q}_{11}\varepsilon_x{}^o + \overline{Q}_{11}z\kappa_x{}^o + \overline{Q}_{12}z\kappa_y{}^o + \overline{Q}_{16}\gamma_{xy}{}^o + \overline{Q}_{16}z\kappa_{xy}{}^o\right]dz \tag{4.46}$$

that becomes

$$\begin{aligned} N_x &= \int_{-H/2}^{H/2} \overline{Q}_{11}\varepsilon_x{}^o dz + \int_{-H/2}^{H/2} \overline{Q}_{12}\varepsilon_y{}^o dz + \int_{-H/2}^{H/2} \overline{Q}_{16}\gamma_{xy}{}^o dz \\ &+ \int_{-H/2}^{H/2} \overline{Q}_{11}z\kappa_x{}^o dz + \int_{-H/2}^{H/2} \overline{Q}_{12}z\kappa_y{}^o + \int_{-H/2}^{H/2} \overline{Q}_{16}z\kappa_{xy}{}^o dz \end{aligned} \tag{4.47}$$

Since reference surface strains and curvatures are independent of z, we can write the above equation in the following from:

$$\begin{aligned} N_x &= \varepsilon_x{}^o\left[\int_{-H/2}^{H/2} \overline{Q}_{11}dz\right] + \varepsilon_y{}^o\left[\int_{-H/2}^{H/2} \overline{Q}_{12}dz\right] + \gamma_{xy}{}^o\left[\int_{-H/2}^{H/2} \overline{Q}_{16}dz\right] \\ &+ \kappa_x{}^o\left[\int_{-H/2}^{H/2} \overline{Q}_{11}zdz\right] + \kappa_y{}^o\left[\int_{-H/2}^{H/2} \overline{Q}_{12}zdz\right] + \kappa_{xy}{}^o\left[\int_{-H/2}^{H/2} \overline{Q}_{16}zdz\right] \end{aligned} \tag{4.48}$$

Since material properties and ply orientations may vary from layer to layer through the thickness of a laminate, the first term of the above equation can be expanded as follows:

$$\int_{-H/2}^{H/2} \overline{Q}_{11} dz = \int_{z_o}^{z_1} \overline{Q}_{11_1} dz + \int_{z_1}^{z_2} \overline{Q}_{11_2} dz + \ldots + \int_{z_{N-1}}^{z_N} \overline{Q}_{11_N} dz \qquad \textbf{(4.49)}$$

where the indices $1 \ldots N$ denote layer numbers

Thus,

$$\begin{aligned} \int_{-H/2}^{H/2} \overline{Q}_{11} dz &= \overline{Q}_{11_1} \int_{z_o}^{z_1} dz + \overline{Q}_{11_2} \int_{z_1}^{z_2} dz + \ldots + \overline{Q}_{11_N} \int_{z_{N-1}}^{z_N} dz \\ &= \overline{Q}_{11_1}(z_1 - z_o) + \overline{Q}_{11_2}(z_2 - z_1) + \ldots + \overline{Q}_{11_N}(z_N - z_{N-1}) \end{aligned} \qquad \textbf{(4.50)}$$

$$\Rightarrow \int_{-H/2}^{H/2} \overline{Q}_{11} dz = \sum_{k=1}^{N} \overline{Q}_{11_k}(z_k - z_{k-1}) = \sum_{k=1}^{N} \overline{Q}_{11_k} h_k \qquad \textbf{(4.51)}$$

Let

$$A_{11} = \sum_{k=1}^{N} \overline{Q}_{11} . h_k \qquad \textbf{(4.52)}$$

Similarly,

$$A_{12} = \sum_{k=1}^{N} \overline{Q}_{12_k} . h_k \qquad \textbf{(4.53)}$$

and

$$A_{16} = \sum_{k=1}^{N} \overline{Q}_{16} . h_k \qquad \textbf{(4.54)}$$

Thus, the first three terms of (4.70) can be denoted as follows:

$$A_{11}\varepsilon_x{}^o + A_{12}\varepsilon_y{}^o + A_{16}\gamma_{xy}{}^o \qquad \textbf{(4.55)}$$

Now, we can obtain the terms which contain curvature terms of (4.47) as follows

$$\int_{-H/2}^{H/2} \overline{Q}_{11} z dz = \overline{Q}_{11_1} \int_{z_o}^{z_1} z dz + \overline{Q}_{11_2} \int_{z_1}^{z_2} z dz + ... + \overline{Q}_{11_N} \int_{z_{N-1}}^{z_N} z dz$$
$$= \overline{Q}_{11_1} \frac{1}{2}(z_1{}^2 - z_o{}^2) + \overline{Q}_{11_2} \frac{1}{2}(z_2{}^2 - z_1{}^2) + ... + \overline{Q}_{11_N} \frac{1}{2}(z_N{}^2 - z_{N-1}{}^2) \quad \textbf{(4.56)}$$
$$= \frac{1}{2}\sum_{k=1}^{N} \overline{Q}_{11_k} (z_k{}^2 - z_{k-1}{}^2)$$

Let

$$B_{11} = \frac{1}{2}\sum_{k=1}^{N} \overline{Q}_{11_k} (z_k{}^2 - z_{k-1}{}^2) \quad \textbf{(4.57)}$$

Similarly,

$$B_{12} = \frac{1}{2}\sum_{k=1}^{N} \overline{Q}_{12_k} (z_k{}^2 - z_{k-1}{}^2) \quad \textbf{(4.58)}$$

$$B_{16} = \frac{1}{2}\sum_{k=1}^{N} \overline{Q}_{16_k} (z_k{}^2 - z_{k-1}{}^2) \quad \textbf{(4.59)}$$

Thus, the fourth, fifth and the sixth terms of (4.70) can be denoted as follows:

$$\kappa_x{}^o B_{11} + \kappa_y{}^o B_{12} + \kappa_{xy}{}^o B_{16} \quad \textbf{(4.60)}$$

Finally,

$$N_x = A_{11}\varepsilon_x{}^o + A_{12}\varepsilon_y{}^o + A_{16}\gamma_{xy}{}^o + B_{11}\kappa_x{}^o + B_{12}\kappa_y{}^o + B_{16}\kappa_{xy}{}^o \quad \textbf{(4.61)}$$

Utilizing the similar methodology, we can obtain the other resultant force components as follows:

$$N_y = A_{12}\varepsilon_x{}^o + A_{22}\varepsilon_y{}^o + A_{26}\gamma_{xy}{}^o + B_{12}\kappa_x{}^o + B_{22}\kappa_y{}^o + B_{26}\kappa_{xy}{}^o \quad \textbf{(4.62)}$$

$$N_{xy} = A_{16}\varepsilon_x{}^o + A_{26}\varepsilon_y{}^o + A_{66}\gamma_{xy}{}^o + B_{16}\kappa_x{}^o + B_{26}\kappa_y{}^o + B_{66}\kappa_{xy}{}^o \quad \textbf{(4.63)}$$

where,

$$A_{22} = \sum_{k=1}^{N} \overline{Q}_{22} h_k \quad \textbf{(4.64)}$$

$$A_{26} = \sum_{k=1}^{N} \overline{Q}_{26} h_k \quad \textbf{(4.65)}$$

$$A_{66} = \sum_{k=1}^{N} \overline{Q}_{66} h_k \tag{4.66}$$

$$B_{22} = \frac{1}{2}\sum_{k=1}^{N} \overline{Q}_{22_k} (z_k^{\ 2} - z_{k-1}^{\ \ 2}) \tag{4.67}$$

$$B_{26} = \frac{1}{2}\sum_{k=1}^{N} \overline{Q}_{26_k} (z_k^{\ 2} - z_{k-1}^{\ \ 2}) \tag{4.68}$$

$$B_{66} = \frac{1}{2}\sum_{k=1}^{N} \overline{Q}_{66_k} (z_k^{\ 2} - z_{k-1}^{\ \ 2}) \tag{4.69}$$

Utilizing the matrix notation, we can obtain the below expression:

$$\begin{bmatrix} N_x \\ N_y \\ N_{xy} \end{bmatrix} = \begin{bmatrix} A_{11} & A_{12} & A_{16} \\ A_{12} & A_{22} & A_{26} \\ A_{16} & A_{26} & A_{66} \end{bmatrix} \begin{bmatrix} \varepsilon_x^{\ o} \\ \varepsilon_y^{\ o} \\ \gamma_{xy}^{\ o} \end{bmatrix} + \begin{bmatrix} B_{11} & B_{12} & B_{16} \\ B_{12} & B_{22} & B_{26} \\ B_{16} & B_{26} & B_{66} \end{bmatrix} \begin{bmatrix} \kappa_x^{\ o} \\ \kappa_y^{\ o} \\ \kappa_{xy}^{\ o} \end{bmatrix} \tag{4.70}$$

4.6.2 Moment Expressions

If we substitute (4.47) into (4.43), we obtain

$$\begin{aligned}
M_x &= \int_{-H/2}^{H/2} \left[\overline{Q}_{11}(\varepsilon_x^{\ o} + z\kappa_x^{\ o}) + \overline{Q}_{12}(\varepsilon_y^{\ o} + z\kappa_y^{\ o}) + \overline{Q}_{16}(\gamma_{xy}^{\ o} + z\kappa_{xy}^{\ o}) \right] \\
&= \int_{-H/2}^{H/2} \left[\overline{Q}_{11}\varepsilon_x^{\ o} z + \overline{Q}_{12}\varepsilon_y^{\ o} z + \overline{Q}_{16}\gamma_{xy}^{\ o} z + \overline{Q}_{11} z^2 \kappa_x^{\ o} + \overline{Q}_{12} z^2 \kappa_y^{\ o} + \overline{Q}_{16} z^2 \kappa_{xy}^{\ o} \right] dz \\
&= \int_{-H/2}^{H/2} \overline{Q}_{11}\varepsilon_x^{\ o} z dz + \int_{-H/2}^{H/2} \overline{Q}_{12}\varepsilon_y^{\ o} z dz + \int_{-H/2}^{H/2} \overline{Q}_{16}\gamma_{xy}^{\ o} z dz + \\
&+ \int_{-H/2}^{H/2} \overline{Q}_{11} z^2 \kappa_x^{\ o} dz + \int_{-H/2}^{H/2} \overline{Q}_{12} z^2 \kappa_y^{\ o} dz + \int_{-H/2}^{H/2} \overline{Q}_{16} z^2 \kappa_{xy}^{\ o} dz \\
&= \varepsilon_x^{\ o} \int_{-H/2}^{H/2} \overline{Q}_{11} z dz + \varepsilon_y^{\ o} \int_{-H/2}^{H/2} \overline{Q}_{12} z dz + \gamma_{xy}^{\ o} \int_{-H/2}^{H/2} \overline{Q}_{16} z dz \\
&+ \kappa_x^{\ o} \int_{-H/2}^{H/2} \overline{Q}_{11} z^2 dz + \kappa_y^{\ o} \int_{-H/2}^{H/2} \overline{Q}_{12} z^2 dz + \kappa_{xy}^{\ o} \int_{-H/2}^{H/2} \overline{Q}_{16} z^2 dz
\end{aligned} \tag{4.71}$$

$$\Rightarrow \int_{-H/2}^{H/2} \overline{Q}_{11} z dz = \int_{z_o}^{z_1} \overline{Q}_{11_1} z dz + \int_{z_1}^{z_2} \overline{Q}_{11_2} z dz + ... + \int_{z_{N-1}}^{z_N} \overline{Q}_{11_N} z dz$$

$$= \frac{1}{2}\overline{Q}_{11_1}(z_1^{\ 2} - z_o^{\ 2}) + \frac{1}{2}\overline{Q}_{11_2}(z_2^{\ 2} - z_1^{\ 2}) + ... + \frac{1}{2}\overline{Q}_{11_N}(z_N^{\ 2} - z_{N-1}^{\ 2})$$

Hence,

$$\int_{-H/2}^{H/2} Q_{11} z dz = \frac{1}{2}\sum_{k=1}^{N} Q_{11_k}(z_k^{\ 2} - z_{k-1}^{\ 2}) \qquad \textbf{(4.72)}$$

This is the same equation obtained earlier in 4.6.1 for force resultants. Thus, the first three components of M_x can be obtained as follows:

$$B_{11}\varepsilon_x^{\ o} + B_{12}\varepsilon_y^{\ o} + B_{16}\gamma_{xy}^{\ o} \qquad \textbf{(4.73)}$$

On the other hand,

$$\int_{-H/2}^{H/2} \overline{Q}_{11} z^2 dz = \int_{z_o}^{z_1} \overline{Q}_{11_1} z^2 dz + \int_{z_1}^{z_2} \overline{Q}_{11_2} z^2 dz + ... + \int_{z_{N-1}}^{z_N} \overline{Q}_{11_N} z^2 dz$$

$$= \frac{1}{3}\overline{Q}_{11_1}(z_1^{\ 3} - z_o^{\ 3}) + \frac{1}{3}\overline{Q}_{11_2}(z_2^{\ 3} - z_1^{\ 3}) + ... + \frac{1}{3}\overline{Q}_{11_N}(z_N^{\ 3} - z_{N-1}^{\ 3}) \qquad \textbf{(4.74)}$$

$$\Rightarrow \int_{-H/2}^{H/2} Q_{11} z^2 dz = \frac{1}{3}\sum_{k=1}^{N} Q_{11_k}(z_k^{\ 3} - z_{k-1}^{\ 3}) \qquad \textbf{(4.75)}$$

Let,

$$D_{11} = \frac{1}{3}\sum_{k=1}^{N} \overline{Q}_{11_k}(z_k^{\ 3} - z_{k-1}^{\ 3}) \qquad \textbf{(4.76)}$$

Similarly,

$$D_{12} = \frac{1}{3}\sum_{k=1}^{N} \overline{Q}_{12_k}(z_k^{\ 3} - z_{k-1}^{\ 3}) \qquad \textbf{(4.77)}$$

$$D_{16} = \frac{1}{3}\sum_{k=1}^{N} \overline{Q}_{16_k}(z_k^{\ 3} - z_{k-1}^{\ 3}) \qquad \textbf{(4.78)}$$

Thus,

(4.79)

$$M_x = B_{11}\varepsilon_x{}^o + B_{12}\varepsilon_y{}^o + B_{16}\gamma_{xy}{}^o + D_{11}\kappa_x{}^o + D_{12}\kappa_y{}^o + D_{16}\kappa_{xy}{}^o$$

Similarly,

$$M_y = B_{12}\varepsilon_x{}^o + B_{22}\varepsilon_y{}^o + B_{26}\gamma_{xy}{}^o + D_{12}\kappa_x{}^o + D_{22}\kappa_y{}^o + D_{26}\kappa_{xy}{}^o \quad \textbf{(4.80)}$$

$$M_{xy} = B_{16}\varepsilon_x{}^o + B_{26}\varepsilon_y{}^o + B_{66}\gamma_{xy}{}^o + D_{16}\kappa_x{}^o + D_{26}\kappa_y{}^o + D_{66}\kappa_{xy}{}^o \quad \textbf{(4.81)}$$

in which,

$$D_{22} = \frac{1}{3}\sum_{k=1}^{N}\overline{Q}_{22_k}(z_k{}^3 - z_{k-1}{}^3) \quad \textbf{(4.82)}$$

$$D_{26} = \frac{1}{3}\sum_{k=1}^{N}\overline{Q}_{26_k}(z_k{}^3 - z_{k-1}{}^3) \quad \textbf{(4.83)}$$

$$D_{66} = \frac{1}{3}\sum_{k=1}^{N}\overline{Q}_{66_k}(z_k{}^3 - z_{k-1}{}^3) \quad \textbf{(4.84)}$$

Finally, we arrange the moment expressions in the following matrix form:

$$\begin{bmatrix} M_x \\ M_y \\ M_{xy} \end{bmatrix} = \begin{bmatrix} B_{11} & B_{12} & B_{16} \\ B_{12} & B_{22} & B_{26} \\ B_{16} & B_{26} & B_{66} \end{bmatrix} \begin{bmatrix} \varepsilon_x{}^o \\ \varepsilon_y{}^o \\ \gamma_{xy}{}^o \end{bmatrix} + \begin{bmatrix} D_{11} & D_{12} & D_{16} \\ D_{12} & D_{22} & D_{26} \\ D_{16} & D_{26} & D_{66} \end{bmatrix} \begin{bmatrix} \kappa_x{}^o \\ \kappa_y{}^o \\ \kappa_{xy}{}^o \end{bmatrix} \quad \textbf{(4.85)}$$

4.6.3 Laminate Stiffness Matrix

If we sum up the force and moment expressions detailed in (4.70) and (4.85), we can obtain the below laminate stiffness matrix expression:

$$\begin{bmatrix} N_x \\ N_y \\ N_{xy} \\ M_x \\ M_y \\ M_{xy} \end{bmatrix} = \begin{bmatrix} A_{11} & A_{12} & A_{16} & B_{11} & B_{12} & B_{16} \\ A_{12} & A_{22} & A_{26} & B_{12} & B_{22} & B_{26} \\ A_{16} & A_{26} & A_{66} & B_{16} & B_{26} & B_{66} \\ B_{11} & B_{12} & B_{16} & D_{11} & D_{12} & D_{16} \\ B_{12} & B_{22} & B_{26} & D_{12} & D_{22} & D_{26} \\ B_{16} & B_{26} & B_{66} & D_{16} & D_{26} & D_{66} \end{bmatrix} \begin{bmatrix} \varepsilon_x{}^o \\ \varepsilon_y{}^o \\ \gamma_{xy}{}^o \\ \kappa_x{}^o \\ \kappa_y{}^o \\ \kappa_{xy}{}^o \end{bmatrix} \quad \textbf{(4.86)}$$

Where,

$$A_{ij} = \sum_{k=1}^{N}\overline{Q}_{ij_k}(z_k - z_{k-1}) \quad \textbf{(4.87)}$$

$$B_{ij} = \frac{1}{2}\sum_{k=1}^{N} \overline{Q}_{ij_k} (z_k{}^2 - z_{k-1}{}^2) \qquad \textbf{(4.88)}$$

$$D_{ij} = \frac{1}{3}\sum_{k=1}^{N} \overline{Q}_{ij_k} (z_k{}^3 - z_{k-1}{}^3) \qquad \textbf{(4.89)}$$

Or,

$$\begin{bmatrix} \varepsilon_x{}^o \\ \varepsilon_y{}^o \\ \gamma_{xy}{}^o \\ \kappa_x{}^o \\ \kappa_y{}^o \\ \kappa_{xy}{}^o \end{bmatrix} = \begin{bmatrix} A & B \\ B & D \end{bmatrix} \begin{bmatrix} N_x \\ N_y \\ N_{xy} \\ M_x \\ M_y \\ M_{xy} \end{bmatrix} \qquad \textbf{(4.90)}$$

5 FIBER REINFORCED LAMINATED PLATES

5.1.1 Governing Rectangular Plate Equations

In order to define the behavior of a laminated plate under a loading condition, given the boundary conditions, we will utilize the Newtonian approach. Consider the below plate:

Details of the derivations in this section can be found in the references [22, 40, 41].

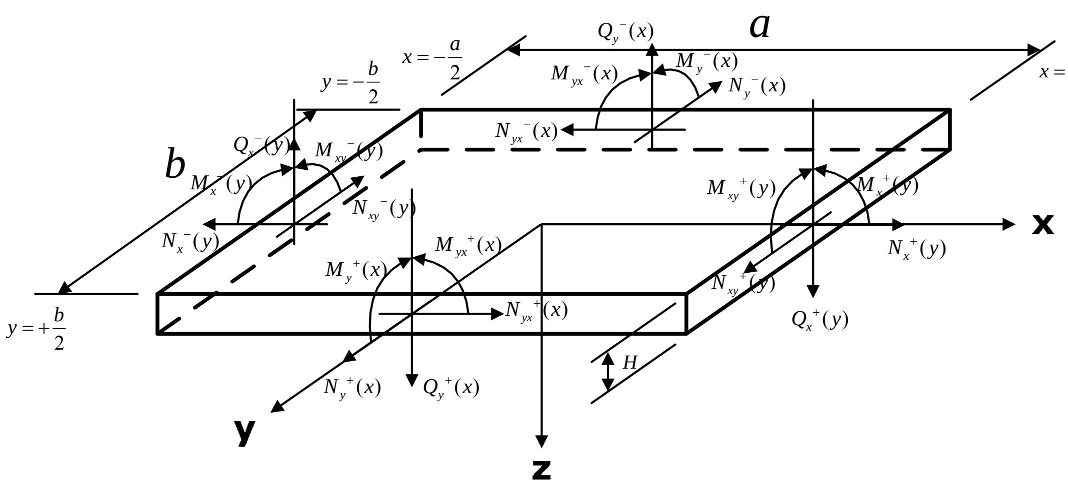

Figure 5.1: Force and Moment Resultants On The Boundaries Of A Plate

Figure notes:

1. xy plane coincides with the reference surface and the midplane of the plate.
2. Coordinate system origin is at the midpoint of the plate.
3. The purpose of using the superscripts + or – is to denote on which side a resultant is; i.e., $-\frac{b}{2}$ or $\frac{b}{2}$. Therefore, obviously; i.e., $N_x^+ = N_x^-$.

We have previously defined all stress resultants in Figure 5.1 except for transverse shear force resultants. Given by

$$Q_x^+(x) = \int_{-H/2}^{H/2} \tau_{xz}(x,y,z)dz \qquad \text{at } x = \frac{a}{2} \tag{5.1}$$

$$Q_x^-(y) = \int_{-H/2}^{H/2} \tau_{xz}(x,y,z)dz \qquad \text{at } x = -\frac{a}{2} \tag{5.2}$$

$$Q_y^+(x) = \int_{-H/2}^{H/2} \tau_{yz}(x,y,z)dz \qquad \text{at } y = \frac{b}{2} \tag{5.3}$$

$$Q_y^-(x) = \int_{-H/2}^{H/2} \tau_{yz}(x,y,z)dz \qquad \text{at } y = -\frac{b}{2} \tag{5.4}$$

However, we have previously showed that, $\tau_{xz} = \tau_{yz} = 0$; namely, in plane stress assumption. Now, we see here that for a plane to prevent its equilibrium under out of plane loading, transverse shear force resultants should exist. This is actually a contradiction though classical laminated plate theory works despite this contradiction.

In order to derive the governing differential equations, forces and moments are summed up for a differential element having the dimensions Δx and Δy within a plate. It is assumed that this differential element is in equilibrium under the forces and moments applied to this element. Although the forces and moments, as illustrated in Figure 5.1, act simultaneously on the differential element for illustrative purposes, they will be shown and they will be summed up separately utilizing the superposition principle.

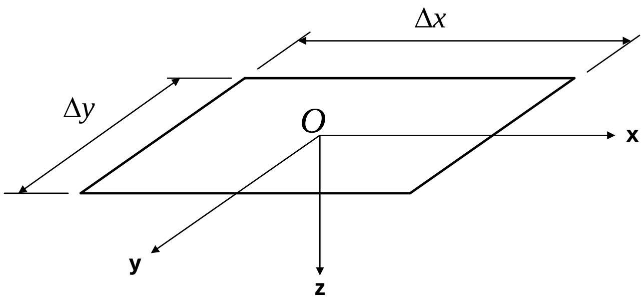

Figure notes:

1. O is at the midpoint of the differential element.
2. The differential element is within a laminated plate away from the boundaries of this plate.

Figure 5.2: Differential Element within a Laminated Plate

5.1.2 Forces along the x-Direction

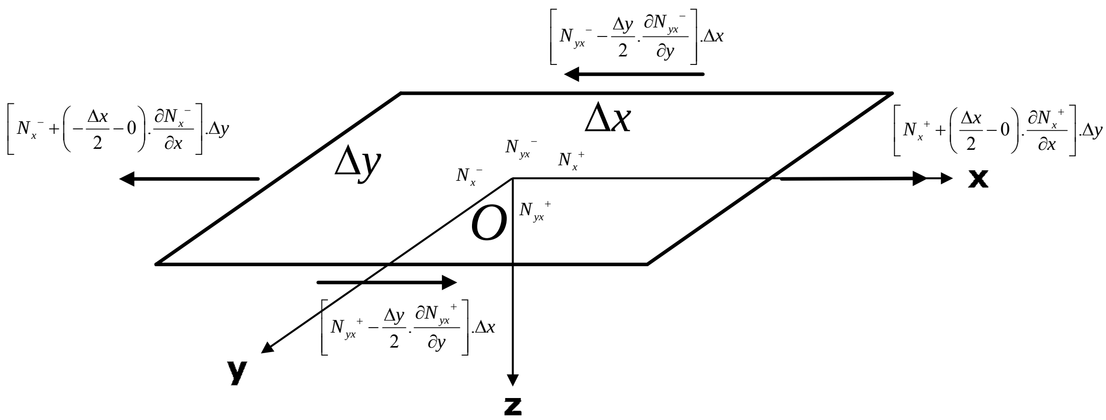

Figure 5.3: Forces Along the x-Direction On The Differential Element

We can obtain the forces and moments acting on the boundaries of the differential element utilizing the Taylor's theorem. Recalling from Appendix A and assuming that the force resultants about O are $N_x^+(y)$, $N_x^-(y)$, $N_{yx}^+(x)$ and $N_{yx}^-(x)$, we can obtain Figure 2.1.

Since, $\Sigma F_x = 0$,

$$\begin{aligned}&\left[N_x + \frac{\Delta x}{2}\frac{\partial N_x}{\partial x}\right]\Delta y - \left[N_x - \frac{\Delta x}{2}\frac{\partial N_x}{\partial x}\right]\Delta y \\ &+\left[N_{yx} + \frac{\Delta y}{2}\frac{\partial N_{yx}}{\partial y}\right]\Delta x - \left[N_{yx} - \frac{\Delta y}{2}\frac{\partial N_{yx}}{\partial y}\right]\Delta x = 0\end{aligned} \tag{5.5}$$

Thus,

$$\frac{\partial N_x}{\partial x}+\frac{\partial N_{yx}}{\partial y}=0 \tag{5.6}$$

Obviously, since $N_{xy}=N_{yx}$

$$\frac{\partial N_x}{\partial x}+\frac{\partial N_{xy}}{\partial y}=0 \tag{5.7}$$

5.1.3 Forces along the y-Direction

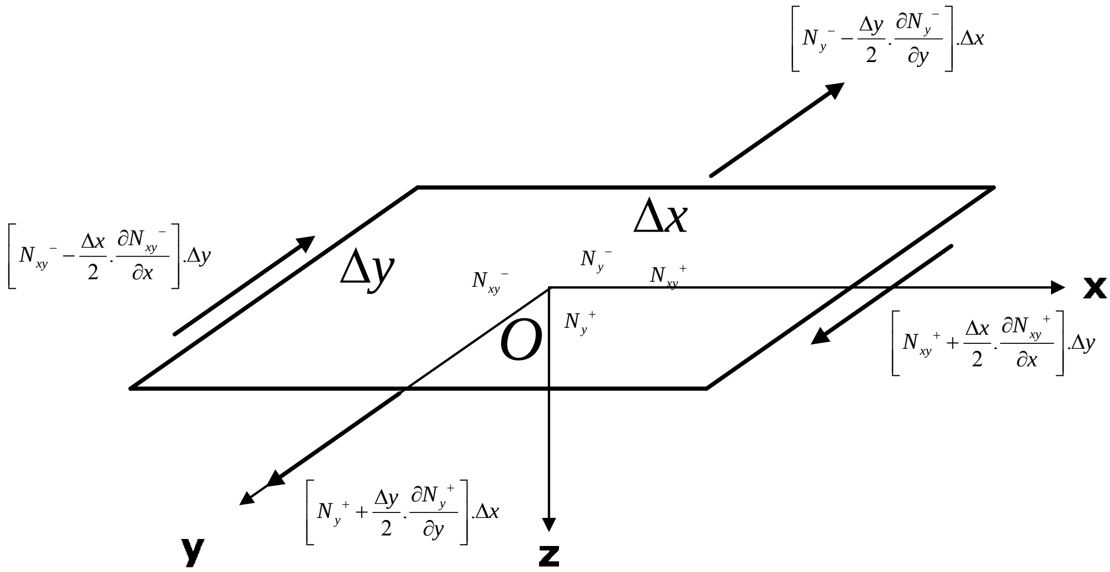

Figure 5.4: Forces Along the y-Direction on the Differential Element

Since $\Sigma F_y = 0$

$$\begin{aligned}&\left[N_y^{+}+\frac{\Delta y}{2}\frac{\partial N_y^{+}}{\partial y}\right]\Delta x-\left[N_y^{-}-\frac{\Delta y}{2}\frac{\partial N_y^{-}}{\partial y}\right]\Delta x\\&+\left[N_{xy}^{+}+\frac{\Delta x}{2}\frac{\partial N_{xy}^{+}}{\partial x}\right]\Delta y-\left[N_{xy}^{-}-\frac{\Delta x}{2}\frac{\partial N_{xy}^{-}}{\partial x}\right]\Delta y=0\end{aligned} \tag{5.8}$$

Thus,

$$\frac{\partial N_y}{\partial y}+\frac{\partial N_{xy}}{\partial x}=0 \tag{5.9}$$

5.1.4 Forces Along the z -Direction

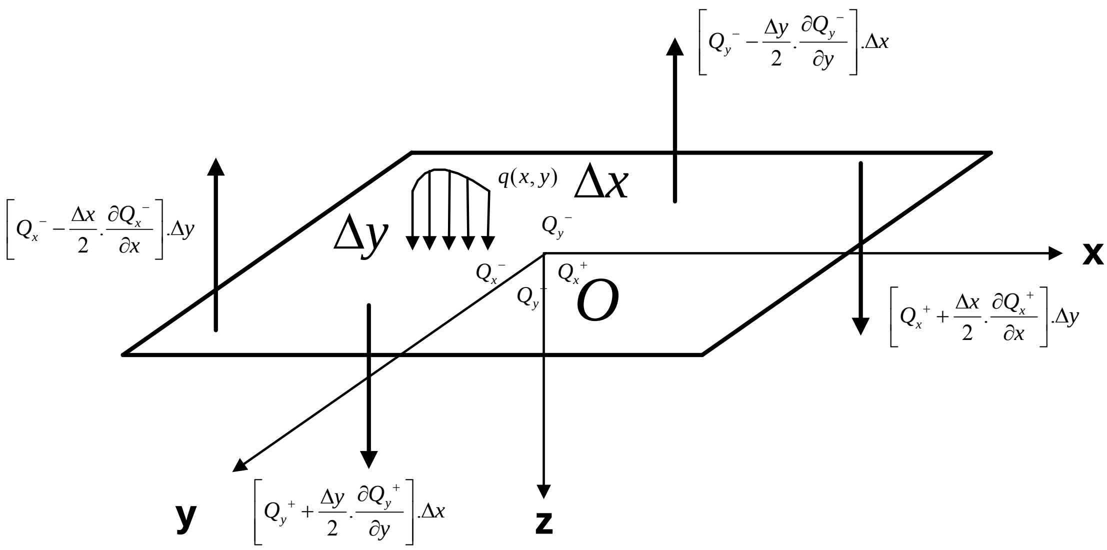

Figure 5.5: Forces Along the z -Direction on the Differential Element

As defined earlier, on the plate boundaries, we can define the transverse shear force resultants accordingly for the differential element.

$$Q_x = \int_{-H/2}^{H/2} \tau_{xz} dz \tag{5.10}$$

and

$$Q_y = \int_{-H/2}^{H/2} \tau_{yz} dz \tag{5.11}$$

Since $\Sigma F_z = 0$,

$$\begin{aligned} &\left[Q_x^+ + \frac{\Delta x}{2}\frac{\partial Q_x^+}{\partial x}\right]\Delta y - \left[Q_x^- - \frac{\Delta x}{2}\frac{\partial Q_x^-}{\partial x}\right]\Delta y \\ &+\left[Q_y^+ + \frac{\Delta y}{2}\frac{\partial Q_y^+}{\partial y}\right]\Delta x - \left[Q_y^- - \frac{\Delta y}{2}\frac{\partial Q_y^-}{\partial y}\right]\Delta x + q\Delta x\Delta y = 0 \end{aligned} \tag{5.12}$$

Thus,

$$\frac{\partial Q_x}{\partial x} + \frac{\partial Q_y}{\partial y} = -q \tag{5.13}$$

5.1.5 Moments About the x-Axis

Utilizing the similar approaches as above, we can sum up the moments about the x-axis:

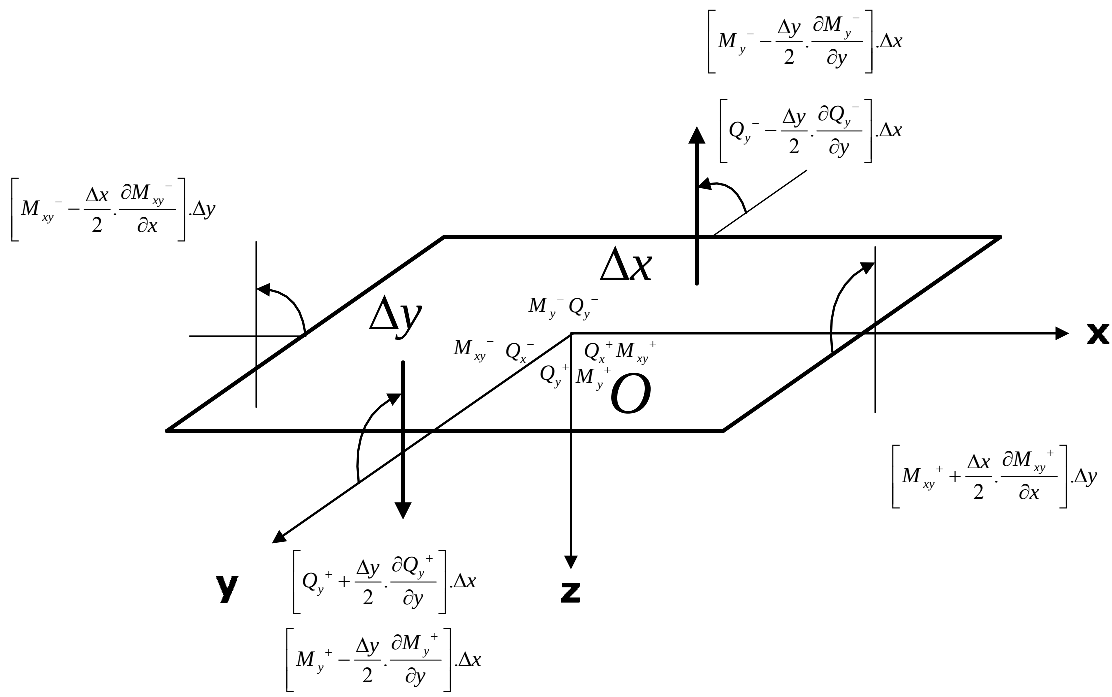

Figure 5.6: Moments about the x-Axis on the Differential Element

Figure notes:

1. Counter clockwise moments are assumed to be positive

Since, $\Sigma M_x = 0$, we get

$$\begin{aligned}
&\left[M_y^- - \frac{\Delta y}{2}\frac{\partial M_y^-}{\partial y}\right]\Delta x + \left[M_{xy}^- - \frac{\Delta x}{2}\frac{\partial M_{xy}^-}{\partial x}\right]\Delta y \\
&-\left[M_{xy}^+ + \frac{\Delta x}{2}\frac{\partial M_{xy}^+}{\partial x}\right]\Delta y - \left[M_y^+ + \frac{\Delta y}{2}\frac{\partial M_y^+}{\partial y}\right]\Delta x \\
&+\left[Q_y^- - \frac{\Delta y}{2}\frac{\partial Q_y^-}{\partial y}\right]\Delta x\frac{\Delta y}{2} + \left[Q_y^+ + \frac{\Delta y}{2}\frac{\partial Q_y^+}{\partial y}\right]\Delta x\frac{\Delta y}{2} = 0
\end{aligned} \qquad \textbf{(5.14)}$$

Thus,

$$Q_y = \frac{\partial M_y}{\partial y} + \frac{\partial M_{xy}}{\partial x} \qquad \textbf{(5.15)}$$

5.1.6 Moments About the y-Axis

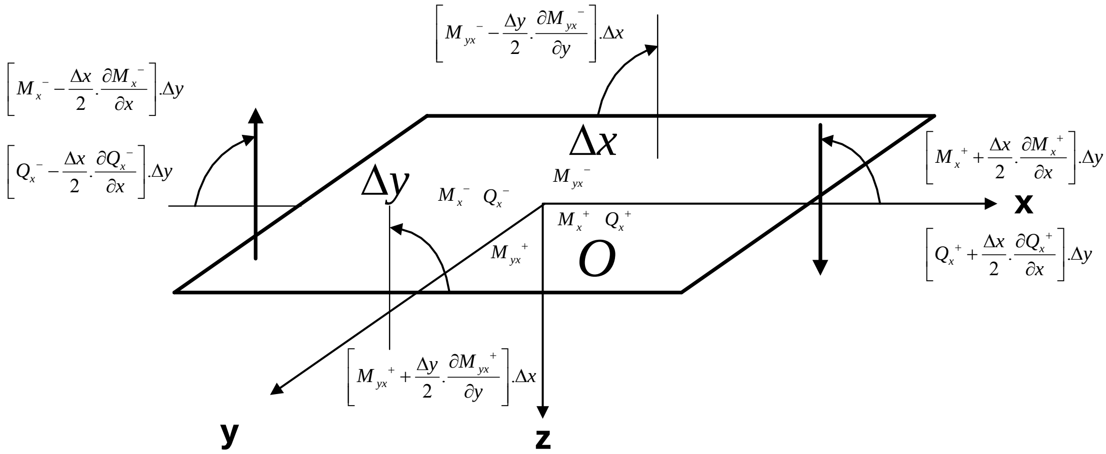

Figure 5.7: Moments about the y-Axis on the Differential Element

Since, $\Sigma M_y = 0$, we get

$$
\begin{aligned}
&\left[M_x^{+} + \frac{\Delta x}{2}\frac{\partial M_x^{+}}{\partial x}\right]\Delta y + \left[M_{yx}^{-} + \frac{\Delta y}{2}\frac{\partial M_{yx}^{-}}{\partial y}\right]\Delta x \\
&-\left[M_x^{-} - \frac{\Delta x}{2}\frac{\partial M_x^{-}}{\partial x}\right]\Delta y - \left[M_{yx}^{+} - \frac{\Delta y}{2}\frac{\partial M_{yx}^{+}}{\partial y}\right]\Delta x \\
&-\left[Q_x^{+} + \frac{\Delta x}{2}\frac{\partial Q_x}{\partial x}\right]\Delta y\frac{\Delta x}{2} - \left[Q_x^{-} - \frac{\Delta x}{2}\frac{\partial Q_x}{\partial x}\right]\Delta y\frac{\Delta x}{2} = 0
\end{aligned}
\tag{5.16}
$$

Thus,

$$
Q_x = \frac{\partial M_x}{\partial x} + \frac{\partial M_{yx}}{\partial y} \tag{5.17}
$$

However, we know that $M_{xy} = M_{yx}$. Therefore,

$$
Q_x = \frac{\partial M_x}{\partial x} + \frac{\partial M_{xy}}{\partial y} \tag{5.18}
$$

5.1.7 Moments about the z-Axis

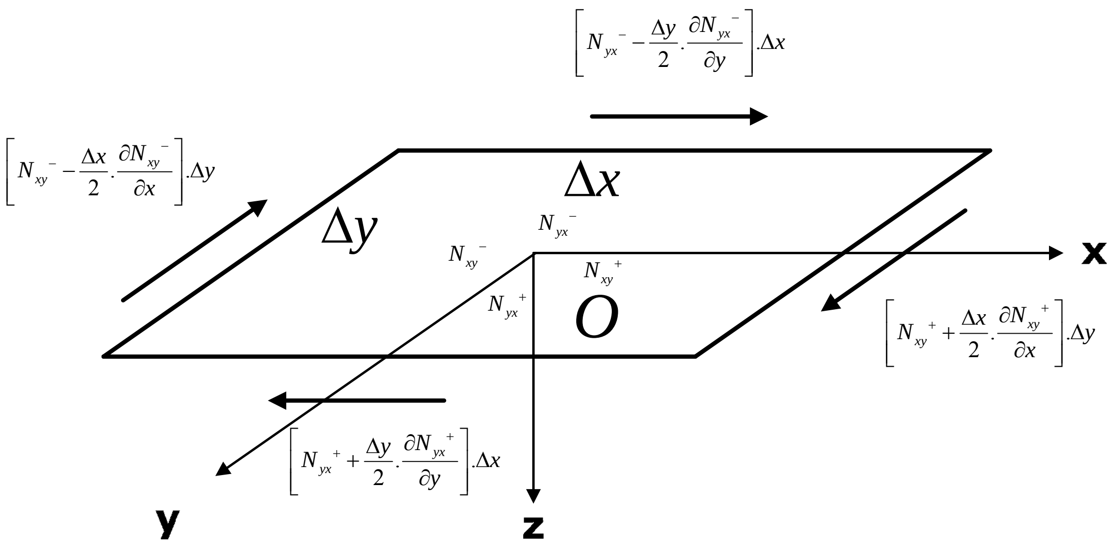

Figure 5.8: Moments about the z -Axis on the Differential Element

Since $\Sigma M_z = 0$, we have

$$\left[N_{yx}^{-}-\frac{\Delta y}{2}\frac{\partial N_{yx}^{-}}{\partial y}\right]\Delta x\frac{\Delta y}{2}+\left[N_{yx}^{+}+\frac{\Delta y}{2}\frac{\partial N_{yx}^{+}}{\partial y}\right]\Delta x\frac{\Delta y}{2}$$
$$-\left[N_{xy}^{+}+\frac{\Delta x}{2}\frac{\partial N_{xy}^{+}}{\partial x}\right]\Delta y\frac{\Delta x}{2}-\left[N_{xy}^{-}-\frac{\Delta x}{2}\frac{\partial N_{xy}^{-}}{\partial y}\right]\Delta y\frac{\Delta x}{2}=0 \quad \textbf{(5.19)}$$

that becomes

$$\Delta x\Delta y N_{yx}-\Delta x\Delta y N_{xy}=0 \quad \textbf{(5.20)}$$

Thus, we conclude that no new information is derived utilizing the equilibrium $\Sigma M_z = 0$.

5.1.8 Generic Rectangular Plate Equations

Utilizing (5.13), (5.15) and (5.17), we can obtain the more generic rectangular plate equations:

$$\frac{\partial N_x}{\partial x}+\frac{\partial N_{xy}}{\partial y}=0 \quad \textbf{(5.21)}$$

$$\frac{\partial N_y}{\partial y}+\frac{\partial N_{xy}}{\partial x}=0 \quad \textbf{(5.22)}$$

$$\frac{\partial^2 M_x}{\partial x^2} + 2\frac{\partial^2 M_{xy}}{\partial x.\partial y} + \frac{\partial^2 M_y}{\partial y^2} + q = 0 \quad \textbf{(5.23)}$$

5.2 Boundary Conditions

In order to solve the differential equations (5.21), (5.22) and (5.23), the below boundary conditions of the plate in question should be specified. [22, 40, 42]

1. At $x = \frac{a}{2}$

   I. $N_x = N_x^+$ or u^o must be specified.

   II. $N_{xy} = N_{xy}^+$ or v^o must be specified.

   III. $\frac{\partial M_x}{\partial x} + 2\frac{\partial M_{xy}}{\partial y} = Q_x^+ + \frac{\partial M_{xy}^+}{\partial y}$ or w^o must be specified.

   IV. $M_x = M_x^+$ or $\frac{\partial w^o}{\partial x}$ (slope at $x = \frac{a}{2}$) must be specified.

At $x = -\frac{a}{2}$

   V. $N_x = N_x^-$ or u^o must be specified.

   VI. $N_{xy} = N_{xy}^-$ or v^o must be specified.

   VII. $\frac{\partial M_x}{\partial x} + 2\frac{\partial M_{xy}}{\partial y} = Q_x^- + \frac{\partial M_{xy}^-}{\partial y}$ or w^o must be specified.

   VIII. $M_x = M_x^-$ or $\frac{\partial w^o}{\partial x}$ (slope at $x = -\frac{a}{2}$) must be specified.

2. At $y = \frac{b}{2}$

   I. $N_y = N_y^+$ or v^o must be specified.

   II. $N_{xy} = N_{xy}^+$ or u^o must be specified.

   III. $\frac{\partial M_y}{\partial y} + 2\frac{\partial M_{xy}}{\partial x} = Q_y^+ + \frac{\partial M_{xy}^+}{\partial y}$ or w^o must be specified.

IV. $M_y = M_y^+$ or $\dfrac{\partial w^o}{\partial y}$ (slope at $y = \dfrac{b}{2}$) must be specified.

3. At $y = -\dfrac{b}{2}$

I. $N_y = N_y^-$ or v^o must be specified.

II. $N_{xy} = N_{xy}^-$ or u^o must be specified.

III. $\dfrac{\partial M_y}{\partial y} + 2\dfrac{\partial M_{xy}}{\partial x} = Q_y^- + \dfrac{\partial M_{xy}^-}{\partial y}$ or w^o must be specified.

IV. $M_y = M_y^-$ or $\dfrac{\partial w^o}{\partial y}$ (slope at $y = -\dfrac{b}{2}$) must be specified.

5.3 Governing Equations in Terms of Displacements

Recalling from (4.86) that

$$
\left.
\begin{aligned}
N_x &= A_{11}\varepsilon_x^{\ o} + A_{12}\varepsilon_y^{\ o} + A_{16}\gamma_{xy}^{\ o} + B_{11}\kappa_x^{\ o} + B_{12}\kappa_y^{\ o} + B_{16}\kappa_{xy}^{\ o} \\
N_y &= A_{12}\varepsilon_x^{\ o} + A_{22}\varepsilon_y^{\ o} + A_{26}\gamma_{xy}^{\ o} + B_{12}\kappa_x^{\ o} + B_{22}\kappa_y^{\ o} + B_{26}\kappa_{xy}^{\ o} \\
N_{xy} &= A_{16}\varepsilon_x^{\ o} + A_{26}\varepsilon_y^{\ o} + A_{66}\gamma_{xy}^{\ o} + B_{16}\kappa_x^{\ o} + B_{26}\kappa_y^{\ o} + B_{66}\kappa_{xy}^{\ o} \\
M_x &= B_{11}\varepsilon_x^{\ o} + B_{12}\varepsilon_y^{\ o} + B_{16}\gamma_{xy}^{\ o} + D_{11}\kappa_x^{\ o} + D_{12}\kappa_y^{\ o} + D_{16}\kappa_{xy}^{\ o} \\
M_y &= B_{12}\varepsilon_x^{\ o} + B_{22}\varepsilon_y^{\ o} + B_{26}\gamma_{xy}^{\ o} + D_{12}\kappa_x^{\ o} + D_{22}\kappa_y^{\ o} + D_{26}\kappa_{xy}^{\ o} \\
M_{xy} &= B_{16}\varepsilon_x^{\ o} + B_{26}\varepsilon_y^{\ o} + B_{66}\gamma_{xy}^{\ o} + D_{16}\kappa_x^{\ o} + D_{26}\kappa_y^{\ o} + D_{66}\kappa_{xy}^{\ o}
\end{aligned}
\right| \qquad \textbf{(5.24)}
$$

On the other hand, by substituting (4.11) and (5.24) into (5.21), (5.22) and (5.23), we can obtain the governing rectangular plate differential equations in terms of displacements as follows:

(5.22) in terms of displacements can be written as; [22, 40]

$$\frac{\partial}{\partial x}\left[A_{11}\frac{\partial u^o}{\partial x}+A_{12}\frac{\partial v^o}{\partial y}+A_{16}(\frac{\partial u^o}{\partial y}+\frac{\partial v^o}{\partial x})-B_{11}\frac{\partial^2 w^o}{\partial x^2}-B_{12}\frac{\partial^2 w^o}{\partial y^2}-2B_{16}\frac{\partial^2 w^o}{\partial x\partial y}\right]$$

$$+\frac{\partial}{\partial y}\left[A_{16}\frac{\partial u^o}{\partial x}+A_{26}\frac{\partial v^o}{\partial y}+A_{66}(\frac{\partial u^o}{\partial y}+\frac{\partial v^o}{\partial x})-B_{16}\frac{\partial^2 w^o}{\partial x^2}-B_{26}\frac{\partial^2 w^o}{\partial y^2}-2B_{66}\frac{\partial^2 w^o}{\partial x\partial y}\right]=0 \quad \textbf{(5.25)}$$

Thus, carrying out some mathematical manipulations, we obtain

$$A_{11}\frac{\partial^2 u^o}{\partial x^2}+(A_{12}+A_{66})\frac{\partial^2 v^o}{\partial x\partial y}+2A_{16}\frac{\partial^2 u^o}{\partial x\partial y}+A_{16}\frac{\partial^2 v^o}{\partial x^2}$$

$$-B_{11}\frac{\partial^3 w^o}{\partial x^3}-(2B_{66}+B_{12})\frac{\partial^3 w^o}{\partial x\partial y^2}-3B_{16}\frac{\partial^3 w^o}{\partial x^2\partial y} \quad \textbf{(5.26)}$$

$$+A_{26}\frac{\partial^2 v^o}{\partial y^2}+A_{66}\frac{\partial^2 u^o}{\partial y^2}-B_{26}\frac{\partial^3 w^o}{\partial y^3}=0$$

(5.21) in terms of displacements:

$$\frac{\partial}{\partial y}\left[A_{12}\frac{\partial u^o}{\partial x}+A_{22}\frac{\partial v^o}{\partial y}+A_{26}(\frac{\partial u^o}{\partial y}+\frac{\partial v^o}{\partial x})-B_{12}\frac{\partial^2 w^o}{\partial x^2}-B_{22}\frac{\partial^2 w^o}{\partial y^2}-2B_{22}\frac{\partial^2 w^o}{\partial x\partial y}\right] \quad \textbf{(5.27)}$$

$$+\frac{\partial}{\partial x}\left[A_{16}\frac{\partial u^o}{\partial x}+A_{26}\frac{\partial v^o}{\partial y}+A_{66}(\frac{\partial u^o}{\partial y}+\frac{\partial v^o}{\partial x})-B_{16}\frac{\partial^2 w^o}{\partial x^2}-B_{26}\frac{\partial^2 w^o}{\partial y^2}-2B_{66}\frac{\partial^2 w^o}{\partial x\partial y}\right]=0$$

Thus, carrying out some mathematical manipulations, we obtain

$$(A_{12}+A_{66})\frac{\partial^2 u^o}{\partial x\partial y}+A_{22}\frac{\partial^2 v^o}{\partial y^2}+A_{26}\frac{\partial^2 u^o}{\partial y^2}+2A_{26}\frac{\partial^2 v^o}{\partial x\partial y}-(B_{12}+2.B_{66})\frac{\partial^3 w^o}{\partial x^2\partial y}$$

$$+B_{22}\frac{\partial^3 w^o}{\partial y^3}-3B_{26}\frac{\partial^3 w^o}{\partial x\partial y^2}+A_{16}\frac{\partial^2 u^o}{\partial x^2}+A_{66}\frac{\partial^2 v^o}{\partial x^2}-B_{16}\frac{\partial^3 w^o}{\partial x^3}=0 \quad \textbf{(5.28)}$$

(5.23) in terms of displacements:

$$\frac{\partial^2}{\partial x^2}\left[B_{11}\frac{\partial u^o}{\partial x}+B_{12}\frac{\partial v^o}{\partial y}+B_{16}(\frac{\partial u^o}{\partial y}+\frac{\partial v^o}{\partial x})-D_{11}\frac{\partial^2 w^o}{\partial x^2}-D_{12}\frac{\partial^2 w^o}{\partial y^2}-2D_{16}\frac{\partial^2 w^o}{\partial x\partial y}\right]$$

$$+2\frac{\partial^2}{\partial x\partial y}\left[B_{16}\frac{\partial u^o}{\partial x}+B_{26}\frac{\partial v^o}{\partial y}+B_{66}(\frac{\partial u^o}{\partial y}+\frac{\partial v^o}{\partial x})-D_{16}\frac{\partial^2 w^o}{\partial x^2}-D_{26}\frac{\partial^2 w^o}{\partial y^2}-2D_{66}\frac{\partial^2 w^o}{\partial x\partial y}\right]$$

$$+\frac{\partial}{\partial y^2}\left[B_{12}\frac{\partial u^o}{\partial x}+B_{22}\frac{\partial v^o}{\partial y}+B_{26}(\frac{\partial u^o}{\partial y}+\frac{\partial v^o}{\partial x})-D_{12}\frac{\partial^2 w^o}{\partial x^2}-D_{22}\frac{\partial^2 w^o}{\partial y^2}-2D_{26}\frac{\partial^2 w^o}{\partial x\partial y}\right]+q=0$$

(5.29)

Thus, carrying out some mathematical manipulations, we obtain;

$$
\begin{aligned}
&-B_{11}\frac{\partial^3 u^o}{\partial x^3}-(B_{12}+2B_{66})\frac{\partial^3 v^o}{\partial x^2\partial y}-3B_{16}\frac{\partial^3 u^o}{\partial x^2\partial y}-B_{16}\frac{\partial^3 v^o}{\partial x^3}\\
&+D_{11}\frac{\partial^4 w^o}{\partial x^4}+2(D_{12}+2D_{66})\frac{\partial^2 w^o}{\partial x^2\partial y^2}+4D_{16}\frac{\partial^4 w^o}{\partial x^3\partial y}\\
&-3B_{26}\frac{\partial^3 v^o}{\partial x\partial y^2}-(B_{12}+2B_{66})\frac{\partial^3 u^o}{\partial x\partial y^2}+4D_{26}\frac{\partial^4 w^o}{\partial x\partial y^3}\\
&-B_{22}\frac{\partial^3 v^o}{\partial y^3}-B_{26}\frac{\partial^3 u^o}{\partial y^3}+D_{22}\frac{\partial^4 w^o}{\partial y^4}=q
\end{aligned}
\qquad \textbf{(5.30)}
$$

5.4 Boundary Conditions in Terms of Displacements

Recalling from 5.2 and 5.3, we can obtain the boundary conditions in terms of displacements as follows: [22, 40]

1. At $x=\frac{a}{2}$

I. $A_{11}\frac{\partial u^o}{\partial x}+A_{12}\frac{\partial v^o}{\partial y}+A_{16}(\frac{\partial u^o}{\partial y}+\frac{\partial v^o}{\partial x})-B_{11}\frac{\partial^2 w^o}{\partial x^2}-B_{12}\frac{\partial^2 w^o}{\partial y^2}-2B_{16}\frac{\partial^2 w^o}{\partial x\partial y}=N_x^{\ +}$

or u^o must be specified.

II. $A_{16}\frac{\partial u^o}{\partial x}+A_{26}\frac{\partial v^o}{\partial y}+A_{66}(\frac{\partial u^o}{\partial y}+\frac{\partial v^o}{\partial x})-B_{16}\frac{\partial^2 w^o}{\partial x^2}-B_{26}\frac{\partial^2 w^o}{\partial y^2}-2B_{66}\frac{\partial^2 w^o}{\partial x\partial y}=N_{xy}^{\ +}$

or v^o must be specified.

III.
$$
\begin{aligned}
&B_{11}\frac{\partial^2 u^o}{\partial x^2}+(B_{12}+2B_{66})\frac{\partial^2 v^o}{\partial x\partial y}+B_{16}(3\frac{\partial^2 u^o}{\partial x\partial y}+\frac{\partial^2 v^o}{\partial x^2})\\
&-D_{11}\frac{\partial^3 w^o}{\partial x^3}-(D_{12}+4D_{66})\frac{\partial^3 w^o}{\partial x\partial y^2}-4D_{16}\frac{\partial^3 w^o}{\partial x^2\partial y}\\
&+2B_{26}\frac{\partial^2 v^o}{\partial y^2}+2B_{66}\frac{\partial^2 u^o}{\partial y^2}-2D_{26}\frac{\partial^3 w^o}{\partial y^3}=Q_x^{\ +}+\frac{\partial M_{xy}^{\ +}}{\partial y}
\end{aligned}
$$

or w^o must be specified.

IV. $B_{11}\frac{\partial u^o}{\partial x}+B_{12}\frac{\partial v^o}{\partial y}+B_{16}(\frac{\partial u^o}{\partial y}+\frac{\partial v^o}{\partial x})-D_{11}\frac{\partial^2 w^o}{\partial x^2}-D_{12}\frac{\partial^2 w^o}{\partial y^2}-2D_{16}\frac{\partial^2 w^o}{\partial x\partial y}=M_x^{\ +}$

or $\frac{\partial w^o}{\partial x}$ must be specified.

V.

2. At $x=-\frac{a}{2}$

I. $$A_{11}\frac{\partial u^o}{\partial x}+A_{12}\frac{\partial v^o}{\partial y}+A_{16}(\frac{\partial u^o}{\partial y}+\frac{\partial v^o}{\partial x})-B_{11}\frac{\partial^2 w^o}{\partial x^2}-B_{12}\frac{\partial^2 w^o}{\partial y^2}-2B_{16}\frac{\partial^2 w^o}{\partial x\partial y}=N_x^{\ -}$$

or u^o must be specified.

II. $$A_{16}\frac{\partial u^o}{\partial x}+A_{26}\frac{\partial v^o}{\partial y}+A_{66}(\frac{\partial u^o}{\partial y}+\frac{\partial v^o}{\partial x})-B_{16}\frac{\partial^2 w^o}{\partial x^2}-B_{26}\frac{\partial^2 w^o}{\partial y^2}-2B_{66}\frac{\partial^2 w^o}{\partial x\partial y}=N_{xy}^{\ -}$$

or v^o must be specified.

III. $$\begin{aligned}&B_{11}\frac{\partial^2 u^o}{\partial x^2}+(B_{12}+2B_{66})\frac{\partial^2 v^o}{\partial x\partial y}+B_{16}(3\frac{\partial^2 u^o}{\partial x\partial y}+\frac{\partial^2 v^o}{\partial x^2})\\ &-D_{11}\frac{\partial^3 w^o}{\partial x^3}-(D_{12}+4D_{66})\frac{\partial^3 w^o}{\partial x\partial y^2}-4D_{16}\frac{\partial^3 w^o}{\partial x^2\partial y}\\ &+2B_{26}\frac{\partial^2 v^o}{\partial y^2}+2B_{66}\frac{\partial^2 u^o}{\partial y^2}-2D_{26}\frac{\partial^3 w^o}{\partial y^3}=Q_x^{\ -}+\frac{\partial M_{xy}^{\ -}}{\partial y}\end{aligned}$$

or w^o must be specified.

IV. $$B_{11}\frac{\partial u^o}{\partial x}+B_{12}\frac{\partial v^o}{\partial y}+B_{16}(\frac{\partial u^o}{\partial y}+\frac{\partial v^o}{\partial x})-D_{11}\frac{\partial^2 w^o}{\partial x^2}-D_{12}\frac{\partial^2 w^o}{\partial y^2}-2D_{16}\frac{\partial^2 w^o}{\partial x.\partial y}=M_x^{\ -}$$

or $\frac{\partial w^o}{\partial x}$ must be specified.

3. At $y=+\frac{b}{2}$

I. $$A_{12}\frac{\partial u^o}{\partial x}+A_{22}\frac{\partial v^o}{\partial y}+A_{26}(\frac{\partial u^o}{\partial y}+\frac{\partial v^o}{\partial x})-B_{12}\frac{\partial^2 w^o}{\partial x^2}-B_{22}\frac{\partial^2 w^o}{\partial y^2}-2B_{26}\frac{\partial^2 w^o}{\partial x\partial y}=N_y^{\ +}$$

or v^o must be specified.

II. $$A_{16}\frac{\partial u^o}{\partial x}+A_{26}\frac{\partial v^o}{\partial y}+A_{66}(\frac{\partial u^o}{\partial y}+\frac{\partial v^o}{\partial x})-B_{16}\frac{\partial^2 w^o}{\partial x^2}-B_{26}\frac{\partial^2 w^o}{\partial y^2}-2B_{66}\frac{\partial^2 w^o}{\partial x\partial y}=N_{xy}^{\ +}$$

or u^o must be specified.

$$(B_{12}+2B_{66})\frac{\partial^2 u^o}{\partial x\partial y}+B_{22}\frac{\partial^2 v^o}{\partial y^2}+B_{26}\frac{\partial^2 u^o}{\partial y^2}+3B_{26}\frac{\partial^2 v^o}{\partial x\partial y}$$

III. $$-(D_{12}+4D_{66})\frac{\partial^3 w^o}{\partial x^2\partial y}-D_{22}\frac{\partial^3 w^o}{\partial y^3}-4D_{26}\frac{\partial^3 w^o}{\partial x\partial y^2}+2B_{16}\frac{\partial^2 u^o}{\partial x^2}$$

$$+2B_{66}\frac{\partial^2 v^o}{\partial x^2}-2D_{16}\frac{\partial^3 w^o}{\partial x^3}=Q_y^{+}+\frac{\partial M_{xy}^{+}}{\partial y}$$

or w^o must be specified.

IV. $$B_{12}\frac{\partial u^o}{\partial x}+B_{22}\frac{\partial v^o}{\partial y}+B_{26}(\frac{\partial u^o}{\partial y}+\frac{\partial v^o}{\partial x})-D_{12}\frac{\partial^2 w^o}{\partial x^2}-D_{22}\frac{\partial^2 w^o}{\partial y^2}-2D_{26}\frac{\partial^2 w^o}{\partial x\partial y}=M_y^{+}$$

or $\frac{\partial w^o}{\partial y}$ must be specified.

4. At $y=-\frac{b}{2}$

I. $$A_{12}\frac{\partial u^o}{\partial x}+A_{22}\frac{\partial v^o}{\partial y}+A_{26}(\frac{\partial u^o}{\partial y}+\frac{\partial v^o}{\partial x})-B_{12}\frac{\partial^2 w^o}{\partial x^2}-B_{22}\frac{\partial^2 w^o}{\partial y^2}-2B_{26}\frac{\partial^2 w^o}{\partial x\partial y}=N_y^{-}$$

or v^o must be specified.

II. $$A_{16}\frac{\partial u^o}{\partial x}+A_{26}\frac{\partial v^o}{\partial y}+A_{66}(\frac{\partial u^o}{\partial y}+\frac{\partial v^o}{\partial x})-B_{16}\frac{\partial^2 w^o}{\partial x^2}-B_{26}\frac{\partial^2 w^o}{\partial y^2}-2B_{66}\frac{\partial^2 w^o}{\partial x\partial y}=N_{xy}^{-}$$

or u^o must be specified.

$$(B_{12}+2B_{66})\frac{\partial^2 u^o}{\partial x\partial y}+B_{22}\frac{\partial^2 v^o}{\partial y^2}+B_{26}\frac{\partial^2 u^o}{\partial y^2}+3B_{26}\frac{\partial^2 v^o}{\partial x\partial y}$$

III. $$-(D_{12}+4D_{66})\frac{\partial^3 w^o}{\partial x^2\partial y}-D_{22}\frac{\partial^3 w^o}{\partial y^3}-4D_{26}\frac{\partial^3 w^o}{\partial x\partial y^2}+2B_{16}\frac{\partial^2 u^o}{\partial x^2}$$

$$+2B_{66}\frac{\partial^2 v^o}{\partial x^2}-2D_{16}\frac{\partial^3 w^o}{\partial x^3}=Q_y^{-}+\frac{\partial M_{xy}^{-}}{\partial y}$$

or w^o must be specified.

IV. $$B_{12}\frac{\partial u^o}{\partial x}+B_{22}\frac{\partial v^o}{\partial y}+B_{26}(\frac{\partial u^o}{\partial y}+\frac{\partial v^o}{\partial x})-D_{12}\frac{\partial^2 w^o}{\partial x^2}-D_{22}\frac{\partial^2 w^o}{\partial y^2}-2D_{26}\frac{\partial^2 w^o}{\partial x\partial y}=M_y^{-}$$

or $\frac{\partial w^o}{\partial y}$ must be specified.

6 PLATE PROBLEM SOLUTION

Utilizing the governing differential equations and the corresponding boundary conditions detailed in Section 5, solution for simply supported, rectangular laminated composite plates under evenly distributed out-of-plane pressure can be obtained.

We assume that the laminates are symmetric, balanced and cross-ply at the same time. However, this is actually the only case where the pre-defined governing differential equations can be solved analytically.

Laminates are called symmetric if there is symmetry of layers, having the same properties, with respect to the reference surface. These properties are obviously thickness, material properties and fiber orientations. On the other hand, laminates are called balanced if every layer has its pair with the opposite fiber orientation somewhere on the opposite of the laminate with respect to the reference surface. Laminates are called cross-ply if layers are oriented either at 0^o or 90^o.

6.1 Simplified Governing Differential Equations

For symmetric, balanced and cross-ply laminates, we have $A_{11} = A_{26} = D_{16} = D_{26} = B_{ij} = 0$ ($i = 1,2,3$). Thus, the governing differential equations (5.26), (5.28) and (5.30) simplify to:

$$A_{11}\frac{\partial^2 u^o}{\partial x^2} + A_{66}\frac{\partial^2 u^o}{\partial y^2} + (A_{12} + A_{66})\frac{\partial^2 v^o}{\partial x \partial y} = 0 \tag{6.1}$$

$$(A_{12} + A_{66})\frac{\partial^2 u^o}{\partial x \partial y} + A_{66}\frac{\partial^2 v^o}{\partial x^2} + A_{22}\frac{\partial^2 v^o}{\partial y^2} = 0 \tag{6.2}$$

$$D_{11}\frac{\partial^4 w^o}{\partial x^4} + 2(D_{12} + 2D_{66})\frac{\partial^4 w^o}{\partial x^2 \partial y^2} + D_{22}\frac{\partial^4 w^o}{\partial y^4} = q_o \tag{6.3}$$

6.2 Simplified Boundary Conditions

In addition to the simplification due to null constants, boundary conditions detailed in section 5.4 further simply to:

1. At $x = \pm \frac{a}{2}$

I. $$N_x = A_{11} \frac{\partial u^o}{\partial x} + A_{12} \frac{\partial v^o}{\partial y} = 0 \qquad \textbf{(6.4)}$$

II. $$N_{xy} = A_{66} (\frac{\partial u^o}{\partial y} + \frac{\partial v^o}{\partial x}) = 0 \qquad \textbf{(6.5)}$$

III. $$w^o = 0 \qquad \textbf{(6.6)}$$

IV. $$M_x = -\left[D_{11} \frac{\partial^2 w^o}{\partial x^2} + D_{12} \frac{\partial^2 w^o}{\partial y^2} \right] = 0 \qquad \textbf{(6.7)}$$

2. At $y = \pm \frac{b}{2}$

I. $$N_y = A_{12} \frac{\partial u^o}{\partial x} + A_{22} \frac{\partial v^o}{\partial y} = 0 \qquad \textbf{(6.8)}$$

II. $$N_{xy} = A_{66} (\frac{\partial u^o}{\partial y} + \frac{\partial v^o}{\partial x}) = 0 \qquad \textbf{(6.9)}$$

III. $$w^o = 0 \qquad \textbf{(6.10)}$$

IV. $$M_y = -\left[D_{12} \frac{\partial^2 w^o}{\partial x^2} + D_{22} \frac{\partial^2 w^o}{\partial y^2} \right] \qquad \textbf{(6.11)}$$

6.3 Solution of the Differential Equations Given the Boundary Conditions

The solution of the governing differential equations (6.1), (6.2) and (6.3), given the boundary conditions detailed in 6.2, is obtained by the Navier Solution utilizing the double Fourier Series. [45] That is;

$$w^o(x, y) = \sum_{m=1,3}^{\infty} \sum_{n=1,3}^{\infty} w_{mn} \cos(\frac{m\pi x}{a}) \cos(\frac{n\pi y}{b}) \qquad \textbf{(6.12)}$$

where,

$$w_{mn} = 16q_o \frac{(-1)^{\frac{m+n}{2}-1}}{mn\pi^6\left[D_{11}\left(\frac{m}{a}\right)^4 + 2(D_{12}+2D_{66})\left(\frac{m}{a}\right)^2\left(\frac{n}{b}\right)^2 + D_{22}\left(\frac{n}{b}\right)^4\right]} \tag{6.14}$$

Considering the above summation up to $m = n = 7$ is sufficient to obtain accurate enough results.

7 ANALYTICAL SOLUTION TOOL

Based on the Classical Lamination Theory and based on the findings on fiber reinforced laminated plates as detailed earlier throughout the study, an analytical solution computer code has been developed for the solution of rectangular simply supported symmetric and balanced laminated plates under uniform out of plane pressure. The tool can easily be tailored to solve for the other boundary and loading conditions. However, the tool is capable of presenting fairly accurate results for sandwich laminated plate problems.

7.1 Analytical Tool Flow Chart

The below flow chart outlines the major steps of the analytical tool. Details of some selected steps are summarized below:

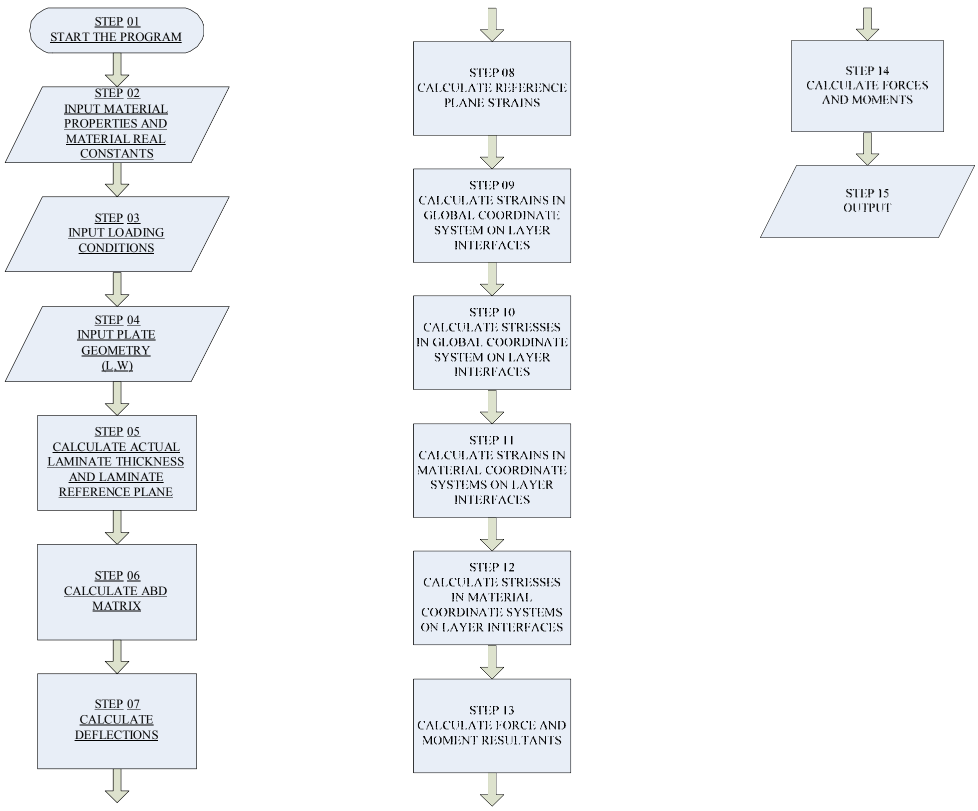

Figure 7.1: Analytical Tool Flow Chart

7.2 Flow Charts' Step Details

STEP 02 : The following material properties and real constants are supplied for each layer the laminate consists of at this step:

- E_1 : Elasticity modulus along the material axis 1 (N/mm^2)
- E_2 : Elasticity modulus along the material axis 2 (N/mm^2)
- E_3 : Elasticity modulus along the material axis 3 (N/mm^2)
- ν_{12} : Poisson ratio 1-2
- ν_{13} : Poisson ratio 1-3
- ν_{23} : Poisson ratio 2-3
- G_{12} : Shear modulus 1-2 (N/mm^2)
- G_{13} : Shear modulus 1-3 (N/mm^2)
- G_{23} : Shear modulus 2-3 (N/mm^2)
- t : Ply thickness (mm)
- θ : Angle between material axis 1 and global axis x

STEP 03 : The default loading is defined as the pressure along z axis, P_z (N/mm^2)

STEP 04 : The below plate dimensions are specified at this step:

- L : Length of the plate, along global axis x, (mm)
- W : Width of the plate, along global axis y, (mm)

STEP 15 : Following output are obtained for each layer the laminate consists of at any location within the plate boundaries at this step:

f_x : Force resultant along the global axis x (N/mm)

f_y : Force resultant along the global axis y (N/mm)

m_x : Moment resultant along the global axis x (N)

m_y : Moment resultant along the global axis y (N)

F_x : Force along the global axis x (N)

F_y : Force along the global axis y (N)

M_x : Moment along the global axis x ($N.mm$)

M_y : Moment along the global axis y ($N.mm$)

σ_x : Stress along the global axis x (N/mm^2)

σ_y : Stress along the global axis y (N/mm^2)

τ_{xy} : Shear stress in global xy plane (N/mm^2)

σ_1 : Stress along the material axis 1 (N/mm^2)

σ_2 : Stress along the global axis 2 (N/mm^2)

σ_{12} : Shear stress in global 1-2 plane (N/mm^2)

w_o : Deflection along the global axis z

8 CONCLUSION AND DISCUSSIONS

Within the context of this thesis a computer code based on CLPT for the analysis of composite sandwich plates is developed. Code results were verified with an experiment. Various plate configurations were analyzed with the code and Ansys 9.0. Code results and FEA results were compared and results are published in Appendix A. Findings are summarized below.

For the rectangular plate configuration case, experimental results and the analytical solution tool results well coincide with each other. Thus, the analytical tool can be considered reliable.

8.1 Trapezoidal Plate Configuration

As can be noticed from the tables and the graphs in Appendix A, for trapezoidal plate configuration, both the stress and deflection values are sensitive to plate geometrical variation, as a function of α, of this sort. Results for both facings of the sandwich plate are affected identically. However up to $\alpha \cong 15^o$, since the deviation of the results is comparably insignificant (less than 10%) , trapezoidal plates can be approximated by equivalent rectangular plates. Thus, the utilization of the analytical approach can be considered reliable.

8.2 Curved Plate Configuration

As for the trapezoidal plate, tables and the graphs for the curved plate configuration in Appendix A show that both the stress and deflection values are sensitive to plate geometrical variation up to some degree. Results for both facings of the sandwich plate are affected, on the contrary dissimilarly in this case. There is much more deviation in results on the facings of the panels where the laminates are subject to tension. However, beyond $R \cong 1000mm$, since the deviation of the results is comparably insignificant (less than 10%), curved rectangular plates can be approximated by equivalent flat rectangular plates. Thus, the utilization of the analytical approach can be considered reliable in this case as well.

9 RECOMMENDATIONS FOR FUTURE STUDY

Within the context of this thesis, a methodology to analytically analyze the mechanical behavior of symmetric and balanced laminated composite sandwich plates, under small deflection assumption, is examined. This methodology is based on CLPT which is an ESL approach. However, the methodology ignored the core shear effects. On the other hand, the problem defined in the thesis is limited to a certain boundary condition and a certain loading condition.

Within the context of a possible future study, the effect various boundary conditions and various loading conditions can be analyzed utilizing the same methodology. Moreover, the effect of core shear can also be incorporated. On the other hand, 3-D layer-wise theories should also be examined to obtain more accurate results especially for local mechanical behavior analysis.

Nevertheless, it should be kept in mind that, analytical approaches are limited to certain problems involving certain structural geometries. For the analysis of more complicated geometries of real life structures, FEA is the inevitable alternative. Therefore, a future study can aim to examine the methodologies of FEA to provide with practical solution tools.

REFERENCES

[1] **Zenkert, D.**, 1997. An Introduction to Sandwich Construction, EMAS Ltd., London.

[2] **Zenkert, D.**, 1997. Composites and Sandwich Structures, EMAS Ltd., London.

[3] **Diab AB**, 1995. Divinycell Technical Manual, Sweden.

[4] **ASM Handbook**, 2001. Volume 21, Composites, ASM International, USA.

[5] **Gay, D.** and Hoa, S. V., and Tsai, S. W., 2003. Composite Materials Design and Applications, CRC Press LLC, USA.

[6] **Hexcel Corporation**, HexWeb Honeycomb Sandwich Design Technology, 2000.

[7] **Smith, C. S.**, 1990. Design of Marine Structures in Composite Materials, Elsevier Science Publishing Co., Inc., Belfast.

[8] **Vinson Jack R.**, 1999. The Behavior of Sandwich Structures of Isotropic and Composite Materials, Technomic Publishing Company, Inc., Lancaster.

[9] **Allen, H. G.**, 1969. Analysis and Design of Structural Sandwich Panels, Pergamon Press Inc., Hungary.

[10] **Plantema, F. J.**, 1966. The Bending and Buckling of Sandwich Beams, Plates and Shells, John Wiley and Sons, Inc., Newyork.

[11] **Garrard, A.**, 1946. Theory of Sanddwich Construction I., Brit. Plastics, vol. 18, pp. 380-388.

[12] **Garrard, A.**, 1946. Theory of Sandwich Construction II., Brit. Plastics, vol. 18, pp. 451-458.

[13] **Hoff, N. J.** and Mautner, S. E., 1944. Sandwich Construction, Aero. Eng. Rev., vol. 3, pp. 29-43.

[14] **Reissner, E.**, 1948. “Finite Deflections of Sandwich Plates”, Journal of Aeronautical Sciences, Vol. 15, No.7, 435-440.

[15] **Libove, C.** and Batdorf, S. B., 1948. A General Samll Deflection Theory for Flat Sandwich Plates, NACA TN-2225, Washington DC.

[16] **Eringen, C.**, 1952. Bending and Buckling of Rectangular Sandwich Plates, Proc. I. U.S. Nat. Congr. Applied Mechanics, New York.

[17] **Bitzer, T. N.**, 1997. Honeycomb Technology, Champman and Hall, London.

[18] **Corden, J.**, 1995. Honeycomb Structures, ASM Handbook I. Composites, pp. 721-728.

[19] **Marshall, A. C.**, 1990. Core Composite and Sandwich Structures, International Encyclopedia of Composites, vol. I, pp. 488-507. VCH Publishers, New York.

[20] **Frostig, Y.**, 1998. Inaccuracies and Validity of Simplified Models in the Theory of Sandwich Structures, Sandwich Construction: 4 Proc. 4th Int. Conf. Sandwich Construction, Stockholm, June 8-12, pp. 167-189, EMAS Publishing, London.

[21] **Librescu, L.** and Hause, T., 2000. Recent Developments in the Modeling and Behavior of Advanced Sandwich Constructions: A Survey, Compos. Struct., vol. 48, pp. 1-17.

[22] **Reddy, J. N.**, 1997. Mechanics of Laminated Composite Plates Theory and Analysis, CRC Press LLC, USA.

[23] **Barut, A.**, Madenci, E., Anderson, T. and Tessler, A., 2002. Equivalent Single-Layer Theory for a Complete Stress Field in Sandwich Panels Under Arbitrarily Distributed Loading, Compos. Struct., vol. 58, pp. 483-495.

[24] **Barut, A.**, Madenci, E., Heinrich, J. and Tessler, A., 2001. Analysis of Thick Sandwich Construction by $\{3,2\}$-Order Theory, Int. J. Solid Struct., vol. 38, pp. 6063-6067.

[25] **Cook, G. M.** and Tessler, A., 1998. A $\{3,2\}$ Order Bending Theory for Laminated Composite and Sandwich Beams, Compos. Part B.-Eng., vol. 29, pp. 565-576.

[26] **Meunier, M.**and Shenoi, R. A., 1999. Free Vibration Analysis of Composite Sandwich Plates, Proc. Inst. Mech. Eng., vol. 213, pp.715-727.

[27] **Meunier, M.** and Shenoi, R. A., 2001. Dynamic Analysis of Composite Sandwich Plates with Damping Modelled Using Higher-Order Shear Deformation Theory, Compos. Struct., vol. 54, pp. 243-254.

[28] **Reddy, J. N.**, 1984. A Simple Higher Order Theory for Laminated Plates, J. Appl. Mech., vol. 51, pp. 745-752.

[29] **Swanson, S. R.**, 1999. An Examination of Higher Order Theory for Sandwich Beams, Compos. Struct., vol. 44, pp. 169-177.

[30] **Pierce, T. R. A.** and Webber, J. P. H., 1972. Buckling of Sandwich Panels with Laminated Face Plates, Aeronaut. Quart., vol. 23, pp. 148-160.

[31] **Pierce, T. R. A.** and Webber, J. P. H., 1973. Experimental Buckling Loads of Sandwich Panels with Carbon Fiber Face Plates, Aeronaut. Quart., vol. 24, pp. 295-312.

[32] **Roa, K. M.** and Meyer-Piening, H. R., 1991. Analysis of Sandwich Plates Using a Hybrid Stress Finite Element, AIAA J., vol. 29, pp. 1498-1506.

[33] **Carrera, E.**, 1998. A Refined Multilayered Finite-Element Model Applied to Linear and Non-Linear Analysis of Sandwich Plates, Compos. Sci. Technol., vol. 58, pp. 1553-1569.

[34] **Ferreira, A. J. M.**, Barbosa, J. T., Cesar de Sa, J. and Marques Torres, A., 1998. Geometric Non-Linear Analysis of Sandwich Structures, Sandwich Construction 4, Proc. 4th Int. Conf. Sandwich Construction, Stockholm, June 8-12, pp. 327-339, EMAS Publishing, London.

[35] **Ferreira, A. J. M.**, Barbosa, J. T., Cesar de Sa, J. and Marques Torres, A., 2000. Non-Linear Analysis of Sandwich Shells: The effect of Core Plasticity, Comput. Struct., vol. 76, pp. 337-346.

[36] **Bisplinghoff, R. L.**, Mar, J. W., and Pian, T. H. H., 1965. Statics of Deformable Solids, Addison Wesley, Massachusetts.

[37] **Boresi, A. P.** and Chong, K. P., 2000. Elasticity in Engineering Mechanics, John Wiley and Sons, Inc., USA.

[38] **Fung, Y. C.**, 1968. Foundations of Solid Mechanics, Y. C., 1968. Foundations of Solid Mechanics, Prentice-Hall of India Private Ltd., New Delhi.

[39] **Wang, C.**, 1953. Applied Elasticity, McGraw-Hill Book Co., Inc., New York.

[40] **Hyer, M. W.**, 1988. Stress Analysis of Fiber Reinforced Composite Materials, McGraw-Hill Book Co., Singapore.

[41] **Gibson, R. F.**, 1994. Principals of Composite Material Mechanics, McGraw-Hill Book Co., Inc., New York.

[42] **Ochoa, O. O.** and Reddy, J. N., 1992. Finite Element Analysis of Composite Laminates, Kluwer Academic Publishers, Netherlands.

[43] **Avallone, E. A.** and Baumeister, T., 1996. Marks' Standard Handbook for Mechanical Engineers Tenth Ed., McGraw-Hill Companies Inc., USA.

[44] **Timoshenko, S.**, and Woinowsky-Kreieger, S., 1959. Theory of Plates and Shells, McGraw-Hill Book Co., Inc., Toronto.

[45] **Yen, K. T.** and Güntürkün, S., and Pohle F. V., 1951. "Deflection of a simply Supported Rectangular Sandwich Plate Subject to Transverse Loads", NACA TN 2581.

[46] **Kreyszig, E.**, 1999. Advanced Engineering Mathematics, John Wiley and Sons., Inc., Singapore.

[47] **Glyn, J.**, Burley, D., Clements, D., Dyke, P., Searl, J. and Wright, J., 2001. Modern Engineering Mathematics, Pearson Education Ltd., Italy.

[48] **Chung, T. J.**, 1988. Continuum Mechanics, Prentice Hall, New Jersey.

[49] **Narasimhan, M. N. L.**, 1993. Principles of Continuum Mechanics, John Wiley and Sons, Inc., USA.

[50] **Housner, G. W.** and Vreeland T. Jr., 1966. The Analysis of Stress and Deformation, The Macmillan Company, USA.

[51] **Timoshenko, S. P.**, and Goodier J. N., 1970. Theory of Elasticity, McGraw-Hill Book Co., Inc., Singapore.

[52] **Ansys Inc.**, Ansys 9.0, Users' Manual.

[53] **Cheng, Q. H.**, Lee, H. P., and Lu, C., 2006. "A Numerical Approach for Evaluating Elastic Constants of Sandwich Structures with Various Cores", Composite Structures, 74 (2006), 226-236.

[54] **Chalmers, D. W.**, 1993. Ministry of Defence Design of Ships' Structures, HMSO, London.

[55] **DNV**, 2004. Rules for Classification of HSLC and NSC, Norway.

[56] **Donnell, L. H.**, 1976. Beams, Plates and Shells, McGraw-Hill Book Co., Inc., USA.

[57] **Heins, C. P.**, 1976. Applied Plate Theory for the Engineer, Lexington Books, Toronto.

[58] **Hildebrand, F. B.** and Reissner, E., and Thomas G. B., 1949. "Notes on the Foundations of the Theory of Small Displacements of Orthotropic Shells", NACA TN 1833.

[59] **Hoff, N. J.**, 1950. "Bending and Buckling of Rectangular Sandwich Plates", NACA TN 2225

[60] **Hollaway, L.**, 1994. Handbook of Polymer Composites for Engineers, Woodhead Publishing Ltd., Cambridge.

[61] **Hohe, J.** and Librescu, L., 2004. "Advances in Structural Modeling of Elastic Sandwich Panels", Mechanics of Advanced Materials and Structures, 11: 395-424.

[62] **March, H. W.**, 1952. "Behavior of a Rectangular Sandwich Panel under a Uniform Lateral Load and Compressive End Loads", U.S. Forest Products Laboratory Report 1834.

[63] **Nguyen, V.** and Caron, J. F., and Sab K., 2005. "A model for Thick Laminates and Sandwich Plates", Composite Science and Technology 65 (2005) 475-489.

[64] **Rao, K. M.**, 1985. Buckling Analysis of Anisotropic Sandwich Plates Faced with Fiber-Reinforced Plastics, AIAA J., vol. 23, pp. 1247-1253.

[65] **Pilkey, W. D.**, 2005. Formulas for Stress and Strain, John Wiley and Sons, Inc., USA.

[66] **Prager, W.**, 1961. Introduction to Mechanics of Continua, Ginn and Company, USA.

[67] **Reissner, E.**, 1984. Finite Deflections of Sandwich Plates, J. Aerospace Sci., vol. 15, pp.435-440.

[68] **Shenoi, H.** and Groves, A., and Rajapakse Y. D. S., 2005. Theory and Applications of Sandwich Structures, University of Southampton, Southampton.

[69] **Srinivas, S. R.**, Joga Rao C. V., and Rao, A. K., 1970. "An Exact Analysis for Vibration of Simply Supported Homogenous and Laminated Thick Rectangular Plates", Journal of Sound and Vibration, Vol. 12, 187-199.

[70] **Swaminathan, K.**, Ragounadin, D., 2004. "Analytical Solutions Using a Higher-order Refined Theory for the Static Analysis of Anti-symmetric Angle-ply Composite and Sandwich Plates", 64 (2004), 405-417.

[71] **Wendt, F. W.** and Liebowitz H., and Perrone, N., 1970. Mechanics of Composite Materials, Pergamon Press Inc., Hungary.

[72] **Yavuzbalkan, E.**, 2005. Free Vibration Analysis of Anisotropic Laminated Shells of Revolution, MSc. Thesis, Middle East Technical University, Ankara.

APPENDIXES

A PLATE SOLUTIONS

A.1 Reference Plate Details

A.1.1 Plate geometry

1000x1000mm rectangular constant thickness sandwich plate.

A.1.2 Construction

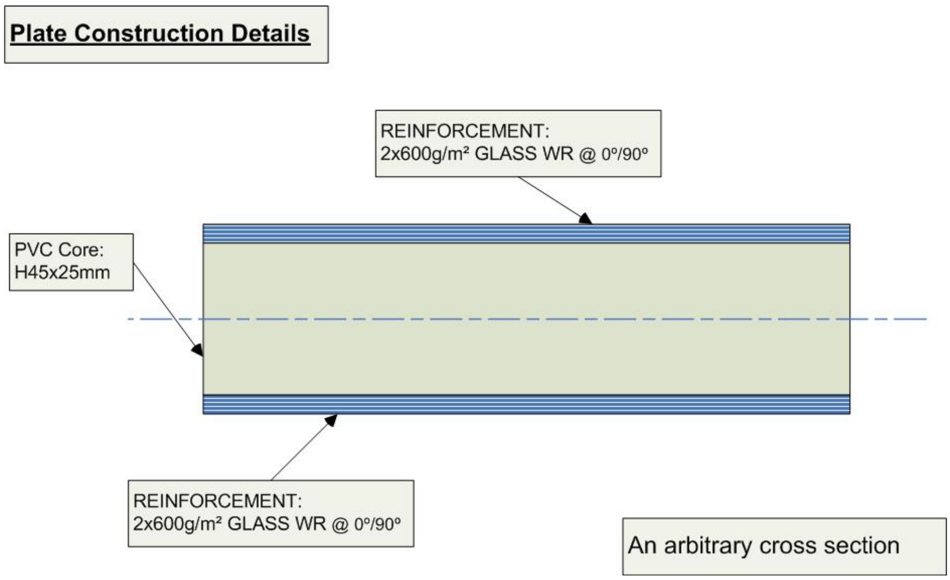

Figure A.1: Reference Plate Cross Section Details

A.1.3 Mechanical properties

1. Reinforcement Material:

   Assumed mechanical properties of the fiber reinforcement are as follows:

   Table A.1: Mechanical Properties of Fiber Reinforcement

E_1	18600	N/mm^2
E_2	5654	N/mm^2
E_3	5654	N/mm^2
ν_{xy}	0.254	
ν_{xz}	0.254	
ν_{yz}	0.428	
G_{xy}	1748	N/mm^2
G_{xz}	1748	N/mm^2
G_{yz}	1220	N/mm^2

2. Core Material:

   Assumed mechanical properties of the core material are as follows:

   Table A.2: Mechanical Properties of Core Material

   E : 50 N/mm^2

   ν : 0.35

A.2 Analytical Solution Tool Results vs. Experiment Results

Analytical solution tool and experiment results are as follows:

Table A.3: Analytical Tool vs. Experiment Results

	Plate configuration	α (deg.)	H (mm)	W_1 (mm)	W_2 (mm)		σ_{max} (N/mm2)			w_{max} (mm)		
Bottom Surface							Analytical	Experiment	Deviation (%)	Analytical	Experiment	Deviation (%)
	01	0	1000	1000	1000	Layer bottom stress	18,340	16,647	10,17%	7,147	8,444	15,36%
Top Surface	Plate configuration	α (deg.)	H (mm)	W_1 (mm)	W_2 (mm)		σ_{max} (N/mm2)			w_{max} (mm)		
							Analytical	Experiment	Deviation (%)	Analytical	Experiment	Deviation (%)
	01	0	1000	1000	1000	Layer top stress	-18,340	-16,368	12,05%	7,147	8,444	15,36%

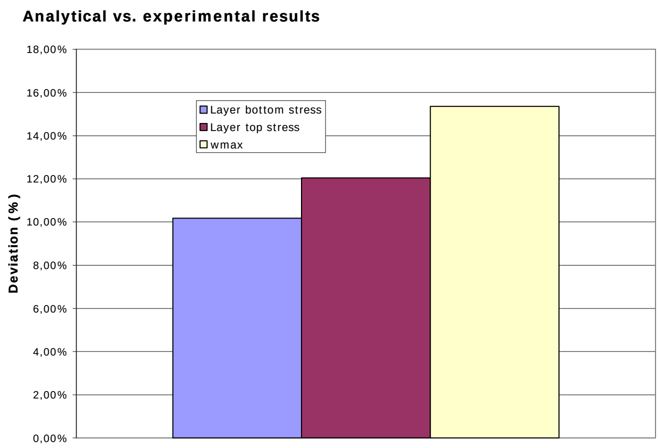

Figure A.2: Deviation, Analytical vs. Experiment Results

A.3 FEA Details

FEA is carried out utilizing Ansys 9.0/ Ansys Inc. commercial software.

A.3.1 Element properties

Table A.4: Element Properties

Element type	:	Shell 91
Maximum number of layers	:	16
Element coordinate system	:	Element orientation
Element output per layer	:	Top and bottom of layer
Interlaminar shear stress output	:	Excluded
Storage of layer data	:	All layers
Thick sandwich option	:	Exclude
Failure criteria print summary	:	Maximum
Node offset option	:	Nodes at midsurf

A.3.2 Mesh properties

Table A.5: Mesh Properties

Element edge length	:	50
Element shape	:	Quadratic

A.3.3 Edge conditions

Table A.6: Constraints on Edges along Direction x

ROTZ	:	Rotations about z axis
ROTY	:	Rotations about y axis
UZ	:	Translations along z axis

Table A.7: Constraints on Edges along Direction y

ROTZ	:	Rotations about z axis
ROTX	:	Rotations about x axis
UZ	:	Translations along z axis

A.3.4 Loading conditions

Table A.8: Loading Conditions

Load type	:	Pressure
Load setting	:	Constant value
Load direction	:	Along $+z$ axis
Load magnitude	:	0.005807 MPa

A.3.5 Type of analysis

Table A.9: Type of Analysis

Discipline	:	Structural
Method	:	H-method
Analysis	:	Linear static

A.4 Analytical Solution Tool Results vs. FEA Results for Trapezoidal Plates

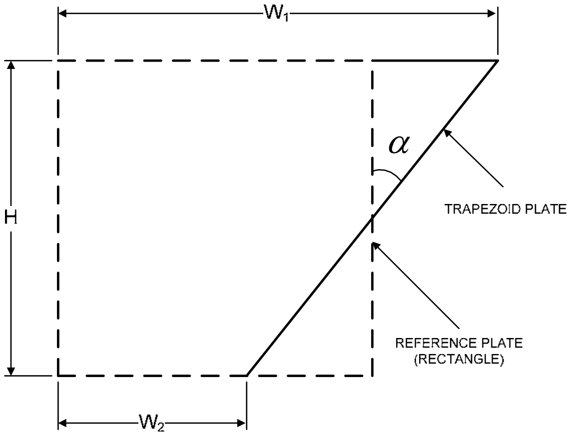

Figure A.3: Trapezoidal Plate Configuration

Analytical solution tool and FEA res. for each layer are as follows:

Table A.10: Analytical Tool vs. FEA Res. For Trapezoidal Plates for L.01

	Plate configuration	α (deg.)	H (mm)	W_1 (mm)	W_2 (mm)	$\sigma_{1\,max}$ (N/mm2)				$\sigma_{2\,max}$ (N/mm2)				w_{max} (mm)		
							Analytical	FEA	Deviation (%)		Analytical	FEA	Deviation (%)	Analytical	FEA	Deviation (%)
Layer 01	01	0	1000	1000	1000	Layer top	-18,340	-18,580	1,29%	Layer top	-6,480	-6,569	1,35%	7,147	7,274	1,75%
		0	1000	1000	1000	Layer bottom	-17,970	-18,204	1,29%	Layer bottom	-6,350	-6,436	1,34%			
	02	10	1000	1088	912	Layer top	-18,340	-18,185	0,85%	Layer top	-6,480	-6,344	2,14%	7,147	7,015	1,88%
		10	1000	1088	912	Layer bottom	-17,970	-17,817	0,86%	Layer bottom	-6,350	-6,216	2,16%			
	03	20	1000	1182	818	Layer top	-18,340	-17,169	6,82%	Layer top	-6,480	-5,577	16,19%	7,147	6,258	14,21%
		20	1000	1182	818	Layer bottom	-17,970	-16,822	6,82%	Layer bottom	-6,350	-5,464	16,21%			
	04	30	1000	1289	711	Layer top	-18,340	-15,834	15,83%	Layer top	-6,480	-4,995	29,73%	7,147	5,236	36,50%
		30	1000	1289	711	Layer bottom	-17,970	-15,514	15,83%	Layer bottom	-6,350	-4,894	29,75%			
	05	40	1000	1420	580	Layer top	-18,340	-13,598	34,87%	Layer top	-6,480	-4,367	48,39%	7,147	4,138	72,72%
		40	1000	1420	580	Layer bottom	-17,970	-13,323	34,88%	Layer bottom	-6,350	-4,279	48,41%			
	06	50	1000	1596	404	Layer top	-18,340	-11,269	62,75%	Layer top	-6,480	-3,834	69,01%	7,147	3,061	133,49%
		50	1000	1596	404	Layer bottom	-17,970	-11,041	62,76%	Layer bottom	-6,350	-3,757	69,03%			

Table A.11: Analytical Tool vs. FEA Res. for Trapezoidal Plates for L.02

	Plate configuration	α (deg.)	H (mm)	W_1 (mm)	W_2 (mm)	$\sigma_{1\,max}$ (N/mm2)				$\sigma_{2\,max}$ (N/mm2)				w_{max} (mm)		
							Analytical	FEA	Deviation (%)		Analytical	FEA	Deviation (%)	Analytical	FEA	Deviation (%)
Layer 02	01	0	1000	1000	1000	Layer top	-17,950	-18,186	1,30%	Layer top	-6,360	-6,441	1,25%	7,147	7,274	1,75%
						Layer bottom	-17,580	-17,180	2,33%	Layer bottom	-6,230	-6,308	1,23%			
	02	10	1000	1088	912	Layer top	-17,950	-17,521	2,45%	Layer top	-6,360	-6,289	1,13%	7,147	7.015	99,90%
						Layer bottom	-17,580	-17,159	2,45%	Layer bottom	-6,230	-6,159	1,15%			
	03	20	1000	1182	818	Layer top	-17,950	-15,788	13,69%	Layer top	-6,360	-5,865	8,45%	7,147	6,258	14,21%
						Layer bottom	-17,580	-15,462	13,70%	Layer bottom	-6,230	-5,744	8,47%			
	04	30	1000	1289	711	Layer top	-17,950	-14,029	27,95%	Layer top	-6,360	-5,351	18,86%	7,147	5,236	36,50%
						Layer bottom	-17,580	-13,739	27,96%	Layer bottom	-6,230	-5,240	18,88%			
	05	40	1000	1420	580	Layer top	-17,950	-12,505	43,54%	Layer top	-6,360	-4,570	39,17%	7,147	4,138	72,72%
						Layer bottom	-17,580	-12,247	43,55%	Layer bottom	-6,230	-4,476	39,19%			
	06	50	1000	1596	404	Layer top	-17,950	-10,888	64,86%	Layer top	-6,360	-3,722	70,89%	7,147	3,061	133,49%
						Layer bottom	-17,580	-10,663	64,87%	Layer bottom	-6,230	-3,645	70,92%			

Table A.12: Analytical Tool vs. FEA Res. for Trapezoidal Plates for L.03

	Plate configuration	α (deg.)	H (mm)	W_1 (mm)	W_2 (mm)	$\sigma_{1\,max}$ (N/mm2)				$\sigma_{2\,max}$ (N/mm2)				w_{max} (mm)		
							Analytical	FEA	Deviation (%)		Analytical	FEA	Deviation (%)	Analytical	FEA	Deviation (%)
Layer 03	01	0	1000	1000	1000	Layer top	-17,600	-17,828	1,28%	Layer top	-6,220	-6,303	1,32%	7,147	7,274	1,75%
						Layer bottom	-17,230	-17,453	1,28%	Layer bottom	-6,090	-6,171	1,31%			
	02	10	1000	1088	912	Layer top	-17,600	-17,450	0,86%	Layer top	-6,220	-6,088	2,17%	7,147	7.015	99,90%
						Layer bottom	-17,230	-17,082	0,87%	Layer bottom	-6,090	-5,959	2,19%			
	03	20	1000	1182	818	Layer top	-17,600	-16,475	6,83%	Layer top	-6,220	-5,474	13,64%	7,147	6,258	14,21%
						Layer bottom	-17,230	-16,128	6,83%	Layer bottom	-6,090	-5,239	16,25%			
	04	30	1000	1289	711	Layer top	-17,600	-15,193	15,84%	Layer top	-6,220	-4,793	29,78%	7,147	5,236	36,50%
						Layer bottom	-17,230	-14,873	15,85%	Layer bottom	-6,090	-4,692	29,80%			
	05	40	1000	1420	580	Layer top	-17,600	-13,048	34,89%	Layer top	-6,220	-4,190	48,43%	7,147	4,138	72,72%
						Layer bottom	-17,230	-12,773	34,89%	Layer bottom	-6,090	-4,102	48,46%			
	06	50	1000	1596	404	Layer top	-17,600	-10,813	62,77%	Layer top	-6,220	-3,679	69,06%	7,147	3,061	133,49%
						Layer bottom	-17,230	-10,585	62,78%	Layer bottom	-6,090	-3,602	69,09%			

Table A.13: Analytical Tool vs. FEA Res. for Trapezoidal Plates for L.04

	Plate configuration	α (deg.)	H (mm)	W_1 (mm)	W_2 (mm)	$\sigma_{1\,max}$ (N/mm2)				$\sigma_{2\,max}$ (N/mm2)				w_{max} (mm)		
							Analytical	FEA	Deviation (%)		Analytical	FEA	Deviation (%)	Analytical	FEA	Deviation (%)
Layer 04	01	0	1000	1000	1000	Layer top	-17,210	-17,454	1,40%	Layer top	-6,100	-6,175	1,21%	7,147	7,274	1,75%
						Layer bottom	-16,860	-17,060	1,17%	Layer bottom	-5,970	-6,042	1,19%			
	02	10	1000	1088	912	Layer top	-17,210	-16,797	2,46%	Layer top	-6,100	-6,029	1,17%	7,147	7.015	99,90%
						Layer bottom	-16,860	-16,436	2,58%	Layer bottom	-5,970	-5,900	1,19%			
	03	20	1000	1182	818	Layer top	-17,210	-15,136	13,70%	Layer top	-6,100	-5,623	8,49%	7,147	6,258	14,21%
						Layer bottom	-16,860	-14,810	13,84%	Layer bottom	-5,970	-5,502	8,51%			
	04	30	1000	1289	711	Layer top	-17,210	-13,450	27,96%	Layer top	-6,100	-5,130	18,91%	7,147	5,236	36,50%
						Layer bottom	-16,860	-13,160	28,12%	Layer bottom	-5,970	-5,020	18,93%			
	05	40	1000	1420	580	Layer top	-17,210	-11,989	43,55%	Layer top	-6,100	-4,382	39,22%	7,147	4,138	72,72%
						Layer bottom	-16,860	-11,731	43,72%	Layer bottom	-5,970	-4,287	39,25%			
	06	50	1000	1596	404	Layer top	-17,210	-10,438	64,88%	Layer top	-6,100	-3,568	70,96%	7,147	3,061	133,49%
						Layer bottom	-16,860	-10,214	65,07%	Layer bottom	-5,970	-3,491	71,00%			

Table A.14: Analytical Tool vs. FEA Res. for Trapezoidal Plates for L.05

	Plate configuration	α (deg.)	H (mm)	W_1 (mm)	W_2 (mm)	$\sigma_{1\,max}$ (N/mm2)				$\sigma_{2\,max}$ (N/mm2)				w_{max} (mm)		
							Analytical	FEA	Deviation (%)		Analytical	FEA	Deviation (%)	Analytical	FEA	Deviation (%)
Layer 05	01	0	1000	1000	1000	Layer top	-0,060	-0,064	6,54%	Layer top	-0,060	-0,064	6,54%	7,147	7,274	1,75%
						Layer bottom	0,060	0,064	6,54%	Layer bottom	0,060	0,064	6,54%			
	02	10	1000	1088	912	Layer top	-0,060	-0,063	4,28%	Layer top	-0,060	-0,063	4,31%	7,147	7.015	99,90%
						Layer bottom	0,060	0,063	4,28%	Layer bottom	0,060	0,063	4,31%			
	03	20	1000	1182	818	Layer top	-0,060	-0,058	3,22%	Layer top	-0,060	-0,056	7,18%	7,147	6,258	14,21%
						Layer bottom	0,060	0,058	3,22%	Layer bottom	0,060	0,056	7,18%			
	04	30	1000	1289	711	Layer top	-0,060	-0,053	13,66%	Layer top	-0,060	-0,049	23,66%	7,147	5,236	36,50%
						Layer bottom	0,060	0,053	13,66%	Layer bottom	0,060	0,049	23,66%			
	05	40	1000	1420	580	Layer top	-0,060	-0,045	33,63%	Layer top	-0,060	-0,043	40,81%	7,147	4,138	72,72%
						Layer bottom	0,060	0,045	33,63%	Layer bottom	0,060	0,043	40,81%			
	06	50	1000	1596	404	Layer top	-0,060	-0,036	65,15%	Layer top	-0,060	-0,037	61,86%	7,147	3,061	133,49%
						Layer bottom	0,060	0,036	65,15%	Layer bottom	0,060	0,037	61,86%			

Table A.15: Analytical Tool vs. FEA Res. for Trapezoidal Plates for L.06

	Plate configuration	α (deg.)	H (mm)	W_1 (mm)	W_2 (mm)	$\sigma_{1\,max}$ (N/mm2)				$\sigma_{2\,max}$ (N/mm2)				w_{max} (mm)		
							Analytical	FEA	Deviation (%)		Analytical	FEA	Deviation (%)	Analytical	FEA	Deviation (%)
Layer 06	01	0	1000	1000	1000	Layer top	16,860	17,060	1,17%	Layer top	5,970	6,042	1,19%	7,147	7,274	1,75%
						Layer bottom	17,210	17,454	1,40%	Layer bottom	6,100	6,175	1,21%			
	02	10	1000	1088	912	Layer top	16,860	16,436	2,58%	Layer top	5,970	5,900	1,19%	7,147	7.015	99,90%
						Layer bottom	17,210	16,797	2,46%	Layer bottom	6,100	6,029	1,17%			
	03	20	1000	1182	818	Layer top	16,860	14,810	13,84%	Layer top	5,970	5,502	8,51%	7,147	6,258	14,21%
						Layer bottom	17,210	15,136	13,70%	Layer bottom	6,100	5,623	8,49%			
	04	30	1000	1289	711	Layer top	16,860	13,160	28,12%	Layer top	5,970	5,020	18,93%	7,147	5,236	36,50%
						Layer bottom	17,210	13,450	27,96%	Layer bottom	6,100	5,130	18,91%			
	05	40	1000	1420	580	Layer top	16,860	11,731	43,72%	Layer top	5,970	4,287	39,25%	7,147	4,138	72,72%
						Layer bottom	17,210	11,989	43,55%	Layer bottom	6,100	4,382	39,22%			
	06	50	1000	1596	404	Layer top	16,860	10,214	65,07%	Layer top	5,970	3,491	71,00%	7,147	3,061	133,49%
						Layer bottom	17,210	10,438	64,88%	Layer bottom	6,100	3,568	70,96%			

Table A.16: Analytical Tool vs. FEA Res. for Trapezoidal Plates for L.07

	Plate configuration	α (deg.)	H (mm)	W_1 (mm)	W_2 (mm)		$\sigma_{1\,max}$ (N/mm2)				$\sigma_{2\,max}$ (N/mm2)			w_{max} (mm)		
							Analytical	FEA	Deviation (%)		Analytical	FEA	Deviation (%)	Analytical	FEA	Deviation (%)
Layer 07	01	0	1000	1000	1000	Layer top	17,230	17,453	1,28%	Layer top	6,090	6,171	1,31%	7,147	7,274	1,75%
						Layer bottom	17,600	17,828	1,28%	Layer bottom	6,220	6,303	1,32%			
	02	10	1000	1088	912	Layer top	17,230	17,082	0,87%	Layer top	6,090	5,959	2,19%	7,147	7.015	99,90%
						Layer bottom	17,600	17,450	0,86%	Layer bottom	6,220	6,088	2,17%			
	03	20	1000	1182	818	Layer top	17,230	16,128	6,83%	Layer top	6,090	5,239	16,25%	7,147	6,258	14,21%
						Layer bottom	17,600	16,475	6,83%	Layer bottom	6,220	5,474	13,64%			
	04	30	1000	1289	711	Layer top	17,230	14,873	15,85%	Layer top	6,090	4,692	29,80%	7,147	5,236	36,50%
						Layer bottom	17,600	15,193	15,84%	Layer bottom	6,220	4,793	29,78%			
	05	40	1000	1420	580	Layer top	17,230	12,773	34,89%	Layer top	6,090	4,102	48,46%	7,147	4,138	72,72%
						Layer bottom	17,600	13,048	34,89%	Layer bottom	6,220	4,190	48,43%			
	06	50	1000	1596	404	Layer top	17,230	10,585	62,78%	Layer top	6,090	3,602	69,09%	7,147	3,061	133,49%
						Layer bottom	17,600	10,813	62,77%	Layer bottom	6,220	3,679	69,06%			

Table A.17: Analytical Tool vs. FEA Res. for Trapezoidal Plates for L.08

	Plate configuration	α (deg.)	H (mm)	W_1 (mm)	W_2 (mm)		$\sigma_{1\,max}$ (N/mm2)				$\sigma_{2\,max}$ (N/mm2)			w_{max} (mm)		
							Analytical	FEA	Deviation (%)		Analytical	FEA	Deviation (%)	Analytical	FEA	Deviation (%)
Layer 08	01	0	1000	1000	1000	Layer top	17,580	-17,180	2,33%	Layer top	6,230	6,308	1,23%	7,147	7,274	1,75%
						Layer bottom	17,950	-18,186	1,30%	Layer bottom	6,360	6,441	1,25%			
	02	10	1000	1088	912	Layer top	17,580	-17,159	2,45%	Layer top	6,230	6,159	1,15%	7,147	7.015	99,90%
						Layer bottom	17,950	-17,521	2,45%	Layer bottom	6,360	6,289	1,13%			
	03	20	1000	1182	818	Layer top	17,580	-15,462	13,70%	Layer top	6,230	5,744	8,47%	7,147	6,258	14,21%
						Layer bottom	17,950	-15,788	13,69%	Layer bottom	6,360	5,865	8,45%			
	04	30	1000	1289	711	Layer top	17,580	-13,739	27,96%	Layer top	6,230	5,240	18,88%	7,147	5,236	36,50%
						Layer bottom	17,950	-14,029	27,95%	Layer bottom	6,360	5,351	18,86%			
	05	40	1000	1420	580	Layer top	17,580	-12,247	43,55%	Layer top	6,230	4,476	39,19%	7,147	4,138	72,72%
						Layer bottom	17,950	-12,505	43,54%	Layer bottom	6,360	4,570	39,17%			
	06	50	1000	1596	404	Layer top	17,580	-10,663	64,87%	Layer top	6,230	3,645	70,92%	7,147	3,061	133,49%
						Layer bottom	17,950	-10,888	64,86%	Layer bottom	6,360	3,722	70,89%			

Table A.18: Analytical Tool vs. FEA Res. for Trapezoidal Plates for L.09

	Plate configuration	α (deg.)	H (mm)	W_1 (mm)	W_2 (mm)		$\sigma_{1\,max}$ (N/mm2)				$\sigma_{2\,max}$ (N/mm2)			w_{max} (mm)		
							Analytical	FEA	Deviation (%)		Analytical	FEA	Deviation (%)	Analytical	FEA	Deviation (%)
Layer 09	01	0	1000	1000	1000	Layer top	17,970	18,204	1,29%	Layer top	6,350	6,436	1,34%	7,147	7,274	1,75%
						Layer bottom	18,340	18,580	1,29%	Layer bottom	6,480	6,569	1,35%			
	02	10	1000	1088	912	Layer top	17,970	17,817	0,86%	Layer top	6,350	6,216	2,16%	7,147	7.015	99,90%
						Layer bottom	18,340	18,185	0,85%	Layer bottom	6,480	6,344	2,14%			
	03	20	1000	1182	818	Layer top	17,970	16,822	6,82%	Layer top	6,350	5,464	16,21%	7,147	6,258	14,21%
						Layer bottom	18,340	17,169	6,82%	Layer bottom	6,480	5,577	16,19%			
	04	30	1000	1289	711	Layer top	17,970	15,514	15,83%	Layer top	6,350	4,894	29,75%	7,147	5,236	36,50%
						Layer bottom	18,340	15,834	15,83%	Layer bottom	6,480	4,995	29,73%			
	05	40	1000	1420	580	Layer top	17,970	13,323	34,88%	Layer top	6,350	4,279	48,41%	7,147	4,138	72,72%
						Layer bottom	18,340	13,598	34,87%	Layer bottom	6,480	4,367	48,39%			
	06	50	1000	1596	404	Layer top	17,970	11,041	62,76%	Layer top	6,350	3,757	69,03%	7,147	3,061	133,49%
						Layer bottom	18,340	11,269	62,75%	Layer bottom	6,480	3,834	69,01%			

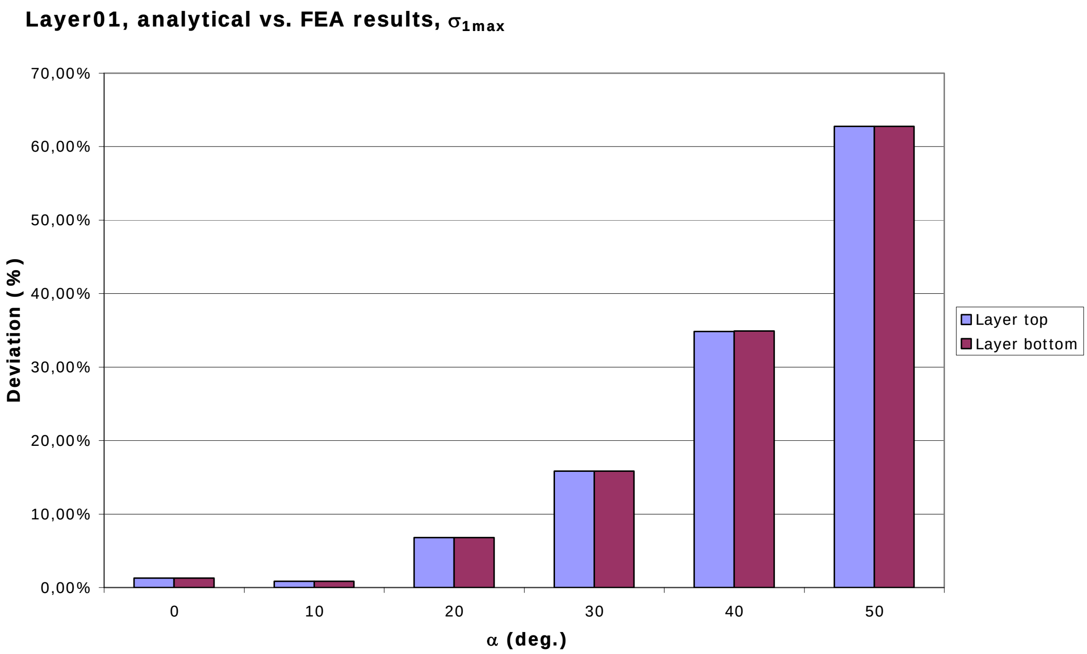

Figure A.4: Analytical Tool vs. FEA for Trapezoidal Plates for $\sigma_{1\max}$ of L.01

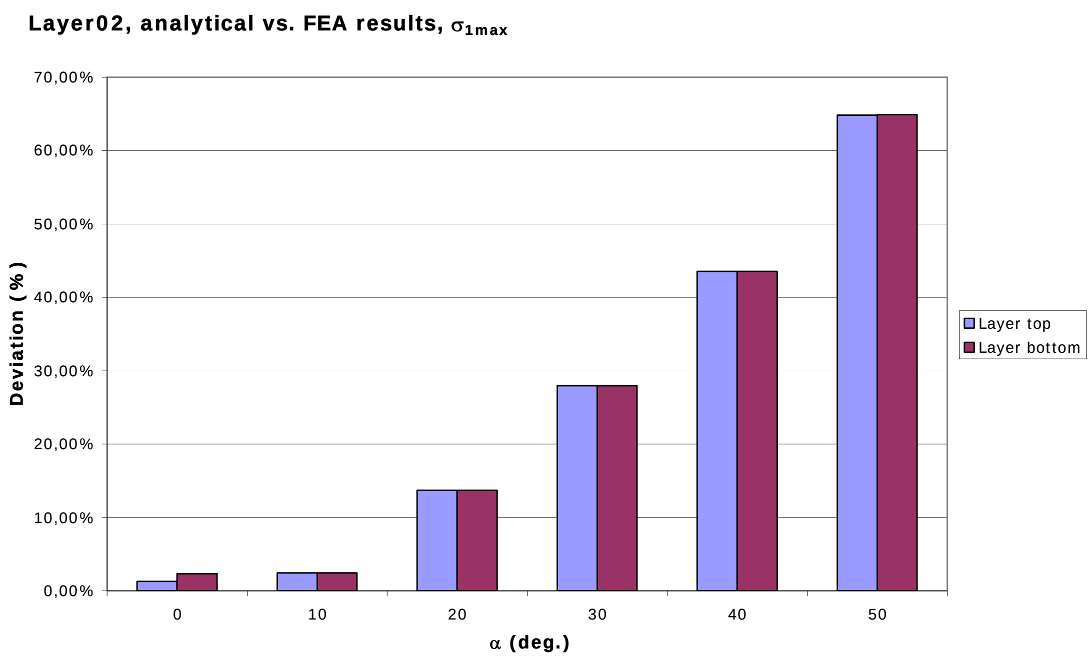

Figure A.5: Analytical Tool vs. FEA for Trapezoidal Plates for $\sigma_{1\max}$ of L.02

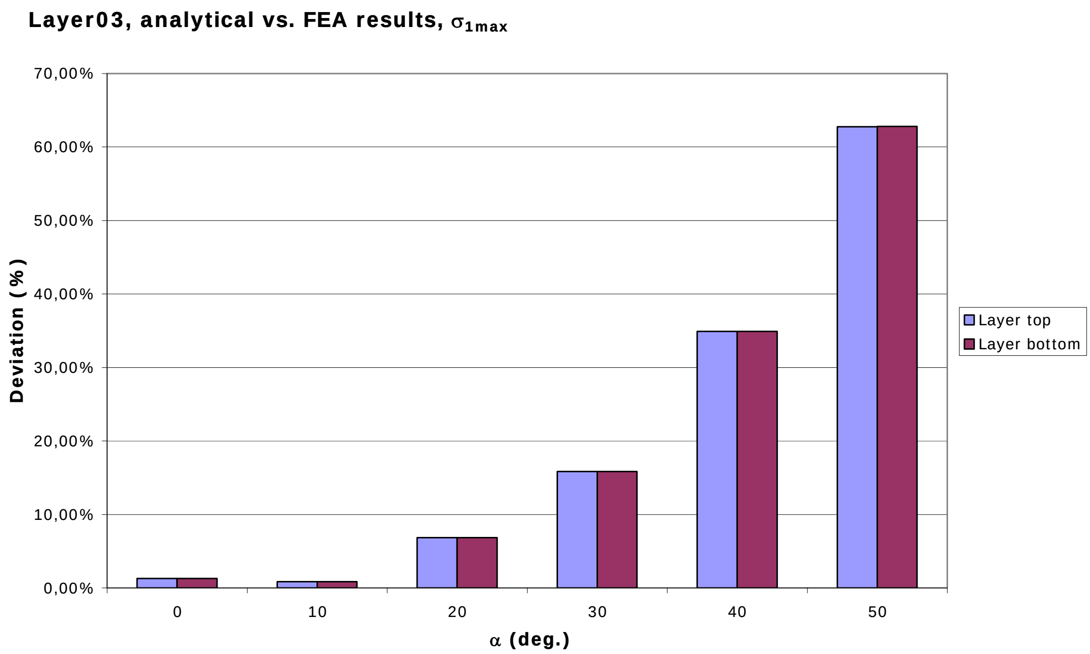

Figure A.6: Analytical Tool vs. FEA for Trapezoidal Plates for $\sigma_{1\max}$ of L.03

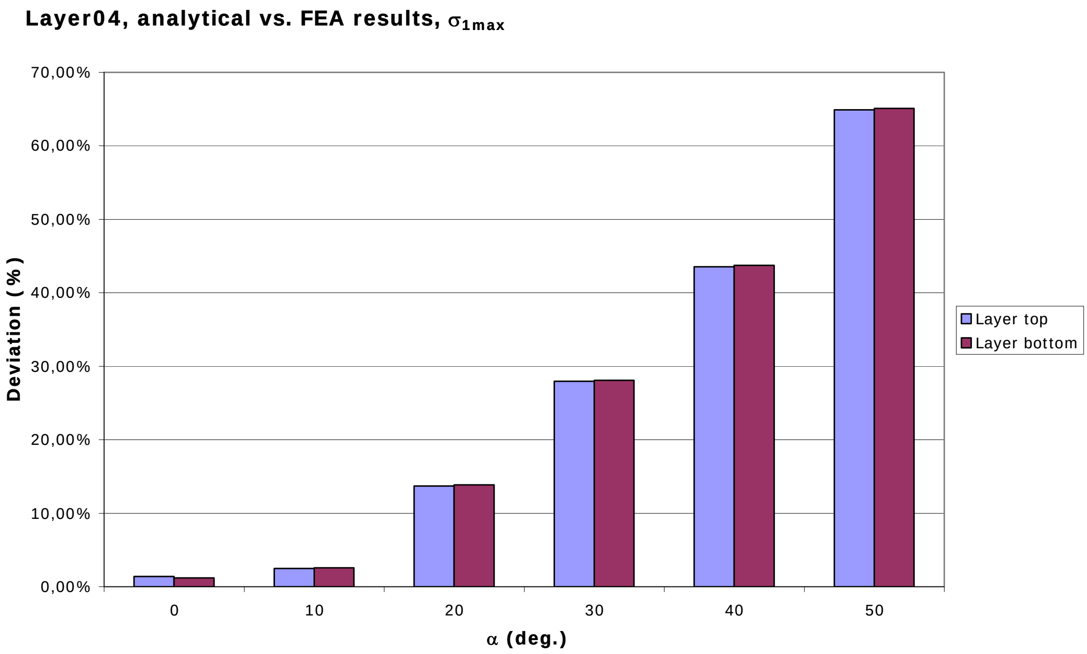

Figure A.7: Analytical Tool vs. FEA for Trapezoidal Plates for $\sigma_{1\max}$ of L.04

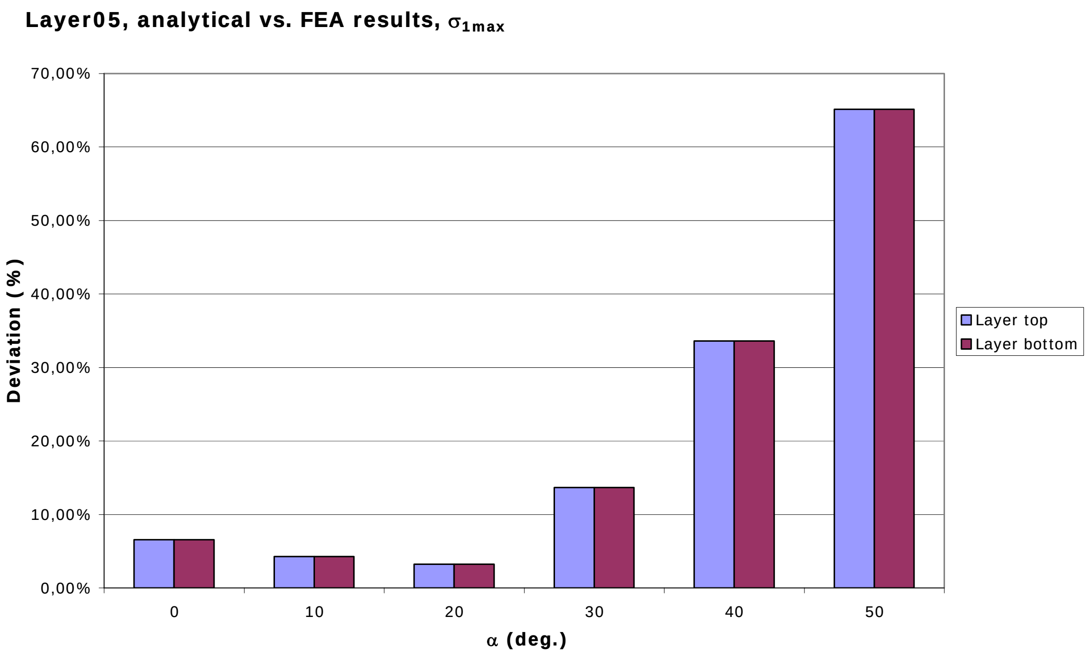

Figure A.8: Analytical Tool vs. FEA for Trapezoidal Plates for $\sigma_{1\max}$ of L.05

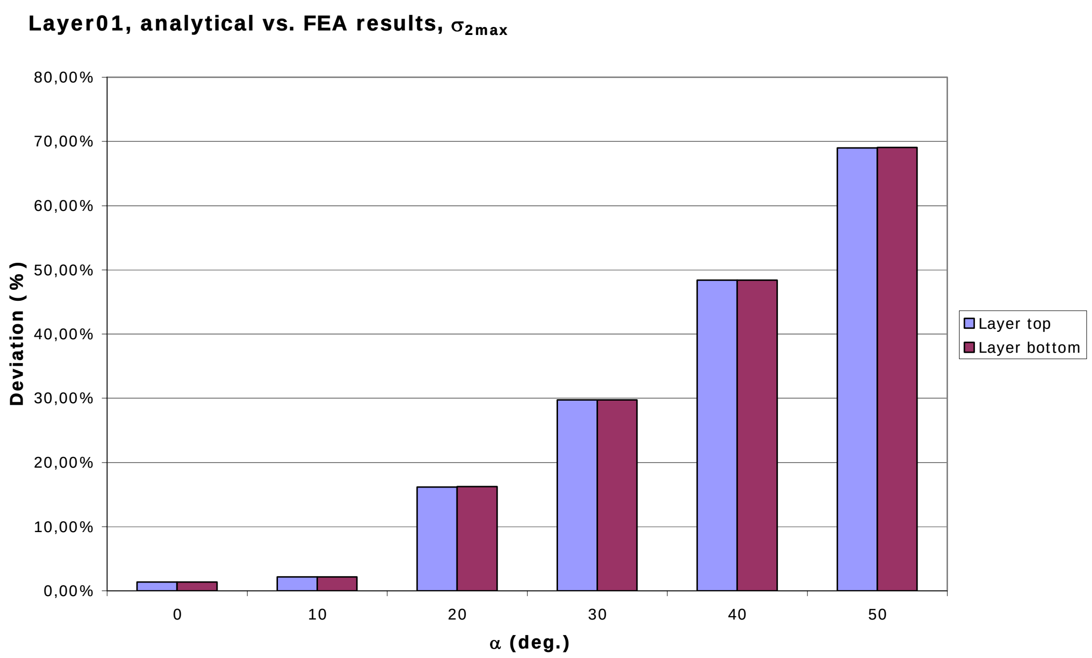

Figure A.9: Analytical Tool vs. FEA for Trapezoidal Plates for $\sigma_{2\max}$ of L.01

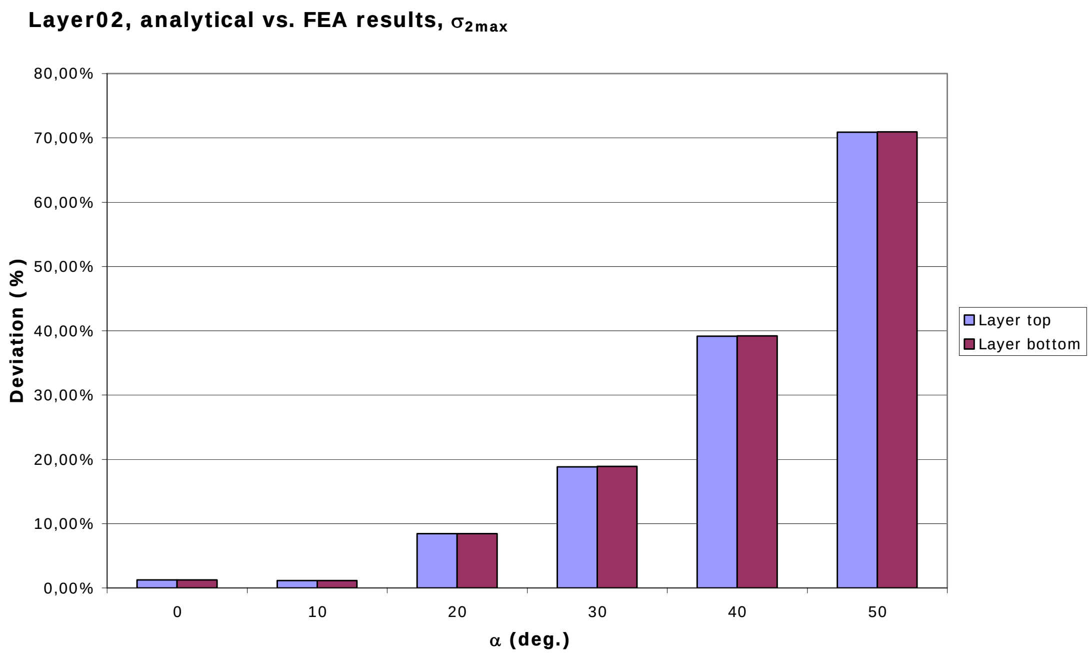

Figure A.10: Analytical Tool vs. FEA for Trapezoidal Plates for $\sigma_{2\max}$ of L.02

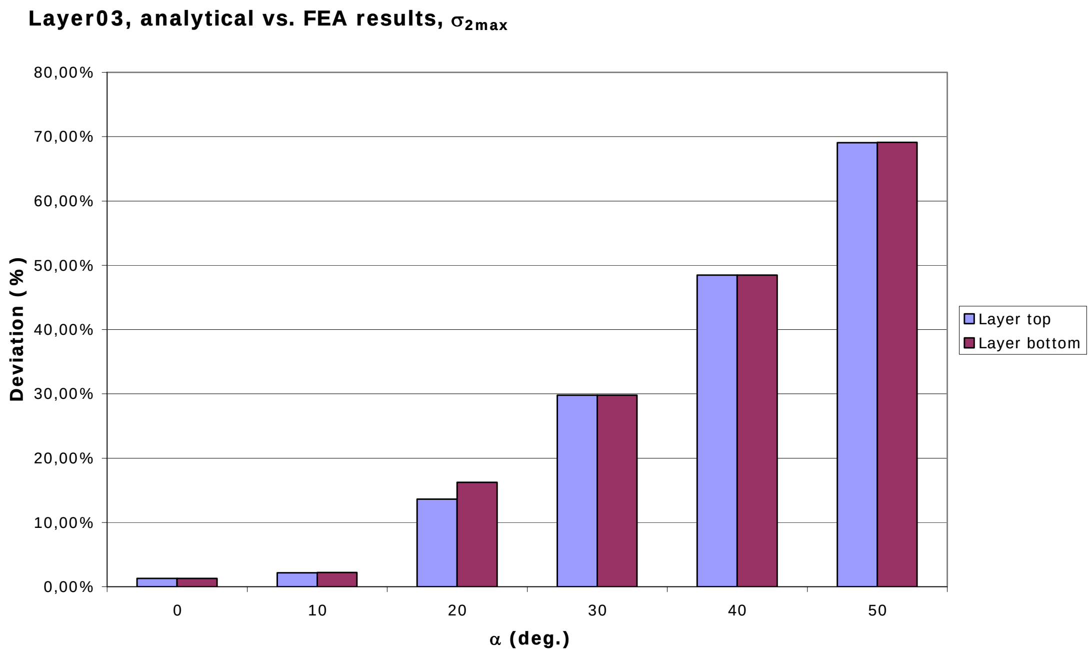

Figure A.11: Analytical Tool vs. FEA for Trapezoidal Plates for $\sigma_{2\max}$ of L.03

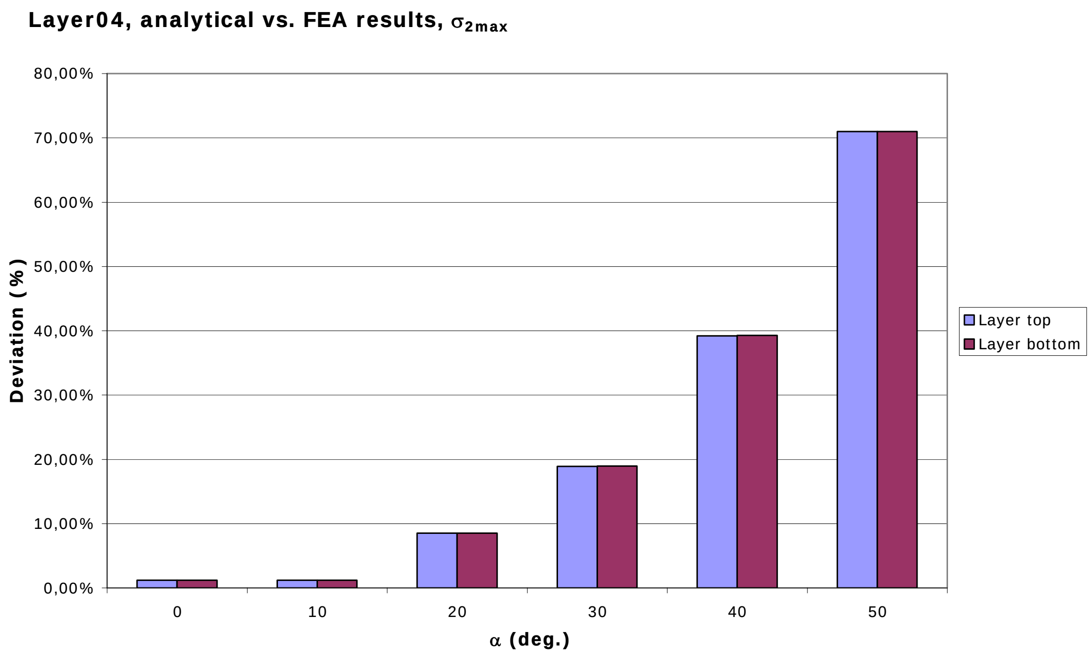

Figure A.12: Analytical Tool vs. FEA for Trapezoidal Plates for $\sigma_{2\max}$ of L.04

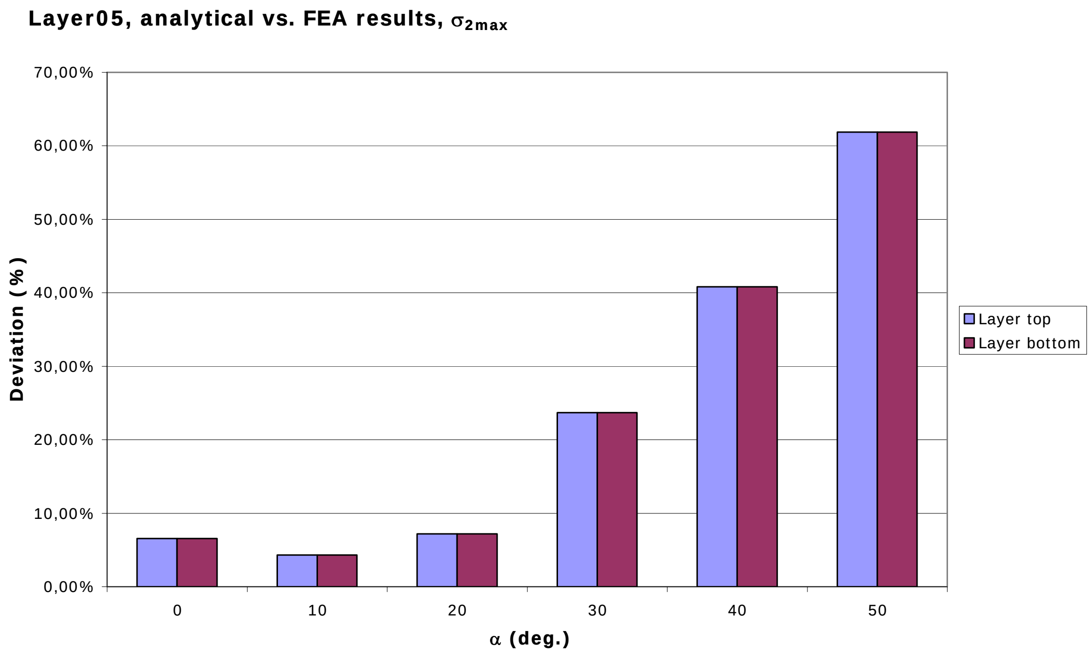

Figure A.13: Analytical Tool vs. FEA for Trapezoidal Plates for $\sigma_{2\max}$ of L.05

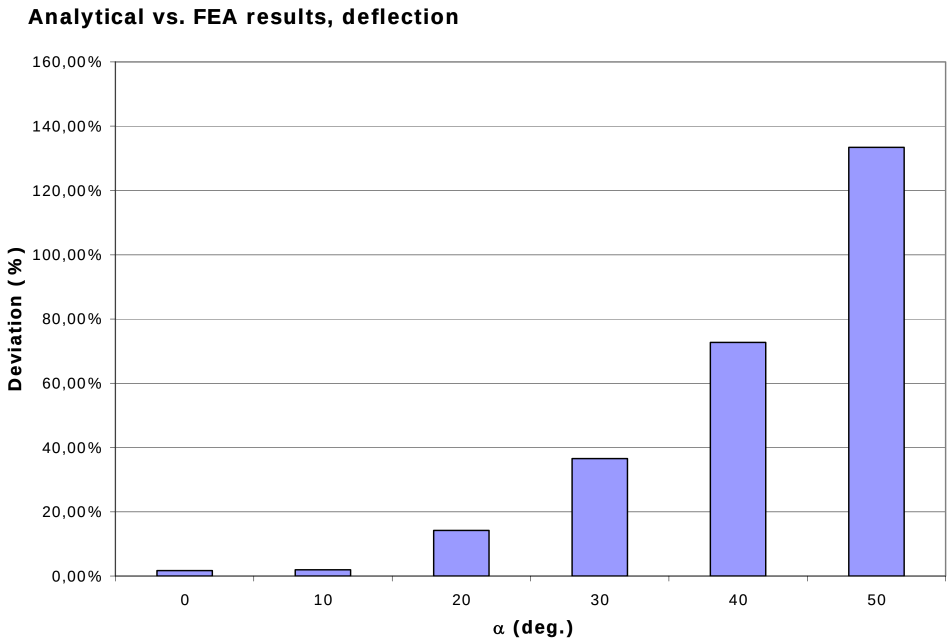

Figure A.14: Analytical Tool vs. FEA for Trapezoidal Plates, $w_{o\max}$

A.5 Analytical Solution Tool Results vs. FEA Results for Curved Plates

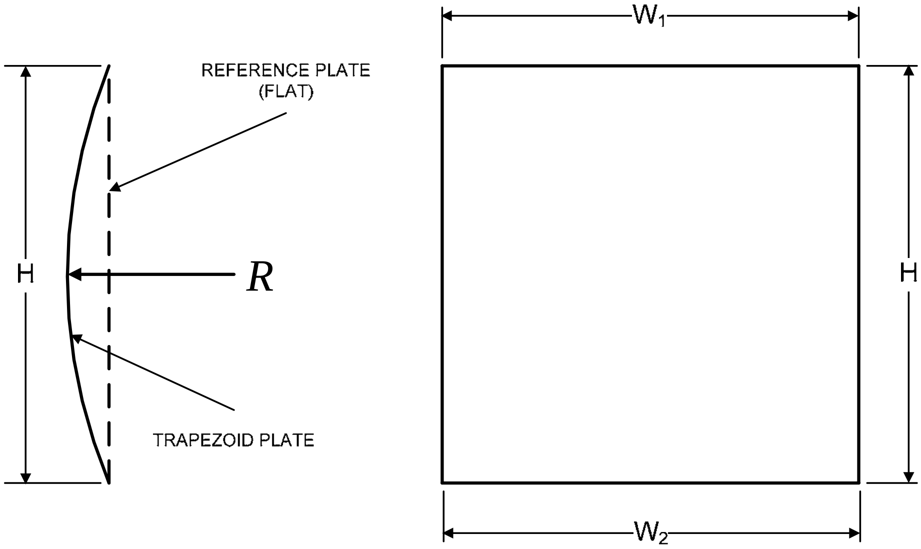

Figure A.15: Curved Plate Configuration.

Typical ship panel curvatures are used for the analysis. However, $R = 5000mm$ can be considered somewhat extreme.

Analytical solution tool and FEA results for each layer are as follows:

Table A.19: Analytical Tool vs. FEA for Curved Plates for L.01

	Plate configuration	R (mm)	H (mm)	W_1 (mm)	W_2 (mm)	$\sigma_{1\,max}$ (N/mm2)				$\sigma_{2\,max}$ (N/mm2)				w_{max} (mm)		
							Analytical	FEA	Deviation (%)		Analytical	FEA	Deviation (%)	Analytical	FEA	Deviation (%)
Layer 01	01	17500	1000	1000	1000	Layer top	-18,340	-18,878	2,85%	Layer top	-6,480	-6,681	3,00%	7,147	7,246	1,37%
		17500	1000	1000	1000	Layer bottom	-17,970	-18,579	3,28%	Layer bottom	-6,350	-6,550	3,05%			
	02	15000	1000	1000	1000	Layer top	-18,340	-18,948	3,21%	Layer top	-6,480	-6,706	3,36%	7,147	7,236	1,23%
		15000	1000	1000	1000	Layer bottom	-17,970	-18,579	3,28%	Layer bottom	-6,350	-6,575	3,42%			
	03	12500	1000	1000	1000	Layer top	-18,340	-18,895	2,94%	Layer top	-6,480	-6,663	2,75%	7,147	7,220	1,01%
		12500	1000	1000	1000	Layer bottom	-17,970	-18,530	3,02%	Layer bottom	-6,350	-6,535	2,83%			
	04	10000	1000	1000	1000	Layer top	-18,340	-19,153	4,24%	Layer top	-6,480	-6,779	4,41%	7,147	7,189	0,58%
		10000	1000	1000	1000	Layer bottom	-17,970	-18,787	4,35%	Layer bottom	-6,350	-6,650	4,51%			
	05	7500	1000	1000	1000	Layer top	-18,340	-19,291	4,93%	Layer top	-6,480	-6,831	5,14%	7,147	7,124	0,32%
		7500	1000	1000	1000	Layer bottom	-17,970	-18,929	5,07%	Layer bottom	-6,350	-6,703	5,27%			
	06	5000	1000	1000	1000	Layer top	-18,340	-19,382	5,38%	Layer top	-6,480	-6,870	5,68%	7,147	6,944	2,92%
		5000	1000	1000	1000	Layer bottom	-17,970	-19,032	5,58%	Layer bottom	-6,350	-6,746	5,87%			

Table A.20: Analytical Tool vs. FEA for Curved Plates for L.02

	Plate configuration	R (mm)	H (mm)	W_1 (mm)	W_2 (mm)	$\sigma_{1\,max}$ (N/mm2)				$\sigma_{2\,max}$ (N/mm2)				w_{max} (mm)		
							Analytical	FEA	Deviation (%)		Analytical	FEA	Deviation (%)	Analytical	FEA	Deviation (%)
Layer 02	01	17500	1000	1000	1000	Layer top	-17,950	-18,510	3,03%	Layer top	-6,360	-6,550	2,90%	7,147	7,246	1,37%
		17500	1000	1000	1000	Layer bottom	-17,580	-18,141	3,09%	Layer bottom	-6,230	-6,419	2,95%			
	02	15000	1000	1000	1000	Layer top	-17,950	-18,581	3,40%	Layer top	-6,360	-6,575	3,27%	7,147	7,236	1,23%
		15000	1000	1000	1000	Layer bottom	-17,580	-18,213	3,48%	Layer bottom	-6,230	-6,444	3,33%			
	03	12500	1000	1000	1000	Layer top	-17,950	-18,455	2,74%	Layer top	-6,360	-6,553	2,95%	7,147	7,220	1,01%
		12500	1000	1000	1000	Layer bottom	-17,580	-18,092	2,83%	Layer bottom	-6,230	-6,424	3,02%			
	04	10000	1000	1000	1000	Layer top	-17,950	-18,793	4,49%	Layer top	-6,360	-6,649	4,34%	7,147	7,189	0,58%
		10000	1000	1000	1000	Layer bottom	-17,580	-18,428	4,60%	Layer bottom	-6,230	-6,519	4,43%			
	05	7500	1000	1000	1000	Layer top	-17,950	-18,945	5,25%	Layer top	-6,360	-6,699	5,06%	7,147	7,124	0,32%
		7500	1000	1000	1000	Layer bottom	-17,580	-18,584	5,40%	Layer bottom	-6,230	-6,571	5,20%			
	06	5000	1000	1000	1000	Layer top	-17,950	-19,070	5,87%	Layer top	-6,360	-6,737	5,59%	7,147	6,944	2,92%
		5000	1000	1000	1000	Layer bottom	-17,580	-18,720	6,09%	Layer bottom	-6,230	-6,613	5,79%			

Table A.21: Analytical Tool vs. FEA for Curved Plates for L.03

	Plate configuration	R (mm)	H (mm)	W_1 (mm)	W_2 (mm)	$\sigma_{1\,max}$ (N/mm2)				$\sigma_{2\,max}$ (N/mm2)				w_{max} (mm)		
							Analytical	FEA	Deviation (%)		Analytical	FEA	Deviation (%)	Analytical	FEA	Deviation (%)
Layer 03	01	17500	1000	1000	1000	Layer top	-17,600	-18,140	2,98%	Layer top	-6,220	-6,419	3,11%	7,147	7,246	1,37%
		17500	1000	1000	1000	Layer bottom	-17,230	-17,770	3,04%	Layer bottom	-6,090	-6,289	3,16%			
	02	15000	1000	1000	1000	Layer top	-17,600	-18,211	3,36%	Layer top	-6,220	-6,445	3,49%	7,147	7,236	1,23%
		15000	1000	1000	1000	Layer bottom	-17,230	-17,842	3,43%	Layer bottom	-6,090	-6,315	3,56%			
	03	12500	1000	1000	1000	Layer top	-17,600	-18,165	3,11%	Layer top	-6,220	-6,406	2,91%	7,147	7,220	1,01%
		12500	1000	1000	1000	Layer bottom	-17,230	-17,800	3,20%	Layer bottom	-6,090	-6,278	2,99%			
	04	10000	1000	1000	1000	Layer top	-17,600	-18,421	4,46%	Layer top	-6,220	-6,521	4,61%	7,147	7,189	0,58%
		10000	1000	1000	1000	Layer bottom	-17,230	-18,056	4,57%	Layer bottom	-6,090	-6,391	4,72%			
	05	7500	1000	1000	1000	Layer top	-17,600	-18,568	5,21%	Layer top	-6,220	-6,575	5,40%	7,147	7,124	0,32%
		7500	1000	1000	1000	Layer bottom	-17,230	-18,206	5,36%	Layer bottom	-6,090	-6,447	5,54%			
	06	5000	1000	1000	1000	Layer top	-17,600	-18,681	5,79%	Layer top	-6,220	-6,622	6,07%	7,147	6,944	2,92%
		5000	1000	1000	1000	Layer bottom	-17,230	-18,331	6,01%	Layer bottom	-6,090	-6,498	6,28%			

Table A.22: Analytical Tool vs. FEA for Curved Plates for L.04

	Plate configuration	R (mm)	H (mm)	W_1 (mm)	W_2 (mm)	$\sigma_{1\,max}$ (N/mm2)				$\sigma_{2\,max}$ (N/mm2)				w_{max} (mm)		
							Analytical	FEA	Deviation (%)		Analytical	FEA	Deviation (%)	Analytical	FEA	Deviation (%)
Layer 04	01	17500	1000	1000	1000	Layer top	-17,210	-17,772	3,16%	Layer top	-6,100	-6,288	3,00%	7,147	7,246	1,37%
		17500	1000	1000	1000	Layer bottom	-16,860	-17,403	3,12%	Layer bottom	-5,970	-6,158	3,05%			
	02	15000	1000	1000	1000	Layer top	-17,210	-17,845	3,56%	Layer top	-6,100	-6,314	3,39%	7,147	7,236	1,23%
		15000	1000	1000	1000	Layer bottom	-16,860	-17,476	3,52%	Layer bottom	-5,970	-6,183	3,45%			
	03	12500	1000	1000	1000	Layer top	-17,210	-17,729	2,93%	Layer top	-6,100	-6,295	3,10%	7,147	7,220	1,01%
		12500	1000	1000	1000	Layer bottom	-16,860	-17,366	2,91%	Layer bottom	-5,970	-6,166	3,18%			
	04	10000	1000	1000	1000	Layer top	-17,210	-18,063	4,72%	Layer top	-6,100	-6,390	4,53%	7,147	7,189	0,58%
		10000	1000	1000	1000	Layer bottom	-16,860	-17,697	4,73%	Layer bottom	-5,970	-6,260	4,64%			
	05	7500	1000	1000	1000	Layer top	-17,210	-18,223	5,56%	Layer top	-6,100	-6,443	5,33%	7,147	7,124	0,32%
		7500	1000	1000	1000	Layer bottom	-16,860	-17,861	5,60%	Layer bottom	-5,970	-6,316	5,47%			
	06	5000	1000	1000	1000	Layer top	-17,210	-18,370	6,31%	Layer top	-6,100	-6,489	5,99%	7,147	6,944	2,92%
		5000	1000	1000	1000	Layer bottom	-16,860	-18,020	6,44%	Layer bottom	-5,970	-6,365	6,20%			

Table A.23: Analytical Tool vs. FEA for Curved Plates for L.05

	Plate configuration	R (mm)	H (mm)	W_1 (mm)	W_2 (mm)	$\sigma_{1\,max}$ (N/mm2)				$\sigma_{2\,max}$ (N/mm2)				w_{max} (mm)		
							Analytical	FEA	Deviation (%)		Analytical	FEA	Deviation (%)	Analytical	FEA	Deviation (%)
Layer 05	01	17500	1000	1000	1000	Layer top	-0,060	-0,066	8,40%	Layer top	-0,060	-0,066	8,40%	7,147	7,246	1,37%
		17500	1000	1000	1000	Layer bottom	0,060	0,061	1,46%	Layer bottom	0,060	0,061	1,51%			
	02	15000	1000	1000	1000	Layer top	-0,060	-0,066	8,77%	Layer top	-0,060	-0,066	8,78%	7,147	7,236	1,23%
		15000	1000	1000	1000	Layer bottom	0,060	0,060	0,67%	Layer bottom	0,060	0,060	0,72%			
	03	12500	1000	1000	1000	Layer top	-0,060	-0,066	8,49%	Layer top	-0,060	-0,066	8,49%	7,147	7,220	1,01%
		12500	1000	1000	1000	Layer bottom	0,060	0,059	1,26%	Layer bottom	0,060	0,059	1,26%			
	04	10000	1000	1000	1000	Layer top	-0,060	-0,067	9,90%	Layer top	-0,060	-0,067	9,91%	7,147	7,189	0,58%
		10000	1000	1000	1000	Layer bottom	0,060	0,059	2,40%	Layer bottom	0,060	-0,059	2,30%			
	05	7500	1000	1000	1000	Layer top	-0,060	-0,067	10,69%	Layer top	-0,060	-0,067	10,73%	7,147	7,124	0,32%
		7500	1000	1000	1000	Layer bottom	0,060	0,057	5,94%	Layer bottom	0,060	0,057	5,78%			
	06	5000	1000	1000	1000	Layer top	-0,060	-0,068	11,39%	Layer top	-0,060	-0,068	11,49%	7,147	6,944	2,92%
		5000	1000	1000	1000	Layer bottom	0,060	0,052	14,70%	Layer bottom	0,060	0,052	14,32%			

Table A.24: Analytical Tool vs. FEA for Curved Plates for L.06

	Plate configuration	R (mm)	H (mm)	W_1 (mm)	W_2 (mm)	$\sigma_{1\,max}$ (N/mm2)				$\sigma_{2\,max}$ (N/mm2)				w_{max} (mm)		
							Analytical	FEA	Deviation (%)		Analytical	FEA	Deviation (%)	Analytical	FEA	Deviation (%)
Layer 06	01	17500	1000	1000	1000	Layer top	16,860	16,188	4,15%	Layer top	5,970	5,725	4,29%	7,147	7,246	1,37%
		17500	1000	1000	1000	Layer bottom	17,210	16,558	3,94%	Layer bottom	6,100	5,855	4,18%			
	02	15000	1000	1000	1000	Layer top	16,860	16,061	4,97%	Layer top	5,970	5,679	5,13%	7,147	7,236	1,23%
		15000	1000	1000	1000	Layer bottom	17,210	16,430	4,75%	Layer bottom	6,100	5,809	5,00%			
	03	12500	1000	1000	1000	Layer top	16,860	15,696	7,42%	Layer top	5,970	5,572	7,14%	7,147	7,220	1,01%
		12500	1000	1000	1000	Layer bottom	17,210	16,060	7,16%	Layer bottom	6,100	5,701	6,99%			
	04	10000	1000	1000	1000	Layer top	16,860	15,589	8,15%	Layer top	5,970	5,508	8,39%	7,147	7,189	0,58%
		10000	1000	1000	1000	Layer bottom	17,210	15,956	7,86%	Layer bottom	6,100	5,638	8,20%			
	05	7500	1000	1000	1000	Layer top	16,860	15,079	11,81%	Layer top	5,970	5,324	12,14%	7,147	7,124	0,32%
		7500	1000	1000	1000	Layer bottom	17,210	15,443	11,44%	Layer bottom	6,100	5,452	11,89%			
	06	5000	1000	1000	1000	Layer top	16,860	13,961	20,76%	Layer top	5,970	4,916	21,44%	7,147	6,944	2,92%
		5000	1000	1000	1000	Layer bottom	17,210	14,315	20,22%	Layer bottom	6,100	5,040	21,02%			

Table A.25: Analytical Tool vs. FEA for Curved Plates for L.07

	Plate configuration	R (mm)	H (mm)	W_1 (mm)	W_2 (mm)	$\sigma_{1\,max}$ (N/mm2)				$\sigma_{2\,max}$ (N/mm2)				w_{max} (mm)		
							Analytical	FEA	Deviation (%)		Analytical	FEA	Deviation (%)	Analytical	FEA	Deviation (%)
Layer 07	01	17500	1000	1000	1000	Layer top	17,230	16,544	4,15%	Layer top	6,090	5,859	3,95%	7,147	7,246	1,37%
		17500	1000	1000	1000	Layer bottom	17,600	16,914	4,06%	Layer bottom	6,220	5,989	3,85%			
	02	15000	1000	1000	1000	Layer top	17,230	16,414	4,97%	Layer top	6,090	5,813	4,76%	7,147	7,236	1,23%
		15000	1000	1000	1000	Layer bottom	17,600	16,783	4,87%	Layer bottom	6,220	5,944	4,65%			
	03	12500	1000	1000	1000	Layer top	17,230	16,121	6,88%	Layer top	6,090	5,686	7,10%	7,147	7,220	1,01%
		12500	1000	1000	1000	Layer bottom	17,600	16,486	6,76%	Layer bottom	6,220	5,815	6,96%			
	04	10000	1000	1000	1000	Layer top	17,230	15,927	8,18%	Layer top	6,090	5,645	7,89%	7,147	7,189	0,58%
		10000	1000	1000	1000	Layer bottom	17,600	16,292	8,03%	Layer bottom	6,220	5,775	7,71%			
	05	7500	1000	1000	1000	Layer top	17,230	15,399	11,89%	Layer top	6,090	5,462	11,49%	7,147	7,124	0,32%
		7500	1000	1000	1000	Layer bottom	17,600	15,761	11,67%	Layer bottom	6,220	5,591	11,25%			
	06	5000	1000	1000	1000	Layer top	17,230	14,231	21,07%	Layer top	6,090	5,061	20,33%	7,147	6,944	2,92%
		5000	1000	1000	1000	Layer bottom	17,600	14,581	20,71%	Layer bottom	6,220	5,186	19,94%			

Table A.26: Analytical Tool vs. FEA for Curved Plates for L.08

	Plate configuration	R (mm)	H (mm)	W_1 (mm)	W_2 (mm)	$\sigma_{1\,max}$ (N/mm2)				$\sigma_{2\,max}$ (N/mm2)				w_{max} (mm)		
							Analytical	FEA	Deviation (%)		Analytical	FEA	Deviation (%)	Analytical	FEA	Deviation (%)
Layer 08	01	17500	1000	1000	1000	Layer top	17,580	16,928	3,85%	Layer top	6,230	5,986	4,08%	7,147	7,246	1,37%
		17500	1000	1000	1000	Layer bottom	17,950	17,288	3,83%	Layer bottom	6,360	6,117	3,98%			
	02	15000	1000	1000	1000	Layer top	17,580	16,800	4,64%	Layer top	6,230	5,940	4,89%	7,147	7,236	1,23%
		15000	1000	1000	1000	Layer bottom	17,950	17,179	4,49%	Layer bottom	6,360	6,070	4,77%			
	03	12500	1000	1000	1000	Layer top	17,580	16,424	7,04%	Layer top	6,230	5,831	6,85%	7,147	7,220	1,01%
		12500	1000	1000	1000	Layer bottom	17,950	16,789	6,92%	Layer bottom	6,360	5,960	6,72%			
	04	10000	1000	1000	1000	Layer top	17,580	16,323	7,70%	Layer top	6,230	5,767	8,03%	7,147	7,189	0,58%
		10000	1000	1000	1000	Layer bottom	17,950	16,690	7,55%	Layer bottom	6,360	5,897	7,86%			
	05	7500	1000	1000	1000	Layer top	17,580	15,806	11,22%	Layer top	6,230	5,580	11,65%	7,147	7,124	0,32%
		7500	1000	1000	1000	Layer bottom	17,950	16,170	11,01%	Layer bottom	6,360	5,708	11,42%			
	06	5000	1000	1000	1000	Layer top	17,580	14,668	19,85%	Layer top	6,230	5,165	20,63%	7,147	6,944	2,92%
		5000	1000	1000	1000	Layer bottom	17,950	15,022	19,49%	Layer bottom	6,360	5,289	20,26%			

Table A.27: Analytical Tool vs. FEA for Curved Plates for L.09

	Plate configuration	R (mm)	H (mm)	W_1 (mm)	W_2 (mm)	$\sigma_{1\,max}$ (N/mm2)				$\sigma_{2\,max}$ (N/mm2)				w_{max} (mm)		
							Analytical	FEA	Deviation (%)		Analytical	FEA	Deviation (%)	Analytical	FEA	Deviation (%)
Layer 09	01	17500	1000	1000	1000	Layer top	17,970	17,283	3,98%	Layer top	6,350	6,120	3,75%	7,147	7,246	1,37%
		17500	1000	1000	1000	Layer bottom	18,340	17,652	3,90%	Layer bottom	6,480	6,251	3,66%			
	02	15000	1000	1000	1000	Layer top	17,970	17,152	4,77%	Layer top	6,350	6,075	4,53%	7,147	7,236	1,23%
		15000	1000	1000	1000	Layer bottom	18,340	17,520	4,68%	Layer bottom	6,480	6,205	4,43%			
	03	12500	1000	1000	1000	Layer top	17,970	16,851	6,64%	Layer top	6,350	5,944	6,82%	7,147	7,220	1,01%
		12500	1000	1000	1000	Layer bottom	18,340	17,216	6,53%	Layer bottom	6,480	6,073	6,69%			
	04	10000	1000	1000	1000	Layer top	17,970	16,658	7,88%	Layer top	6,350	5,904	7,55%	7,147	7,189	0,58%
		10000	1000	1000	1000	Layer bottom	18,340	17,024	7,73%	Layer bottom	6,480	6,034	7,39%			
	05	7500	1000	1000	1000	Layer top	17,970	16,123	11,46%	Layer top	6,350	5,719	11,03%	7,147	7,124	0,32%
		7500	1000	1000	1000	Layer bottom	18,340	16,485	11,25%	Layer bottom	6,480	5,848	10,81%			
	06	5000	1000	1000	1000	Layer top	17,970	14,932	20,35%	Layer top	6,350	5,311	19,57%	7,147	6,944	2,92%
		5000	1000	1000	1000	Layer bottom	18,340	15,282	20,01%	Layer bottom	6,480	5,436	19,21%			

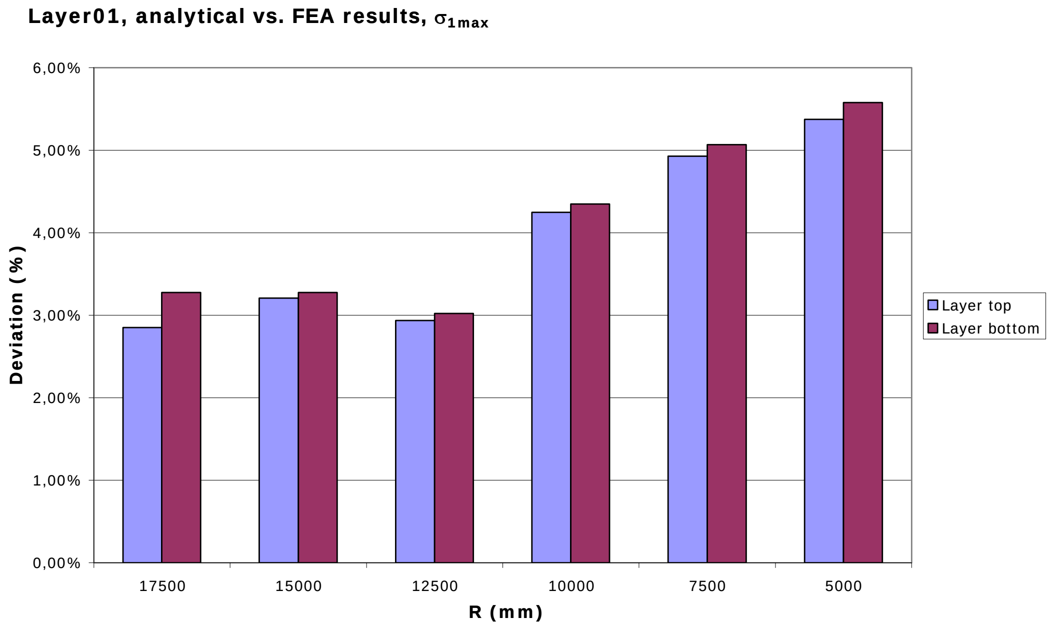

Figure A.16: Analytical Tool vs. FEA for Curved Plates for $\sigma_{1\max}$ of L.01

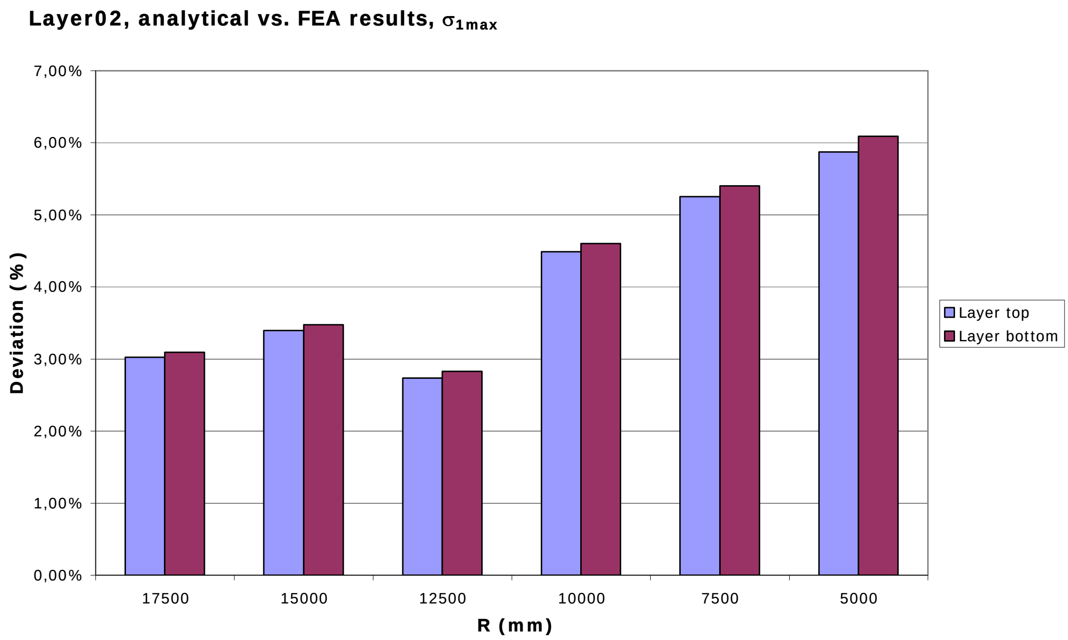

Figure A.17: Analytical Tool vs. FEA for Curved Plates for $\sigma_{1\max}$ of L.02

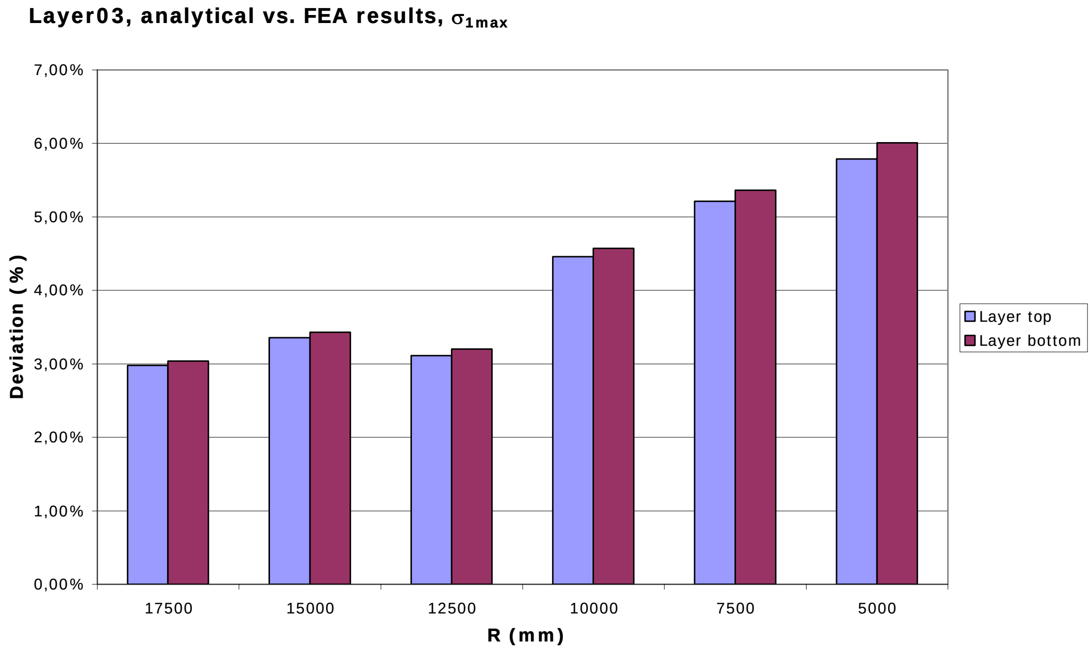

Figure A.18: Analytical Tool vs. FEA for Curved Plates for $\sigma_{1\max}$ of L.03

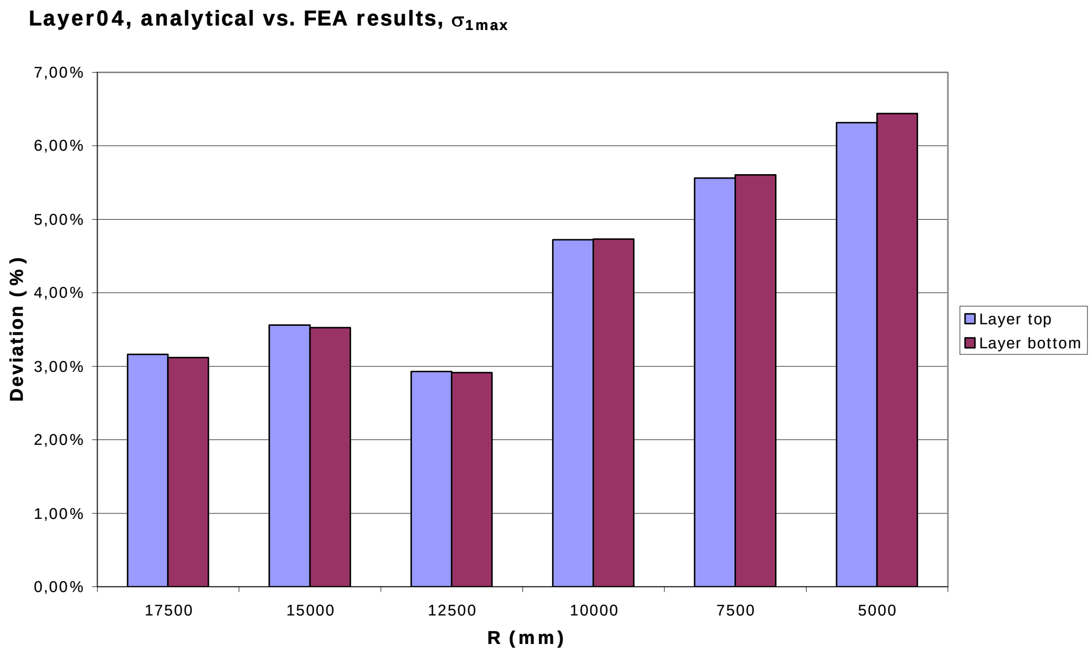

Figure A.19: Analytical Tool vs. FEA for Curved Plates for $\sigma_{1\max}$ Of L.04

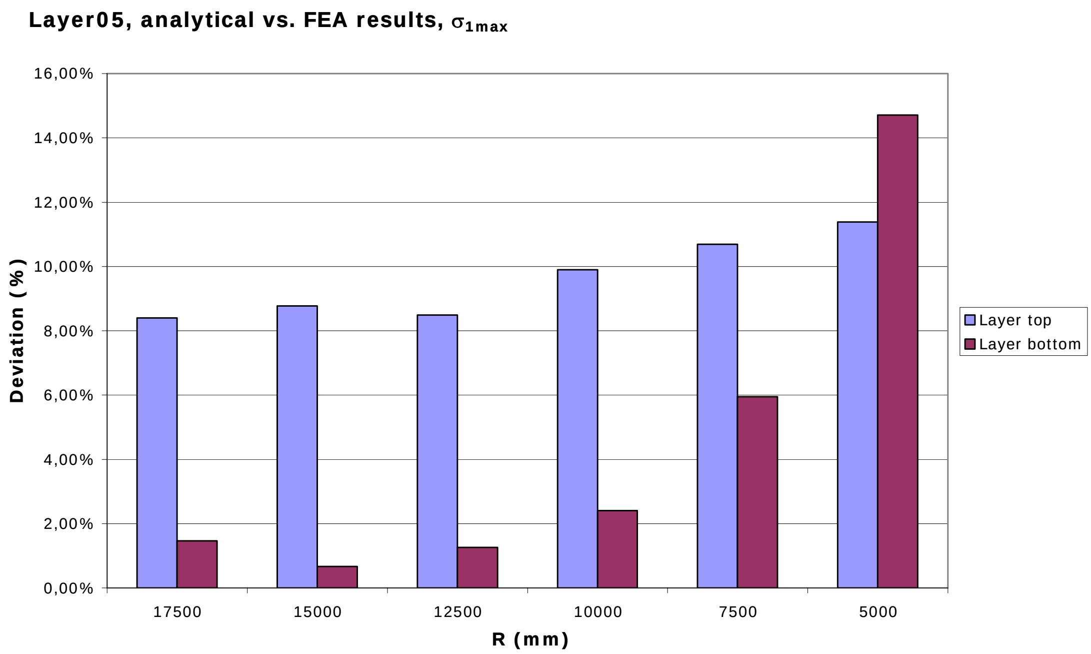

Figure A.20: Analytical Tool vs. FEA for Curved Plates for $\sigma_{1\max}$ of L.05

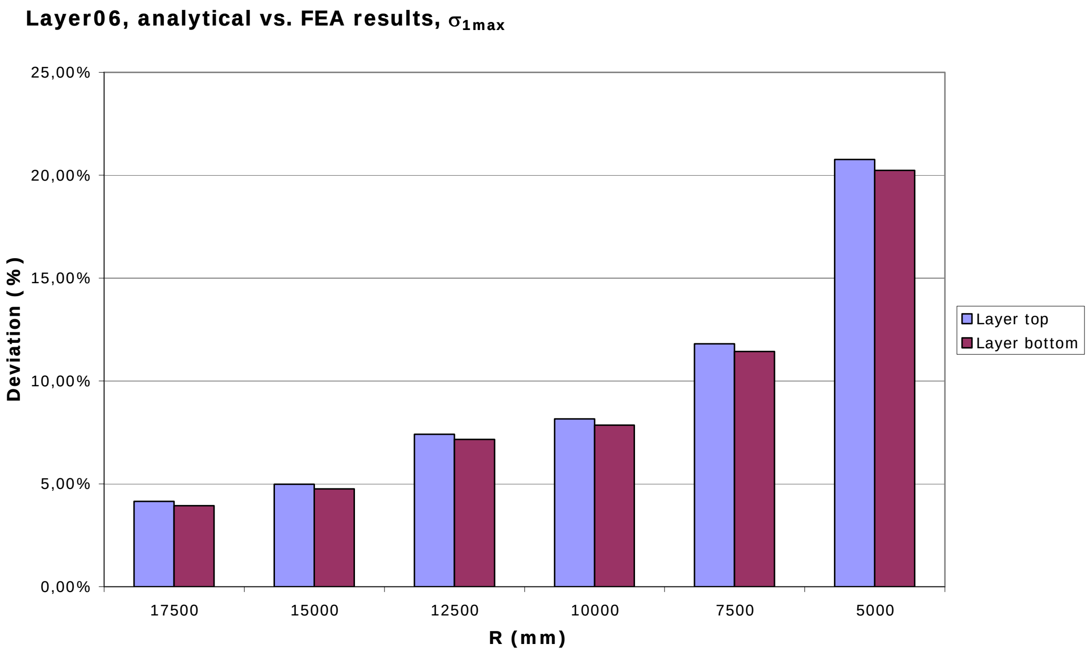

Figure A.21: Analytical Tool vs. FEA for Curved Plates for $\sigma_{1\max}$ of L.06

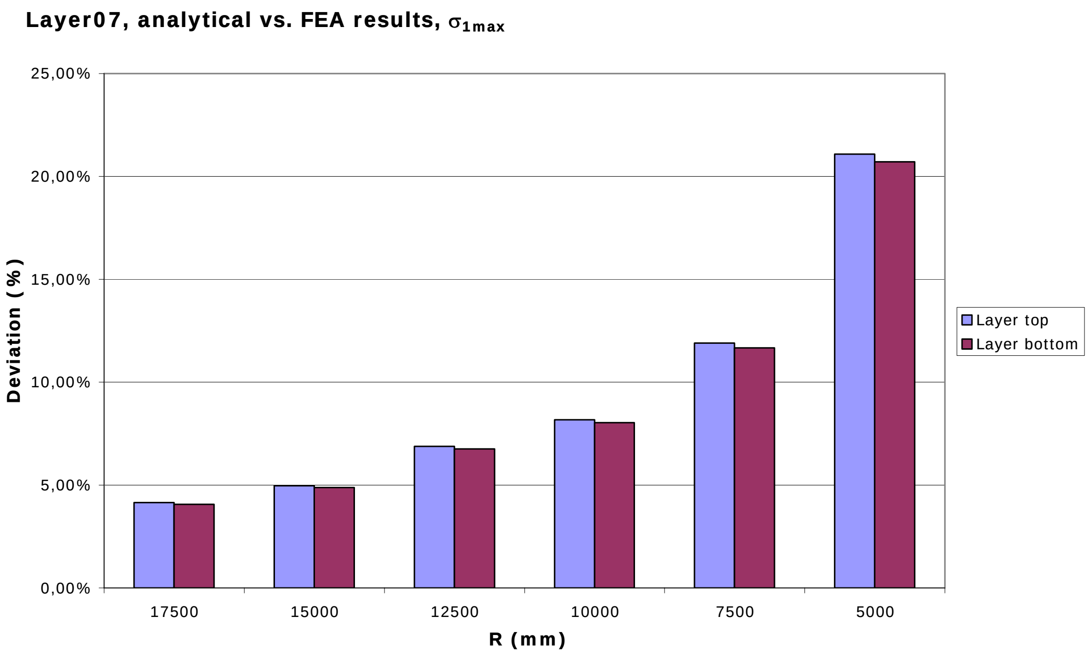

Figure A.22: Analytical Tool vs. FEA for Curved Plates for $\sigma_{1\max}$ of L.07

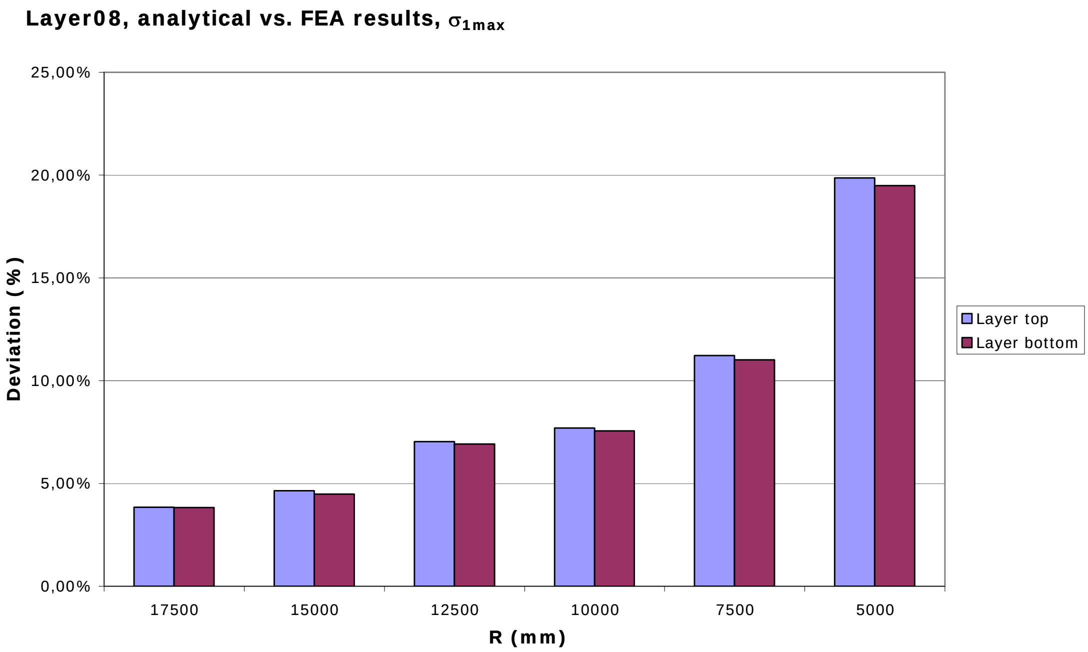

Figure A.23: Analytical Tool vs. FEA for Curved Plates for $\sigma_{1\max}$ of L.08

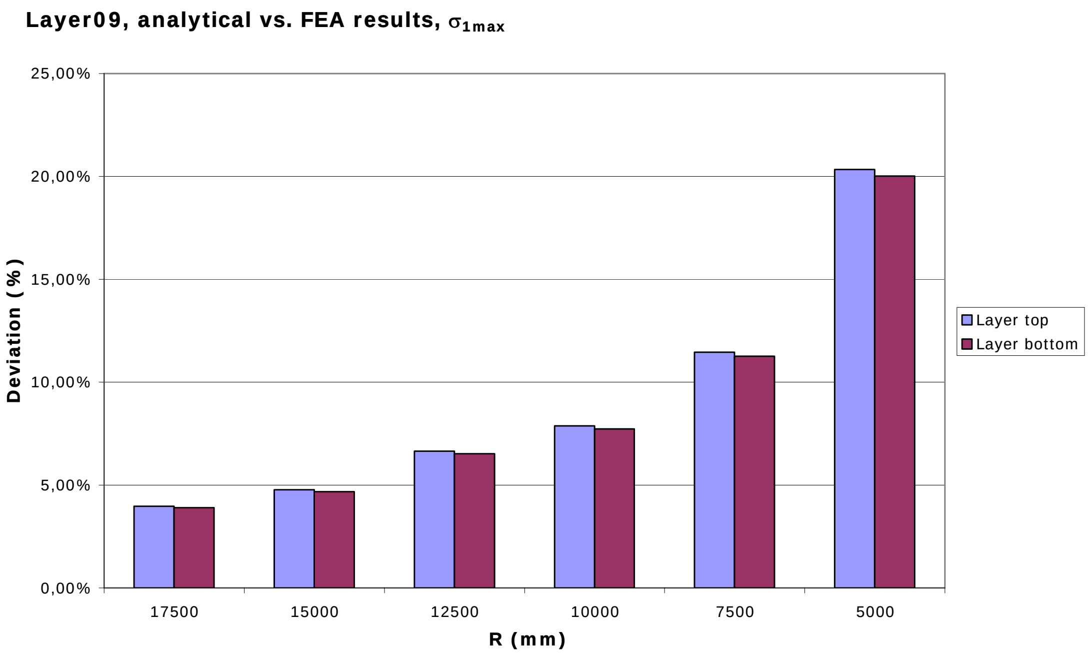

Figure A.24: Analytical Tool vs. FEA for Curved Plates for $\sigma_{1\max}$ of L.09

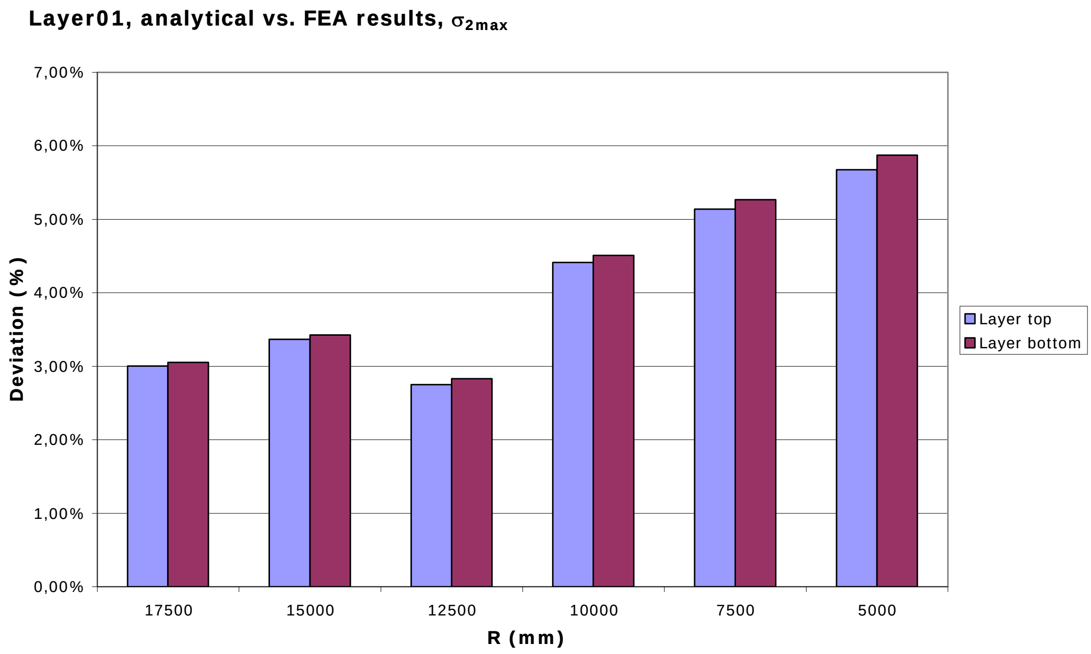

Figure A.25: Analytical Tool vs. FEA for Curved Plates for $\sigma_{2\max}$ of L.01

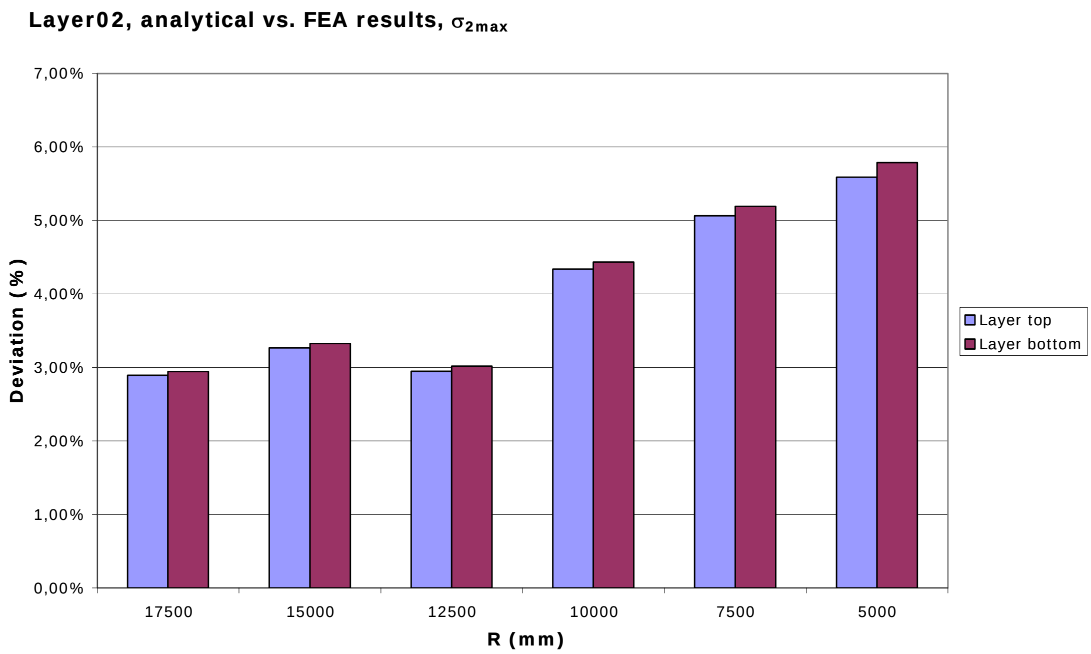

Figure A.26: Analytical Tool vs. FEA for Curved Plates for $\sigma_{2\max}$ of L.02

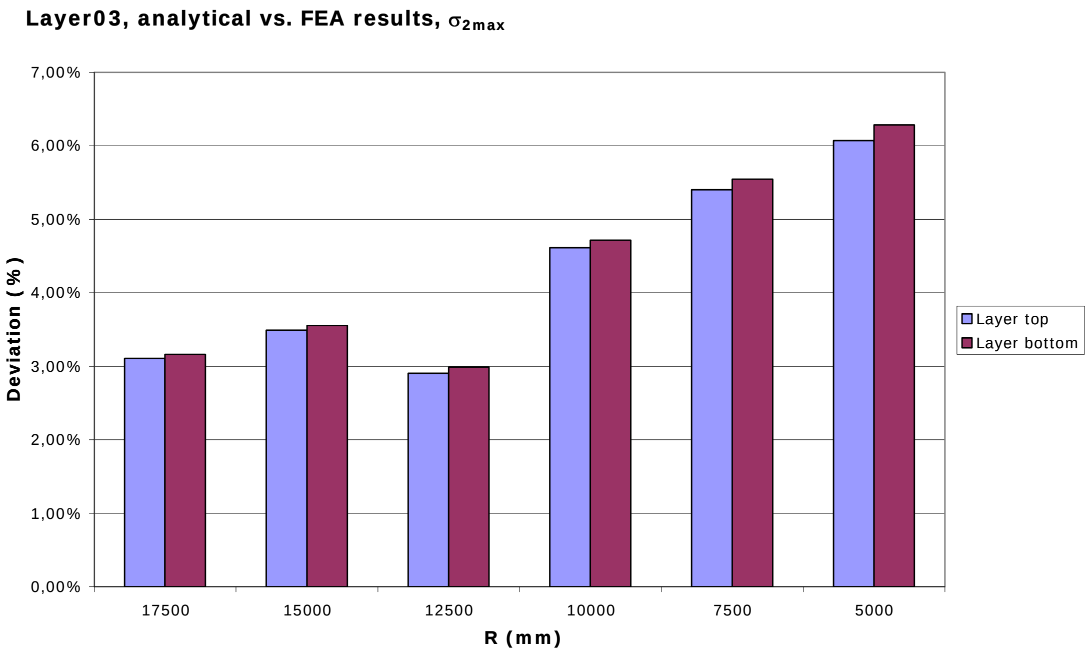

Figure A.27: Analytical Tool vs. FEA for Curved Plates for $\sigma_{2\max}$ of L.03

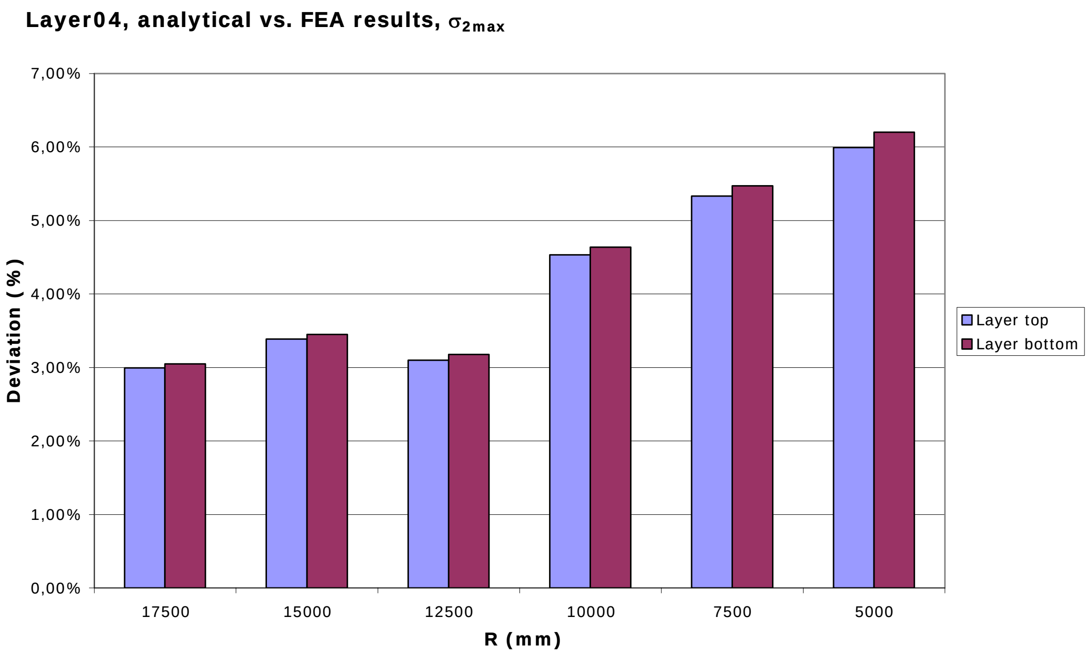

Figure A.28: Analytical Tool vs. FEA for Curved Plates for $\sigma_{2\max}$ of L.04

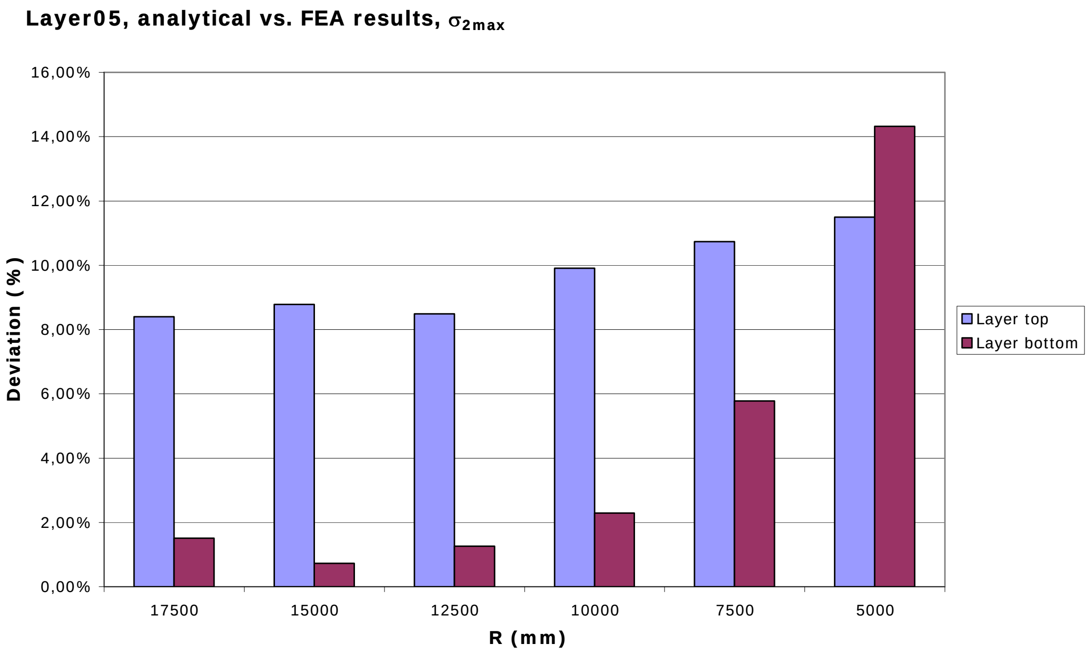

Figure A.29: Analytical Tool vs. FEA for Curved Plates for $\sigma_{2\max}$ of L.05

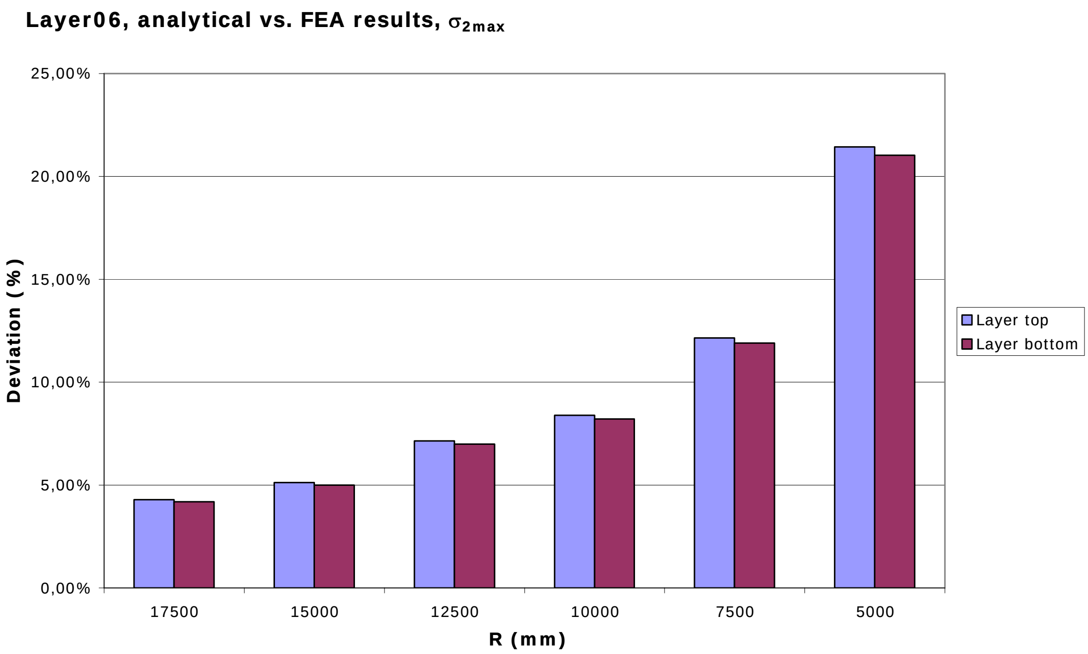

Figure A.30: Analytical Tool vs. FEA for Curved Plates for $\sigma_{2\max}$ of L.06

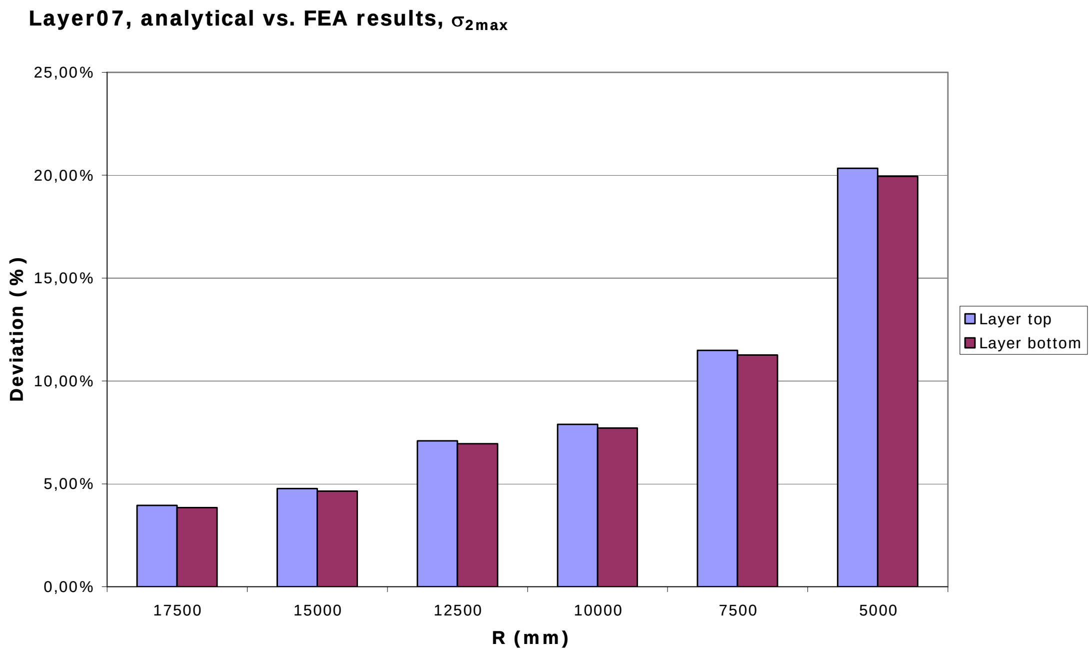

Figure A.31: Analytical Tool vs. FEA for Curved Plates for $\sigma_{2\max}$ of L.07

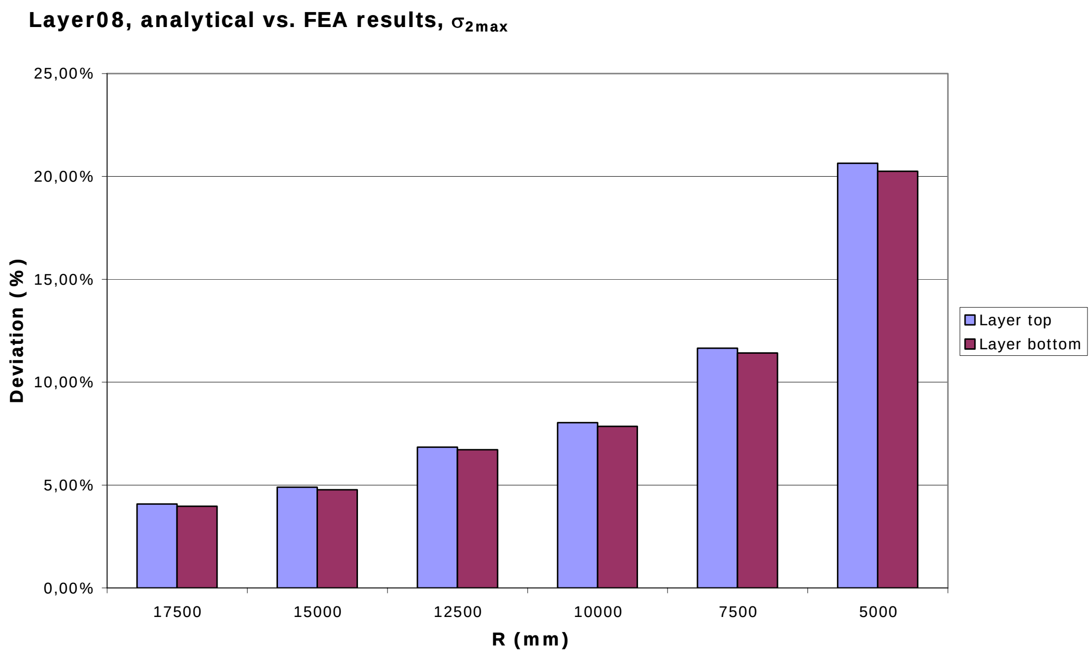

Figure A.32: Analytical Tool vs. FEA for Curved Plates for $\sigma_{2\max}$ of L.08

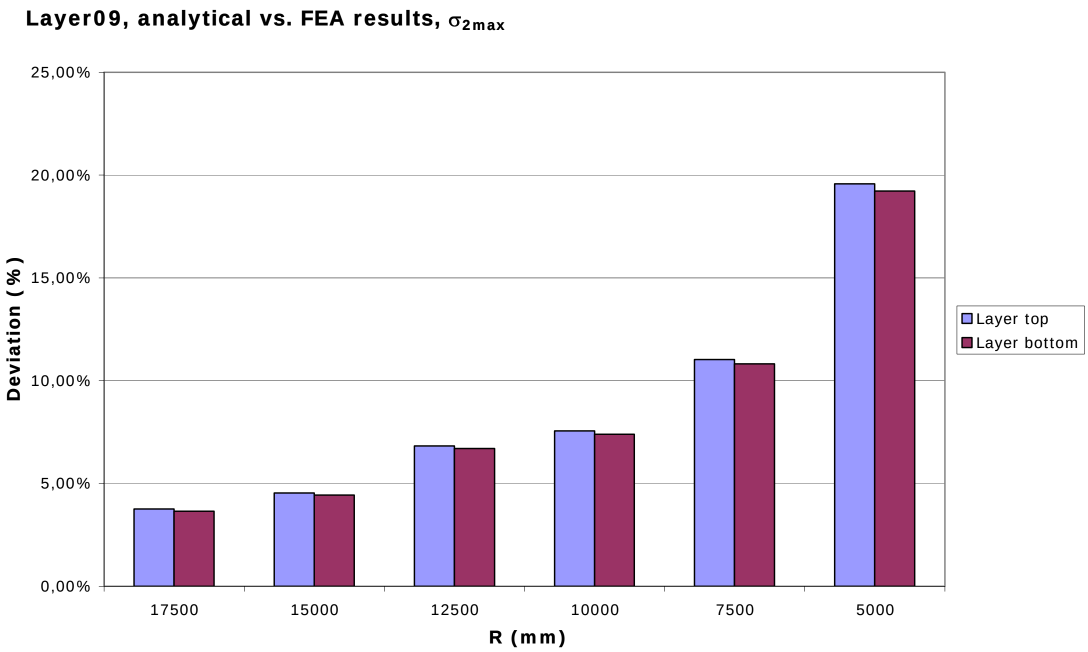

Figure A.33: Analytical Tool vs. FEA for Curved Plates for $\sigma_{2\max}$ of L09

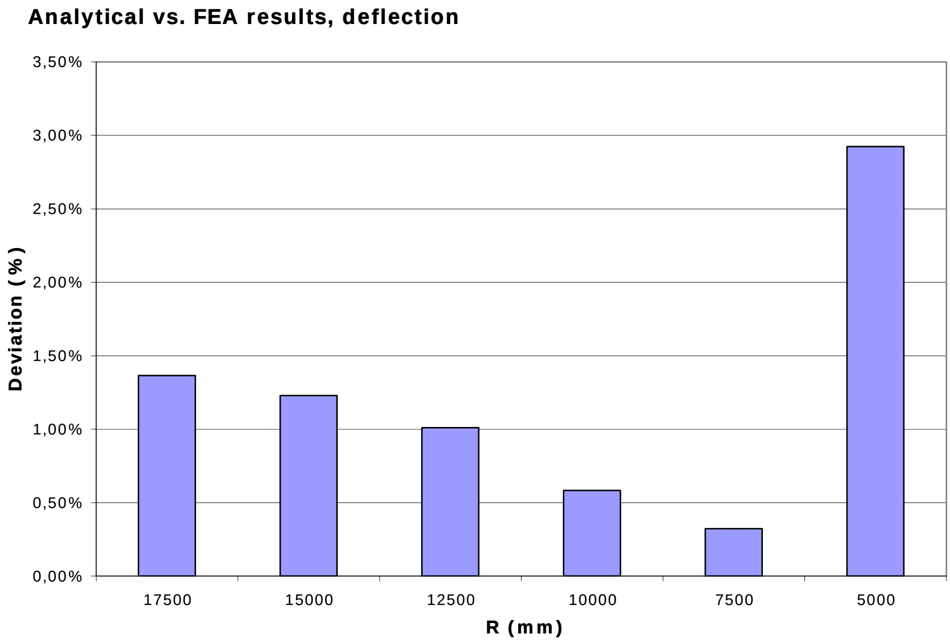

Figure A.34: Analytical Tool vs. FEA for Curved Plates, $w_{o\max}$

B STRESS DISTRIBUTION ABOUT x_o

According to Taylor's theorem for a continuous function one can write the below Taylor series expansion about x_0 [46, 47];

$$f(x) = f(x_0) + \frac{x - x_0}{1!} f'(x_0) + \frac{(x - x_0)^2}{2!} f''(x_0) + \ldots + \frac{(x - x_0)^n}{n!} f^{(n)}(x_0) + \frac{(x - x_0)^{n+1}}{(n+1)!} f^{(n+1)}(x_0 + \theta h) \quad \textbf{(B.1)}$$

where $0 < \theta < 1$.

According to this theorem, there exists only one Taylor series with center x_0 which represents $f(x)$.

If we assume that there exists no discontinuity within a material, then the stress distribution within this material can be represented by a continuous function, i.e., by a Taylor series.

For the infinitesimal cubic element case;

$$f(x_0) = \sigma_{11}, \; f'(x_0) = \frac{\partial \sigma_{11}}{\partial x_1} \text{ and } x - x_0 = dx_1 - 0 = dx_1$$

Taking the first two terms of the Taylor series we can obtain the below equation which represents the stress value at a distance dx_1 from x_0 [39]:

$$f(dx_1) \cong \sigma_{11} + \frac{\partial \sigma_{11}}{\partial x_1}.dx_1 \quad \textbf{(B.2)}$$

It is not mandatory to use the remaining terms of the series since the first two terms can represent the stress function with well enough computational accuracy. This can easily be demonstrated as follows:

The third term of the series is given by;

$$\frac{(dx_1)^2}{2} \cdot \frac{\partial^2 \sigma_{11}}{\partial {x_1}^2} \tag{B.3}$$

We already know that $dx << 1$. Therefore, ${dx_1}^2$ is even a considerably smaller quantity that has a negligible effect on the final result.

C LENGTH OF AN INFINITESIMAL LINE ELEMENT

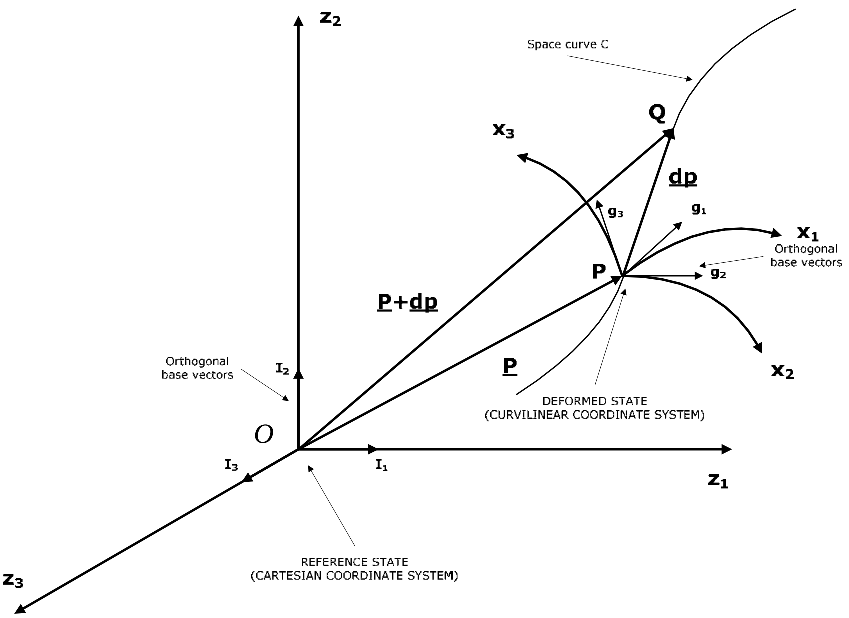

Figure C.1: Length of an Infinitesimal Line Element

Details of the derivations in this section can be found in the references [36, 37, 38, 39, 48, 49]

Consider a space curve C in E^3 where C: p(t)=p, $t \in [a,b]$ and b>a, a and b are real.

$$\overrightarrow{PQ} = \underline{dp} \qquad \textbf{(C.1)}$$

Let arc length PQ along curve C be denoted by ds. As P approaches to Q, arc length ds approaches to zero. Hence, the line element length ds can be taken equal to $|dp|$.

We know that the inner product of two vectors is a scalar which represents a magnitude of length of the resultant vector. Therefore, obviously, the dot product a vector with itself yields the square of the length of the vector.

Thus,

$$ds^2 = \underline{dp} \bullet \underline{dp} \quad \textbf{(C.2)}$$

From Figure C.1,

$\underline{P}(z) = z_1\underline{I_1} + z_2\underline{I_2} + z_3\underline{I_3}$ or shortly, $\underline{P}(z) = z_k\underline{I_k}$

or,

$\underline{P}(x) = x_1\underline{g_1} + x_2\underline{g_2} + x_3\underline{g_3}$ or shortly, $\underline{P}(z) = z_k\underline{I_k}$ **(C.3)**

Obviously, as can be seen from the figure and as shown above, $\underline{P}$ can be defined in both reference and deformed coordinate systems.

Since there is one to one mapping between z_k and x_k;

$z_k = z_k(x_1, x_2, x_3)$ and **(C.4)**

$$x_k = x_k(z_1, z_2, z_3) \quad \textbf{(C.5)}$$

$\Rightarrow \underline{I_k} = \dfrac{\partial \underline{P}(z)}{\partial z_k}$ likewise, **(C.6)**

$$\Rightarrow \underline{g_m} = \frac{\partial \underline{P}(x)}{\partial x_m} \quad \textbf{(C.7)}$$

Thus,

$$\begin{aligned}
\underline{dp} &= \frac{\partial \underline{P}(x)}{\partial x_m} dx_m \\
&= \frac{\partial \underline{P}(x)}{\partial x_1} dx_1 + \frac{\partial \underline{P}(x)}{\partial x_2} dx_2 + \frac{\partial \underline{P}(x)}{\partial x_3} dx_3 \\
&= \underline{g_1} dx_1 + \underline{g_2} dx_2 + \underline{g_3} dx_3
\end{aligned} \quad \textbf{(C.8)}$$

On the other hand, we know that $\underline{P}(z) = \underline{P}(x)$ thus,

$$\frac{\partial \underline{P}(z)}{\partial x_m} = \underline{I_k} \frac{\partial z_k}{\partial x_m} = \frac{\partial \underline{P}(x)}{\partial x_m} = \underline{g_m}$$

$$\Rightarrow \underline{g_m} = \underline{I_k} \frac{\partial z_k}{\partial x_m} \quad \textbf{(C.9)}$$

Hence,

$$ds^2 = \underline{dp} \bullet \underline{dp} = \underline{g_k} dx_k \bullet \underline{g_l} dx_l = g_{kl} dx_k dx_l \tag{C.10}$$

The same equation can be written in the following matrix form as follows:

$$ds^2 = dx_k \begin{bmatrix} \underline{g_1} \\ \underline{g_2} \\ \underline{g_3} \end{bmatrix} \bullet dx_l \begin{bmatrix} \underline{g_1} & \underline{g_2} & \underline{g_3} \end{bmatrix} \tag{C.11}$$

If we write the result of this dot product explicitly, we will see more obviously that k and l are interchangeable, that is,

$$\begin{aligned} ds^2 &= \underline{g_1} \bullet \underline{g_1} dx_1 dx_1 + \underline{g_1} \bullet \underline{g_2} dx_1 dx_2 + \underline{g_1} \bullet \underline{g_3} dx_1 dx_3 \\ &+ \underline{g_2} \bullet \underline{g_1} dx_2 dx_1 + \underline{g_2} \bullet \underline{g_2} dx_2 dx_2 + \underline{g_2} \bullet \underline{g_3} dx_2 dx_3 \\ &+ \underline{g_3} \bullet \underline{g_1} dx_3 dx_1 + \underline{g_3} \bullet \underline{g_2} dx_3 dx_2 + \underline{g_3} \bullet \underline{g_3} dx_3 dx_3 \end{aligned} \tag{C.12}$$

equivalently,

$$\begin{aligned} ds^2 &= g_{11} dx_1 dx_1 + g_{12} dx_1 dx_2 + g_{13} dx_1 dx_3 \\ &+ g_{21} dx_2 dx_1 + g_{22} dx_2 dx_2 + g_{23} dx_2 dx_3 \\ &+ g_{31} dx_3 dx_1 + g_{32} dx_3 dx_2 + g_{33} dx_3 dx_3 \end{aligned} \tag{C.13}$$

Therefore, we can conclude that fundamental metric coefficients are symmetrical i.e.:

$$g_{kl} = g_{lk}$$

This requires that metric of the space, $ds^2 = \underline{dp} \bullet \underline{dp}$, should also be symmetrical.

Notice that if we had used Cartesian coordinate system instead of curvilinear coordinate system to define the deformed state, due to orthogonality of base vectors, then we would obtain;

$$ds^2 = \underline{dp} \bullet \underline{dp} = I_{kk} (dx_k)^2 \tag{C.14}$$

D DEFORMATION OF A PARTICLE

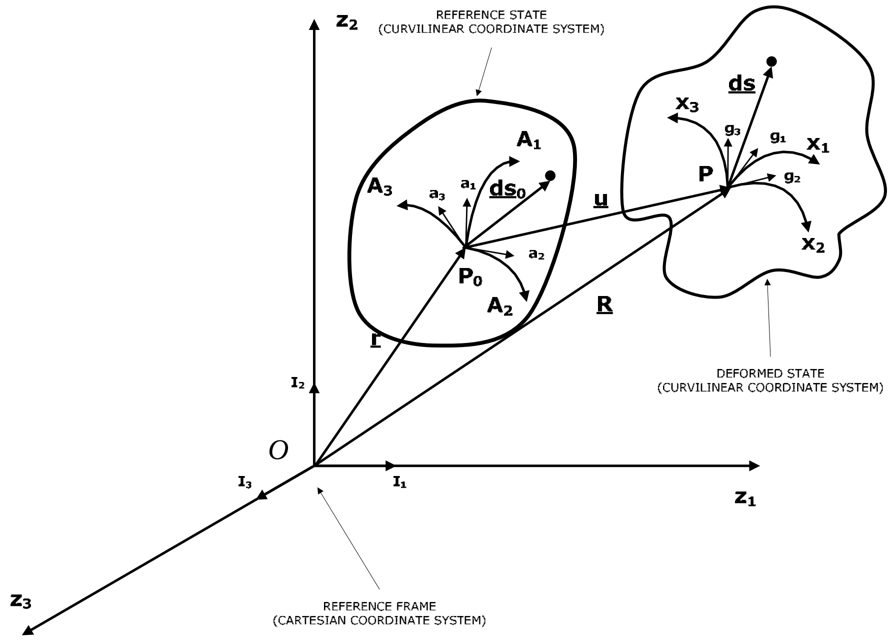

Figure D.1: Deformation of a Particle.

Details of the derivations in this section can be found in the references [37, 38, 39]

As detailed in Appendix B;

$$ds_0^{\ 2} = a_{kl} dA_k dA_l \tag{D.1}$$

and

$$ds^2 = g_{kl} dx_k dx_l \tag{D.2}$$

Hence,

$$ds^2 - ds_0^{\ 2} = g_{kl} dx_k dx_l - a_{mn} dA_m dA_n$$

Since we assume that there is one to one mapping between z_i to A_i and z_i to x_i ($i = 1,2,3$), as shown earlier;

$$A_i = A_i(z_1, z_2, z_3) \tag{D.3}$$

and

$$x_i = x_i(z_1, z_2, z_3) \quad \textbf{(D.4)}$$

Thus, using the concept of total differential we can write;

$$dA_i = \frac{\partial A_i}{\partial z_j} dz_j, \; dx_i = \frac{\partial x_1}{\partial z_j} dz_j \quad \textbf{(D.5)}$$

accordingly,

$$\begin{aligned} ds^2 - ds_0{}^2 &= g_{kl} \frac{\partial x_k}{\partial z_j} dz_j \frac{\partial x_l}{\partial z_i} dz_i - a_{kl} \frac{\partial A_k}{\partial z_j} dz_j \frac{\partial A_l}{\partial z_i} dz_i \\ &= \left[g_{kl} \frac{\partial x_k}{\partial z_j} \frac{\partial x_l}{\partial z_i} - a_{kl} \frac{\partial A_k}{\partial z_j} \frac{\partial A_l}{\partial z_i} \right] dz_j dz_i \end{aligned} \quad \textbf{(D.6)}$$

Let us define the difference between the two space metrics, $ds^2 - ds_0{}^2$, as follows:

$$ds^2 - ds_0{}^2 = 2\gamma_{kl} dz_j dz_i \quad \textbf{(D.7)}$$

where,

$$\gamma_{kl} = \frac{1}{2}\left[g_{kl} \frac{\partial x_k}{\partial z_j} \frac{\partial x_l}{\partial z_i} - a_{kl} \frac{\partial A_k}{\partial z_j} \frac{\partial A_l}{\partial z_i} \right] \quad \textbf{(D.8)}$$

is the strain tensor.

Obviously, the above equation dictates that because fundamental metric coefficients are symmetric, strain tensor is also symmetric.

E MTDSC BASICS; COORDINATE TRANSFORMATIONS

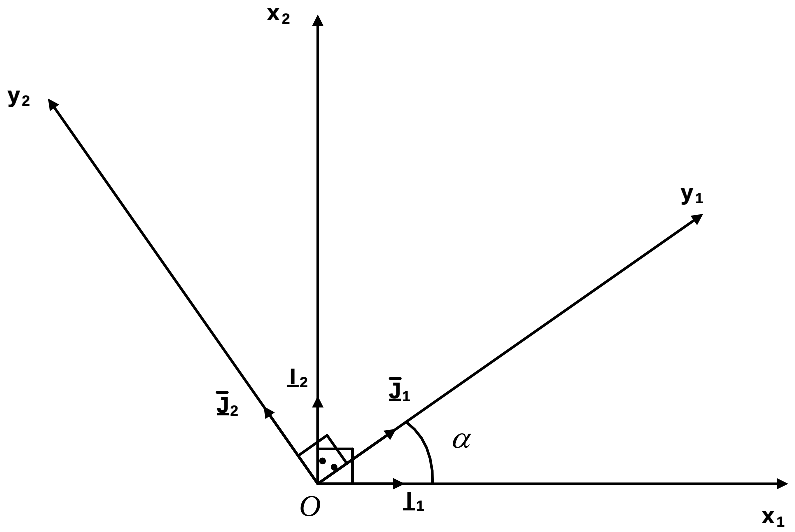

Figure E.1: 2D Coordinate System Transformation

$$\underline{\bar{J}_1} = a_{\bar{1}1}\underline{I_1} + a_{\bar{1}2}\underline{I_2} \tag{E.1}$$

$$\underline{\bar{J}_2} = a_{\bar{2}1}\underline{I_1} + a_{\bar{2}2}\underline{I_2} \tag{E.2}$$

On the other hand,

$$\underline{I_1} = a_{1\bar{1}}\underline{\bar{J}_1} + a_{1\bar{2}}\underline{\bar{J}_2} \tag{E.3}$$

$$\underline{I_2} = a_{2\bar{1}}\underline{\bar{J}_1} + a_{2\bar{2}}\underline{\bar{J}_2} \tag{E.4}$$

Where,

$$a_{\bar{1}1} = \underline{\bar{J}_1} \bullet \underline{I_1} = \left|\bar{J}_1\right|\left|I_1\right|\cos(\alpha) = \cos(\alpha) \tag{E.5}$$

$$a_{\bar{1}2} = \underline{\bar{J}_1} \bullet \underline{I_2} = \left|\bar{J}_1\right|\left|I_2\right|\cos(90-\alpha) = \cos(90-\alpha) \tag{E.6}$$

$$\Rightarrow \underline{\bar{J}_1} = \cos(\alpha)\underline{I_1} + \cos(90-\alpha)\underline{I_2} \tag{E.7}$$

and,

$$a_{\bar{2}1} = \underline{\bar{J}_2} \bullet \underline{I_1} = |\bar{J}_2||I_1|\cos(90+\alpha) = \cos(90+\alpha) \quad \textbf{(E.8)}$$

$$a_{\bar{2}2} = \underline{\bar{J}_2} \bullet \underline{I_2} = |\bar{J}_2||I_2|\cos(\alpha) = \cos(\alpha) \quad \textbf{(E.9)}$$

$$\Rightarrow \underline{\bar{J}_2} = \cos(90+\alpha)\underline{I_1} + \cos(\alpha)\underline{I_2} \quad \textbf{(E.10)}$$

similarly,

$$a_{1\bar{1}} = \underline{I_1} \bullet \underline{\bar{J}_1} = |I_1||\bar{J}_1|\cos(\alpha) = \cos(\alpha) \quad \textbf{(E.11)}$$

$$a_{1\bar{2}} = \underline{I_1} \bullet \underline{\bar{J}_2} = |I_1||\bar{J}_2|\cos(90+\alpha) = \cos(90+\alpha) \quad \textbf{(E.12)}$$

$$a_{2\bar{1}} = \underline{I_2} \bullet \underline{\bar{J}_1} = |I_2||\bar{J}_1|\cos(90-\alpha) = \cos(90-\alpha) \quad \textbf{(E.13)}$$

$$a_{2\bar{2}} = \underline{I_2} \bullet \underline{\bar{J}_2} = |I_2||\bar{J}_2|\cos(\alpha) = \cos(\alpha) \quad \textbf{(E.14)}$$

and thus,

$$\underline{I_1} = \cos(\alpha)\underline{\bar{J}_1} + \cos(90+\alpha)\underline{\bar{J}_2} \quad \textbf{(E.15)}$$

$$\underline{I_2} = \cos(90-\alpha)\underline{\bar{J}_1} + \cos(\alpha)\underline{\bar{J}_2} \quad \textbf{(E.16)}$$

Now, we can extend our findings to three dimensional coordinate system transformation cases.

$$\underline{\bar{J}_1} = a_{\bar{1}1}\underline{I_1} + a_{\bar{1}2}\underline{I_2} + a_{\bar{1}3}\underline{I_3} \quad \textbf{(E.17)}$$

$$\underline{\bar{J}_2} = a_{\bar{2}1}\underline{I_1} + a_{\bar{2}2}\underline{I_2} + a_{\bar{2}3}\underline{I_3} \quad \textbf{(E.18)}$$

$$\underline{\bar{J}_3} = a_{\bar{3}1}\underline{I_1} + a_{\bar{3}2}\underline{I_2} + a_{\bar{3}3}\underline{I_3} \quad \textbf{(E.19)}$$

$$\Rightarrow \underline{\bar{J}_m} = a_{\bar{m}n}\underline{I_n} \text{ or } \underline{\bar{J}_m} = a_{n\bar{m}}\underline{I_n} \quad \textbf{(E.20)}$$

On the other hand,

$$\underline{I_1} = a_{1\bar{1}}\underline{\bar{J}_1} + a_{1\bar{2}}\underline{\bar{J}_2} + a_{1\bar{3}}\underline{\bar{J}_3} \quad \textbf{(E.21)}$$

$$\underline{I_2} = a_{2\bar{1}}\underline{\bar{J}_1} + a_{2\bar{2}}\underline{\bar{J}_2} + a_{2\bar{3}}\underline{\bar{J}_3} \quad \textbf{(E.22)}$$

$$\underline{I_3} = a_{3\bar{1}}\underline{\bar{J}_1} + a_{3\bar{2}}\underline{\bar{J}_2} + a_{3\bar{3}}\underline{\bar{J}_3} \quad \textbf{(E.23)}$$

$$\Rightarrow \underline{I_m} = a_{m\bar{n}} \underline{\bar{J}_n} \text{ or } \underline{I_m} = a_{\bar{n}m} \underline{\bar{J}_n} \tag{E.24}$$

F STRAIN TENSOR TRANSFORMATIONS

Details of the derivations in this section can be found in the reference [37].

We know from (D.7) that,

$$ds^2 - ds_0^2 = 2\gamma_{ml} dx_m dx_l \qquad \textbf{(F.1)}$$

where γ_{ml} are reference strains. As shown earlier, the magnitude $ds^2 - ds_0^2$ represented the extension of a line element. Therefore this magnitude should remain unchanged under any coordinate transformation. Thus,

$$ds^2 - ds_0^2 = 2\gamma'_{kp} dy_k dy_p \qquad \textbf{(F.2)}$$

Where γ'_{kp} are transformed strains.

Under the above transformation, $x_m \to y_k$, the relationship between the unit lengths according to the transformation rule detailed in Appendix D is follows:

$$dx_m = a_{\bar{k}m} dy_k \qquad \textbf{(F.3)}$$

From (E.20) and (E.24);

$$2\gamma'_{kp} dy_k dy_p = 2\gamma_{ml} a_{\bar{k}m} dy_k a_{\bar{p}l} dy_p \qquad \textbf{(F.4)}$$

$$\Rightarrow \gamma'_{kp} dy_k dy_p = \gamma_{ml} a_{\bar{k}m} a_{\bar{p}l} dy_k dy_p \qquad \textbf{(F.5)}$$

$$\Rightarrow \bar{\gamma}_{kp} = \gamma_{ml} a_{\bar{k}m} a_{\bar{p}l} \qquad \textbf{(F.6)}$$

G STRESS TENSOR TRANSFORMATIONS

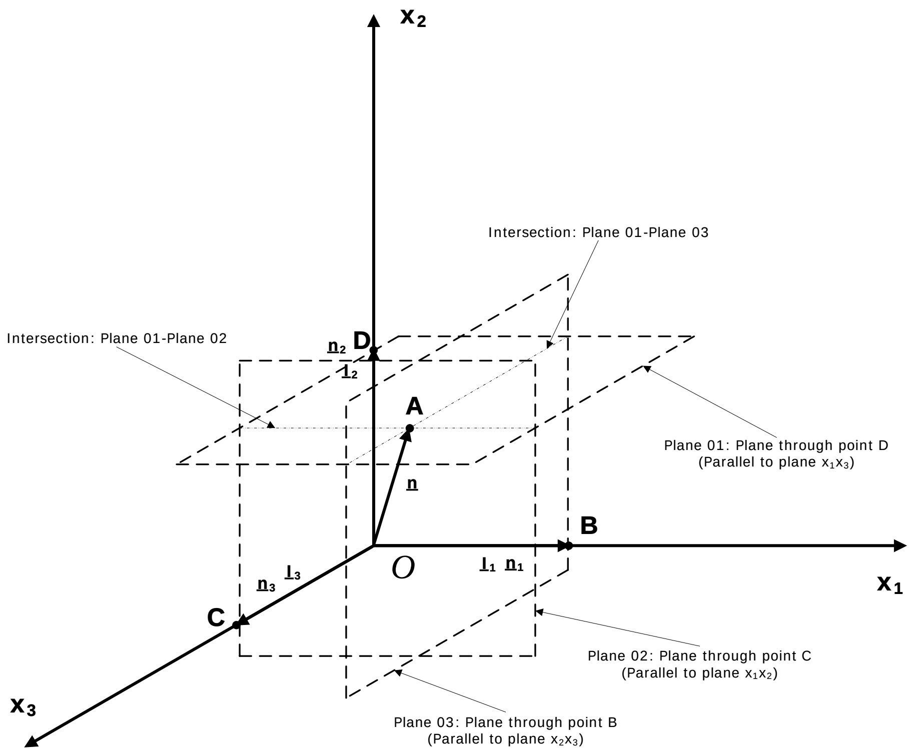

Figure G.1: Stress Tensor Transformations 01

Details of the derivations in this section can be found in the references [36, 37].

As can be seen from Figure G.1,

$$\underline{n_1} = n_1 \underline{I_1} \quad \textbf{(G.1)}$$

$$\underline{n_2} = n_2 \underline{I_2} \quad \textbf{(G.2)}$$

$$\underline{n_3} = n_3 \underline{I_3} \quad \textbf{(G.3)}$$

Obviously,

$$\begin{aligned} \underline{n} &= \underline{n_1} + \underline{n_2} + \underline{n_3} \\ &= n_1 \underline{I_1} + n_2 \underline{I_2} + n_3 \underline{I_3} \end{aligned} \quad \textbf{(G.4)}$$

where n_1, n_2, n_3 are direction cosines.

$$n_1 = \cos(\underline{OA} - \underline{OB}\hat{)} = \frac{|\underline{OB}|}{|\underline{OA}|} \tag{G.5}$$

If we assume that $\underline{n}$ is unit vector then,

$$|\underline{n}| = |\underline{OA}| = 1 \tag{G.6}$$

Therefore,

$$n_1 = \cos(OA - OB\hat{)} = |\underline{OB}| \tag{G.7}$$

Similarly,

$$n_2 = |\underline{OD}| \tag{G.8}$$

$$n_3 = |\underline{OC}| \tag{G.9}$$

Consider also the infinite number of planes perpendicular to $\underline{n}$. However, there is only one plane which is perpendicular to $\underline{n}$ at point A. For the rest of the discussion below, we will consider this plane and the stress vector acting on it.

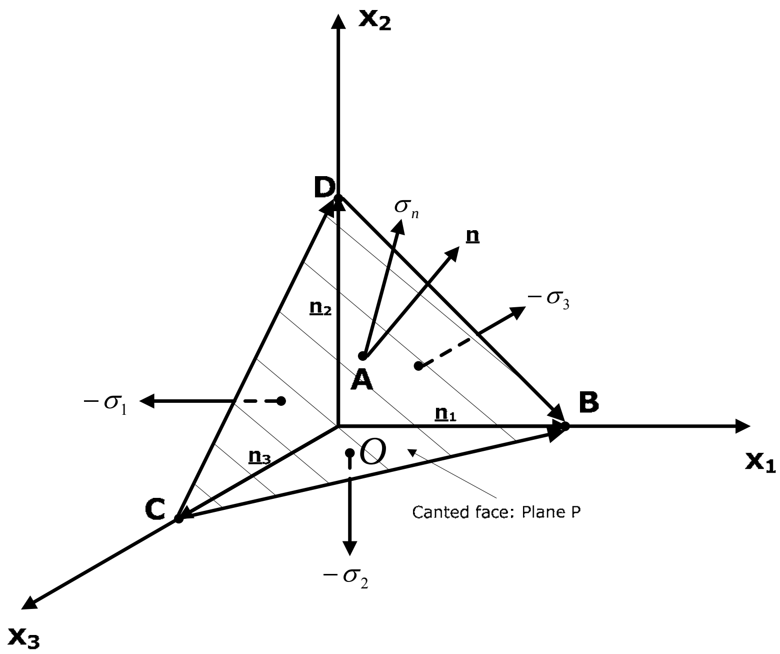

Figure notes:

The canted face of the tetrahedron has the surface normal $\underline{n}$ as explained above.

σ_n is the stress vector acting on the canted face BCD

Stress vectors are not necessarily along the face normal.

The tetrahedron is assumed to be infinitesimally small.

Figure G.2: Stress Tensor Transformations 02

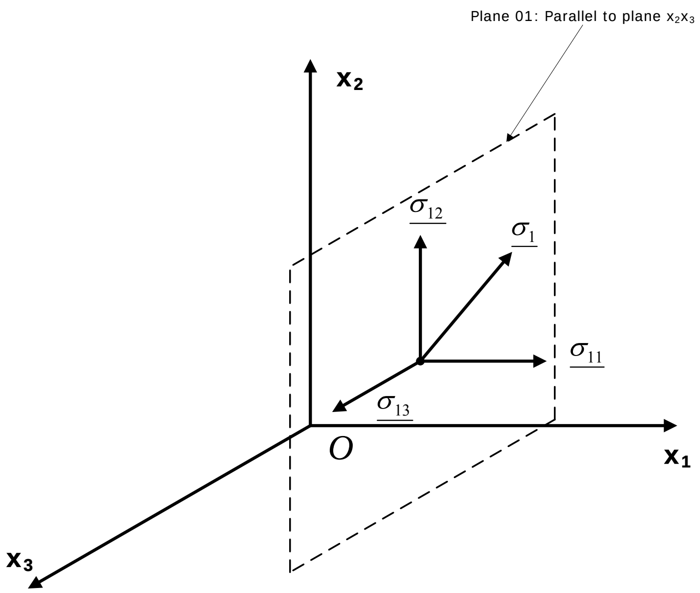

Figure notes:

1. The stress vector acting on Plane 01 is $\underline{\sigma_1}$ and it has its components along the coordinate axes. Obviously,

$\underline{\sigma_1} = \sigma_{11}\underline{I_1} + \sigma_{12}\underline{I_2} + \sigma_{13}\underline{I_3}$

Figure G.3: Stress Tensor Transformations 03

Now, let's write the vectorial force equilibrium for the tetrahedron shown in Figure G.2.

$$\underline{\sigma_n}A(BCD)-\underline{\sigma_1}A(COD)-\underline{\sigma_2}A(COB)-\underline{\sigma_3}A(DOB)+\underline{F}dV=0 \tag{G.10}$$

Where $\underline{F}dV$ is the internal force due to gravity.

Since the tetrahedron is assumed to be infinitesimally small, dV is a considerably smaller term than the area terms. Thus the forces including the gravitational loads are neglected. Hence,

$$\underline{\sigma_n}.A(BCD)=\underline{\sigma_1}A(COD)+\underline{\sigma_2}A(COB)+\underline{\sigma_3}A(DOB) \tag{G.11}$$

Let,

$$A(BCD)=A_n \tag{G.12}$$

$$A(COD)=A_1 \tag{G.13}$$

$$A(COB)=A_2 \tag{G.14}$$

$$A(DOB)=A_3 \tag{G.15}$$

$$\Rightarrow \underline{\sigma_n}A_n=\underline{\sigma_1}A_1+\underline{\sigma_2}A_2+\underline{\sigma_3}A_3 \tag{G.16}$$

$$\Rightarrow \underline{\sigma_n}A_n=\underline{\sigma_m}A_m \tag{G.17}$$

$$\Rightarrow \underline{\sigma_n}=\underline{\sigma_m}\frac{A_m}{A_n} \tag{G.18}$$

We know that the cross product of two vectors yields a vector whose magnitude is equal to the area of the parallelogram formed by these two vectors. Thus,

$$2.\underline{n}.A(BCD)=\underline{CB}\times\underline{CD} \tag{G.19}$$

$$\underline{CB}=\underline{n_1}-\underline{n_3} \tag{G.20}$$

$$\underline{CD}=\underline{n_2}-\underline{n_3} \tag{G.21}$$

$$\begin{aligned}&\Rightarrow 2A_n n=(\underline{n_1}-\underline{n_3})\times(\underline{n_2}-\underline{n_3})\\&=\underline{n_1}\times\underline{n_2}-\underline{n_1}\times\underline{n_3}-\underline{n_3}\times\underline{n_2}+\underline{n_3}\times\underline{n_3}\\&=\underline{n_1}\times\underline{n_2}-\underline{n_1}\times\underline{n_3}-\underline{n_3}\times\underline{n_2}\end{aligned} \tag{G.22}$$

On the other hand,

$$2A(COD)\underline{n_1} = 2A_1\underline{n_1} = \underline{n_2} \times \underline{n_3} = -\underline{n_3} \times \underline{n_2} \quad \textbf{(G.23)}$$

$$2A(COB)\underline{n_2} = 2A_2\underline{n_2} = \underline{n_3} \times \underline{n_1} = -\underline{n_1} \times \underline{n_3} \quad \textbf{(G.24)}$$

$$2A(DOB)\underline{n_3} = 2A_3\underline{n_3} = \underline{n_1} \times \underline{n_2} \quad \textbf{(G.25)}$$

thus,

$$2A_n\underline{n} = 2A_3\underline{n_3} + 2A_2\underline{n_2} + 2A_1\underline{n_1} \quad \textbf{(G.26)}$$

or,

$$A_n\underline{n} = A_m\underline{n_m} \quad \textbf{(G.27)}$$

hence,

$$\underline{n} = \frac{A_m}{A_n}\underline{n_m} \quad \textbf{(G.28)}$$

If we compare (G.28) with (E.24) will get;

$$a_{nm} = \frac{A_m}{A_n} \quad \textbf{(G.29)}$$

We can combine this equation with (G.17) to obtain;

$$\underline{\sigma_n} = a_{nm}\underline{\sigma_m} \quad \textbf{(G.30)}$$

This equation can be written in the following explicit from as follows:

$$\underline{\sigma_n} = a_{n1}\underline{\sigma_1} + a_{n2}\underline{\sigma_2} + a_{n3}\underline{\sigma_3} \quad \textbf{(G.31)}$$

Recall that $\underline{\sigma_n}$ is the stress vector acting on the canted face of the tetrahedron and it is not necessarily along $\underline{n}$ which is the surface normal. However, a_{nm} are the cosines of the angles between $\underline{n}$ and x_m. These were, as shown previously, n_m. Thus,

$$\underline{\sigma_n} = n_1\underline{\sigma_1} + n_2\underline{\sigma_2} + n_3\underline{\sigma_3} \quad \textbf{(G.32)}$$

It is intuitive from Figure G.3 that;

$$\left.\begin{aligned}\underline{\sigma_1} &= \underline{I_1}\sigma_{11} + \underline{I_2}\sigma_{12} + \underline{I_3}\sigma_{13} \\ \underline{\sigma_2} &= \underline{I_1}\sigma_{21} + \underline{I_2}\sigma_{22} + \underline{I_3}\sigma_{23} \\ \underline{\sigma_3} &= \underline{I_1}\sigma_{31} + \underline{I_2}\sigma_{32} + \underline{I_3}\sigma_{33}\end{aligned}\right| \qquad \textbf{(G.33)}$$

We can combine these equations with (G.32) to obtain:

$$\begin{aligned}&\underline{\sigma_n} = n_1(\underline{I_1}\sigma_{11} + \underline{I_2}\sigma_{12} + \underline{I_3}\sigma_{13}) \\ &+n_2.(\underline{I_1}\sigma_{21} + \underline{I_2}\sigma_{22} + \underline{I_3}\sigma_{23}) \\ &+n_3.(\underline{I_1}\sigma_{31} + \underline{I_2}\sigma_{32} + \underline{I_3}\sigma_{33})\end{aligned} \qquad \textbf{(G.34)}$$

$$\begin{aligned}&\Rightarrow \underline{\sigma_n} = \underline{I_1}(n_1\sigma_{11} + n_2\sigma_{21} + n_3\sigma_{31}) \\ &+\underline{I_2}.(n_1\sigma_{12} + n_2\sigma_{22} + n_n\sigma_{32}) \\ &+\underline{I_3}.(n_1\sigma_{13} + n_2\sigma_{23} + n_3\sigma_{33})\end{aligned} \qquad \textbf{(G.35)}$$

or in the closed form:

$$\underline{\sigma_n} = \underline{I_1}\sigma_{n1} + \underline{I_2}\sigma_{n2} + \underline{I_3}\sigma_{n3} \qquad \textbf{(G.36)}$$

where;

$$\left.\begin{aligned}\underline{\sigma_{n1}} &= \underline{n_1}\sigma_{11} + \underline{n_2}\sigma_{21} + \underline{n_3}\sigma_{31} \\ \underline{\sigma_{n2}} &= \underline{n_1}\sigma_{12} + \underline{n_2}\sigma_{22} + \underline{n_3}\sigma_{32} \\ \underline{\sigma_{n3}} &= \underline{n_1}\sigma_{13} + \underline{n_2}\sigma_{23} + \underline{n_3}\sigma_{33}\end{aligned}\right| \qquad \textbf{(G.37)}$$

So far we have obtained $\underline{\sigma_n}$ and $\underline{n}$. Now we are at the stage to project $\underline{\sigma_n}$ onto $\underline{n}$ in order to obtain the magnitude of the stress acting perpendicular on plane P. And after that we will obtain the tangent components as identified in Figure G.3.

Stress acting perpendicular on plane P is;

$$\sigma_{nn} = \underline{n} \bullet \underline{\sigma_n} \qquad \textbf{(G.38)}$$

Using (G.4) and (G.35), we can obtain the following expression:

$$\begin{aligned}&\sigma_{nn} = n_1(n_1\sigma_{11} + n_2\sigma_{21} + n_3\sigma_{31}) \\ &+n_2(n_1\sigma_{12} + n_2\sigma_{22} + n_{32}\sigma_{32}) \\ &+n_3(n_1\sigma_{13} + n_2\sigma_{23} + n_3\sigma_{33})\end{aligned} \qquad \textbf{(G.39)}$$

Since we know that $\sigma_{nm} = \sigma_{mn}$, then,

$$\sigma_{nn} = n_1^2\sigma_{11} + n_2^2\sigma_{22} + n_3^2\sigma_{33} + 2n_1n_2\sigma_{12} + 2n_1n_3\sigma_{13} + 2n_2n_3\sigma_{23} \tag{G.40}$$

On the other hand, having found the magnitude of the stress acting along the plane normal, we can easily obtain the stress components tangent to the plane as follows:

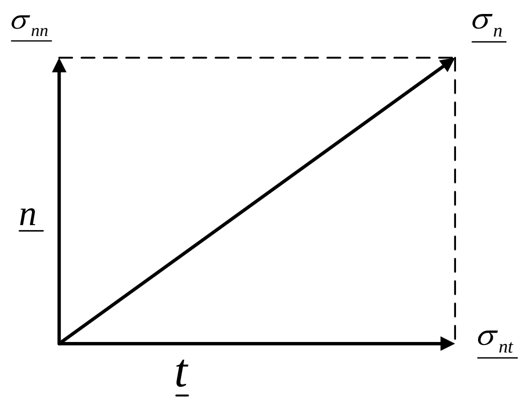

Figure G.4: Stress Tensor Transformations 04

Obviously,

$$\sigma_{nt}^2 = \sigma_n^2 - \sigma_{nn}^2 \tag{G.41}$$

Form (G.35);

$$\sigma_n^2 = \sigma_{n1}^2 + \sigma_{n2}^2 + \sigma_{n3}^2 \tag{G.42}$$

$$\Rightarrow \sigma_{nt}^2 = \sigma_{n1}^2 + \sigma_{n2}^2 + \sigma_{n3}^2 - \sigma_{nn}^2 \tag{G.43}$$

Up to this point, we have obtained the stress components acting on plane P in explicit form. For convenience, we can write these expressions in short form using the index notation as follows:

From (G.40), components along coordinate system axes:

$$\underline{\sigma_{n\alpha}} = \underline{n_\beta}\sigma_{\beta\alpha} = \underline{n_\beta}\sigma_{\alpha\beta} \tag{G.44}$$

From (G.40), component along plane P normal:

$$\underline{\sigma_{nn}} = \underline{n_\alpha}\,\underline{n_\beta}\sigma_{\alpha\beta} \tag{G.45}$$

Let's consider a coordinate system transformation $x_m \rightarrow y_k$ detailed as follows:

$$\begin{array}{ccccc} & & x_1 & x_2 & x_3 \\ \underline{n_1} \leftarrow & y_1 & a_{11} & a_{12} & a_{13} \\ \underline{n_2} \leftarrow & y_2 & a_{21} & a_{22} & a_{23} \\ \underline{n_3} \leftarrow & y_3 & a_{31} & a_{32} & a_{33} \end{array}$$

$\underline{n_1}$, $\underline{n_2}$, $\underline{n_3}$ are unit vectors along y_1, y_2, y_3 respectively i.e.

$$\underline{n_1} = a_{11}\underline{I_1} + a_{12}\underline{I_2} + a_{13}\underline{I_3} \quad \textbf{(G.46)}$$

$$\underline{n_2} = a_{21}\underline{I_1} + a_{22}\underline{I_2} + a_{23}\underline{I_3} \quad \textbf{(G.47)}$$

$$\underline{n_3} = a_{31}\underline{I_1} + a_{32}\underline{I_2} + a_{33}\underline{I_3} \quad \textbf{(G.48)}$$

And a_{nm} are the direction cosines; i.e., a_{23} is the cosine of the angle between y_2 and x_3.

Using (G.43), we can calculate the magnitude of any stress vector acting perpendicular on any transformed plane.

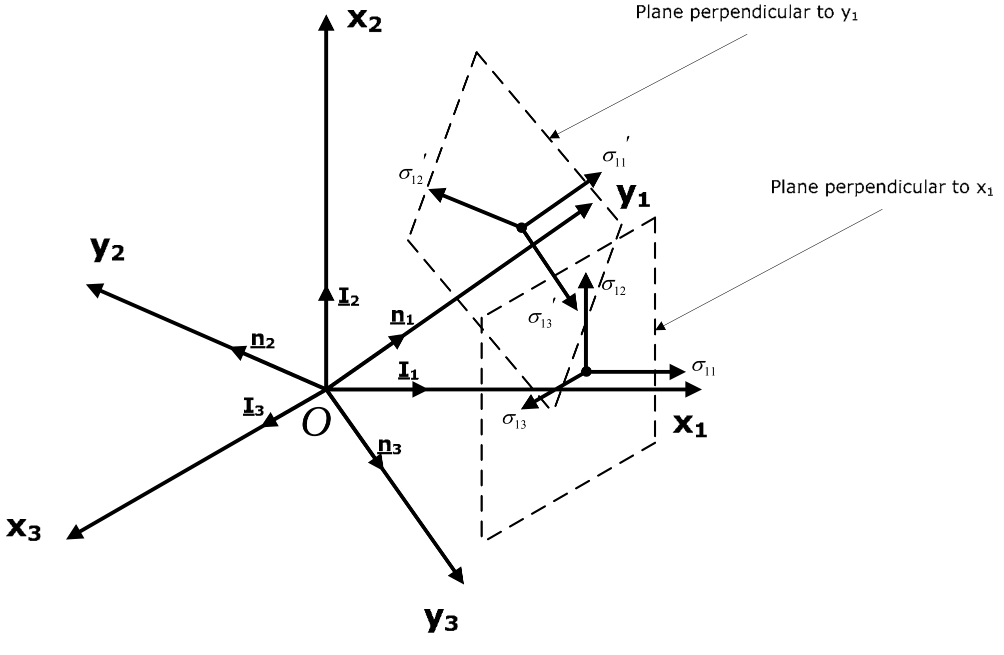

Figure G.5: Stress Tensor Transformations 05

Hence,

$$\sigma_{11}' = a_{11}^2\sigma_{11} + a_{12}^2\sigma_{22} + a_{13}^2\sigma_{33} + 2a_{11}a_{12}\sigma_{12} + 2a_{11}a_{13}\sigma_{13} + 2a_{12}a_{13}\sigma_{23} \quad \textbf{(G.49)}$$

$\Rightarrow$

$$\sigma_{11}' = a_{1\alpha} a_{1\beta} \sigma_{\alpha\beta} \tag{G.50}$$

similarly,

$$\sigma_{22}' = a_{2\alpha} a_{2\beta} \sigma_{\alpha\beta} \tag{G.51}$$

$$\sigma_{33}' = a_{3\alpha} a_{3\beta} \sigma_{\alpha\beta} \tag{G.52}$$

On the other hand, if we are able to obtain for instance the stress vector acting on the plane perpendicular to y_1, then we can find the magnitude of its components (shear stresses) which are along the y_2 and y_3 by mapping it onto the unit vectors n_2 and n_3. Recalling from (G.35);

$$\begin{aligned} \underline{\sigma_1'} &= \underline{I_1}(a_{11}\sigma_{11} + a_{12}\sigma_{21} + a_{13}\sigma_{31}) \\ &+ \underline{I_2}(a_{11}\sigma_{12} + a_{12}\sigma_{22} + a_{13}\sigma_{32}) \\ &+ \underline{I_3}(a_{11}\sigma_{13} + a_{12}\sigma_{23} + a_{13}\sigma_{33}) \end{aligned} \tag{G.53}$$

and

$n_2 = \underline{I_1} a_{21} + \underline{I_2} a_{22} + \underline{I_3} a_{23} \rightarrow$ vector along y_2

If we map $\underline{\sigma_1'}$ onto $\underline{n_2}$ we can obtain the magnitude of the component along y_2.

Thus,

$$\sigma_{12}' = \underline{\sigma_1'} \, \underline{n_2} \tag{G.54}$$

$$\begin{aligned} \Rightarrow \sigma_{12}' &= a_{21}(a_{11}\sigma_{11} + a_{12}\sigma_{21} + a_{13}\sigma_{31}) \\ &+ a_{22}(a_{11}\sigma_{12} + a_{12}\sigma_{22}) \end{aligned} \tag{G.55}$$

$$\begin{aligned} \Rightarrow \sigma_{12}' &= a_{21}(a_{11}\sigma_{11} + a_{12}\sigma_{21} + a_{13}\sigma_{31}) \\ &+ a_{22}(a_{11}\sigma_{12} + a_{12}\sigma_{22} + a_{13}\sigma_{32}) \\ &+ a_{23}(a_{11}\sigma_{31} + a_{12}\sigma_{23} + a_{13}\sigma_{33}) \end{aligned} \tag{G.56}$$

The above equation can also be written in index notation as follows:

$$\sigma_{12}' = a_{1\alpha} a_{2\beta} \sigma_{\alpha\beta} \tag{G.57}$$

Similarly,

$$\sigma_{13}{}' = a_{1\alpha} a_{3\beta} \sigma_{\alpha\beta} \qquad \textbf{(G.58)}$$

$$\sigma_{12}{}' = a_{2\alpha} a_{3\beta} \sigma_{\alpha\beta} \qquad \textbf{(G.59)}$$

Thus, utilizing our findings so far we can obtain the general stress transformation formula in index notation as follows:

$$\sigma_{\gamma\delta}{}' = a_{\gamma\alpha} . a_{\delta\beta} . \sigma_{\alpha\beta} \qquad \textbf{(G.60)}$$

where $\sigma_{\gamma\delta}{}'$ are the transformed stresses and $\sigma_{\alpha\beta}$ are the reference stresses

H MAXWELL-BETTI RECIPROCAL THEOREM

Details of the derivations in this section can be found in the references [50, 61].

Consider two sets of forces, $\underline{P_1}...\underline{P_n}$ and $\underline{p_1}...\underline{p_m}$ (n, m=1, N), to be applied on different locations of a body.

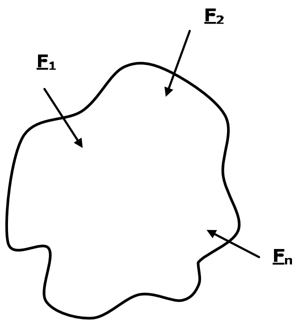

Figure H.1: Maxwell-Betti Reciprocal Theorem 01

First, let's apply $\underline{F_n}$ on the undeformed body as shown in Figure H.1. The body is deformed; however, let's keep this deformation out of concern for the moment. Apply $\underline{f_m}$ following the application of $\underline{F_n}$ on the same body; the body is further deformed. Assume deformation caused by the application of $\underline{f_m}$ to be denoted as $\underline{d_n}$. These deformations are at the points of application of the load set $\underline{F_n}$. Thus, we can write the work done by $\underline{F_n}$ due to displacements caused by the application of $\underline{f_m}$ as follows:

$$W_{F/f} = \sum_{n=1}^{N} \underline{F_n}\,\underline{d_n} \tag{H.1}$$

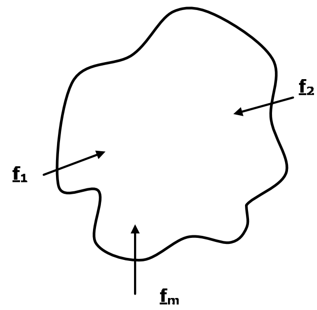

Figure H.2: Maxwell-Betti Reciprocal Theorem 02.

Now, unlike above, let's apply $\underline{f_m}$ on the undeformed body first as shown in Figure H.2. The body is deformed; however, this deformation is out of concern for the moment. Apply $\underline{F_n}$ following the application of $\underline{f_m}$ on the body. Assume deformations caused by the application of $\underline{F_n}$ denoted as $\underline{D_m}$. These deformations are at the points of application of the load set $\underline{f_m}$. Thus we can write the work done by $\underline{f_m}$ due to the displacements caused by the application of the load set $\underline{F_n}$ as follows:

$$W_{f/F} = \sum_{m=1}^{N} \underline{f_m} \underline{D_m} \tag{H.2}$$

Maxwell-Betti Reciprocal Theorem states that;

$$W_{F/f} = W_{f/F} \tag{H.3}$$

Thus,

$$\sum_{n=1}^{N} F_n d_n = \sum_{m=1}^{N} f_m D_m \tag{H.4}$$

In practical terms, Maxwell-Betti Reciprocal Theorem states that deformations are proportional to the applied forces.

I GRADIENT (SLOPE) OF A CURVE AT A POINT

Details of the derivations in this section can be found in the references [46, 47]

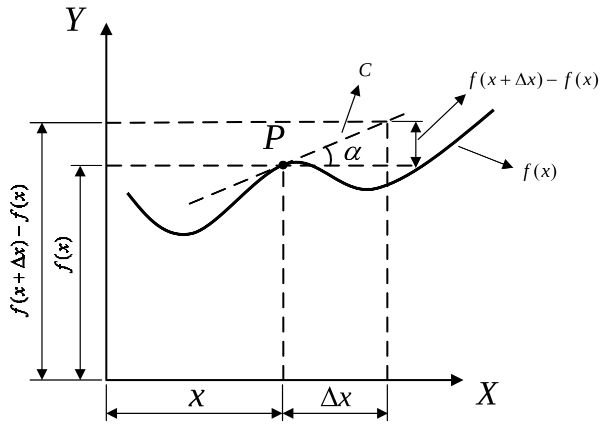

Figure I.1: Gradient (slope) of a Curve.

Figure notes:

1. $f(x)$ is an arbitrary curve defined in E^3.
2. Curve C is tangent to curve $f(x)$ at point P.

Thus, the slope of curve $f(x)$ at $X = x$ can be defined as follows:

$$\alpha = \lim_{\Delta x \to 0} \frac{f(x+\Delta x) - f(x)}{\Delta x} \tag{I.1}$$

Hence,

$$\alpha = \frac{\mathrm{df(x)}}{\mathrm{dx}} = \lim_{\Delta x \to 0} \frac{\Delta f}{\Delta x} = \lim_{\Delta x \to 0} \frac{f(x+\Delta x) - f(x)}{\Delta x} \tag{I.2}$$

J STRAIN TENSOR

Details of the derivations in this section can be found in the references [37, 38, 39]

Recalling our findings from Appendix C, we deduce the strain tensor components as follows:

From (D.8), we know that

$$\gamma_{kl} = \frac{1}{2}\left[g_{kl} \frac{\partial x_k}{\partial z_j} \frac{\partial x_l}{\partial z_i} - a_{kl} \frac{\partial A_k}{\partial z_j} \frac{\partial A_l}{\partial z_i} \right] \qquad \textbf{(J.1)}$$

If we assume that the reference coordinate system z_i ($i = 1,2,3$) coincides with the undeformed state coordinate system A_i ($i = 1,2,3$) then,

$$\frac{\partial A_k}{\partial z_j} = 1 \ (k = 1,2,3 \text{ and } j = 1,2,3)$$

Hence,

$$E_{kl} = \gamma_{kl} = \frac{1}{2}\left[g_{kl} \frac{\partial x_k}{\partial z_j} \frac{\partial x_l}{\partial z_i} - a_{kl} \right] \text{ (Lagrangian strain tensor)} \qquad \textbf{(J.2)}$$

If we assume that the reference coordinate system z_i ($i = 1,2,3$) coincides with the deformed state coordinate system x_i ($i = 1,2,3$), then,

$$\frac{\partial x_k}{\partial z_j} = 1 \ (k = 1,2,3 \text{ and } j = 1,2,3) \qquad \textbf{(J.3)}$$

Hence,

$$e_{kl} = \gamma_{kl} = \frac{1}{2}\left[g_{kl} - a_{kl} \frac{\partial A_k}{\partial z_j} \frac{\partial A_l}{\partial z_i} \right] \text{ (Eulerian strain tensor)} \qquad \textbf{(J.4)}$$

In Lagrangian approach, we fix our attention to the undeformed state and select a_{kl} arbitrarily, the aim is to watch the change from this state to the deformed state.

Whereas, in Eulerian approach, we fix our attention to an arbitrarily selected region or a point and try to determine the undeformed state from this region or point backwards. This approach is utilized mostly in fluid mechanics and large deformation solid problems.

We can use the same rectangular Cartesian coordinate system to describe both the deformed and undeformed states.

Then, due to orthogonality of base vectors;

$$a_{ij} = g_{ij} = \delta_{ij} \;\; (i = 1,2,3 \text{ and } j = 1,2,3)$$

where δ_{ij} is the Kronecker Delta function.

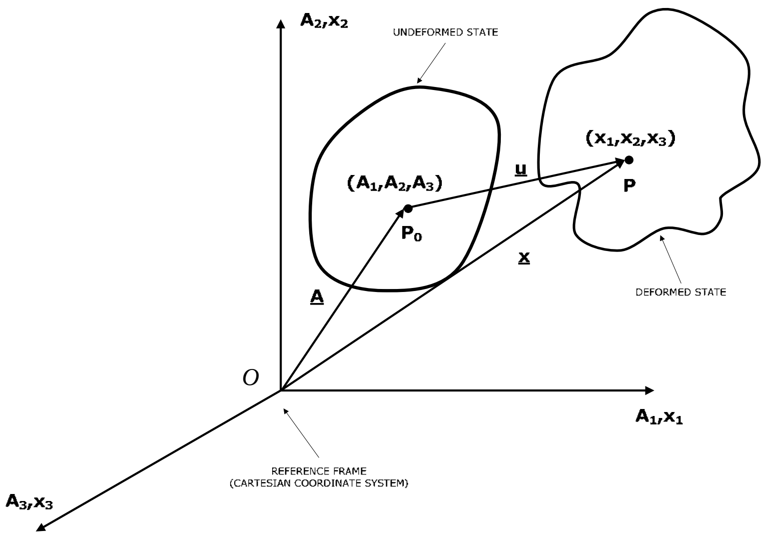

Figure J.1: Strain Tensor.

It is intuitive from the drawing that

$$u_i = x_i - A_i \quad \textbf{(J.5)}$$

thus,

$$x_i = u_i + a_i \quad \textbf{(J.6)}$$

and

$$a_i = x_i - u_i \quad \textbf{(J.7)}$$

Hence,

$$\frac{\partial x_i}{\partial A_m} = \frac{\partial u_i}{\partial A_m} + \frac{\partial A_i}{\partial A_m} = \frac{\partial u_i}{\partial A_m} + \delta_{im} \tag{J.8}$$

and

$$\frac{\partial A_i}{\partial x_m} = \frac{\partial x_i}{\partial x_m} - \frac{\partial u_i}{\partial x_m} = \delta_{im} - \frac{\partial u_i}{\partial x_m} \tag{J.9}$$

We can now substitute the above findings in strain tensor definitions of (J.2) and (J.4) to obtain the below expressions.

$$E_{ml} = \frac{1}{2}\left[\delta_{ij}\left(\frac{\partial u_i}{\partial A_m} + \delta_{ml}\right)\left(\frac{\partial u_j}{\partial A_l} + \delta_{jl}\right) - \delta_{ml} \right] \tag{J.10}$$

After some mathematical manipulations and replacement of dummy indices, we can obtain the strain tensor in the following more familiar form,

$$E_{ij} = \frac{1}{2}\left[\frac{\partial u_j}{\partial A_i} + \frac{\partial u_i}{\partial A_j} + \frac{\partial u_\alpha}{\partial A_i}\frac{\partial u_\alpha}{\partial A_j} \right] \tag{J.11}$$

Similarly,

$$e_{ml} = \frac{1}{2}\left[\delta_{ml} - \delta_{ij}\left(\delta_{im} - \frac{\partial u_i}{\partial x_m}\right)\left(\delta_{jl} - \frac{\partial u_j}{\partial x_l}\right) \right] \tag{J.12}$$

that gives,

$$e_{ij} = \frac{1}{2}\left[\frac{\partial u_j}{\partial x_i} + \frac{\partial u_i}{\partial x_j} - \frac{\partial u_\alpha}{\partial x_i}\frac{\partial u_\alpha}{\partial x_j} \right] \tag{J.13}$$

Removing the non-linear terms we can obtain the engineering strains as follows:

$$E_{ij} = \frac{1}{2}\left[\frac{\partial u_j}{\partial A_i} + \frac{\partial u_i}{\partial A_j} \right] \tag{J.14}$$

and

$$e_{ij} = \frac{1}{2}\left[\frac{\partial u_j}{\partial x_i} + \frac{\partial u_i}{\partial x_j} \right] \tag{J.15}$$

Under small deformation assumption, there is no distinction between A_i and x_i. Therefore,

$$E_{ij} = e_{ij} = \frac{1}{2}\left[\frac{\partial u_j}{\partial x_i} + \frac{\partial u_i}{\partial x_j}\right] \tag{J.16}$$

Explicitly,

$$\left.\begin{aligned} E_{11} &= \frac{\partial u_1}{\partial x_1} \text{ or } \varepsilon_x = \frac{\partial u}{\partial x} \\ E_{22} &= \frac{\partial u_2}{\partial x_2} \text{ or } \varepsilon_y = \frac{\partial v}{\partial y} \\ E_{33} &= \frac{\partial u_3}{\partial x_3} \text{ or } \varepsilon_z = \frac{\partial w}{\partial z} \end{aligned}\right| \tag{J.17}$$

and

$$\left.\begin{aligned} \varepsilon_{xy} &= \frac{1}{2}\gamma_{xy} = \frac{1}{2}\left[\frac{\partial u}{\partial y} + \frac{\partial v}{\partial x}\right] \\ \varepsilon_{xz} &= \frac{1}{2}\gamma_{xz} = \frac{1}{2}\left[\frac{\partial u}{\partial z} + \frac{\partial w}{\partial x}\right] \\ \varepsilon_{yz} &= \frac{1}{2}\gamma_{yz} = \frac{1}{2}\left[\frac{\partial v}{\partial z} + \frac{\partial w}{\partial y}\right] \end{aligned}\right| \tag{J.18}$$

K NOTES ON DISPLACEMENT COMPONENTS

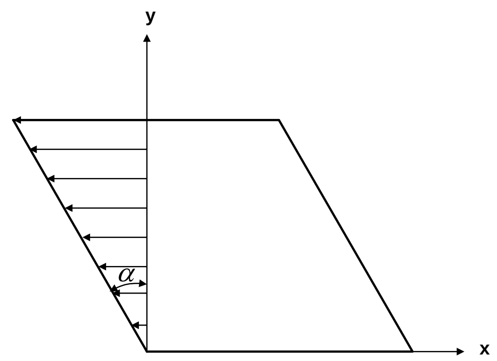

Figure K.1: Displacement Components, $\underline{u}$.

$$\alpha = -\frac{\partial u(x,y)}{\partial y} \tag{K.1}$$

In Figure K.1, α represents the change of displacement vector $\underline{u}$ with y.

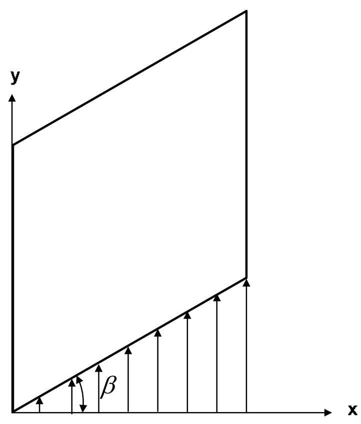

Figure K.2: Displacement Components, $\underline{v}$.

$$\beta = \frac{\partial v(x,y)}{\partial x} \tag{K.2}$$

In Figure K.2, β represents the change of displacement vector $\underline{v}$ with x.

We can represent the above deformations on the same figure as follows:

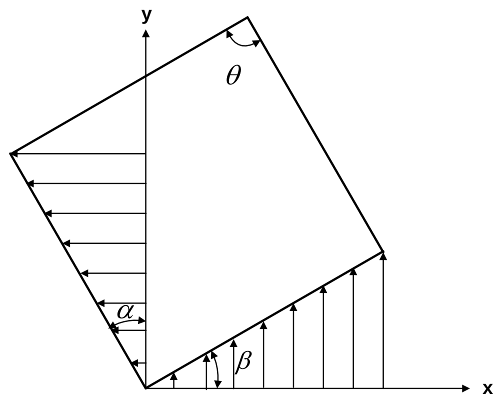

Figure K.3: Displacement Components; $\underline{u}$ and $\underline{v}$.

Obviously, $\theta = 90^o$ before deformation. If following the deformation $\alpha = \beta$, then $\theta = 90^o$. This means that there is no shear deformation but there is only a rigid body rotation about z.

If $\alpha \neq \beta$, then $\theta \neq 0$. This means that there is shear deformation and some rigid body rotation.

Thus,

$\beta - \alpha$ represents the total change in angle θ which corresponds to shear deformation; namely,

$$\beta - \alpha = \frac{\partial v(x,y)}{\partial x} + \frac{\partial u(x,y)}{\partial y} = \gamma_{xy} \tag{K.3}$$

Therefore, when we assume that $\gamma_{xy}{}^o = 0$, and when $u^o(x,y) \neq 0$ and $v^o(x,y) \neq 0$, rigid body rotation is obtained as a result of the mathematical manipulation.

L SIGN CONVENTIONS

- Negative and positive curvatures:

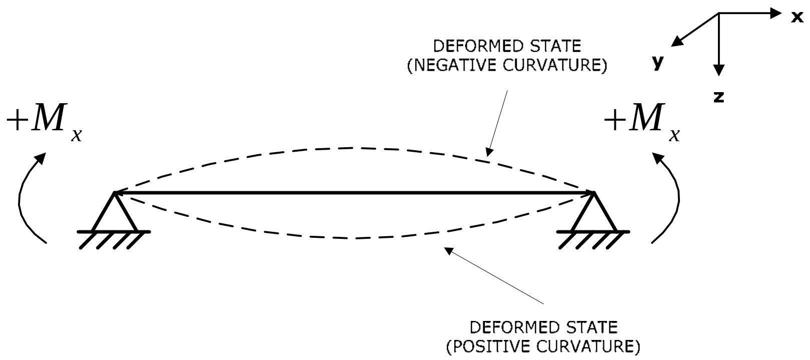

Figure L.1: Typical Plate Cross Section

- Positive moments:

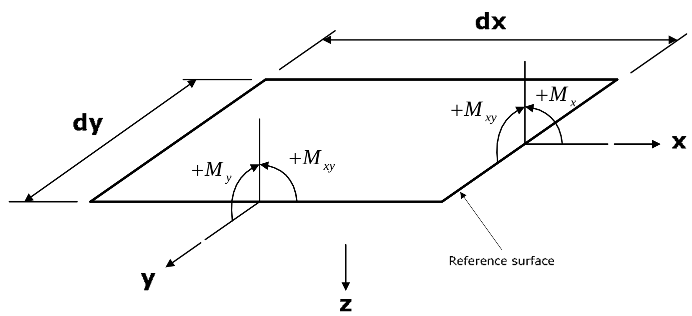

Figure L.2: Moments Acting on a Plate Reference Surface

Thus, moments about $+y$ are (using the right hand rule):

$$M_x.dx \tag{L.1}$$

$$M_{xy}.dx \tag{L.2}$$

Moments about $+x$ are (using the right hand rule):

$$M_y.dy \tag{L.3}$$

M EXPERIMENT

PROBLEM DEFINITION

Bending of a rectangular, simply supported, fiber reinforced sandwich plate under uniformly distributed pressure.

OBJECTIVES OF THE EXPERIMENT

Examining the bending behavior of the rectangular simply supported, fiber reinforced sandwich plate under uniformly distributed pressure with an experiment and provide with a benchmark for analytical and computational solution models.

Objectives of the Experiment

The objectives of the experiment are summarized below:

Measurement of maximum panel deflection

Maximum panel deflection is measured in the middle of the plate facing the support side.

Measurement of maximum inner skin stress

Maximum inner skin strain (compression) is measured in the middle of the plate facing the loaded side. Maximum inner skin stress is then obtained using the corresponding measured strain value. Strain is measured in three principal axes lying on the same horizontal plane, namely; 0º, 90º (corresponding to warp and weft directions of the fiber cloth used as reinforcement) and ±45º. The rationale behind the selection and measurement along these axes is to verify each measurement by comparing one another. It is assumed that the reinforcement shows same mechanical properties along warp and weft directions.

Measurement of maximum outer skin stress

Maximum outer skin strain (tension) is measured in the middle of the plate facing the support side. Maximum outer skin stress is then obtained using the corresponding measured strain value. Strain is measured in three principal axes lying on the same horizontal plane, namely; 0º, 90º (corresponding to warp and weft directions of the fiber cloth used as reinforcement) and ±45º as for the measurement of maximum inner skin stress.

EXPERIMENT PLAN

1. Design and construction of the fiber reinforced sandwich plate
2. Design and construction of the supporting structure
3. Determination of the amount and the way of loading
4. Measurement of the panel deflection with a displacement gauge and measurement of strain values using strain gauges.

EXPERIMENT SET LAY-OUT

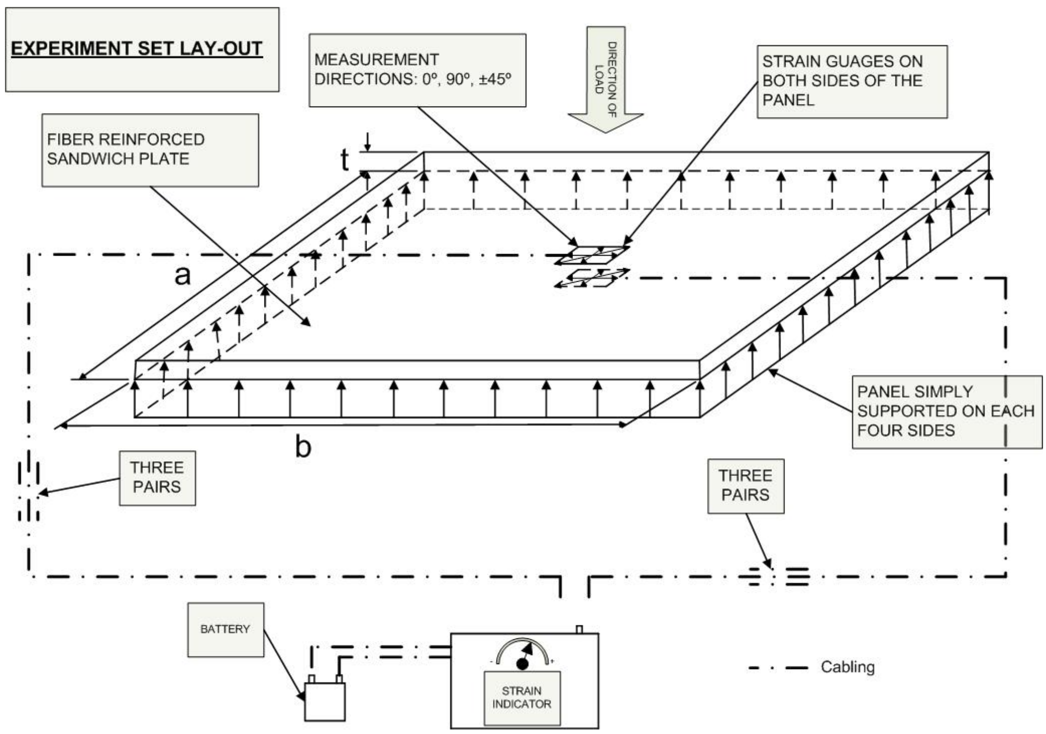

Figure M.1: Experiment Set Lay-Out

DETAILS OF THE COMPONENTS

Composite Plate

Plate geometry

1000x1000mm rectangular constant thickness sandwich plate.

Plate construction

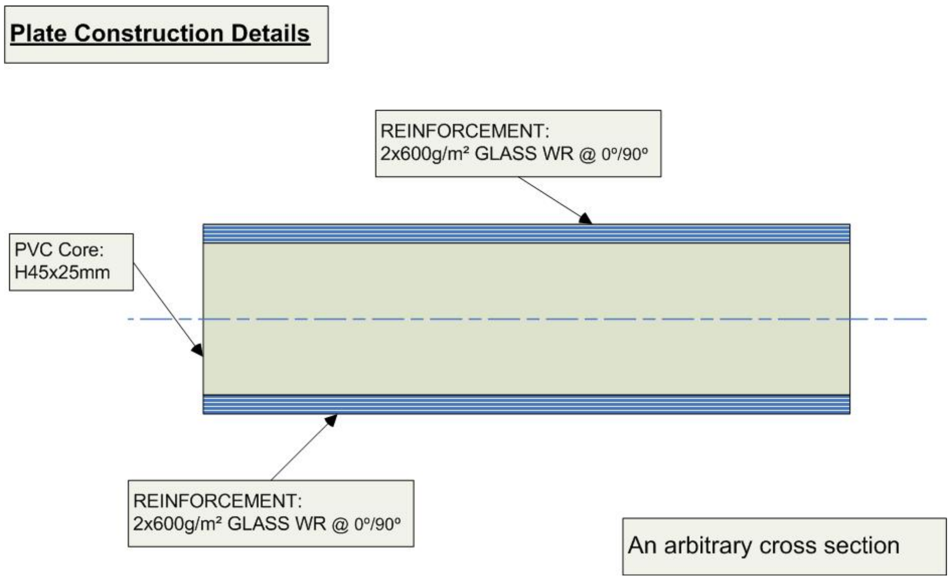

Figure M.2: Plate Cross Section Details

Mechanical properties

1. Reinforcement Material:

   Assumed mechanical properties of the fiber reinforcement are as follows:

Table M.1: Mechanical Properties of Fiber Reinforcement

E_1 :	18600	N/mm^2
E_2 :	5654	N/mm^2
E_3 :	5654	N/mm^2
ν_{xy} :	0.254	
ν_{xz} :	0.254	
ν_{yz} :	0.428	
G_{xy} :	1748	N/mm^2
G_{xz} :	1748	N/mm^2
G_{yz} :	1220	N/mm^2

2. Core Material:

   Assumed mechanical properties of the fiber reinforcement are as follows:

Table M.2: Mechanical Properties of Fiber Reinforcement

E	50	N/mm^2
ν	0.35	

Supporting Structure

The supporting structure is designed so that the "simply supported" boundary condition is ensured. On the other hand, the supporting structure should also present an ideally rigid behavior. In practical terms, this means that the deformations of the supporting structure should be so small, compared to the deformations of the plate, that they can be ignored. A factor of 1/100 is assumed to be acceptable.

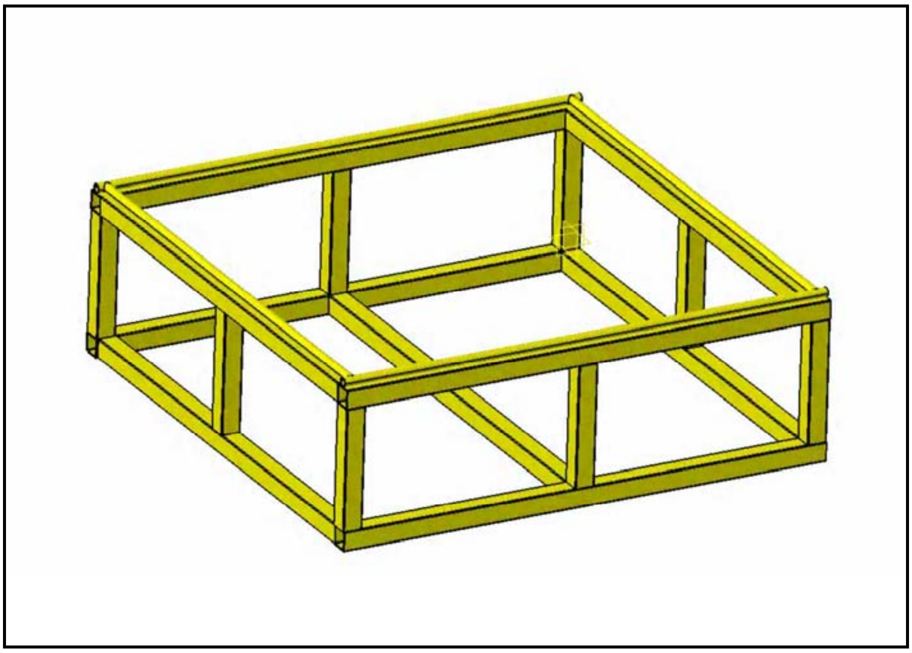

Figure M.3: 3-D Model of the Supporting Structure

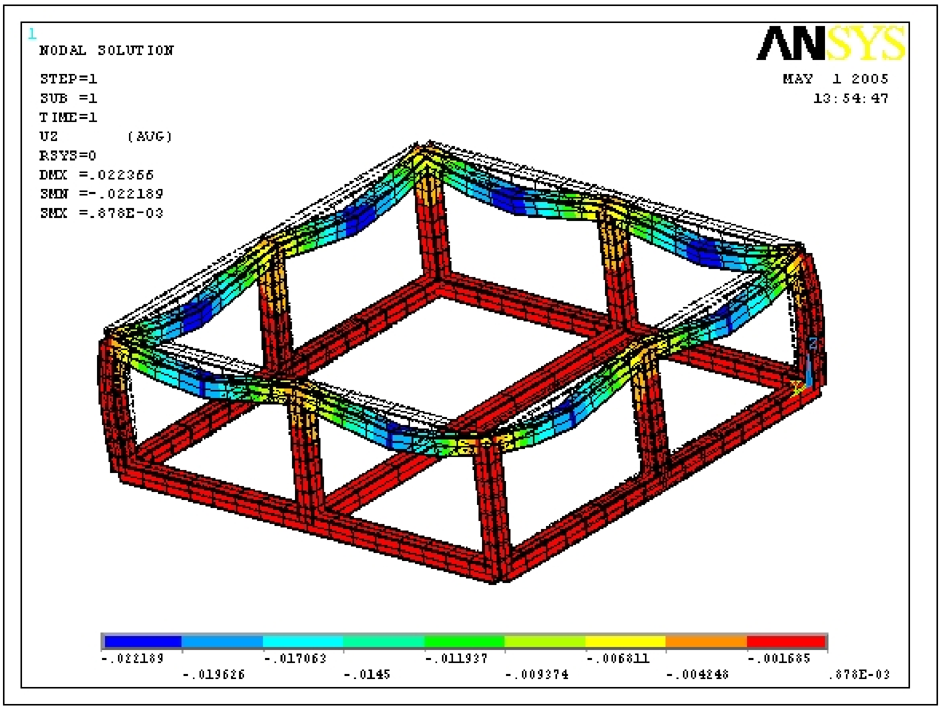

Figure M.4: FEA Results: Maximum Deformation along the Vertical Axis

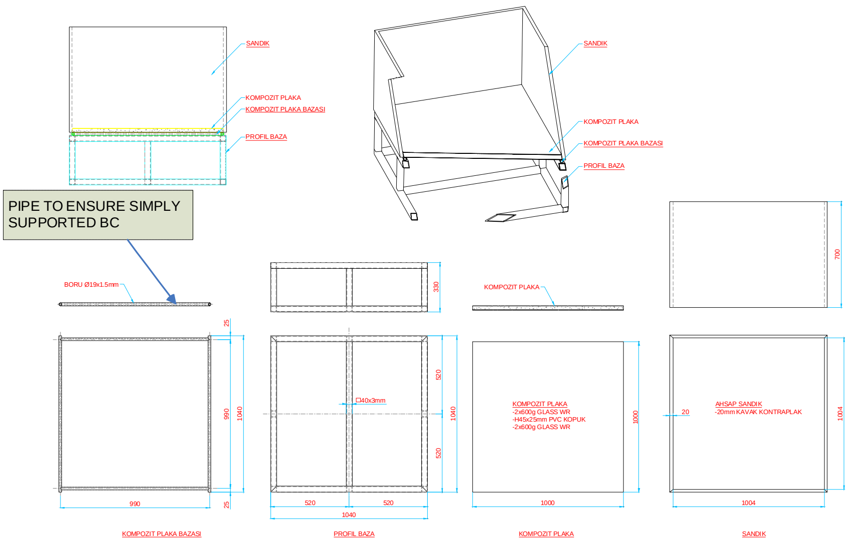

Figure M.5: Shop Drawing Of The Supporting Structure

Loading

To ensure that the panel is loaded under uniformly distributed pressure and for convenience, sand is used. Determination of the amount of sand to be used for the experiment is obtained by preliminary bending analysis of the sandwich plate. The figure shows the maximum panel deflection under an evenly distributed pressure of 5.807×10^{-3} N/mm². This pressure can be obtained using a 1000x1000x600mm sand block. The specific weight of the sand used is 9.865×10^{3} N/m³.

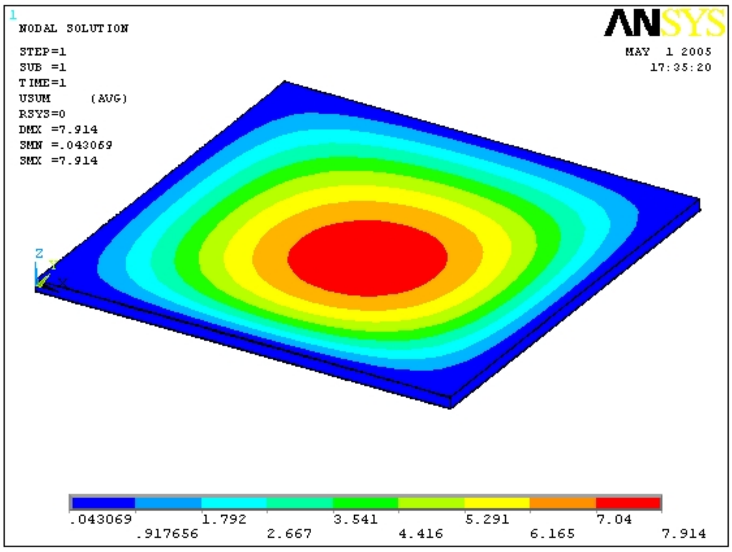

Figure M.6: FEA Results: Maximum Deflection along Vertical Axis

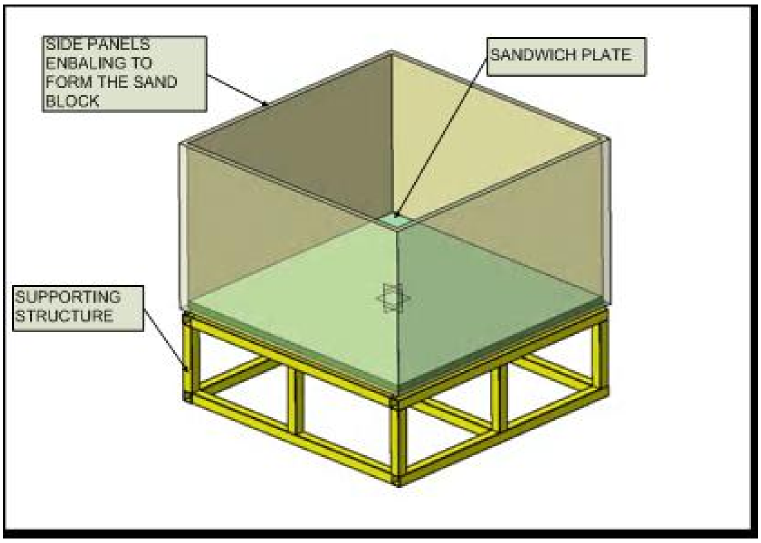

Figure M.7: Support Structure: Sandwich Plate and Side Panels

Strain Gauge and Indicator Details

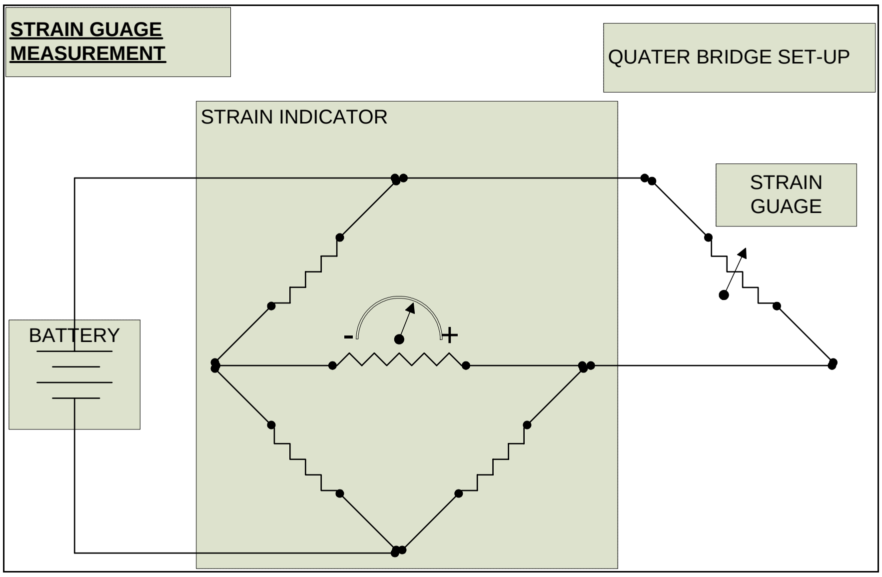

Figure M.8: Measurements and Calculations

EXPERIMENT

Venue

The experiment was carried out on 22.08.2006.

Measurements

The experiment was carried out in five subsequent load steps. Measurements were noted at each load step. The table below and the corresponding graph summarize the experiment and measurements.

Table M.3: Measurements Summary Table.

SIDE B (Tension)

Sand Block Height form Panel Face	Corresponding load x 10^3 N/mm²	Strain Value, Red x E6	Neutralized Strain Value, Red x E6	Strain Value, Blue x E6	Neutralized Strain Value, Blue x E6	Strain Value, Green x E6	Neutralized Strain Value, Green x E6	Average Strain x E6	Gauge Reading (mm)	Corrected Reading (mm)	Panel Deflection x 100 (mm)
H: 0mm	0,000	0,0	0,0	-3480,0	0,0	-210,0	0,0	0,0	3,000	3,000	0,0
H: 150mm	1,452	249,0	249,0	-3232,5	247,5	9,0	219,0	238,5	6,199	6,597	340,4
H: 300mm	2,904	472,5	472,5	-2992,5	487,5	232,5	442,5	467,5	7,847	8,351	515,8
H: 450mm	4,355	682,5	682,5	-2782,5	697,5	435,0	645,0	675,0	9,396	9,998	680,6
H: 600mm	5,807	900,0	900,0	-2557,5	922,5	652,5	862,5	895,0	10,935	11,636	844,4

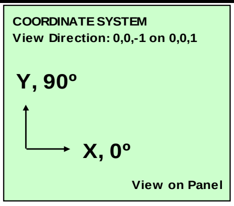

SIDE A (Compression)

Sand Block Height form Panel Face	Corresponding load x 10^3 N/mm²	Strain Value, Red x E6	Neutralized Strain Value, Red x E6	Strain Value, Blue x E6	Neutralized Strain Value, Blue x E6	Strain Value, Green x E6	Neutralized Strain Value, Green x E6	Average Strain x E6
H: 0mm	0,000	1507,5	0,0	180,0	0,0	945,0	0,0	0,0
H: 150mm	1,452	1230,0	-277,5	-120,0	-300,0	690,0	-255,0	-277,5
H: 300mm	2,904	1012,5	-495,0	-232,5	-412,5	480,0	-465,0	-457,5
H: 450mm	4,355	820,5	-687,0	-547,5	-727,5	255,0	-690,0	-701,5
H: 600mm	5,807	667,5	-840,0	-742,5	-922,5	67,5	-877,5	-880,0

Notes:
- Side B faces the support
- Side A faces the load
- Label red corresponds to gauge along 0º-180º axis
- Label blue corresponds to gauge along 90º-270º direction
- Label green corresponds to gauge along 45º-225º direction
- Panel deflection is measured in the middle of the plate, side facing the support
- Gauge reading for panel deflection is corrected for 20º (with respect to horizontal axis) misalignment of the gauge

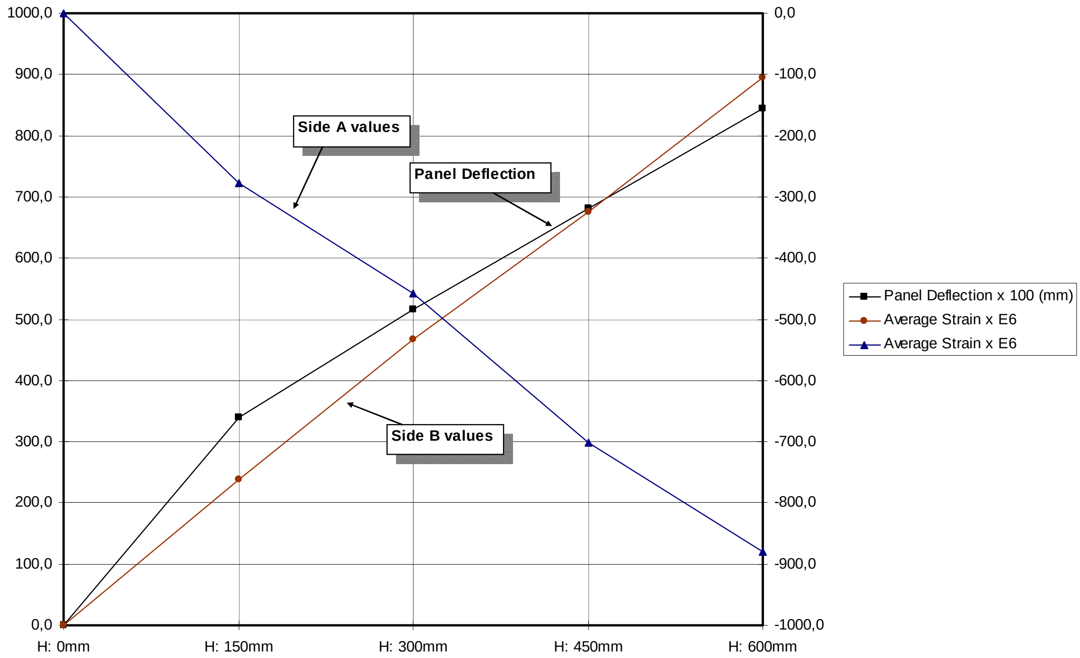

Figure M.9: Measurements Summary Graph.

PHOTO GALLERY

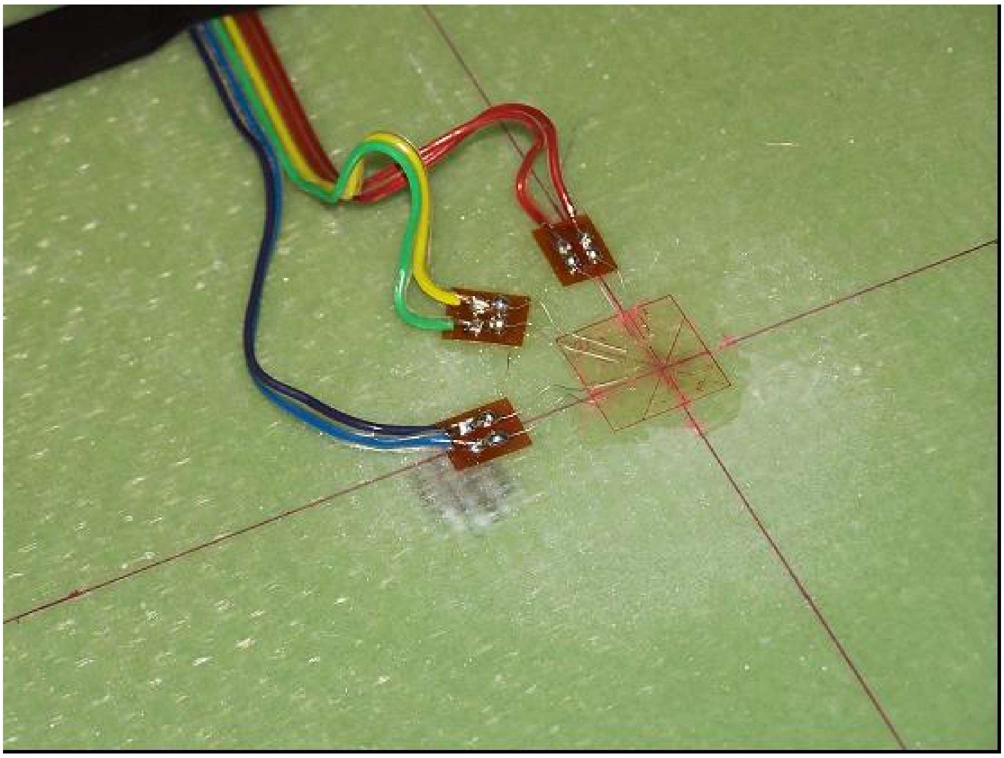

Figure M.10: Strain Gauge Installation.

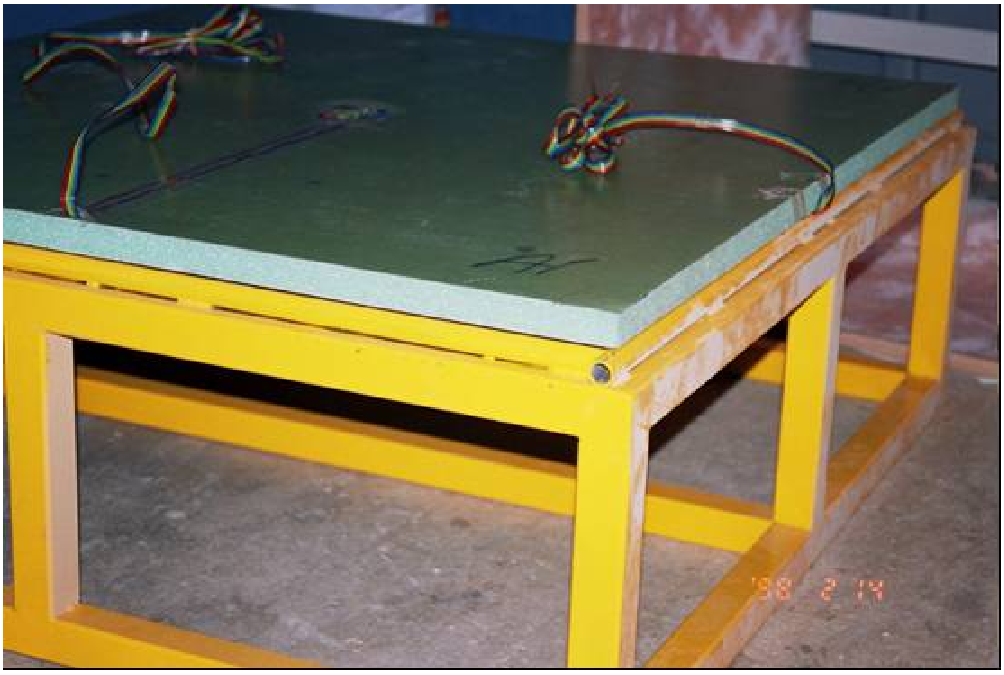

Figure M.11: The Supporting Structure and the Sandwich Panel.

Figure M.12: The Sand Block at 450mm Height.

Figure M.13: The Strain Indicator.

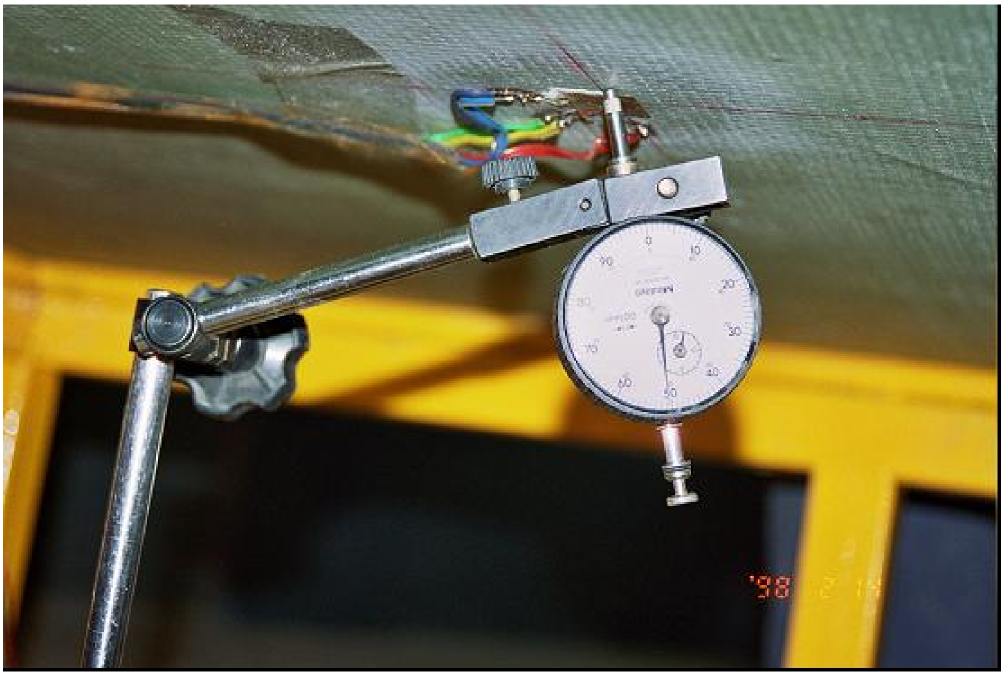

Figure M.14: The Deflection Gauge.

RESUME

I was born in 1975 in Istanbul. Following my graduation form the High School, I started Istanbul Technical University, Faculty of Naval Architecture and Ocean Engineering, Department of Naval Architecture for my Bachelor's degree in 1993. I graduated in 1997. Following my graduation, I started working at Yonca-Onuk JV/ Istanbul as the Engineering in Charge in the Operations Department in 1997. Following the completion of my military service in 1999, I again started at Yonca-Onuk JV from where I had left. In the year 2000, I was assigned as the Director Engineering. In 2005, I co-founded BGM Mühendislik Hizmetleri Ltd. in Istanbul. I also hold an MBA degree from Sabancı University.

I am interested in the design and the construction of vessels incorporating composite materials.